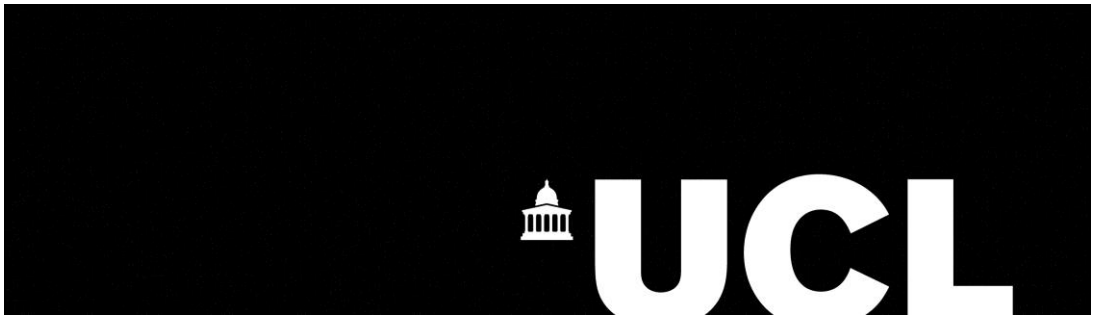

The use of microfluidic chambers to study action potential propagation and stimulus transduction in sensory neurons *in vitro*

Alex James Clark

SUBMITTED FOR THE DEGREE OF

DOCTOR OF PHILOSOPHY

I, Alex James Clark, confirm that the work presented in this thesis is my own. Where information has been derived from other sources, I confirm that this has been indicated in the thesis

Abstract

Primary afferent sensory neurons can be incredibly long single cellular structures, often traversing distances of over one metre in the human. Cutaneous sensory stimuli are transduced in the periphery by specialised end-organs or free nerve endings which enable the coding of the stimulus into electrical action potentials that propagate towards the central nervous system.

Despite significant advances in our knowledge of sensory neuron physiology and ion channel expression, many commonly used techniques fail to accurately model the primary afferent neuron in its entirety. *In vitro* experiments often focus on the cell somata and neglect the fundamental processes of peripheral stimulus transduction and action potential propagation. Despite this, these experiments are frequently used as a model for cellular investigations of the receptive terminals. Crucially, somal responses may not represent the functional expression of ion channels in the axon and end terminals.

The aim of this thesis was to develop a system using compartmentalised culture chambers and ratiometric calcium imaging to directly and accurately compare the sensitivity and functional protein expression of isolated neuronal regions *in vitro*.

Using this preparation I demonstrate that the nerve terminals of cultured DRG neurons can be depolarised to induce action potential propagation, which has both a TTX-resistant and TTX-sensitive component. Furthermore, I show that there is a differential regulation of proton sensitivity between the sensory terminals and somata in cultured sensory neurons. I also go on to show that capsaicin sensitivity is highly dependent on embryonic dissection age.

This novel approach enables a comprehensive method to study the excitability characteristics and regional sensitivity differences of cultured sensory neurons on a single cell level. Examination of the sensory terminals is crucial to further understand the properties and diversity of DRG sensory neurons.

Acknowledgements

First and foremost I would like to thank my supervisor Martin, for his help and guidance throughout my PhD. I greatly appreciate the skills and knowledge he has passed on to me during my time in his lab, and I'm sure these will help hugely during the course of my scientific career. To the other members of the Koltzenburg lab, both past and present, thank you for everything you have all done to help me on my way. I have learnt so much from your help in the lab to the conversations over many cups of coffee! I gratefully acknowledge Mona, who has been a constant source of good advice over the years. It has been a pleasure to work with all of you during my PhD.

I would like to particularly thank Guillermo and Gipi for helping me to establish the microfluidic chambers in Martin's lab. Thank you for taking your time to answer my questions and showing me the ropes. Your help was pivotal in getting me up and running in the lab!

I am very grateful to Niral and Erik, for their helpful insight into using radioactivity.

To 'the boys', thanks for always being there for beers and darts - the 'Cittie' has become a home away from home! Your enthusiasm for celebrations has made for some very memorable occasions!

To my parents, you are a constant source of love and encouragement and for that I am forever grateful. You have always believed in me and endlessly supported me. You have taught me to work hard and take pride in all I do. I would not be where I am today without the support from both of you.

To my best friend and fiancée Carol, you have always been there for me, to bear the brunt of the frustrations and share in the joy of success. Thank you for your editing help (!), your culinary delights and for always being able to cheer me up and keep a smile on my face. Finally, we can begin to plan our big day!

Finally, I dedicate the work in this thesis to my Grandad, Czes Mitmanski. You were such a warm and friendly person, constantly interested in all I do and always ready to listen over a glass of Rioja! Your stories, smiles and hugs will never be forgotten. I hope I have made you proud.

Contents page

List of tables

Abbreviations

ΔF/F	Delta ratio of 340nm fluorescence/380nm fluorescence
ADP	Adenosine diphosphate
AMH	A-fibre mechano-heat-sensitive nociceptors
ANOVA	Analysis of variance
araC	Cytosine β-D-arabinofuranoside
ASIC	Acid-sensing ion channel
ATF-1	Activating transcription factor -1
ATP	Adenosine triphosphate
BCL-2	B-cell lymphoma-2
BDNF	Brain-derived neurotrophic factor
cAMP	Cyclic adenosine monophosphate
CCI	Chronic constriction injury
CFA	Complete Freund's adjuvant
CGRP	Calcitonin gene-related peptide
CIEP	Congenital inability to experience pain
CMH	C-fibre mechano-heat-sensitive afferents
CM_I	C-fibre mechano-insensitive afferents
CREB	cAMP response element binding protein
CREM	cAMP response element modulator
CTB	Cholera toxin B-subunit
DDSA	Dodecenyl Succinic Anhydride
DiI	1,1'-dioctadecyl-3,3,3',3'-tetramethylindocarbocyanine perchlorate
DiO	3,3'-Dioctadecyloxacarbocyanine perchlorate

DIV	Days *in vitro*
DMP-30	2.4.6-tri (Dimethyl Aminomethyl).
DMSO	Dimethyl sulfoxide
DRASIC	Dorsal root acid-sensing ion channel
DRG	Dorsal root ganglion
E12.5	Embryonic day 12.5 (for example)
EC50	Half-maximal effective concentration
ECF	Extracellular fluid
eRET	Early Ret
Fura-2 AM	Fura-2 acetoxymethyl
G2A	G2 accumulation
GDNF	Glial cell line-derived neurotrophic factor
GPCR	G-protein coupled receptor
GTP	Guanosine triphosphate
HEK	Human embryonic kidney
HEPES	4-(2-Hydroxyethyl)piperazine-1-ethanesulfonic acid
HBSS	Hank's balanced salt solution
HRP	Horseradish peroxidase
K2p	Two pore K^+ channel
^{125}I	^{125}Iodine
IB4	Isolectin B4
IC50	Half-maximal inhibitory concentration
IgG	Immunoglobulin G
L5 DRG	Fifth lumbar dorsal root ganglion (for example)
LTMC	Low-threshold C-fibre mechanoreceptor

LTM	Low-threshold mechanoreceptor
MAP	Mitogen activated protein
MBq	Megabecquerel
MEK	Mitogen-activated protein kinase kinase
MIA	Mechanically insensitive afferents
MNA	Methyl Nadic Anhydride
Mrgpr	Mas-related G protein coupled receptor
mRNA	Messenger ribonucleic acid
mTOR	Mammalian target of rapamycin
Na_v	Voltage-gated sodium channels
NCC	Neural crest cell
NF-AT	Nuclear factor of activated T cells
NGF	Nerve growth factor
NGN1	Neurogenin 1
NGN2	Neurogenin 2
NT-3	Neurotrophin-3
NT-4	Neurotrophin-4
OGR1	Ovarian cancer G-protein coupled receptor 1
P0	Postnatal day 0 (for example)
$p75^{NTR}$	p75 neurotrophin receptor
PBS	Phosphate buffered saline
PDMS	Polydimethylsiloxane
PHA-L	Phaseolus vulgaris leucoagglutinin
PE	Primary erythromelalgia
PEPD	Paroxysmal extreme pain disorder

PGMEA	Propyleneglycolmethylether acetate
PI3-k	Phosphatidylinositide 3-kinase
PKA	Protein kinase A
PKC	Protein kinase C
PLAP	Placental alkaline phosphatise
PLC	Phospholipase C
PLL	Poly-L-lysine
p-Trk	Phosphorylated tropomysin receptor kinase
RA (I or II)	Rapidly adapting (type I or II)
RAR	Retinoic acid receptor
RARE	Rentinoic acid-response element
ROI	Region of interest
RTX	Resiniferatoxin
RXR	Retinoid C receptors
SA (I or II)	Slowly adapting (type I or II)
SEM	Standard error of the mean
siRNA	Small interfering ribonucleic acid
SLP3	Stomatin-like protein 3
SP	Substance P
TASK	TWIK-related acid sensing K^+ channel
TBHP	*tert*-butyl hydroperoxide
TDAG8	T-cell death associated gene 8
TG	Trigeminal ganglion
Tlx3	T-cell leukemia homeobox 3
Trk	Tropomyosin-receptor kinase

TRP	Transient receptor potential
TRPA	Transient receptor potential ankyrin subfamily
TRPC	Transient receptor potential classic subfamily
TRPM	Transient receptor potential melastatin subfamily
TRPML	Transient receptor potential mucolipin subfamily
TRPP	Transient receptor potential polycystin subfamily
TRPV	Transient receptor potential vanilloid subfamily
TTX	Tetrodotoxin
TTX-r	Tetrodotoxin-resistant
TTX-s	Tetrodotoxin-sensitive
TWIK	Tandem of P domains in a weak inwardly rectifying K+ channel
VGCC	Voltage gated calcium channel
VGSC	Voltage gated sodium channel

Chapter 1

Introduction

1.1. Sensory neurons

Thermal, mechanical and chemical stimuli are detected and encoded by a group of specialised primary afferent neurons. The cell bodies of these sensory neurons are located in the dorsal root ganglion (DRG) and trigeminal ganglion (TG) and have both a peripheral and central branch. Sensory neurons are vitally important and are implicated in virtually every task we carry out. The importance of a functioning sensory nervous system becomes particularly evident when it is disrupted. Several genetic mutations in genes encoding proteins preferentially expressed in sensory neurons have been shown to severely impact upon the sensory nervous system. For example, congenital inability to experience pain (CIEP) is a classic loss of sensory function that can be caused by a mutation in SCN9A (Cox et al., 2006), the gene encoding the voltage gated sodium channel subtype 1.7 ($Na_v1.7$). This condition results in the inability to guard oneself against potentially tissue damaging stimuli which can lead to disabling and sometimes life-threatening injuries. Conversely, sensory gain of function mutations such as Inherited Erythromelalgia can result in bursts of excruciating pain that are highly debilitating. Inherited Erythromelalgia is caused by a point mutation (Yang et al., 2004a) or a substitution mutation (Dib-Hajj et al., 2005) in SCN9A. Both mutations result in a gain of function of $Na_v1.7$ by causing a hyperpolarising shift in activation and a slow deactivation (Cummins et al., 2004).

These examples are just some of the many genetic disorders that can affect the somato-sensory nervous system. Whether inherited or acquired, chronic pain has been estimated to affect 46.5 % of the UK population at some point during their lifetime, in a single, self-reported study based on the most commonly used definition of chronic pain, that of the International Association for the Study of Pain (Elliott et al., 1999). The extent of affected individuals makes the study of the sensory nervous system imperative. Advances in this field of research will not only help to understand the progression of diseases affecting the sensory nervous system, perhaps contributing to therapeutic interventions, but will also expand our knowledge of how this intricate system correctly functions in the face of constantly changing stimuli.

1.1.1. Sensory afferent subtypes

DRG sensory neurons have two processes, one projecting into the central nervous system and the other projecting and innervating a peripheral tissue such as skin, viscera, joints or muscle. Sensory neurons can be broadly divided into two categories, depending upon their myelination and cell size characteristics. A-fibres have fast-conducting myelinated axons and larger cell bodies, whilst C-fibres have small cell bodies with slower conducting, unmyelinated axons (Meyer et al., 2006) (Table 1.1). A-fibres can be further divided into subpopulations. Aβ fibres are the largest with thick, heavily myelinated axons, allowing these fibres to conduct rapidly at velocities over 10 m/s in the rodent (Koltzenburg et al., 1997) and predominantly function as mechano- and proprio-receptors (Meyer et al., 2006). The thin, myelinated Aδ fibres conduct at approximately 1 – 10 m/s in the rodent and are activated by both cold and pressure stimuli (Meyer et al., 2006). Many of these are

classified as nociceptors, responding to noxious, potentially tissue damaging stimuli for example mechanical pin-prick. A subpopulation of Aδ fibres constitute the D-hair mechanoreceptors, which are mechano-sensitive afferents that have conduction velocities in the Aδ range (Leem et al., 1993). The small diameter C-fibres are unmyelinated, conducting at velocities less than 1m/s in the rodent (Lawson et al., 1993) and less than 2 m/s in the human (Serra et al., 1999). These comprise the majority of DRG sensory neurons and are principally nociceptors, responding to noxious thermal, chemical and mechanical stimuli (Meyer et al., 2006).

	Aβ-fibres	**Aδ-fibres**	**C-fibres**
Cell body size	> 50 µm diameter	25-50 µm diameter	< 25 µm diameter
Myelination	Heavily myelinated	Thinly myelinated	Unmyelinated
Conduction velocity	> 10 m/s	1-10 m/s	< 1 m/s
Stimulus modalities	Low-threshold mechanical Proprioception	Low and high-threshold mechanical Chemical Thermal	Low and high-threshold mechanical Chemical Thermal
Neurotrophic dependence for survival	BDNF NT-3	NGF NT-4	NGF NT-3 GDNF
Cellular markers	Parvalbumin Neurofilament GM1 ganglioside (receptor for CTB)	Neurofilament GM1 ganglioside	Peripherin CGRP, Substance P (peptidergic C-fibres) IB4 (nonpeptidergic C-fibres)

Table 1.1.1
A summary of the primary afferent characteristics in mouse DRG neurons. Sensory fibres can be differentiated by histological, electrophysiological and functional properties.

Nociception is an essential process for all higher organisms. Nociceptors ordinarily have high thresholds, and are excited by noxious stimulus intensities. In the skin there are two major categories of nociceptors, the unmyelinated, small diameter C-fibres and the medium diameter, thinly myelinated Aδ fibres. Due to their myelination, and therefore faster nerve conduction, the latter are responsible for the 'first pain', that is the sharp, prickling pain experienced after a noxious stimulus. C-fibres conduct slower, and are responsible for the longer lasting, burning 'second pain'

(Price et al., 1977). A-fibre nociceptors respond with higher discharge frequencies and provide greater discriminatory information than C-fibres (Slugg et al., 2000). These A-fibre nociceptors can be divided into two classes according to their individual characteristics (Treede et al., 1998). Type I are polymodal in their activation profile as they respond to heat, mechanical and chemical stimuli, and are therefore referred to as AMH-type I (A-fibre mechano-heat-sensitive nociceptors) (Table 1.1.2). Thermal stimuli activate AMHs but only at temperatures greater than 50 ˚C; although this threshold can reduce by 10 ˚C if the heat stimulus is prolonged for 30 seconds (Treede et al., 1998). The mean conduction velocities of type I nociceptors in monkey is between that of Aδ and Aβ fibres at 25 m/s (Treede et al., 1998).

Type II Aδ nociceptors are considerably more sensitive to heat, but have a very high mechanical threshold compared to type I, and are therefore known as mechanically insensitive afferents (MIAs). Type II fibres are commonly found in hairy skin and are not present in the glabrous skin of the hand. The conduction velocity of type II fibres at 15 m/s is slower than that of type I fibres and heat responses differ between the two populations (Treede et al., 1995). Type I display a gradual increasing response to heat and sensitize after burn injury implicating them in the development of hyperalgesia. Type II fibres resemble C-fibre mechano-heat-sensitive afferents (CMHs) which have an early peak frequency and a slowly adapting response to heat (Treede et al., 1995). First pain sensation from heat stimuli applied to the glabrous skin of the human hand is absent, correlating with the lack of type II fibres in this location (Meyer et al., 2006).

C-fibre nociceptors can similarly be divided by their activation properties. CMH fibres are a common cutaneous afferent that are considered polymodal due to their activation by mechanical, thermal and chemical stimuli (Meyer et al., 2006) (Table 1.1.2). CMH firing rate typically increases in response to an increasing heat stimulus, within the detected temperature range. The temperature range detected by CMHs has proven difficult to study due to the large differences in the skin depth of the terminals. However, if this is taken into consideration, the heat threshold of the majority of CMHs is between 39-41˚C – an extraordinarily narrow range (Tillman et al., 1995). Another main feature of CMHs is that their response can be strongly modified by previous activity. For example, an identical heat stimulus separated by an interval of one minute can result in a fatigued response of 40% less than the first response (Peng et al., 2003). Enhanced responses can occur in sensitised hairy skin CMHs as a result of burn injury, which appears to contribute to heat hyperalgesia; however, CMHs that innervate the glabrous skin do not sensitise after burn (Campbell and Meyer, 1983), indicating that sensitisation is not a uniform property of nociceptors. C-fibre mechano-insensitive afferents (CM_I) are a heterogeneous population that differ in their responses to chemical and heat stimuli (Table 1.1.2). Many CM_I fibres respond to capsaicin and the itch mediator – histamine (Schmelz et al., 1997), suggesting pronounced chemosensitivity. Some CM_I fibres do not respond to heat stimuli and have therefore been regarded as ‘silent’ nociceptors, these have been shown to be recruited in sensitised states leading to spatial summation, which in turn contributes to primary heat and mechanical hyperalgesia following chemical irritants applied to the skin (Schmidt et al., 1995).

Location	Axon	Receptor	Sensation
Skin	Aβ	RA I – Meissner's corpuscle	Slippage, flutter vibration
		RA II Pacinian corpuscle	Vibration
		SA I – Merkel cell	Pressure, surface texture
		SA II – Ruffini corpuscle	Skin stretch
		G-Hair	Hair movement
	Aδ	AMH I – free nerve endings	Pain
		AMH II – free nerve endings	Pain
		D-Hair	Hair movement
	C	CMH – free nerve endings	Pain
		CM_I – free nerve endings	Pain, itch
		LTMC – free nerve endings	Pleasant touch
Muscle	Ia	Primary muscle spindle afferents	Proprioception
	Ib	Golgi tendon organ	Proprioception
	II	Secondary muscle spindle afferents	Proprioception
	III	Free nerve endings	Pain, pressure
	IV	Free nerve endings	Pain, pressure
Joint	II	?	Pain, pressure
	III	Free nerve endings	Pain, pressure
	IV	Free nerve endings	Pain, pressure
Viscera	Aδ	Free nerve endings	Pain/pressure/reflex control
	C	Free nerve endings	Pain/pressure/reflex control

Table 1.1.2
Table displaying the axon nomenclature for sensory neurons, the receptor organ and the sensation elicited by its excitation.

Itch and pain are clearly two very different sensations; however, there remains a long standing question whether these share a common neuronal pathway. Itch has been defined as an 'unpleasant skin sensation that elicits the desire or reflex to scratch' (Ikoma et al., 2006), therefore in terms of behaviour, itch is far removed from acute pain which induces a rapid withdrawal reflex. The best characterised mediator of itch is histamine, which is secreted by skin mast cells and acts on histamine receptors, predominantly exciting CM_I sensory fibres (Alving et al., 1991). However, there are histamine independent mechanisms of itch, including that induced by cowhage, the spicules covering the pod of the tropical legume *Macuna pruriens* (Shelley and Arthur, 1955; Johanek et al., 2008) and that induced by the anti-malaria drug, Chloroquine (Davidson and Giesler, 2010). The latter has been suggested to act largely through the human MrgprX1 (Mas-related G protein coupled receptor member X1) expressed by primary sensory neurons (Liu et al., 2009). The expression of *Mrgprs* is restricted to primary sensory neurons and their function has been linked to distinct roles in somatosensation (Bandell and Patapoutian, 2009).

A population of low-threshold C-fibre mechanoreceptors (LTMC) that are insensitive to heat have been described in several species, including cat (Bessou and Perl, 1969) and human (Nordin, 1990). These afferents are strongly activated by slowly moving innocuous mechanical stimuli within their receptive field (Table 1.1.2). Interestingly, supraspinal areas associated with touch perception such as the somatosensory cortex were not activated by the activation of these fibres, instead the insula was activated which is associated with affiliative behaviour, these fibres may therefore mediate the sensation of pleasant touch (Olausson et al., 2002).

1.1.2. DRG neurogenesis

DRG neurons can be divided according to the modality they detect. Each functional subtype expresses a unique composition of ion channels and receptors allowing it to respond to a specific set of stimuli. The development of the individual molecular characteristics is based on specific gene programmes which run in each neuronal subpopulation (Marmigère and Ernfors, 2007). The transcription and translation of genes encoding proteins in sensory neurons is initiated by crucial signalling factors which turn on at specific embryonic time points, and are highly dependent on which neurogenesis 'wave' the neuron is born in (Lewin and Barde, 1996). The first wave of sensory neuron neurogenesis is initiated by expression of the transcription factor – neurogenin-2 and begins from the early migrating neural crest cells (NCC) which begin to coalesce and form the early DRG. In chick these have been shown to have limited cell division, with each multipotent NCC producing approximately 3 neurons on average (Frank and Sanes, 1991). Neurons born in the first wave predominantly differentiate into the large-diameter mechanoreceptive and proprioceptive neurons, accounting for approximately 4 % of the total DRG population (Frank and Sanes, 1991). The second, neurogenin-1 mediated wave gives rise to approximately 91 % of all DRG neurons, as these cells have a much higher division rate (approximately 36 neurons per NCC) and are also able to differentiate into all DRG subtypes (Frank and Sanes, 1991). The remaining 5% are born in the third neurogenesis wave and differentiate from boundary cap cells – a neural crest derived group of cells,

located at the neuronal entry point of the dorsal horn (Hjerling-Leffler et al., 2005). These generate TrkA positive neurons, which are mainly small diameter, nociceptive neurons (Maro et al., 2004).

1.1.3. Neurotrophin dependence and role of the Runx transcription factors

During embryonic development, DRG neurons depend on neurotrophic factors for survival. Neurotrophic factors bind to tropomyosin-receptor kinase (Trk) receptors which are members of the receptor tyrosine kinase family (Figure 1.1.1). Different DRG subpopulations can be identified by the expression of Trk proteins (Ernfors, 2001). The first neurogenesis wave gives rise to mechano- and proprio-ceptive neurons which have been identified to express the neurotrophin receptors TrkB and TrkC (Rifkin et al., 2000) (Green column, Figure 1.1.2). TrkB preferentially binds brain-derived neurotrophic factor (BDNF) and neurotrophin-4 (NT4), whilst TrkC binds neurotrophin-3 (NT3) with a high affinity (Figure 1.1.1) and NGF to a lesser degree. Very early in development TrkB and TrkC is highly coexpressed, however the incidence of coexpression drops from approximately 75 % at E11.5 to only 10 % at E12.5 in the mouse (Kramer et al., 2006). The erosion of TrkB in these initially coexpressing neurons is controlled by expression of a runt-related transcription factor – Runx3, which promotes a selective TrkC phenotype and the consequent development into a proprioceptive neuron. On the other hand, the exclusion of Runx3 is crucial to allow TrkB expression and the subsequent consolidation into cutaneous mechanoreceptors (Kramer et al., 2006).

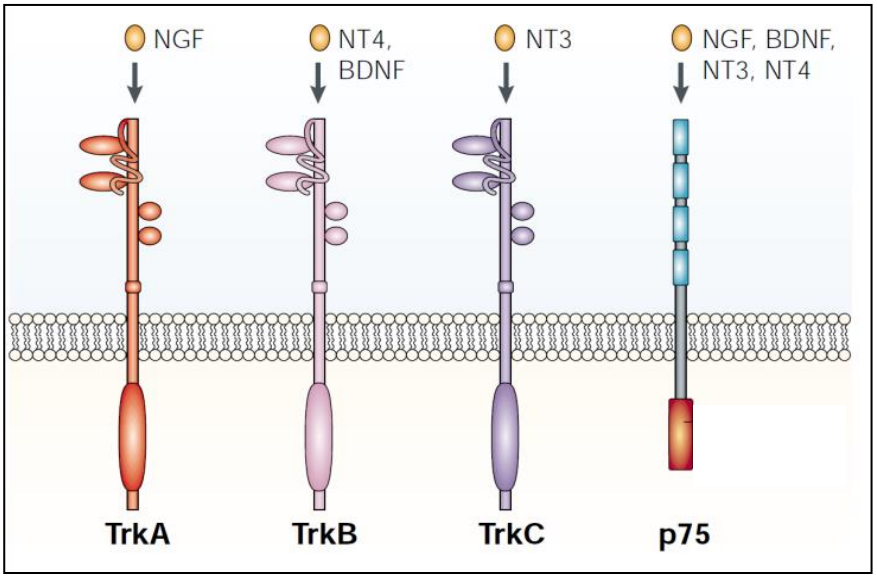

Figure 1.1.1
Neurotrophins and their receptors. Neurotrophins bind to selective Trk receptors, whereas all neurotrophins bind to the low affinity p75 neurotrophin receptor. The extracellular portion of Trk receptors consists of an immunoglobulin G (IgG) domain for ligand binding, whereas the intracellular portion contains a tyrosine kinase sequence for initiating cellular cascades. Adapted from Chao, 2003.

In addition to the Trk receptors, the glial cell line-derived neurotrophic factor (GDNF) receptor – Ret, is also expressed at early developmental ages. This early Ret (eRet) population is first detected between E11.5 and E12, and predominantly express TrkB early in development (brown column,

Figure 1.1.2). However this is downregulated in many neurons as the onset of TrkC expression begins (Kramer et al., 2006). The eRet lineage diversifies into neurons with a mechanosensory function. In the adult these are large diameter, neurofilament 200 positive, which can innervate Meissner and Pacinian corpuscles that participate in touch sensation (Luo et al., 2009).

The nerve growth factor (NGF) receptor – TrkA, is first detected at E11.5 (grey, red and orange column, Figure 1.1.2) and is expressed in approximately 80% of all DRG neurons at E15 in the mouse (Molliver et al., 1997), these give rise to the small and medium diameter DRG populations (Pezet and McMahon, 2006). The second of the runt-related transcription factors to be characterised – Runx1, is initially expressed in most of these TrkA expressing cells, and in all prospective nociceptors. However, at E16, under the control of Runx1, approximately half of the TrkA expressing neurons start to express the GDNF receptor, Ret (Molliver and Snider, 1997; Luo et al., 2007) and downregulate TrkA. The extinguishment of TrkA in these neurons begins at postnatal day (P) 1, and continues until P21. In adulthood, these Ret expressing nociceptors are largely non-peptidergic and can be identified by the binding of isolectin B4 (IB4) from *Griffonia simplicifolia* and project to lamina II inner of the dorsal horn (Molliver et al., 1997) (orange column, Figure 1.1.2). Conversely, the other 50 % preserve TrkA expression and switch off Runx1, and remain TrkA positive into adulthood. These are characterised by their ability to release neuropeptides including calcitonin gene-related peptide (CGRP) and substance P (SP) and project to lamina I and lamina II outer (Golden et al., 2010) (red column, Figure 1.1.2).

The persistent expression of Runx1 delineates the population of nociceptors that undergo the developmental TrkA to Ret transition. In mice, the conditional knockout of Runx1 in the peripheral nervous system impairs this transition, with a dramatic favouring of the TrkA positive neurons (Chen et al., 2006). Furthermore, the expression of many nociceptive ion channels and receptors are negatively affected in the conditional Runx1 knock out. For example, the transient receptor potential (TRP) channels are highly affected by Runx1 knockout. The menthol receptor, TRP melastatin-8 (TRPM8), and the mustard oil receptor TRP ankyrin-1 (TRPA1) are entirely absent, and high expression of the capsaicin receptor TRP vanilloid-1 (TRPV1) is also absent in the L5 DRG. The ATP-gated channel P2X3, and the tetrodotoxin-resistant (TTX-r) Na^+ channel, $Na_v1.9$ are also both markedly reduced. Behaviourally, these mice exhibit profound defects in noxious heat detection, and do not develop mechanical allodynia after induction of neuropathic injury (Chen et al., 2006). Runx1 is therefore a major determinant of the molecular and physiological characteristics of Ret^+ nociceptors.

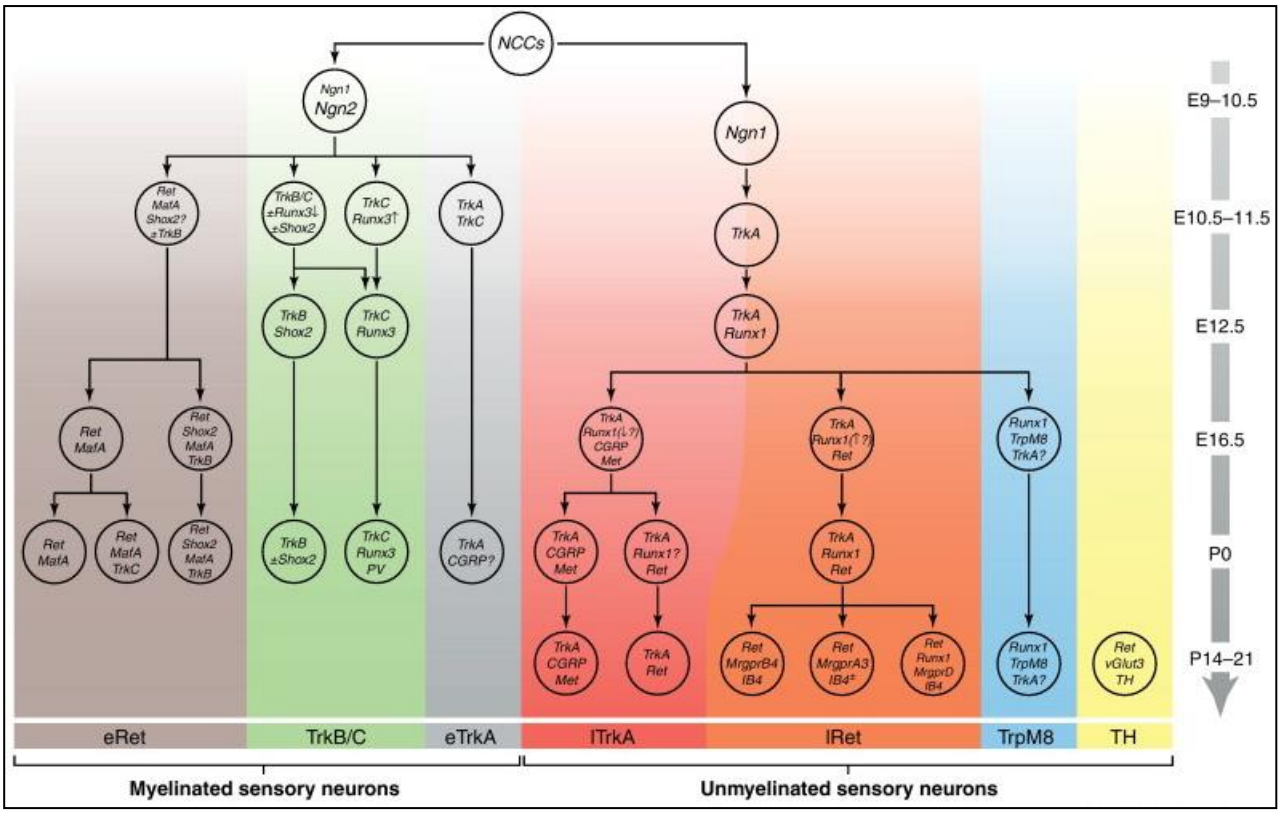

Figure 1.1.2
DRG neuron diversification during mouse development. Neurons originate from neural crest cells (NCCs). The development of myelinated neurons is initiated by neurogenin-2, whereas the unmyelinated neurons depend on neurogenin-1. Myelinated neurons consist of the eRet and TrkB/C lineages which develop to have a mechanosensory role, and the early TrkA lineage, which develop into the lightly myelinated neurons, with conduction velocities in the Aδ range. Unmyelinated neurons can also be developmentally divided. The late TrkA population predominantly form the peptidergic nociceptors and can be identified by the expression of CGRP, whilst the late Ret population largely differentiate into the non-peptidergic nociceptors, and can be identified by IB4 binding. Finally the TRPM8^{+} population which are activated by cooling and cooling compounds are neither peptidergic or IB4^{+} and probably arise from Runx1^{+}/TrkA^{+} progenitors. (Adapted from *Lallemend and Ernfors, 2012).*

1.1.4. The role of the low affinity p75 neurotrophin receptor

In addition to the Trk receptors, neurotrophins are also capable of binding to the p75 neurotrophin receptor (p75^{NTR}). These receptors share no sequence homology to the Trks in terms of cytoplasmic domains and ligand binding. The p75^{NTR} is commonly referred to as low affinity neurotrophin receptor, as although it is capable of binding to NGF, BDNF, NT3 and NT4 it does so with lower affinity than the respective Trks. Within the developing sensory nervous system, p75^{NTR} mRNA has been detected at very early stages, for example, migrating neural crest cells and all cells of the nascent DRG at E4 – E4.5 in the chick are p75^{NTR} positive (Rifkin et al., 2000). Null mutation of p75^{NTR} by targeting exon IV of the *p75^{NTR}* locus in the mouse resulted in a profound phenotype which included an abnormal waddling gait, reduced diameter of the sciatic nerve, a reduction in Schwann cells number during development and over a 50 % decrease in the number of sensory neurons in the

L5 DRG (von Schack et al., 2001). This knockout mouse provides compelling evidence that $p75^{NTR}$ is required for the normal development of sensory neurons.

Whilst Trk receptors and $p75^{NTR}$ are independently activated by neurotrophins, they have also been shown to interact, producing high affinity binding sites and enhancing NGF mediated TrkA activation (Barker and Shooter, 1994). In support of this, Trk activation in the presence of $p75^{NTR}$ has been shown to be enhanced in response to low neurotrophin concentrations (Verdi et al., 1994), this is especially critical during development when neurons must bind neurotrophins released from target tissues in the sub-picomolar range (Barde, 1989). Trk receptor function is positively modulated in several ways by $p75^{NTR}$, as discussed, ligand binding is enhanced, but the presence of $p75^{NTR}$ also increases Trks accessibility to neurotrophins, ultimately promoting axonal growth and target innervation.

Independent of the complex formation with Trks, $p75^{NTR}$ can be activated alone by neurotrophin binding. In stark contrast to the pro-survival signals facilitating through Trk/$p75^{NTR}$ complex signalling, the activation of $p75^{NTR}$ alone has a well-known function in promoting cell death (Hempstead, 2002), which may be a means of refining the neuronal population and establishing correct target innervation. Interestingly, pro-neurotrophins, the precursors of mature neurotrophins, display a far greater binding selectivity for $p75^{NTR}$ than the Trk receptors, and are considerably more effective at initiating $p75^{NTR}$ dependent apoptosis. It has been shown that pro-NGF creates a signalling complex by binding to both $p75^{NTR}$ and sortilin, a protein expressed in a variety of tissues, and this complex constitutes a molecular switch mediating the pro-apoptotic signals of pro-NGF (Nykjaer et al., 2004).

In conclusion, neurotrophin mediating signalling promotes both survival and death, which depends upon the relative abundance of the pro-neurotrophin and the mature form. Furthermore, functional interactions between $p75^{NTR}$ and Trk receptors also influence the direction of signalling.

1.2. Sensory transduction

Primary afferents neurons are highly effective at conveying sensory stimuli to the central nervous system. This process involves several key processes. Firstly, the stimulus is transduced into an electrically encoded action potential, which upon cutaneous stimulation occurs in the very distal regions of the neuron terminating in the skin (Figure 1.2.1). Secondly, the action potential is rapidly propagated from the peripheral receptor to the dorsal horn of the spinal cord (Figure 1.2.1). Thirdly, synaptic transmission of the encoded response from the sensory neuron to a spinal projecting or interneuron then takes place; this is the process whereby mainly glutamatergic synaptic transmission from the peripheral primary afferent to the CNS neuron occurs (Figure 1.2.1).

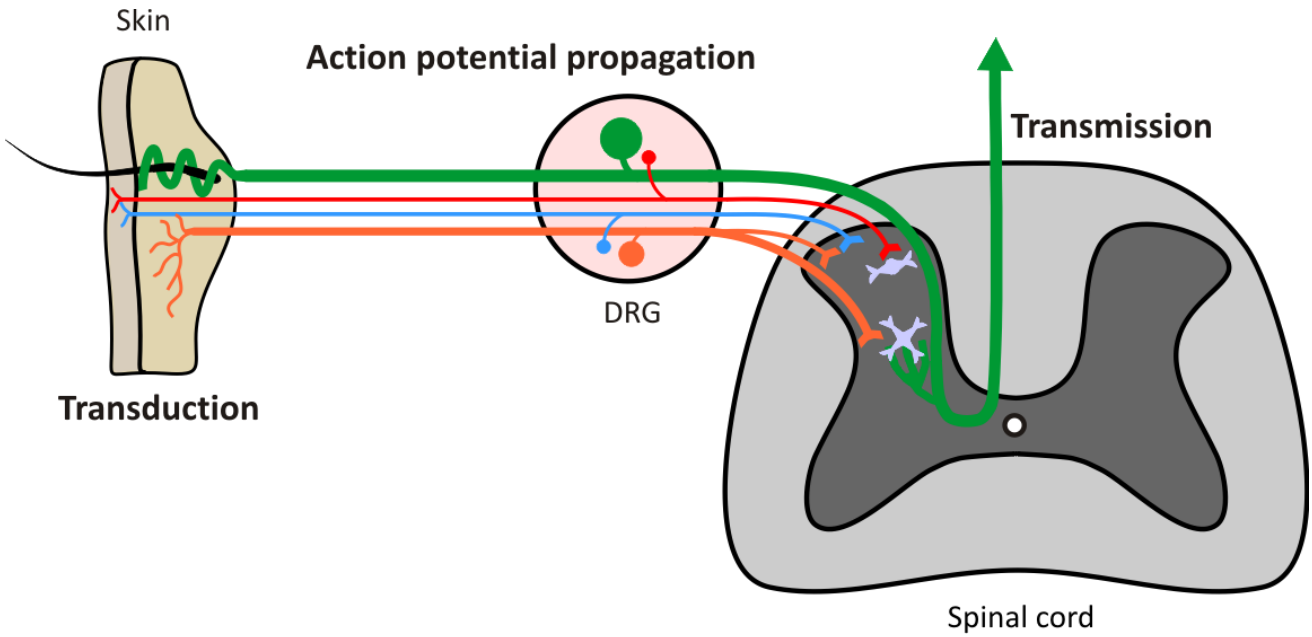

Figure 1.2.1
Central and peripheral terminations of the major process involved in somatosensory sensation. Transduction encodes the peripheral stimulus into an electrical signal. The action potential is then propagated from the periphery into the dorsal horn of the spinal cord along the primary afferent axon. Synaptic transmission in the spinal cord or brain stem allows the central nervous system to process the peripheral stimulus. Four types of afferent fibre are depicted, the thickly myelinated mechanoceptor illustrated in green with a specialised end organ. An unmyelinated peptidergic nociceptor illustrated in blue with central processes terminating in lamina I and lamina II outer of the dorsal horn and free nerve endings terminating in the epidermis. An unmyelinated nonpeptidergic nociceptor in red with central processes terminating in lamina II inner of the dorsal horn, and free nerve endings terminating in the superficial epidermal layer. Finally, an Aδ fibre is illustrated in orange, with central terminals in superficial lamina I and in deep lamina V, and peripheral extensions terminating in the dermal layer of the skin.

Sensory neurons have a distinct embryonic development that results in a large diversity, with each subpopulation finely tuned to detect distinct sensory modalities. Each subpopulation expresses a unique combination of ion channels and receptor proteins, which are under the control of crucial transcription factors, several of which have been discussed. The molecular characteristics

of each neuron dictate the phenotype and therefore the sensitivity to each stimulus. Runx1 dependant neurons are capable of transducing multiple sensory modalities and develop into nociceptors, thermoceptors and the itch sensing, pruriceptors by adulthood (Lopes et al., 2012). Many of these neurons, born originally from the TrkA lineage express TRP channels. TRP channels have a restricted pattern of expression amongst sensory neuron subpopulations, for example the capsaicin receptor – TRPV1, is used as a characteristic marker of polymodal nociceptors (Caterina et al., 2000).

1.2.1. TRP channel architecture and activation properties

In mammals, six families comprise the TRP superfamily; the classic TRPs (TRPCs), the vanilloid receptor TRPs (TRPVs), the malastatin TRPs (TRPMs), the mucolipins (TRPMLs), the polycystins (TRPPs) and the ankyrin-like with transmembrane domain 1 (TRPAs). The primary TRP channel structure consists of four subunits each with six transmembrane helices (S1 – S6), with a pore domain between the fifth and sixth segment. All of the TRP channels are permeable to cations, and are predominantly selective for sodium and calcium ions, TRPs therefore play important roles in generating depolarisation in excitable cells (Clapham et al., 2005). A selectivity filter, formed by the extracellular-facing pore loop select cations for permeation, which are then held in place by the S5 and S6 α-helices. Both the amino- and carboxy-terminals are located intracellularly, with the amino-terminal believed to have an important role in anchoring the protein to the plasma membrane and contain sites for protein-protein interactions. The carboxyl-terminal of the S6 helix form the lower gate which is able to swing into open and closed conformations to regulate cation entry (Clapham, 2003).

TRP channels are a diverse super-family of ion channels, consequently, their activation properties are equally as varied. The thermoreceptive properties of TRP channels have been extensively researched, and a wide temperature range has been demonstrated to be detected by several TRP channels. In order to detect temperature, it has been suggested these channels possess a temperature sensing domain, which would undergo large conformational changes in the structure upon an increase in temperature. TRP activation by cold temperatures is attributed to weakening of hydrophobic interactions resulting in denaturation and loss of tertiary and quaternary interactions (Latorre et al., 2007). Temperature activation of TRP channels therefore results in structural rearrangements of temperature sensitive domains, which can affect the pore and gating region of the protein influencing the probability of cation entry.

1.2.2. TRP channel chemo- and thermoreception

With respect to thermosensation, Caterina and colleagues made a seminal discovery in 1997, by cloning the capsaicin receptor, and demonstrating that human embryonic kidney (HEK) cells expressing TRPV1 exhibited an increase in intracellular calcium in response to a 45˚C heat stimulus (Figure 1.2.2) (Caterina et al., 1997). In human psychophysical experiments, capsaicin injection produces profound burning pain and molecular identification of TRPV1 confirmed this pain

is due to the depolarisation of specific C and Aδ nociceptors, on which capsaicin receptors are expressed. Mice lacking TRPV1 exhibit a complete insensitivity to capsaicin *in vivo*, demonstrating the specificity of capsaicin for TRPV1 (Caterina et al., 2000; Davis et al., 2000). TRPV1 is expressed on the majority of heat-sensitive nociceptors, which typically exhibit an activation temperature of approximately 43˚C – correlating with the temperature at which humans usually regard as painful (Figure 1.2.2). Heat evokes an inward current through TRPV1 when heterologously expressed (Caterina et al., 1997), in addition, cultured DRG neurons from TRPV1 knockout mice exhibited an absent or significantly reduced heat current further implicating TRPV1 as an important thermoreceptor (Caterina et al., 2000; Davis et al., 2000).

To further investigate the role of TRPV1 expressing afferents in a selective manner, the central terminals of TRPV1 positive C-fibres can be destroyed with an intrathecal injection of capsaicin (Cavanaugh et al., 2009). Behavioural testing with a 55˚C heat plate revealed that these mice had a complete insensitivity to acute noxious heat indicating that the TRPV1 expressing afferents mediate the entire response to the heat stimulus. Interestingly, behavioural analysis of mice with global TRPV1 knockout demonstrated no change in thermal sensitivity when assessed with the hotplate test (Davis et al., 2000). Furthermore, another group demonstrated a reduced heat sensitivity but only at temperatures well above the thermal activation threshold for TRPV1 (Caterina et al., 2000). The behavioural heat pain phenotype of the global TRPV1 knockout mouse therefore contrasts with that in which the TRPV1 positive, central terminals have been destroyed. Together, these studies suggest the existence of an additional heat transduction mechanism that acts through TRPV1 positive primary afferents.

The important discovery of the thermoreceptive properties of TRPV1 paved the way for the identification of several more temperature activated TRP channels. Other TRPV subtypes have been suggested as potential heat transducers which may account for TRPV1 independent thermoreceptors. TRPV2 has been shown to be have an activation threshold of approximately 52˚C when expressed *in vitro* (Figure 1.2.2) (Caterina et al., 1999), furthermore TRPV2 has also been shown to be present on Aδ fibres that respond to high threshold noxious heat (Leffler et al., 2007). In accordance, many TRPV2 expressing rat DRG neurons were shown to be positive for neurofilament heavy-chain (Lewinter et al., 2004), a marker generally associated with myelinated axons. Type I AMHs have a thermal threshold of approximately 53˚C (Treede et al., 1995), suggesting that TRPV2 expression may account for the high thermal threshold of type I AMHs; high temperatures such as these are potentially very damaging, therefore expression of TRPV2 on the faster conducting myelinated fibres rather than the slower conducting C-fibres seems practical. The remaining presence of a neuronal population that could be excited with noxious temperatures (> 55˚C) in *Trpv1* (-/-) *in vitro* DRG neurons (Caterina et al., 2000), suggests these neurons express a TRPV1 independent, noxious heat detector. However, recordings from the skin nerve preparation suggest that *in vitro* heat sensitivity is normal in *Trpv2* (-/-) mice compared to wildtype animals (Park

et al., 2011). Furthermore, a population of heat sensitive nociceptors have been detected that lack both TRPV1 and TRPV2 expression, suggesting an alternative mechanism (Woodbury et al., 2004).

TRPM3 has recently been demonstrated to be expressed in DRG neurons, and chemical activation of this channel with pregnenolone sulphate results in strong nocifensive responses in mice (Vriens et al., 2011). HEK cells transiently expressing TRPM3 were insensitive to capsaicin but strongly activated by a 40˚C heat stimulus. Furthermore, *Trpm3* knockout animals exhibited a significantly longer reaction time to temperatures between 52˚C and 58˚C on the hot plate test, but were indistinguishable from controls when tested for noxious mechanical thresholds. This study suggests TRPM3 could account for a noxious thermal, TRPV1-independent transduction mechanism.

The detection of warm, innocuous temperatures is also important to the survival of an organism. Warm sensitive fibres have been shown to fire continuous low rate action potentials at a skin temperature of approximately 34˚C, with firing frequency increasing with a rise in temperature. (Hensel, 1981). Cutaneous, warm receptors can be divided into two populations according to their maximum average response at certain temperatures (Tominaga and Caterina, 2004), these temperatures correspond to the activation properties of two other TRPV channels. TRPV3 is first activated by temperatures in the range of 34-38˚C, and continues to be activated into the noxious range (Smith et al., 2002). TRPV4 begins to be activated by slightly cooler temperatures, in the region of 27-34˚C (Figure 1.2.2), with the amplitude of heat evoked responses from TRPV4 quickly diminishing over 42˚C (Guler et al., 2002). Further to their expression in sensory neurons, TRPV3 (Peier et al., 2002b) and TRPV4 (Guler et al., 2002) have also both been shown to be expressed in keratinocytes. The role of keratinocytes in inflammation has been widely studied, however it is unknown whether they have a direct role in thermosensation. Keratinocytes are closely linked with the free nerve endings of sensory neurons, therefore TRP channel expression in these cells suggests that they may indeed play some role in the sensing of temperature.

In regard to cold thermal detection, two cold thermo-transducers have been proposed, and in the same way that TRPV1 is capsaicin sensitive, natural cooling agents have been exploited as probes for these channels. A member of the melastatin subfamily - TRPM8, is a cold and menthol sensitive channel, and has been shown to be expressed in approximately 10% of small diameter sensory neurons (McKemy et al., 2002). *In* vitro TRPM8 expression studies have revealed an activation temperature of approximately 25-28˚C (Figure 1.2.2), which corresponds to the activation temperatures of innocuous, cold sensitive fibres in the skin (Patapoutian et al., 2003). The second proposed thermo-transducer is a member of the ankyrin subfamily – TRPA1, is activated by isothiocyanate compounds including mustard oil, and in heterologous expression systems has been shown to be activated by noxious cold temperatures (<15˚C) (Figure 1.2.2) (Story et al., 2003), although this has also been disputed (Jordt et al., 2003). TRPA1 knockout animals have added to the controversy, by providing contradictory evidence both for (Kwan et al., 2006; Karashima et al., 2009) and against (Bautista et al., 2006) the role of TRPA1 in cold transduction. Behavioural analysis in

mice with destruction of TRPA1 central terminals by capsaicin (TRPA1 and TRPV1 are expressed in largely overlapping populations (Figure 1.2.2)) do not display any changes to cool and noxious cold stimuli compared to controls (Cavanaugh et al., 2009). Therefore this suggests that TRPA1 expressing fibres are not essential for the transduction of acute noxious cold stimuli, but may serve a sensitising role to cold stimuli after tissue injury (Basbaum et al., 2009).

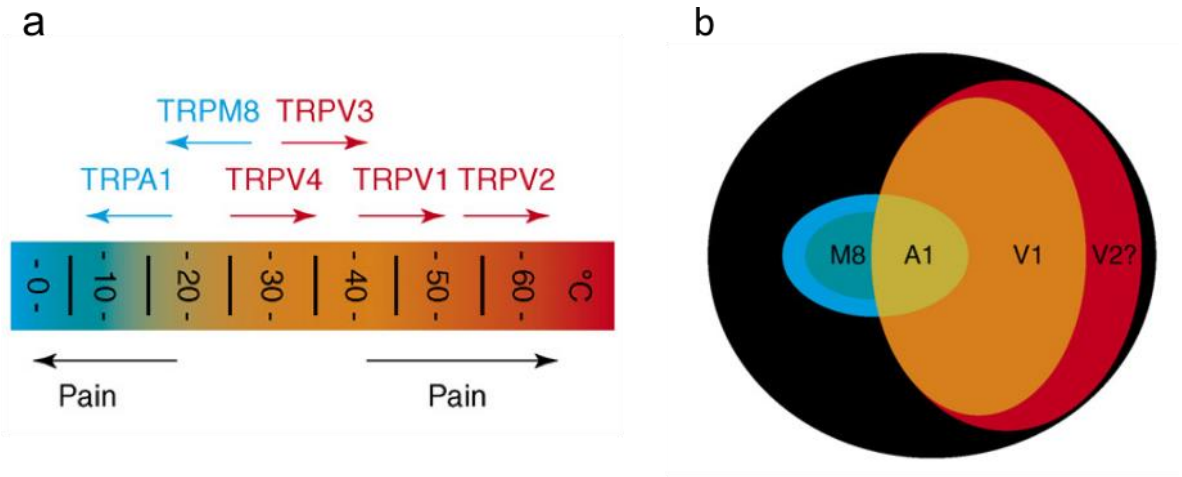

Figure 1.2.2
TRP channels play a major role in thermosensation. (a) Diagram illustrating the range of temperatures that are suggested to activate certain TRP channels involved in thermoreception. The roles of TRPA1 and TRPV2 as temperature sensors in vivo are disputed, although both display robust activation at the illustrated temperatures in heterologous expression systems. (b) Composition of sensory neurons based on their thermal and chemical activation properties. Warm and hot sensitive neurons include the capsaicin sensitive (TRPV1 expressing – orange) population and potentially a small subpopulation that express TRPV2 and are capsaicin insensitive (red). The cold sensitive population is suggested to contain 3 populations - the menthol sensitive, TRPM8 expressing cells (blue), the menthol and mustard oil sensitive cells, expressing both TRPM8 and TRPA1, and the TRPA1-positive neurons that are also capsaicin sensitive. Adapted from Talavera et al., 2008.

1.2.3. Embryonic emergence of TRP channel expression

Sensory neurons are born at approximately E11-E12, when they exit the cell cycle and no longer undergo cellular division. At this time point, neural crest cells are committed to the sensory lineage, and also express voltage-gated calcium channels, which are present in DRG neurons, but not in non-neuronal cells (Hjerling-Leffler et al., 2007). At E12.5 the very first capsaicin sensitive, and therefore TRPV1 expressing cells are detected. Functional evaluations revealed that just 2 days later, the proportion of capsaicin sensitive cells dramatically increases to 64% of the total population at E14.5 in the mouse (Hjerling-Leffler et al., 2007). Lineage studies have demonstrated that prospective mechanoreceptive and nociceptive neurons can be differentiated as early as E10-E12 in the mouse based on transcription factor expression such as neurogenin and Runx. With the first detectable TRP channel expression at E12.5-E13.5 there is therefore a delay of approximately 1 day from the birth of the neuron to expression of functional TRP receptors.

Other TRP channels commonly studied in sensory physiology include TRPM8 and TRPA1. Similar to TRPV1 these are also robustly activated by chemical agonists, with menthol and

cinnamaldehyde/mustard oil commonly used in functional studies of TRPM8 and TRPA1 expression, respectively. Expression of these two TRP channels begins later than TRPV1. Functional and mRNA detection of TRPM8 begins at E16.5, and steadily increases to adult expression levels of 5 % by postnatal day 0 (P0). Functional TRPA1 expression begins even later, with the first cinnamaldehyde induced responses not detected until P0 and the first consistent responses appearing at P7. A large overlap of menthol and capsaicin responses were detected during early development, whereas this started to decrease at E18.5 to reach approximately 50 % overlap in the adult (Hjerling-Leffler et al., 2007). This is likely to be due to the loss of capsaicin sensitivity in a subpopulation of menthol sensitive neurons, rather than the selective death of some TRPV1 expressing neurons and an induction of TRPM8 expression in another subset. In support of this, menthol sensitive neurons are severely reduced in mice neonatally treated with systemic capsaicin, which kills all TRPV1 expressing neurons (Holzer, 1991). Similarly, mustard oil responses in the systemic capsaicin treated mice are abolished, indicating that most of the TRPM8 and TRPA1 expressing neurons are ultimately derived from an embryonically TRPV1 positive population (Holzer, 1991).

1.2.4. Detection of protons

Tissue acidification is commonly found in inflamed tissues and a variety of other pathologies. The local acidosis is thought to be a major contributing factor in the generation of pain and hyperalgesia associated with inflammation (Reeh and Steen, 1996). Therefore, acidic conditions have a direct effect on sensory neurons, with low pH solutions evoking a prolonged activation of sensory neurons. Psychophysical experiments have confirmed the algogenic effect of protons, by demonstrating cutaneous injection of acid at pH 5 results in sustained, stinging pain in humans (Lindahl, 1961). It has been known for several decades that nociceptors are excited by protons through the activation of cation channels (Krishtal and Pidoplichko, 1981), sensory neurons have also been demonstrated to be activated by H^+ -ions in dissociated cultures (Bevan and Yeats, 1991). In response to acid stimulation, DRG neurons usually respond with either a transient, rapidly inactivating current or a sustained current (Bevan and Yeats, 1991; Leffler et al., 2006), leading to the suggestion that there appears to be more than one molecular mechanism for proton transduction.

One of the main candidate mechanisms for proton transduction is activation of the capsaicin receptor, TRPV1. Initial interest into the role of TRPV1 in acid-sensing began when Bevan and Yeats, 1991, demonstrated proton sensitive cells were also activated by capsaicin. In agreement, capsaicin induced activation was significantly potentiated by pH 5.5, illustrating an interaction between TRPV1 and protons (Caterina et al., 1997). A few years later, the same group generated the TRPV1 knockout mouse and demonstrated that proton evoked responses were almost entirely abolished with only 1 % of all DRG neurons responsive to acid *in vitro* (Caterina et al., 2000). Subsequent studies using *Trpv1* (-/-) mice have demonstrated a significant reduction of proton induced current in unmyelinated fibres detected by using an *in vitro* skin-nerve preparation (Leffler et al., 2006), this reduction suggests TRPV1 is required to mediate proton induced excitation in C-

fibres. However, in the same study proton responses were unaffected among the thin myelinated nociceptive population indicating the presence of a TRPV1-independent proton detector in these afferents.

Another candidate for proton transduction was proposed when complimentary DNA encoding a protein sharing homology with members of the amiloride-sensitive Na^+/degenerin family of ion channels was isolated and expressed in *Xenopus* oocytes. Known as acid-sensing ion channels (ASICs), these have been shown to respond to a drop in extracellular pH to below 6.9 with a fast-rising, rapidly inactivating current. These channels were only sensitive to pH on the extracellular surface, suggesting they constituted a detector of extracellular protons (Waldmann et al., 1997). Immunohistochemistry has demonstrated that the majority of DRG neurons express the ASIC1a and ASIC1b isoforms (Hughes et al., 2007). ASIC2a is only expressed on larger DRG neurons, whereas ASIC2b is abundant throughout the different DRG subpopulations (García-Añoveros et al., 2001). Finally, ASIC3a has been shown to be present in peripheral sensory neurons (Sutherland et al., 2001). Overall, within all DRG neurons, ASICs have a wider distribution of expression than TRPV1. Complicating matters further, is the fact that ASICs are able to assemble as functional heteromeric as well as homomeric channels with the specific combination of subunits determining the functional pH sensitivity (Hesselager et al., 2004).

ASIC3 (also referred to as Dorsal Root Acid Sensing Ion Channel – DRASIC) is expressed in sensory neurons ranging from large mechanoreceptors to small nociceptors, in addition its peripheral presence in Meissener corpuscles and free nerve endings (Price et al., 2001) make it a particularly attractive proton transduction candidate. Specific pharmacological block of ASIC3 in the rat skin-nerve preparation using the sea anemone toxin, APETx2 (Diochot et al., 2004), entirely inhibits C-fibre firing when stimulated with moderate acidifications (Deval et al., 2008), suggesting it plays a role in the transduction of mild acidic stimuli. However, studies using ASIC3 knockout mice have provided contradictory evidence as to the involvement of ASIC3 in acute nociception to acid stimuli (Price et al., 2001; Chen et al., 2002). Interestingly, pH 5 and noxious heat (52 ˚C) induced responses in single C-fibre recordings were substantially attenuated in *Asic3 -/-* mice (Price et al., 2001), perhaps indicating this channel is required for a maximal receptor response to acid. The reduced neural response to a noxious heat stimuli was accounted for by a ~30 % reduction in spike activity, however this was unexpected as ASIC3 is not gated by noxious heat. These results point to the possibility that ASIC3 and TRPV1 may functionally interact to transduce noxious stimuli, and may both be required for a maximal response.

Inflammation is a common pain condition that can result in local acidosis and induce high expression of ASICs. ASIC3 mRNA was increased by more than 15 times in the DRG soma when inflammation was induced by complete Freund's adjuvant (CFA) injection into the hindpaw of a rat (Voilley et al., 2001). *In vitro* studies have confirmed this; increases in ASIC-expressing neurons and ASIC-like current amplitude have been observed in DRG cultures supplemented with

proinflammatory mediators including NGF, bradykinin and interleukin-1 (Mamet et al., 2002). In addition to increasing the expression of ASIC3, proinflammatory molecules have been shown to modulate the activity of ASICs. Serotonin and bradykinin, for example, have been demonstrated to induce activity in the protein kinase C (PKC) pathway after binding to their G-protein coupled receptors (GPCRs). PKC activity can facilitate channel phosphorylation, potentiating ASIC currents (Deval et al., 2004), suggesting these channels play an important role in pain sensitisation in inflammatory conditions. The increase in ASIC current is also accompanied by a shift in its pH dependence towards physiological levels, suggesting nociceptor excitability would increase as a result of ASIC activity during inflammation. Inflammation is a major cause of acidosis induced pain, and Deval et al., 2008 report that specific pharmacological blockade of ASIC3 with APETx2 and siRNA (small interfering RNA) knockdown of ASIC3 both induce potent antinociceptive effects in a rat model of primary hyperalgesia, heavily implicating these channels in inflammatory induced hyperalgesia.

In addition to TRPV1 and ASICs, the ovarian cancer G-protein coupled receptor 1 (OGR1) family, consisting of OGR1, GPR4, T-cell death associated gene 8 (TDAG8) and G2 accumulation (G2A) have been shown to be activated by acid stimuli, in the region of pH 6.4 – 6.8. All of these receptors are found in the DRG, with many localised to small diameter, IB4 positive nociceptors (Huang et al., 2007). After CFA induced inflammation, TDAG8 was shown to dramatically increase its expression in the DRG. Co-expression with TRPV1 in A-fibres was also considerably increased, and TDAG8 expression was also shown to increase in both IB4 positive and negative populations (Chen et al., 2009). Increased expression of TDAG8 in IB4 positive neurons has been suggested to increase the sensitivity to protons and capsaicin through modulating the activation properties of ASICs and TRPV1. This is confirmed by studies showing cells that co-express TDAG8 and TRPV1 show enhanced responses to capsaicin stimulation after pre-treatment with pH 6.4, suggesting that when TDAG8 is expressed, protons can potentiate the calcium influx through TRPV1 activation (Chen et al., 2009). In response to extracellular protons, TDAG8 responses leads to activation of protein kinase A (PKA) pathways which can phosphorylate TRPV1 – modulating its function, and potentially leading to a sensitised pain state. This provides evidence that increases in H^+-ions during inflammation not only directly activate ASIC3 and TRPV1 to cause pain, but also are detected by GPCRs that can then further enhance the sensitivity of neurons, which may contribute to the development of inflammatory-induced hyperalgesia.

Acid is an algogenic stimulus that is commonly associated with inflammation. Its detection is common across all vertebrates examined, with one exception. Remarkably, the African naked mole rat is entirely acid insensitive. Detailed investigations have revealed the nociceptors of these mammals possess some exceptional characteristics (Smith et al., 2011). The classical acid sensors – TRPV1 and ASICs are not dissimilar in the naked mole rat to other vertebrates, yet application of a pH 6 solution to naked mole rat DRG neurons resulted in a 63 % decrease in voltage-gated inward conductance (Smith et al., 2011). Furthermore, the potency of pH 4 and pH 6 evoked-inhibition of

mechanically induced C-fibre activity in the naked mole rat was significantly greater than in mouse neurons. The molecular basis of the acid insensitivity lies with a specific variant of the voltage gated sodium channel (VGSC) subtype 1.7 ($Na_v1.7$). This is crucial in determining the excitability threshold for nociceptors, and has proved to be indispensable for the detection of pain. A highly conserved positively charged motif in the pore loop region between S5 and S6 in domain IV (Figure 1.3.1) was found to be negatively charged in the naked mole rat. This charge difference renders $Na_v1.7$ in the mole rat more sensitive to proton block. Therefore, despite the presence of acid sensors in the form of TRPV1 and ASICs, the depolarising input through these channels is unable to overcome the block on $Na_v1.7$ by H^+ -ions, meaning acid evoked action potentials are not evoked. This fascinating phenotype was shown to be of major biological importance for the naked mole rat; they live in subterranean burrows which experience unusually high CO_2 levels, which can drive tissue acidosis. Similarly, $Na_v1.7$ in the cave-roosting microbat, which also experiences high CO_2 levels, was found to also have a negatively charged motif in the same pore loop region (Smith et al., 2011). Therefore, convergent evolution has selected $Na_v1.7$ to reduce acid induced nociception in these mammals.

Collectively, the current literature heavily implicates TRPV1 and ASICs as the primary acid sensors, although to what degree each contributes to the overall detection of protons is unclear. The OGR1 family of GPCRs are also implicated in acid detection, however, these appear to be predominantly involved with modulating the primary detectors which can influence the onset of inflammatory induced hyperalgesia. Overall, it seems likely that TRPV1, expressed on unmyelinated C-fibres play an important role in the transduction of strong acidic pH values, whereas ASICs, expressed on thin myelinated nociceptors are tuned to detect smaller fluctuations from physiological pH.

1.2.5. Mechanoreception

A diverse range of mechanical stimuli is detected by specialised receptor organs, which are innervated by the peripheral terminations of sensory neurons. Low threshold, large diameter Aβ DRG neurons are mechanoreceptors responsible for innervating the end organs. The morphology of the end organ differs according to the specific mechanical modality it detects, and are further distinguished by their adaptation profiles. Rapidly adapting (RA) mechanoreceptors terminate as Meissner's corpuscles in the dermal papillae - detecting light touch and vibration (Brown and Iggo, 1967) or Pacinian corpuscles – primarily detecting vibration in the skin (Loewenstein and Mendelson, 1965). Longitudinal lanceolate endings associated with guard hair follicles respond to skin movement and indentation (Brown and Iggo, 1967). The predominant slowly adapting (SA) mechanoreceptors are Merkel discs – enriched in the touch sensitive areas of the skin they are responsible for the discrimination of shape and texture (Iggo and Muir, 1969) and Ruffini corpuscles – detecting skin stretch (Iggo and Andres, 1982).

Mechanically evoked currents have been recorded in many cells, but the exact transduction mechanism remain unidentified. Recent expression profiling in neuroblastoma cell lines have

indicated the transmembrane proteins, Piezo 1 and 2 are required for mechanically induced currents (Coste et al., 2010). The use of siRNAs against Piezo 2 in mouse DRG neurons selectively and significantly reduced the number of cells expressing rapidly adapting, mechanically evoked currents. Furthermore, the same study illustrated that the expression of Piezo 2 overlapped with immunohistochemical markers present in mechanosensory neurons including peripherin and neurofilament 200. Another mechanotransducer recently identified include a stomatin-like protein 3 (SLP3)(Wetzel et al., 2007). Transgenic mice in which this protein was disrupted displayed 40% and 30% mechanically insensitive Aβ and Aδ fibres, respectively, with over 90% of sensory fibres in wildtype litter mates mechanically sensitive. The development of mechanical allodynia after chronic constriction injury (CCI) was significantly impaired in the *SLP3* mutant, suggesting this protein is required for a subset of cutaneous mechanoreceptors.

To conclude, DRG neurons are a highly heterogeneous population that detect a wide range of stimulus modalities and intensities. The peripheral terminals of the respective subpopulations are highly adapted to detect specific stimuli. This adaptation is due in part to the preferential expression of certain transduction proteins in precise subpopulations, endowing sensitivity of a precise modality to that neuron. Additionally, defined innervation of an end-organ ensures these finely tuned receptors detect specific stimuli. Mutations in genes encoding several of these proteins have proved critical in our understanding of their properties. However, certain areas of peripheral somatosensation are still ambiguous. Therefore fundamental research into the functioning and expression of these proteins can greatly further our knowledge of these crucial sensory transducers.

1.3. Action potential propagation – Voltage Gated Sodium Channels

Sensory transduction is responsible for the local depolarisation of the receptive terminals. The depolarisation must then be propagated to the CNS in the form of action potentials. Initiation of the action potential and subsequent propagation is dependent upon voltage-gated sodium channels (VGSCs) of which there are nine subtypes, $Na_v1.1$ through $Na_v1.9$. These can be divided into two main subgroups, based on their sensitivity to the pufferfish derived neurotoxin – Tetrodotoxin (TTX). TTX binds to the external channel vestibule in 1:1 stoichiometry, and blocks sodium current by occluding the channel pore (Hille, 1975). Those which are inhibited by low-nanomolar concentrations of TTX are referred to as TTX-sensitive (TTX-s) and include $Na_v1.1$, 1.2, 1.3, 1.4, 1.6 and 1.7. Conversely, the channels which display insensitivity to TTX up to 1 μM are known as the TTX-resistant (TTX-r) and comprise $Na_v1.5$, 1.8 and 1.9.

Sodium channels consist of an α-subunit and auxiliary β-subunits. The α-subunit is composed of 4 homologous domains (I – IV), each containing a 6 transmembrane spanning region (S1 – S6) (Figure 1.3.1). This subunit constitutes the pore forming region, and alone is sufficient for sodium ion influx, however the co-expression of β-subunits regulates the kinetics and voltage dependence of the sodium channel. β-subunits are also crucial in channel localisation and interaction with the intracellular cytoskeleton and cell adhesion molecules (Catterall et al., 2005). The pore is lined by the S5 and S6 region of each domain (Figure 1.3.1), whilst the pore loops between S5 and S6 form the outer, narrow entry to the pore which is crucial for ion selectivity. The S4 segments in each domain are crucial for the voltage dependent properties of VGSCs. With a positively charged amino acid at every third position, these residues serve as gating charges, and in response to membrane depolarisation move across the membrane to initiate channel activation (Catterall et al., 2005). During the activated state, sodium ions influx into the cell down their electro-chemical gradient, resulting in the upstroke of the action potential. Each sodium channel is tightly controlled by two gates, the activation and inactivation gates, both of which are open during the rising phase of the action potential. The channel then inactivates within 1-2 ms of depolarisation as a result of the intracellularly located inactivation gate between domains III and IV (Figure 1.3.1). This cytoplasmic gate and a receptor site become available after S4 activation, the gate can then bind to a receptor site, blocking the pore and inactivating the channel (Vassilev et al., 1988). The inactivation gate is partly responsible for limiting the rising phase, and makes repolarisation to the resting membrane potential (through potassium channel opening) easier (Bezanilla and Armstrong, 1977). Upon repolarisation conformational changes results in the closure of the activation gate, so that both gates are now closed, leading to closed state inactivation. The two gates have characteristically opposing effects, so that when one is open the other is usually closed. Therefore, once the activation gate has closed, approximately 2-5 ms later, the inactivation gate swings back to unblock the intracellular pore of the channel resulting in the closed, resting state, where the channel is primed for another depolarisation (Armstrong, 2006). This time delay from the closing of the activation gate to the opening of the inactivation gate accounts for the refractory period.

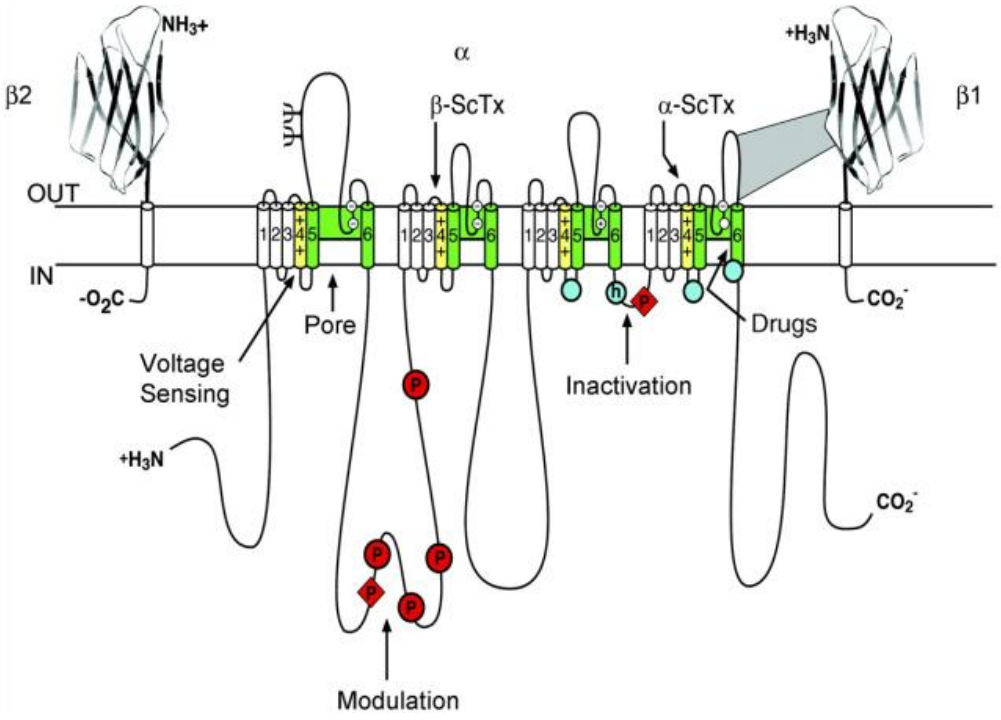

Figure 1.3.1
The primary structure of the subunits which comprise the voltage gated sodium channels. The α-subunit is composed of 4 domains, each with 6 membrane spanning α-helices, represented by cylinders. S5 and S6 (green cylinders) line the pore, whilst the extracellular loops between them form the outer entry to the pore, and contain outer and inner rings of amino residues (white circles) that form the ion selectivity filter and TTX binding site. S4 (yellow cylinders) carry a positive charge and serve as voltage sensors. Inactivation gate (h in blue circle) blocks the pore after activation by binding to a receptor site (blue circles are implicated in forming the inactivation gate receptor). Red sites are known phosphorylation locations by PKA (circles) and PKC (diamonds). The extracellular domains of the β1 and β2 subunits are shown, along with the probable α-subunit interaction site with β1. Adapted from Catterall, 2012.

VGSCs are abundantly expressed throughout the nervous system, although most have a preferential location of expression. For example, $Na_v1.7$, $Na_v1.8$ and $Na_v1.9$ are preferentially associated with nociceptors and $Na_v1.2$ and $Na_v1.6$ are predominantly found at the nodes of Ranvier in myelinated axons. The VGSCs expressed in DRG neurons are the TTX-sensitive - $Na_v1.1$, $Na_v1.3$ and $Na_v1.6$, $Na_v1.7$, and the TTX-resistant, $Na_v1.8$ and $Na_v1.9$.

1.3.1. $Na_v1.1$

$Na_v1.1$ is expressed in both the CNS and the PNS, however its function in sensory neurons is unclear. In situ hybridisation studies suggest $Na_v1.1$ mRNA is expressed at highest levels in large diameter sensory neurons, with limited expression in the smaller neurons (Black et al., 1996). Therefore it is unlikely to be implicated in cutaneous pain transmission of small diameter neurons (Cummins et al., 2007).

1.3.2. $Na_v1.3$

In the DRG, $Na_v1.3$ is highly expressed in embryonic neurons and is undetectable in adult sensory neurons. However, after peripheral nerve injury the expression of this channel is upregulated, potentially implicating $Na_v1.3$ in the hyperexcitable state that follows nerve injury. Furthermore, this channel is also thought to encode the rapidly repriming response in injured neurons (Cummins et al., 2001). Interestingly the injury-induced upregulation in DRG neurons is reversed by NGF administration, suggesting that loss of neurotrophic signalling may account for the subsequent gene transcription (Dib-Hajj et al., 2010).

1.3.3. $Na_v1.6$

$Na_v1.6$ is expressed in several types of neuron, and there is evidence showing this ion channel is highly concentrated at the nodes of Ranvier of sensory and motor neurons (Caldwell et al., 2000). $Na_v1.6$ exhibits rapid activation and fast inactivation which is similar to other TTX-sensitive channels, however, $Na_v1.6$ can recover approximately five times faster from inactivation than $Na_v1.7$ (Herzog et al., 2003) which would mean $Na_v1.6$ expressing neurons should be able to sustain high frequency firing. Indeed, large DRG neurons with myelinated axons can fire at high frequencies and also exhibit rapid recovery from inactivation similar to $Na_v1.6$ channels (Everill et al., 2001).

1.3.4. $Na_v1.7$

DRG and sympathetic ganglion neurons both express $Na_v1.7$; this channel is responsible for producing a fast activating, fast inactivating and slowly repriming, TTX-s current (Dib-Hajj et al., 2010). Based on its properties, this channel largely controls the threshold of firing by amplifying generator potentials (Rush et al., 2007). NGF and other inflammatory mediators have been demonstrated to regulate $Na_v1.7$ expression, and increased levels of $Na_v1.7$ have been detected in a rat model of painful diabetic neuropathy (Chattopadhyay et al., 2008). $Na_v1.7$ antisense knock-down animals display a reduction of thermal hyperalgesia after intraplantar administration of CFA (Yeomans et al., 2005), confirming a role for $Na_v1.7$ in inflammatory pain. $Na_v1.7$ is preferentially expressed in small-diameter nociceptive neurones, explaining why pain detection is altered in these knock-down animals. Immunocytochemisty has revealed that 100 % of C-, 90% of Aδ-, and 40% of Aα/β-fibre units were positively stained for $Na_v1.7$, and that a higher proportion of nociceptive than low-threshold mechanoreceptive (LTM) neurons were positive for this channel (Djouhri et al., 2003b). The same study also positively correlated $Na_v1.7$ staining with action potential duration, and negatively correlated the staining with conduction velocity and soma size, all of which are characteristics of nociceptive neurons.

Mutations in SCN9A, the gene encoding $Na_v1.7$, have proved this VGSC is absolutely critical for action potential propagation in nociceptors. A specific loss of function mutation in SCN9A CAN result in congenital inability to experience pain (CIEP) (Cox et al., 2006), a debilitating and sometimes life threatening disorder in which the patients do not feel pain. Conversely, gain of function mutations in SCN9A have also been described, resulting in Erythromelalgia and Paroxysmal Extreme

Pain Disorder (PEPD). Inherited Erythromelalgia is caused by a point mutation (Yang et al., 2004b) or a substitution mutation (Dib-Hajj et al., 2005). Both mutations result in a gain of function of $Na_v1.7$ by causing a hyperpolarising shift in activation and a slow deactivation (Cummins et al., 2004). Clinical presentation is usually in the first decade and often causes excruciating distal pain. PEPD is caused by the mutant $Na_v1.7$ channel recovering faster from fast inactivation and producing larger currents in response to ramp stimuli (Dib-Hajj et al., 2008). PEPD patients suffer from extreme pain attacks that usually last several minutes.

These mutations in SCN9A further emphasise the importance of $Na_v1.7$ in the propagation of nociceptive action potentials. Consequently these make $Na_v1.7$ an attractive target for analgesic development, however, in order to study this channel a selective blocker is necessary. The tarantula venom peptide ProTx-II interacts with $Na_v1.7$, inhibiting this channel with at least a hundred fold selectively over other Na_v1 channels. In desheathed sensory nerves, this toxin was able to completely inhibit evoked C-fibre compound action potential with little effect on Aβ-fibre conduction (Schmalhofer et al., 2008). This specific $Na_v1.7$ blocking toxin could prove very useful in the search for novel analgesics.

1.3.5. $Na_v1.8$

$Na_v1.8$ is expressed preferentially in sensory neurons and is therefore very common in the DRG and trigeminal ganglia. In addition $Na_v1.8$ is also found along peripheral axons and in free nerve terminals in the skin. $Na_v1.8$ produces a slow inactivating, rapidly repriming TTX-r current, that contributes most of the sodium current to the action potential upstroke (in neurons that express it) (Renganathan et al., 2001). The ability for this channel to rapidly reprime means it has a critical role in repetitive firing, furthermore, its presence in free nerve endings indicates its involvement in the transmission of nociceptive information. Studies of neuropathic pain patients have revealed an increase in expression of this channel in axons within painful neuromas (Black et al., 2008), whilst animal studies have shown that by silencing $Na_v1.8$ with siRNA, tactile allodynia in the chronic constriction injury (CCI) rat model of painful neuropathy could be reversed (Dong et al., 2007). $Na_v1.8$ has a relatively high threshold of activation which combined with its abundant expression in nociceptive neurons may underlie the high threshold of these neurons (Djouhri et al., 2003a).

The TTX-r $Na_v1.8$ channel is expressed on the superficial endings of nociceptive fibres, and it is this channel that is essential for the excitability of nociceptors when the skin is cooled (Zimmermann et al., 2007). Cooling enhances the voltage dependent slow inactivation of all TTX-s channels, however, the excitability of $Na_v1.8$ is entirely cold-resistant. In fact, during cooling, the activation threshold for $Na_v1.8$ is reduced. $Na_v1.8$-null mice (Akopian et al., 1999) support this finding by showing negligible responses to noxious cold and mechanical stimulation at low temperatures.

1.3.6. $Na_v1.9$

$Na_v1.9$ produces a persistent TTX-R current; this is due to its ultraslow inactivation kinetics and the activation threshold lying close to the resting membrane potential of neurons (Dib-Hajj et al., 2010). The expression of this channel is largely limited to small diameter, nonpeptidergic DRG neurons, most of which are nociceptors. $Na_v1.9$–like immunoreactivity was found in 64% of C-fibre units measured from lumbar rat DRGs, all of which were high threshold nociceptors (Fang et al., 2002). 91% of C-unresponsive units were also positive for $Na_v1.9$, based on their membrane properties these were classed as nociceptive, and probably account for the silent nociceptor population. All low threshold mechanoreceptors were negative for $Na_v1.9$. $Na_v1.9$ expression is regulated by GDNF and not NGF, similarly the nonpeptidergic C-fibres which express this channel, lose their TrkA expression and upregulate the GDNF signalling receptor – Ret, during early post-natal development. This specific regulation may account for some of the functional differences observed between the peptidergic and nonpeptidergic C-fibre population. The ultraslow inactivation of the $Na_v1.9$ current suggests that it does not contribute to the action potential upstroke, but rather prolong the response to subthreshold depolarisations, thereby acting to lower the overall action potential threshold (Dib-Hajj et al., 2010).

1.4. Axonal Transport

In terms of size, neurons represent the largest single cells. In humans, the axon of a sensory neuron can extend to over a metre in length. Protein synthesis usually occurs in the cell body, therefore, neurons are dependent on an efficient anterograde active transport system to distribute mitochondria and newly synthesised proteins such as ion channels to peripheral destinations. Alternatively, retrograde transport is responsible for the shipping of target derived factors, from peripheral target cells to the soma of the neuron. Retrograde signalling of target derived signals is crucial for neuronal growth, target innervation, synaptogenesis and the establishment of distinct neuronal phenotypes (Ginty and Segal, 2002).

In the past few decades a wealth of knowledge has been uncovered about the mechanisms that govern active transport. The microtubular network has been shown to be vital for transport, with side arms linking the microtubule to the transport cargo (Hirokawa, 1982). These delicate side arms were shown to be motor proteins with ATPase activity that are able to generate the force required for movement (Brady et al., 1982).

Motor proteins vary according to the direction of transport. The kinesin motor protein superfamily is primarily responsible for transporting cargo towards the positive end of the microtubule, and therefore constitute the major anterograde transport mechanism. Kinesins are composed of heavy and light chains, connected by a tail region. In most cases, the globular head of the heavy chain contains the motor, which is responsible for ATP binding and ADP release (Scholey et al., 1989). ADP release results in conformational changes which gives rise to the motion of the motor protein. A host of regulatory proteins can interact with the tail region creating a large variety of kinesin motors, each of which is responsible for shuttling a specific cargo (Goldstein and Yang, 2000).

Retrograde transport is primarily due to the dynein motor proteins. Dynein is a large cytoplasmic protein with several motor domains (Paschal, 1987), and associates with dynactin, a protein complex which is required for most of dyneins motor functions and can also associate with cargos (Dahlstrom, 2010).

1.4.1. Retrograde neurotrophin signalling

Unlike other growth factors that directly bind to receptors in the cell body plasma membrane – usually located less than a micron from the nucleus, neurotrophins bind to receptors that can be located over 1 metre from the nucleus. This long journey can take hours or days to eventually reach the somata and induce gene expression. Retrograde signalling is therefore heavily implicated in the neurotrophin signalling process. During development, peripheral neurons are dependent upon target derived neurotrophins, including NGF, GDNF, NT3 and NT4, for survival. The now heavily supported neurotrophic hypothesis, suggests that these factors are in limited supply, so that the neurons which successfully innervate their target survive, whereas those that are less

competitive undergo cell death (Yuen et al., 1996). This is suggested to account for the extensive neuronal pruning and refinement that occurs during development, in which approximately 50 % of all neurons die. In addition to the survival effects during development, neurotrophins also play a major role in neural repair and neuroprotection in mature neurons.

Neurotrophins bind to their respective Trk receptors and the common, low affinity P75 receptor. In order for the neurotrophin mediated effects to take place, a signal must be sent from the neurotrophin binding location in the peripheral terminals to the nucleus. Evidence implicates the neurotrophin receptor themselves as the signalling molecule. Sciatic nerve ligation studies demonstrate the accumulation of activated, phosphorylated Trks (P-Trks) distal to the nerve ligation site (Ehlers et al., 1995), furthermore P-Trks also accumulate in the cell body of sensory neurons cultured in compartmentalised Campenot chambers which separate the cell soma and peripheral terminals, when only the terminals are exposed to the neurotrophin (Watson et al., 1999). Both of these experiments suggest Trk receptors are retrogradely transported upon binding and activation by their neurotrophin, which supports the signalling endosome theory. This suggests that neurotrophin mediated effects are brought about by the direct transport of the neurotrophin and its receptor (Beattie et al., 1996; Ginty and Segal, 2002). In order for the receptor-ligand complex to be transported it must first be internalised by endocytosis at the axon terminal. The protein complex and additional signalling molecules are then sorted into membrane bound organelles called signalling endosomes. These are then associated with dynein motors which shuttles the cargo towards the cell body. The speeds observed for fast axonal transport are in the region of 0.2–3 μm/s (Lalli and Schiavo, 2002), with 1.3 μm/s suggested to be the average (Cui et al., 2007). At this speed, and with an axon 1 metre in length, transport would take approximately 9 days to reach the cell somata.

There is a wealth of evidence to support the pro-survival role of Trk receptor/ligand complex arrival at the cell soma. Interestingly, TrkA can bind both NGF and NT3, with both able to induce axonal growth in sympathetic neurons, however it is only NGF induced phosphorylation of TrkA that is able to generate robust receptor-ligand internalisation, trafficking and survival. The binding of NT3 to TrkA also induces robust TrkA phosphorylation, but is unable to induce internalisation. Instead, NT3 induces local signalling to promote axonal growth through differential control of TrkA activation (Kuruvilla et al., 2004). One of the main downstream effects in neurotrophin signalling is the phosphorylation of CREB (cAMP response element binding protein). CREB belongs to a subfamily of transcription factors that also includes CREM (cAMP response element modulator) and ATF-1 (activating transcription factor-1). Upon phosphorylation, CREB forms homodimers with itself, or heterodimers with CREM or ATF-1, which are then able to bind to the CRE palindromic sequence promoters in the genome. 4710 palindromic CRE promoters are present in the human genome, and many genes involved in transcription, metabolism, neurotransmission and growth factor synthesis are under the control of this promoter sequence. In terms of neuronal survival, NGF has been shown to drive CREB-induced expression of B-cell

lymphoma -2 (BCL-2) in sympathetic neurons (Riccio et al., 1999). BCL-2 is an anti-apoptotic protein, therefore NGF induced expression of BCL-2 could explain the pro-survival effects of NGF in sympathetic neurons.

NGF mediated, CREB signalling is also required for DRG neuronal survival and NGF supplement is crucial for the survival of embryonic DRG cultures *in vitro.* In addition to the pro-survival effects of NGF, the ability of nerve tips to extend properly requires TrkA/NGF signalling, furthermore, CREB knockout animals show impaired axonal outgrowth *in vitro* (Lonze et al., 2002), suggesting this is also under the control of CREB. Compartmentalised chambers exploit the survival and growth inducing properties of NGF by using this neurotrophin as a chemo-attractant. As a result, neuronal processes grow towards a higher concentration of NGF, as they would during target innervation, into an isolated compartment where they can be separately studied.

1.5. Methods to investigate the properties of DRG neurons

DRG sensory neurons can be studied using a variety of techniques, these can include *in vivo*, *ex vivo* or *in vitro* methods. *In vivo* electrophysiological recordings offer a method whereby the 'natural' environment of the cell is minimally disrupted. One of the earliest examples of *in vivo* single fibre recordings was described by Adrian in 1926, this comprehensive report detailed the use of a capillary electrometer in combination with an amplifier, where a teased nerve fibre was placed over a recording electrode whilst stimuli was applied to the end organ. This preparation was used to record from both proprioceptive single fibres in the frog sciatic nerve in response to stretching of the gastrocnemius muscle, and nociceptive single fibres in the cat saphenous nerve when the skin of the foot is nipped or pricked (Adrian, 1926). The crucial step made by Adrian was the amplification of the signal above background noise, which at the time gave unprecedented insights into action potential propagation in a single fibre. By the mid-20th century all experimental data had come from reduced preparations, using decerebrate or anesthetised animals. There was therefore a growing requirement to investigate how electrophysiological findings in animals compare to that in humans, Hensel and Boman took the first step to record from cutaneous afferents in awake human volunteers. After an initial general anaesthetic during which the radial nerve was exposed, single afferent impulses were recorded when the subject was fully awake. They presented recordings of mechanoreceptive fibres responding to prodding of the receptive field and the bending of a hair, furthermore, a cold sensitive unit that was insensitive to mechanical stimuli was also identified (Hensel and Boman, 1960). Whilst these recordings in awake humans were a significant step forward, correlations of afferent activity with elicited sensation were not possible as the selected nerve branch was cut proximally. Development of a hard and non-brittle tungsten electrode with a tip just 5 – 15 µm allowed for the first time intraneural recordings from an intact single afferent in awake subjects (Vallbo and Hagbarth, 1968). This experiment correlated the perceived sensation of smooth and rough mechanical stimulation of the skin to the neural response, and provided one of the earliest examples of microneurography single fibre recording.

Whilst advances were being made in microneurography, alternative methods for investigating sensory neurons were simultaneously being developed. The skin nerve preparation was first described in the mid-1980's and involves dissection of the saphenous nerve complete with a patch of innervated skin (Reeh, 1986). This *in vitro* preparation allows recordings from either a single fibre by teasing an individual unit away from a nerve bundle, or compound action potential recordings from the entire nerve. The dissection of both nerve and innervated skin allows discrete application of stimuli to the receptive field; furthermore, this preparation is also highly suitable for pharmacological investigations, as application of drugs can easily be directed to the nerve. Responses obtained from this preparation are also comparable to *in vivo* data from the same species (Cain et al., 2001) and the relatively fast dissection which can then be used for many hours make for a useful tool in sensory physiology (Koltzenburg et al., 1997; Zimmermann et al., 2009).

Both *in vivo* and *in vitro* electrophysiological techniques are indispensable tools in studying sensory neurons, however, they provide limited information on the cellular properties. Therefore, alternative methods for studying neuronal excitability have been devised that involve intracellular recording. The earliest examples of intracellular recordings in DRG neurons were described by Perl and colleagues; a micro-electrode was inserted into the nerve to penetrate a single afferent and they were able to define a population of cutaneous mechanical nociceptors (Burgess and Perl, 1967). The use of micro-electrodes soon progressed to be used for direct recordings from the DRG cell somata which provided an excellent signal to noise ratio (Bessou et al., 1971). More recently, an *ex vivo* technique has been described by Koerber and Woodbury whereby the spinal cord, DRGs, nerves and skin are dissected intact, allowing individual sensory somata to be impaled with a microelectrode to record responses from stimulation of the receptive field (Koerber and Woodbury, 2002). This method has the advantage that the entire peripheral sensory system is intact, however the dissection is technically demanding, taking many hours for a successful preparation.

Labelling of DRG neurons is a commonly used technique to map the central terminals in the dorsal horn of the spinal cord. The major breakthrough in neuronal staining came with the use of horseradish peroxidise (HRP) first described by Snow and colleagues in 1976. Before the use of HRP, neuronal labelling was often limited to the somata and immediate dendrites, making tracing of peripheral terminals difficult. Intracellular HRP labelling relied on axonal transport so instead of depending on diffusion as previous dyes had done, HRP was transported throughout the cell (Snow et al., 1976). Subsequent experiments have combined cell labelling with intracellular recordings. For example, Sugiura and Perl recorded intracellularly from DRG cell bodies whilst exploring the receptive field with a range of stimuli. After determining the functional properties of the individual neuron, a plant lectin (*Phaseolus vulgaris leucoagglutinin*, PHA-L) was deposited intracellularly by iontophoresis (Sugiura et al., 1986). 2-6 days later, immunohistological analysis revealed that the termination zone of unmyelinated nociceptors was in the superficial dorsal horn and predominantly lamina II (Sugiura et al., 1986).

The *in vivo* and *in vitro* electrophysiological methods discussed involve stimulation of the receptive field or nerve itself. *In vitro* methods using dissociated DRG cultures have also been developed which are now common practise to study sensory neuron physiology. The feasibility of *in vitro* DRG experiments also makes them a popular alternative to the technically demanding *in vivo* and *ex vivo* experiments. *In vitro* electrophysiology such as patch clamp recording allows access to the intracellular environment with only a single configuration to attach the cell. Variations of the technique allow the recording of currents through a single channel in excised patch configurations, or the activity across the entire membrane in whole-cell configurations. One disadvantage of patch clamping however is the slow accumulation of data, as only a single neuron is investigated at any one time.

Ratiometric calcium imaging is another commonly used *in vitro* method to study DRG neurons. This technique can allow the simultaneous evaluation of over 100 dissociated DRG cell bodies, furthermore it provides excellent data on the functional expression of sensory receptors and ion channels, and can be used to define neuronal subpopulations based on their functional responses. Calcium imaging of a DRG mass cultures involves loading the cell somata with a calcium indicator, and directly stimulating them whilst capturing the fluorescent change with a camera. This technique has been used extensively to study sensory neurons, in one example the emergence of TRP channel expression was demonstrated by recording the functional responses to a range of TRP channel agonists using DRG neurons dissected at various embryonic stages (Hjerling-Leffler et al., 2007).

Whilst the soma of DRG neurons can be isolated, dissociated and recorded from relatively simply, two important issues must be considered when evaluating the results. Firstly, acutely dissociated DRGs represent a model of axotomy and therefore may not reflect normal functionality. Secondly, recordings from DRG cell bodies are used as a model for cellular investigations of the receptive terminals. Somal responses may not represent the functional expression of ion channels and receptors in the receptive terminals or axonal collaterals. Importantly, it is the peripheral terminals that are primarily responsible for the transduction of stimuli into electrically encoded action potentials. Conventional mass culture of DRG neurons does not allow manipulation of neuronal microenvironments, making it difficult to study discrete neuronal regions. Therefore, compartmentalised chambers in which the terminals and soma are separated have been developed, which allow the study of peripheral neuronal regions in isolation from the cell soma.

1.5.1. Compartmentalised chambers

The first of these were the compartmentalised 'Campenot' chambers which were developed to study the effect of NGF on DRG neurons (Campenot, 1977). These chambers use a compartmentalised Teflon divider attached to a Petri dish with a layer of grease (Figure 1.5.1a). DRG neurites are able to pierce the grease layer and enter an adjacent compartment, in which they can be treated separately to the soma. The hydrophobic grease layer provides a barrier between each compartment, it is not however fluidically isolating, therefore allowing the migration of some soluble factors. This is demonstrated by the directional growth of the axons towards the high concentration of NGF, if the compartments were fluidically isolated axons would grow randomly in all directions. Campenot chambers have also proved extremely challenging to fabricate and assemble, with large variations between laboratories and investigators. In addition, many chambers develop a leak due to an imperfect grease seal (Figure 1.5.1b). Neurites within the Campenot chambers are also very susceptible to lesioning due to mechanical disturbances.

a

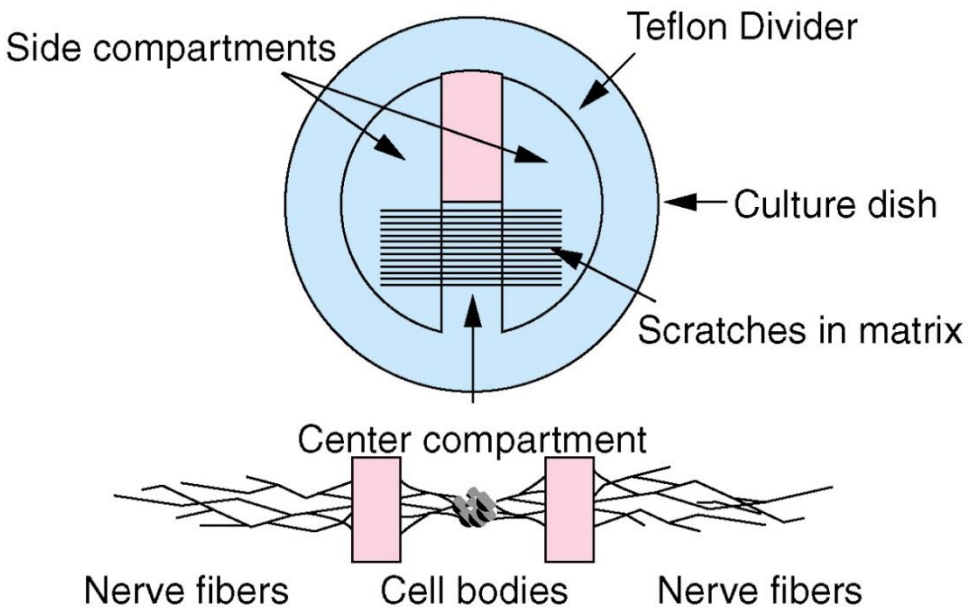

b

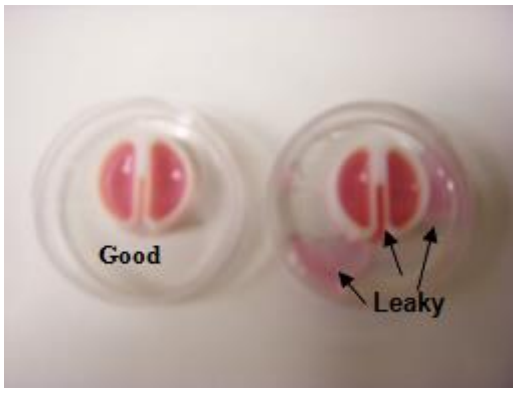

Figure 1.5.1
(a) Schematic of a Campenot chamber showing the separate side compartments and the scratches which direct the growth of the axons into the side compartments. Adapted from Miller and Kaplan, 2001. (b) Photo of 2 Campenot chambers, showing a chamber on the left which is successfully sealed with grease, and a chamber on the right which has leaked. Adapted from Pazyra-Murphy and Segal, 2008.

Advances in microfluidic technology have allowed the development of improved compartmentalised chambers. Microfluidics uses microfabrication techniques to develop a device suitable for biological experimentation. This technology has been utilised for a number of purposes, for example, microfluidic chips have been designed to facilitate the handling of volumes much smaller than a microlitre, which has been suggested to aid drug screening and testing on live cells (Dittrich and Manz, 2006). Another group has used microfluidic technology to fabricate a device to secure and immobilise the nematode *Caenorhabditis elegan*, so that submicron precision nanosurgery using lasers can be performed to axotomise axons in order to study nerve regeneration

(Ben-Yakar and Bourgeois, 2009). One of the earliest descriptions of using microfluidics for neuronal cell culture was in 2003 by the Jeon laboratory, here they report that the growth of cortical neurites can be directed through microgrooves resulting in the separation of somata from peripheral processes (Taylor et al., 2003). Two years later, the same group published an article describing the use of compartmentalised microfluidic chambers for the study of axonal injury, and go on to describe methods to isolate pure CNS axons without somata or dendrites (Taylor et al., 2005). A year later the Jeon group published a comprehensive Nature Protocols paper explaining the fabrication of the moulds by soft lithography (Park et al., 2006).

The advantage of using soft lithography is that it does not limit the spatial resolution of the design, therefore, fabrication of microscopic microgrooves that are only 3 µm in height is possible. The microgrooves are embedded into a barrier and are the only link between two identical compartments (Figure 1.5.2). The microscopic dimensions of the microgrooves are crucial as they acts as a 'filter' preventing the passage of cell somata from one side to the other, yet allowing the growth of neurites through to the adjacent compartment. Furthermore the resistance created by the microgroove array allows the fluidic isolation between neuronal microenvironments by establishing a volume difference between the compartments (Taylor et al., 2005). This can facilitate the delivery of treatments to isolated neuronal regions.

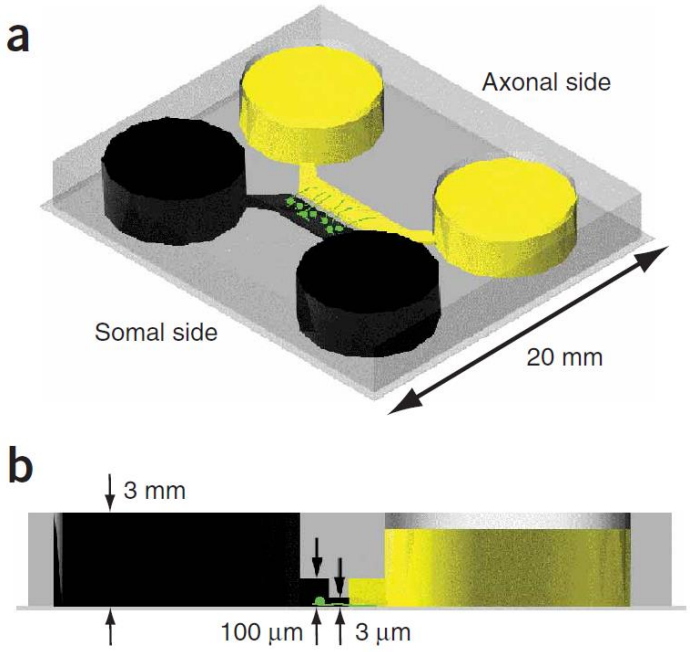

Figure 1.5.2
(a-b) Schematic and dimensions of the microfluidic chamber described by Tayler et al., 2005 showing the somal and axonal compartment separated by a microgroove array. Each compartment is 100 µm in height and are connected by microgrooves 3 µm in height. Adapted from Taylor et al., 2005.

The compatibility of microfluidic chambers with high-resolution microscopy and the long-term culture of neurons have made them a popular tool in neuroscience research. Importantly, they can be reproducibly fabricated, during which they are irreversibly adhered to a glass coverslip, allowing robust and leak-free experiments (Park et al., 2006). Variations of these compartmentalised chambers have been manufactured and applied to different biological questions. Recently, a chamber with a cushion gel has been designed, allowing the precise delivery of mechanical stimulation to the axons whilst synchronous calcium imaging was used to detect the somal response (Usoskin et al., 2010). This experimental paradigm revealed three previously uncharacterised populations of mechanically sensitive neurons, those responding to static indentation, and two vibration responsive populations. Compartmentalised microfluidic chambers represent an alternative method to Campenot chambers that serve as a robust method to study the properties of neuronal terminals and axons in isolation from the cell soma.

In conclusion, the development of the technology required for the fabrication of microfluidic chambers has opened a new opportunity for *in vitro* investigations of DRG sensory terminals in isolation from the cell somata. The highly reproducible and leak free chambers provide an attractive alternative to the classical Campenot chambers, that often fail due to an imperfect seal resulting in a leaking chamber. This thesis concentrates on using the microfluidic chambers in combination with functional calcium imaging. This novel combination enables the characterisation of functional protein expression in specific neuronal regions. Furthermore, the fluidic isolation between compartments enables the investigation of compounds applied specifically to the axons and the effects these have on action potential propagation in a relatively simple and high throughput *in vitro* system.

1.6. Aims

The aims of this thesis project were as follows:

- The initial aim was to establish a system whereby stimulation of peripheral neuronal regions could be detected by recording the changes in calcium concentration in the cell soma. Therefore, terminals were stimulated and time-locked somal calcium responses were measured.
- Next, I investigated whether all neurons which had successfully projected an axon into an adjacent compartment could be activated by a neuronal depolarising agent with an aim to see if functional responses are only observed in a subpopulation of DRG neurons. Retrograde tracing experiments were therefore correlated with functional recordings.
- A key question was can the microfluidic chambers be used to pharmacologically investigate action potential propagation *in vitro*. To investigate this, I used the 3 compartment chambers in which voltage gated sodium channel blockers were selectively applied to the middle axonal compartment, whilst stimulating the terminals and recording from the soma. This enabled a robust method to quantify neurons in which action potential propagation was inhibited by the application of compounds to their axon.
- Protons are established activators of nociceptive neurons with TRPV1 and ASICs regarded as the main molecular transducers of proton stimuli. There is however a discrepancy in the reported literature as to their respective contribution to the overall detection of acid stimuli. This in part, has been complicated by the use of techniques that only investigate specific neuronal regions. The novel combination of microfluidic technology and functional calcium imaging allows for the simultaneous investigation of the soma and peripheral neuronal regions. Therefore, a major aim was to functionally investigate proton transduction by comparing the sensitivity of the terminals, axon and soma to acid stimuli in order to see if proton sensitivity is differentially regulated between neuronal regions.
- Furthermore, another objective was to uncover the contribution of ASICs and TRPV1 to acid transduction by using pharmacological blockers.
- TRPV1 is also gated by noxious heat and the plant derived irritant – capsaicin. Its expression is restricted to a subpopulation of nociceptive neurons. A major aim of this thesis was to study the functional expression of TRPV1 throughout neuronal regions of cultured cells, to determine if there is a differential regulation of capsaicin sensitivity in the periphery compared to the soma.
- In addition, the expression of TRPV1 was specifically investigated on the axon by studying the ability for high concentration capsaicin to induce a conduction block.
- An important question in cell biology is does the *in vitro* culture of primary cells affect the properties of the cells. To investigate this, functional TRP channel expression was studied throughout embryogenesis and during time in culture. The focus was directed at

investigating if the onset of TRP channel expression and the maintenance of expression continued after long-term culture of embryonic DRG neurons.

- The final aim involved examining the role of various neurotrophins in promoting TRP channel expression *in vitro*.

Chapter 2

Materials and Methods

The work in my thesis describes a new method to functionally study DRG neurons in a compartmentalised culture system in which the compartments are fluidically isolated. First I describe the manufacture of the microfluidic chambers. This includes the fabrication of silicon master moulds, containing the microgroove pattern, the transfer of the pattern to an epoxy resin mould and replication of the pattern onto a Polydimethylsiloxane (PDMS) piece. An important step is the process of irreversibly adhering the PDMS to a glass bottomed culture dish which finalises the manufacture of a microfluidic chamber. Next I describe the details of how fluid flow in this new culture system was tested in order to quantify the rate of flow between different compartments. Finally the DRG culture procedure and the details of using the microfluidic chambers with functional calcium imaging are explained.

2.1. Fabrication of master moulds by soft lithography

Compartmentalised microfluidic culture chambers are comprised of a PDMS piece in which a relief pattern of channels and microgrooves is moulded (Figure 2.1.1). This moulded piece is subsequently adhered to a glass bottom culture dish. The PDMS piece is fabricated from an epoxy resin master mould by replica moulding, meaning all 'daughter moulds' are exact replicas of the master, ensuring consistency between experiments.

The process of fabricating compartmentalised microfluidic chambers by soft lithography was first described by Park et al., 2006. In this paper, a master mould was fabricated using a two-step soft lithography approach in order to produce a two layered three-dimensional relief pattern. The same process was followed under the guidance of Guillermo Menendez at the London Centre for Nanotechnology. Two layers are required due to the differing heights of the microgrooves and channels. The first layer constitutes the microgrooves and the second layer, which is built up on top of the first, constitutes the channels. The two layers are built from an epoxy based photosensitive compound - SU-8 photoresist (Microchem, MA, USA), on a 3 inch silicon wafer substrate (Compart Technology, Peterborough, UK). Initially, the wafer (Figure 2.1.2a) is coated with a 3 µm thick layer of SU-8 5 photoresist using a spin-coater at 2000 rpm for 1 minute, then baked for 2 minutes at 95˚C (Figure 2.1.2b). The microgroove pattern is transferred onto the wafer by irradiating the photosensitive SU-8 layer through a photomask (JD Photo, Oldham, UK) containing the microgroove pattern (Figure 2.1.2c). The irradiated SU-8 is polymerised and crosslinked to the silicon wafer. Non-irradiated SU-8 is then removed with a 30 second propyleneglycolmethylether acetate (PGMEA) photoresist developer (Chestech, Rugby, UK) wash, leaving behind the microgroove relief pattern (Figure 2.1.2d). The next step is a repetition of this process by spinning a second layer of SU-8 50 photoresist with a thickness of 100 (3 compartment chambers) or 150 µm (2 compartment chambers) onto the previously patterned silicon wafer (Figure 2.1.2e). A photomask containing the channel pattern is perfectly aligned on top of the wafer and transferred by a second UV exposure (Figure 2.1.2f). Another PGMEA wash removed all un-polymerised SU-8 completing the silicon master. This ultimately creates a master mould containing the relief pattern of the channels that are

linked by a microgroove array (Figure 2.1.2f). The fabrication process of a 3 compartment mould uses the same 2 layered technique. The only difference is the photomask design which imprints 2 microgroove arrays into the first layer, and 3 channels into the second layer.

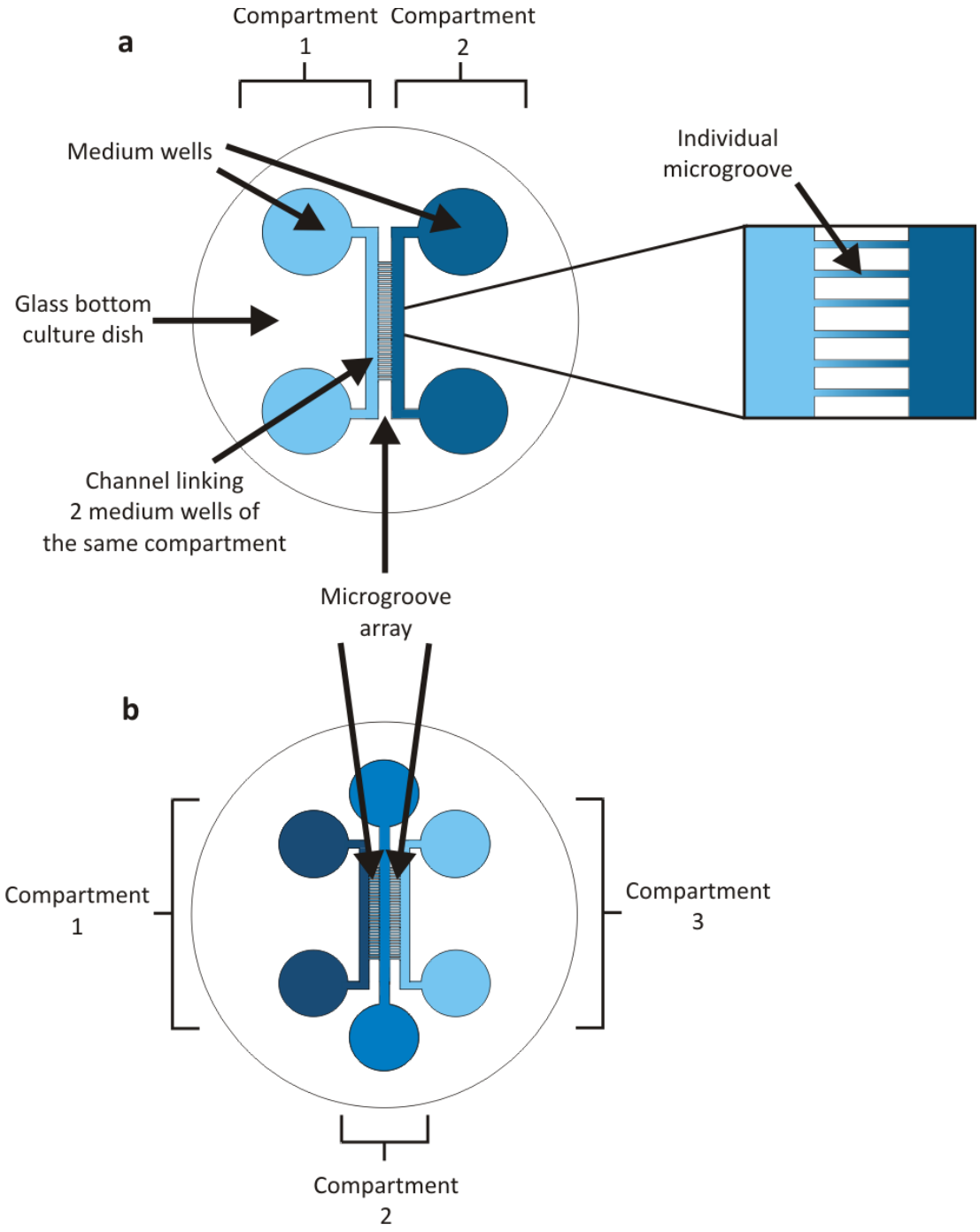

Figure 2.1.1
Schematic of a 2 (a) and 3 (b) compartment chamber showing the medium wells, channels and microgrooves. Dimensions of the channels and microgrooves in these schematics are approximate.

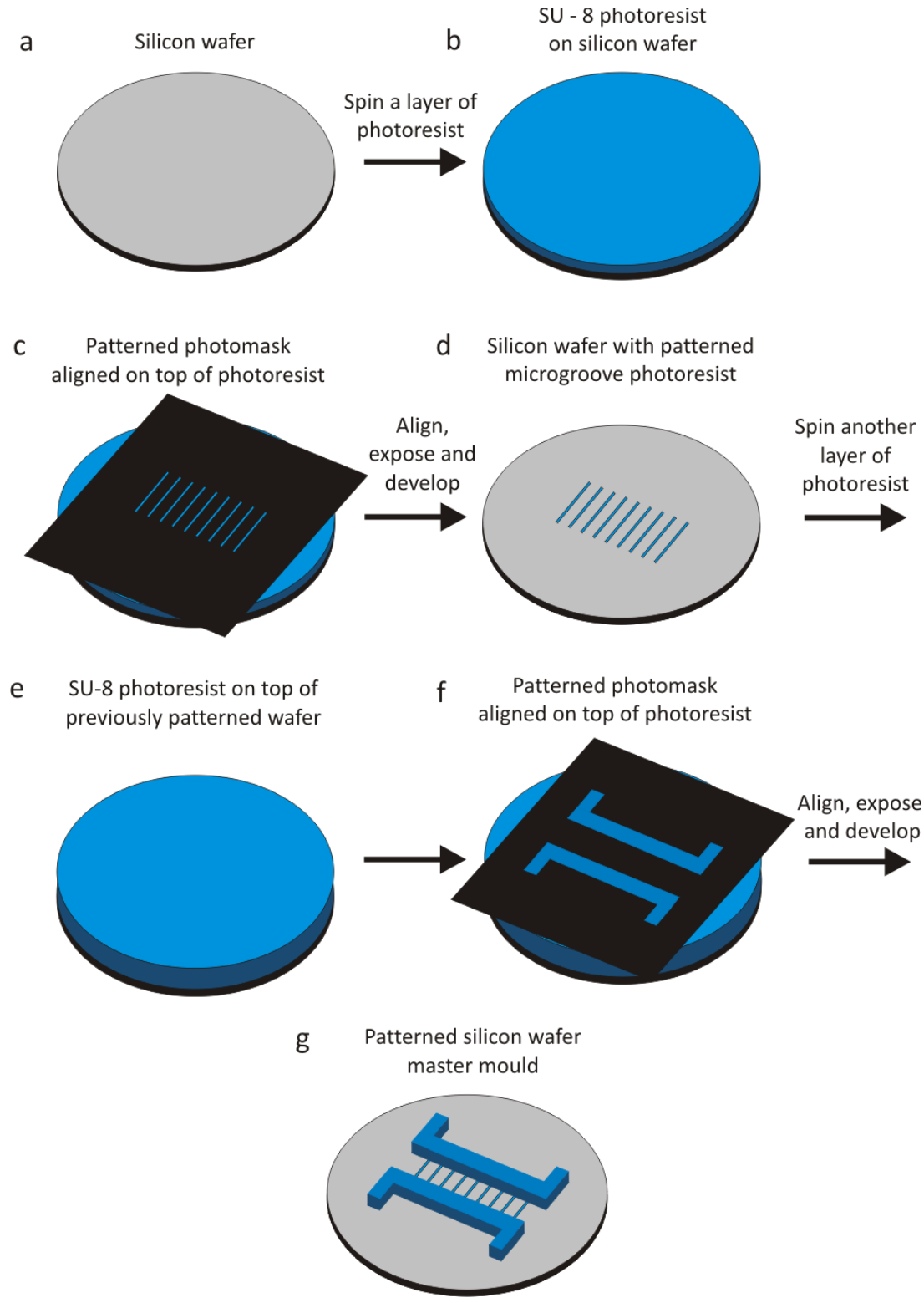

Figure 2.1.2
Fabrication of a 2 compartment master mould by soft lithography. The master mould contains 2 layers of patterned photoresist structures on a silicon wafer. The process begins with a silicon wafer (a) which is then spin coated with a layer of SU-8 photoresist (b). A microgroove patterned photomask is aligned on top of the photoresist (c). Irradiation through the patterned photomask polymerises and crosslinks the irradiated photoresist to the silicon wafer. A wash with PGMEA removes non-irradiated photoresist to leave only the microgroove pattern on the silicon wafer (d). A second thicker layer of photoresist is spun on top of the same silicon wafer (e) and the second photomask containing the channel pattern is aligned (f). The channels are aligned so that they are connected by the previously patterned microgrooves. Another wash with PGMEA removes all non-irradiated photoresist to leave the final patterned mast mould (g).

The 2 compartment chamber consists of 2 pairs of medium wells (Figure 2.1.1a). Each pair of wells are connected by a channel which is 2 cm long, 1 mm wide and 150 µm high. The relatively large dimensions of the channel permit rapid fluid exchange (<1 sec) between connected medium wells. The channels of each compartment are connected by a microgroove array containing approximately 100 individual microgrooves, each of which are 800 µm in length, 10 µm in width and 3 µm in height. Due to the very small dimensions of each microgroove, fluid exchange between compartments occurs over many hours.

The 3 compartment chamber consists of 3 pairs of medium wells (Figure 2.1.1b), each connected by a channel. The middle channel is 1.5 cm in length, whilst the 2 outer channels are 1.2 cm in length; all 3 channels are 1 mm in width and 100 µm in height. The 2 microgroove arrays each consist of approximately 80 microgrooves. The individual microgrooves are 500 µm in length, 10 µm in width and 3 µm in height.

2.2. Fabrication of epoxy templates

In the original description of using soft lithography for the fabrication by Park et al., 2006, the silicon wafer master mould was used to repeatedly transfer the microgroove/channel pattern to a PDMS piece. However, regularly using these as templates proved to be problematic, and after only 10-20 uses of the silicon wafer, the SU-8 layers begin to delaminate affecting the transfer of the microgroove pattern to the PDMS (Menendez, 2010). Furthermore, as mentioned in the original description (Park et al., 2006) the silicon wafer is fragile, which can easily crack when removing the solidified PDMS piece (Menendez, 2010). Bearing in mind the relatively lengthy process of transferring the layers to the wafer which requires reserving time in a clean room, the longevity of the silicon masters was unsatisfactory. To circumvent these issues, Guillermo Menendez describes in his PhD thesis a method to manufacture an intermediate epoxy resin template which replicates the original silicon master. There are several advantages of performing this intermediate step. First, many epoxy moulds can be fabricated using a single patterned PDMS piece generated from the original silicon wafer. Second, each epoxy mould was considerably stronger and could be used to generate a far greater number of PDMS pieces than the silicon wafer, without deterioration of the microgroove pattern. It is estimated that each epoxy mould can be used for thousands of transfers (Menendez, 2010), ultimately saving considerable time and cost. For the manufacture of epoxy resin templates, all components of the Taab 812 epoxy resin (Taab, Berkshire, UK) were thoroughly mixed (Table 2.2.1).

Taab 812 RESIN (g)	MNA (g)	DDSA (g)	ACCELERATOR DMP-30 (g)	FINAL WEIGHT (g)
9.6	6.6	3.8	0.4	20
19.2	13.2	7.6	0.8	40
28.8	19.8	11.4	1.2	60
38.4	26.4	15.2	1.6	80
48	33	19	2	100

Table 2.2.1
Components required for epoxy resin preparation. MNA - Methyl Nadic Anhydride, DDSA - Dodecenyl Succinic Anhydride, DMP-30 - 2.4.6-tri (Dimethyl Aminomethyl).

To remove air bubbles, the mixture was degassed for 30 minutes in a bell jar which was vented by connecting the hose to a vacuum pump. The mixture was then poured into a plastic petri dish measuring 5 cm in diameter and 1.5 cm in height. A PDMS piece copied from the original silicon master was used as a template to transfer the pattern into the epoxy resin. The PDMS device was set to float on the liquid mix of epoxy resin with the pattern facing downwards. With the PDMS piece floating on top, the epoxy resin was polymerised at 65°C overnight, after which the PDMS piece was peeled from the hardened epoxy block. To fabricate a single mould, approximately 20 g of epoxy resin mixture is required. Using this method, seven 2 compartment, and four 3 compartment epoxy resin templates were fabricated. Each epoxy template was highly alike to their counterparts as the same PDMS piece patterned from the original silicon wafer was used to pattern the epoxy resin moulds.

2.3. PDMS replication

All PDMS pieces were replica moulded from the epoxy resin templates. To fabricate the PDMS pieces, a 10:1 ratio of PDMS prepolymer and curing agent (Sylgard 184, Dow Corning, MI, USA) is thoroughly mixed and kept for 30 minutes at room temperature and pressure to allow the mixture to degass. The mixture is poured into the epoxy resin templates to approximately 3 mm thickness and allowed to cure for 45 minutes at 70˚C. Once solidified, the PDMS piece is removed from the template by cutting around the perimeter of the piece with a scalpel and carefully pealing the PDMS away from the epoxy mould. The reservoir wells are cut at either end of the channels using Harris Uni-Core cutters (Electron Microscopy Sciences, PA, USA). 5 mm diameter cutters are used for the 6 wells in the 3 compartment chamber, whereas the 8 mm cutters are used for the 4 wells in the 2 compartment chambers. The cutters are aligned so that when pressure is applied a circular piece of PDMS is removed, these ‘holes’ in the patterned PDMS piece form the individual medium wells. The cutters must be aligned so that they cut into the channel but not into the microgroove array. This ensures that two wells are connected by a channel, yet remain separated from adjacent compartments by the microgroove array.

2.4. Irreversible binding using a plasma cleaner

A leak-free environment is created by irreversibly adhering the PDMS piece to the glass bottom of a WillCo culture dish (Intracell, Royston, UK) or MatTek glass bottomed dishes (MatTek, MA, USA) using a Plasma Cleaner (Femto model, Diener Electronics, Ebhausen, Germany). Both of the culture dishes used have a glass bottom with a diameter of 30 mm and a thickness of 0.17mm allowing use with inverted microscopes. The PDMS piece is first cleaned of dust and debris by applying Scotch Magic tape to the patterned side and peeling it off. Any debris will stick to the tape and be removed upon peeling the tape off. This tape was used as it does not leave any residual glue on the PDMS piece upon peeling it away. The dish and the PDMS piece (microgroove side up) are placed inside the treatment chamber within the plasma cleaner. The chamber is vented and the pressure allowed to drop below 200 mTorr which takes approximately 20 seconds. The PDMS and glass surfaces are then treated with two separate plasma treatments, separated by approximately 5 seconds and each lasting 25 seconds at <100W power. Plasma cleaning involves the removal of impurities and contaminants from surfaces through the use of energetic plasma created by exciting gas atoms in air to a higher excitable state. High frequency voltages are used to ionise the gas, creating the excitable plasma. The plasma interacts with the surfaces placed in the cleaner and breaks apart organic bonds of surface contaminants, resulting in an ultra clean surface. Venting the plasma cleaner removes all contaminants, the PDMS piece is then placed microgroove side down in the centre of the glass bottom. By running curved forceps around all regions of the PDMS piece, and applying gentle pressure the PDMS evenly adheres to the glass bottom. To complete the binding reaction, microfluidic chambers are incubated at 75˚C for 10 minutes. After that approximately 200 µl of sterile water is added to each medium well, flooding the channel and microgrooves. Plasma treatment renders the treated surfaces hydrophilic and therefore water readily flows through the microgrooves. However, hydrophobic recovery begins soon after plasma treatment, therefore if water is not added whilst the surfaces are hydrophilic, water will no longer flow through the microgrooves. If this occurs, any fluid such as tissue culture medium, is unable to flow into the microgrooves. Neuronal processes are unable to grow through a microgroove which has dried out. Therefore, if the chambers are stored for several weeks before use for cell culture, the reservoir wells are topped up with sterile water weekly, to prevent the chambers from drying out. Chambers can be stored in a sterile environment for several weeks before using them for cell culture.

2.5. Quantifying the flow across the microgroove array

The microgroove array establishes a high fluidic resistance between compartments. However, only one published study has examined this isolation and only at a single time point, which suggested that a volume difference of 30 µl in the two compartment system will take over 24 hours to equilibrate (Park et al., 2006). This demonstrates that the compartment with the greater volume will remain fluidically isolated for at least 24 hours. To investigate the rate of equilibration in more detail and over a longer time period, a highly sensitive radioactive method was used. Niral Patel and Erik Arstad provided training with using radioactive solutions and the phosphorimager. All handling

of the highly radioactive stock solution was performed by Niral Patel, handling of the diluted solutions was then performed by myself. Experiments were conducted at the UCL Department of Chemistry.

A series of optimisation and calibration experiments were initially carried out to determine the radioactivity level and exposure time. To optimise the levels of activity used, a calibration experiment was conducted to identify the minimum detection threshold of the phosphorimager. This was important to know as a volume difference of 40 µl (200 µl and 160 µl are loaded in the separate compartments) was used, therefore only 10 % (20 µl of 200 µl) of the volume needs to flow across the microgrooves to equilibrate the volumes resulting in 180 µl in each compartment. Therefore, in order to detect this movement using phosphorimaging, a sufficient radioactivity level must be initially loaded, so that less than 10 % of this loaded activity can be detected when it has diluted in the phosphate buffered saline (PBS) of the adjacent unloaded compartment. Seven levels of activity - 0.01, 0.05, 0.1, 0.25, 0.5, 1 and 4 Megabecquerel (MBq) of ^{125}Iodine (^{125}I, Perkin Elmer Life and Analytical Sciences, MA, USA) were assessed in duplicate (Figure 2.5.1), by loading the activity in a volume of 200 µl in a single compartment of a 2 compartment chamber. ^{125}I was serially diluted from stock (3.7 GBq/ml) into 200 µl phosphate buffered solutions. The activity of each solution was measured using a PTW Curiementor 4 isotope calibrator (Freisburg, Germany). The chambers were immediately exposed for 1 hour on an unmounted 20 x 25 cm phosphor screen (VWR international, PA, USA). Phosphor screens are coated with photo-reactive phosphor crystals that are a europium-activated barium fluorohalide compound. When these are exposed to high-energy radiation such as beta particles and gamma rays, an electron of the Eu^{2+} is ejected and Eu^{3+} is formed (Robertson et al., 2001). The screen was subsequently scanned by a Typhoon 9410 Trio+ phosphorimager (GE Healthcare, UK), with the scanning parameters set to 'best resolution'- 25 microns. During the phosphorimaging, the screen is scanned with a laser of visible light, which converts Eu^{3+} ions back to Eu^{2+}. The conversion of europium back to its ground state releases a photon that is detected during the scanning (Robertson et al., 2001), the photon intensity is displayed as a false colour image to quantitatively and spatially give a representation of the radioactivity levels and location. Scanning a 20 x 25 cm screen at these parameters took approximately 2 hours. The resulting signal was quantified as a pixel count using ImageQuant software. Using this calibration graph, 1 MBq was chosen as the activity level to use as it is well within the threshold levels for detection (Figure 2.5.1). 0.01 MBq was near the lower detection threshold, therefore by choosing an activity level which was a hundred fold greater, a movement of just 1 % radioactive solution could be detected. It is also clear that even at 4 MBq the pixel representation of the radioactive signal is not saturated and continues to increase linearly (Figure 2.5.1). However, in order to minimise exposure to ionising radiation, 1 MBq was selected as this still produced reliable images.

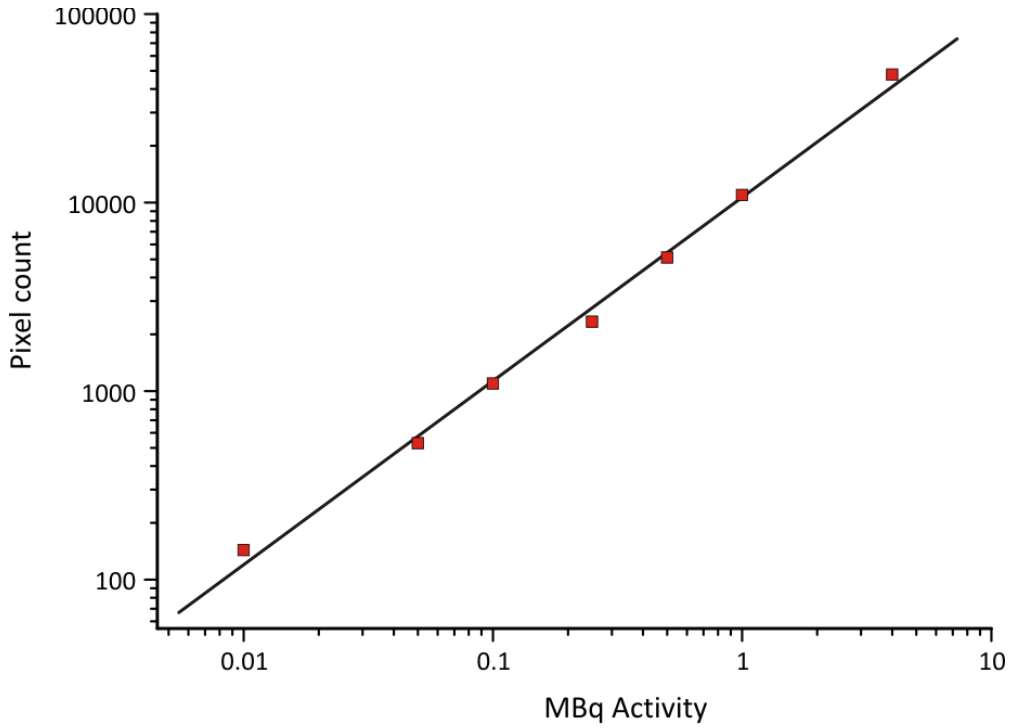

Figure 2.5.1
Calibration graph of loaded activity levels and resulting pixel count with linear line of best fit. Each point is the mean of 2 replicates.

In order to optimise the exposure time of chambers to the phosphor screen, a series of experiments were conducted by loading one compartment with 1 MBq activity in 200 µl and immediately exposing the chamber to the screen for 5 minutes, 30 minutes, 1 hour and 3 hours (Figure 2.5.2). The detected signal proportionately increased with exposure time. 1 hour was chosen as the optimal length of time as the detected signal was large enough to accurately quantify the pixel count, and the 'halo effect' around the wells was reduced compared to 3 hour exposure.

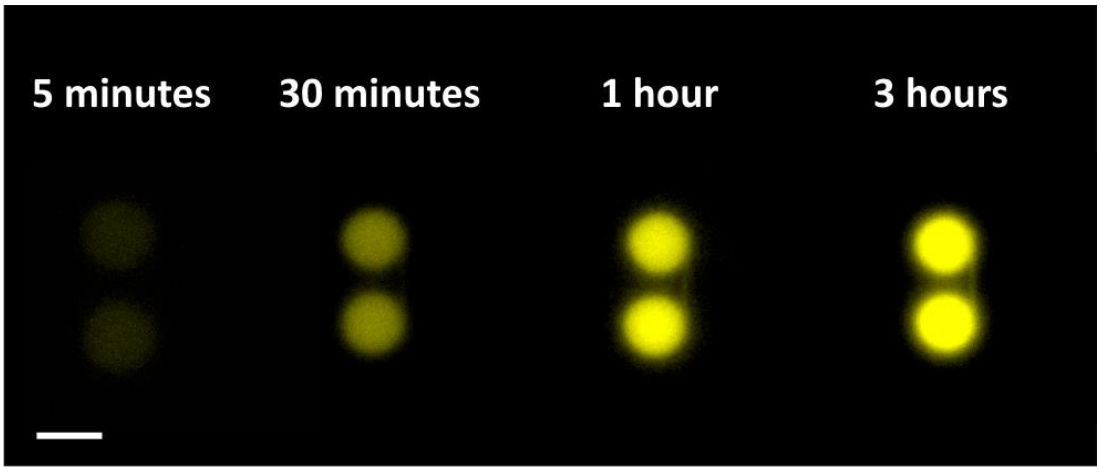

Figure 2.5.2
False colour phosphor-images showing exposure times of 5 minutes, 30 minutes, 1 hour and 3 hours of 1 MBq activity. Scale bar, 1 cm.

Using 1 MBq activity and a 1 hour exposure time, the flow across the microgroove array was assessed over 5 days. Radioactive solution was added to one compartment of a 2 compartment chamber and these were exposed for 1 hour on a phosphor screen at 0, 24, 48, 72 and 96 hours after addition of the solutions. The phosphor screens were subsequently scanned using the same phosphorimager and scanning parameters as in the calibration experiments. Three volume conditions were investigated in 4 separate 2 compartment culture chambers (Table 2.5.1), in which compartment A (Figure 2.5.3) contained a greater, equal or lower volume of ^{125}I solution than PBS in compartment B (Figure 2.5.3). ^{125}I was serially diluted into either 160 µl or 200 µl phosphate buffered solutions. Each solution was made up to 1 MBq activity measured using a PTW Curiementor 4 isotope calibrator (Freisburg, Germany).

	Compartment A	**Compartment B**
Condition 1	200 µl ^{125}I	160 µl PBS
Condition 2	160 µl ^{125}I	160 µl PBS
Condition 3	160 µl ^{125}I	200 µl PBS

Table 2.5.1
Table showing the 3 different volume conditions that were investigated with phosphorimaging.

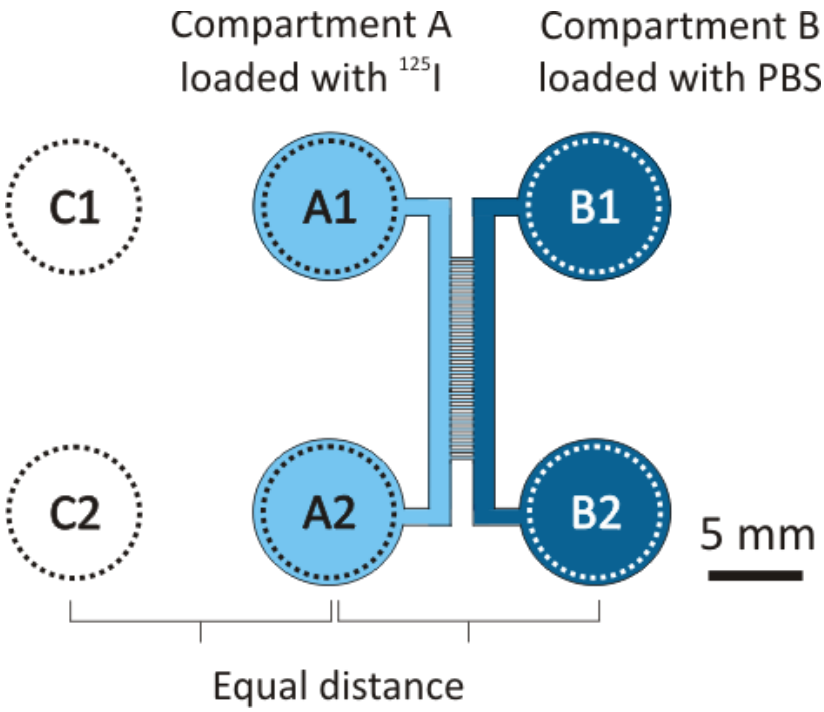

Figure 2.5.3
Schematic of the 2 compartment chamber showing the addition of ^{125}I to compartment A, and PBS to compartment B. The dashed circles in each of the medium wells represent the ROI used when quantifying the signal. In each compartment the signal was always quantified in the pair of medium wells, hence there are 2 values (1 and 2) for each compartment. C1 and C2 are ROI's placed the same distance from compartment A, as compartment B is from compartment A. These are used to quantify the signal produced by radioactive shine from the loaded compartment.

To quantify the flow of radioactive solution through the microgrooves, circular regions of interest (ROI) were drawn in ImageQuant that measured 6 mm in diameter (Figure 2.5.3). These ROI's were placed in each of the 4 medium wells, measuring 8 mm in diameter and pixel counts of detected signal were recorded. For each chamber, the values from the 2 wells of the compartment loaded with radioactivity, and the values from the 2 wells of the unloaded compartment were separately averaged. Despite the relatively long half-life of ^{125}I (60 days), this isotope is constantly decaying and emitting gamma rays in all directions, a process known as radioactive 'shine'. This is a continual process that will still occur during the 1 hour exposure of the chamber to the phosphor screen, as a result, upon scanning the screen a slight halo is sometimes observed around the radioactive sample. Therefore the effect of shine has to be taken into consideration when quantifying the signal in the unloaded compartment. To do this, control regions of interest which are the same size are placed the same distance from compartment A, as the distance between compartment A and compartment B. These regions of interest termed 'C' (Figure 2.5.3) will give a precise quantification of the signal produced by shine. As shine occurs in all directions, this value can be deducted from the values quantified in the regions of interest in compartment B. This gives a value that corresponds to the amount of radioactive solution that has moved from compartment A to compartment B. Due to the constant decay of the isotope over the 5 experimental days, the

movement is expressed as a percentage of total activity in a single chamber. This ensures the percentage of signal in compartment B is always relative to total signal, as this total will fractionally decrease over the 5 days due to the decay of the isotope. To calculate the level of activity that has moved from compartment A to compartment B whilst taking into account shine and isotope decay the following would need to be calculated:

= [(signal in compartment B – shine) / (total signal in the whole chamber – shine)] x 100

Therefore the equation using the ROI's in Figure 2.5.3 to quantify the percentage of total activity that has moved from compartment A to compartment B is:

= [(B1 + B2) – (C1 + C2) / (A1 + A2) + ((B1 + B2) – (C1 + C2))] x 100

2.6. Preparation for culture

Microfluidic chambers are prepared for culture 24 hours in advance by removing water from all medium wells and flooding the channels with 70 % ethanol to reduce microbiological contamination. The wells and glass bottomed culture dish are then also filled with 70 % ethanol to a level that covers the PDMS piece and left for a minimum of 30 minutes. Excess ethanol is then removed from the culture dish and medium wells. To ensure the channels are free of ethanol, a single medium well of all compartments is filled with sterile water. The water is then allowed to flow through the channel until the connected well is half full, meaning the volume in that compartment has equilibrated between the 2 wells. Water from all wells is then removed and this process is repeated 3 times. On the final wash, all water in the medium wells is removed and 20 µl of Poly-L-lysine (PLL, 0.1mg/ml in water, Biochrom AG, Berlin, Germany) is added into each compartment allowing the entire channel to be filled. The channel itself only has a fluid volume of approximately 3 µl, and this is the only region that needs to be treated with PLL. Excess PLL is however applied to each compartment to ensure the channel does not dry out during the incubation time. Chambers are then stored at 4˚C overnight. On dissection day, PLL is removed from the medium wells, and 20 µl laminin (30mg/ml in 50 mM Tris-HCl (pH 7.4), Invitrogen, Paisley, UK) is subsequently added to each compartment. A minimum of 2 hours at 4˚C is required for laminin incubation, after which excess laminin is removed before the cells are plated into the chambers.

2.7. DRG neuron culture

Time mated pregnant Sprague Dawley rats at E14.5, E15.5 and E16.5 or C57BL/6 mice at E13.5, E14.5 and E16.6 were culled humanely according to the Animals (Scientific Procedures) Act 1986, by a rising concentration of CO_2 or by cervical dislocation. The animals were housed in university facilities, on a 12-hour light-dark cycle and with food and water provided *ad libitum*. All embryos were harvested, and transferred to calcium-, magnesium- and phenol red-free Hank's balanced salt solution (HBSS) which contained 1X HBSS, (10 x HBSS, Invitrogen, Paisley, UK) 5 mM 4-(2-Hydroxyethyl)piperazine-1-ethanesulfonic acid) HEPES, and 10 mM D-glucose. Embryonic DRGs from all cervical, thoracic, lumbar and sacral segments were dissected in HBSS. This was performed

by pinning an embryo facedown onto a dissecting mat and carefully removing the skin from head to tail down the midline of the back allowing access to the spinal cord. Forceps are gently run down either side of the cord to free it from surrounding tissue. The cord is cut at the most rostral point before entry into the *foramen magnum* and gently removed intact from the embryo. Any remaining meninges are removed leaving all DRGs intact and easily accessible for dissection. The collected DRGs are then emzymatically digested in a solution containing 10 mg/ml collagenase type IV (Worthington Biochemical Corp. NJ, USA) and 12 mg/ml dispase type II (Roche Products Ltd. UK) (made up in HBSS) for 45 minutes at 37˚C. A single cell suspension is achieved by mechanically triturating the ganglia using fire-polished Pasteur pipettes. Cells were then loaded onto a Percoll (Sigma, Gillingham, UK) gradient to remove non-neuronal debris and centrifuged for 8 minutes (280 *x* g). After washing the cells in Neurobasal medium (1 x Neurobasal medium, L-glutamine free, Invitrogen Paisley, UK) to remove Percoll, cells were resuspended in complete Neurobasal medium supplemented with NGF, containing Neurobasal medium (Invitrogen, Paisley, UK), 2 % (v/v) B27 supplement (50 x B27 Supplement, Invitrogen, Paisley, UK), 0.416 mM L-Glutamine (Invitrogen, Paisley, UK), 1 % (v/v) penicillin-streptomycin (100 x penicillin-streptomycin solution, containing 10,000 units penicillin and 10 mg/ml streptomycin, Sigma, Gillingham, UK) and 200 ng/ml recombinant human NGF (gift from Genentech, CA, USA). 10 µl of complete Neurobasal medium, plus 200 ng/ml NGF was added to all compartments other than the somal compartment. Cells were plated in a volume of 2.5 µl into one of the openings of the somal compartment channel (Figure 2.7.1). Capillary action drew the cell suspension along the entire compartment length, resulting in an even distribution of cells throughout the somal channel. 2.5 µl is approximately the volume required to fill the channel. In later imaging experiments, only cells which have adhered in the channel can be functionally analysed, therefore plating a larger volume will result in cells flowing into the medium wells, increasing wastage of the cell suspension. Cells were left to adhere for a minimum of 2 hours before flooding each compartment with 200 µl (2 compartment) or 100 µl (3 compartment) of complete Neurobasal medium plus 200 ng/ml NGF.

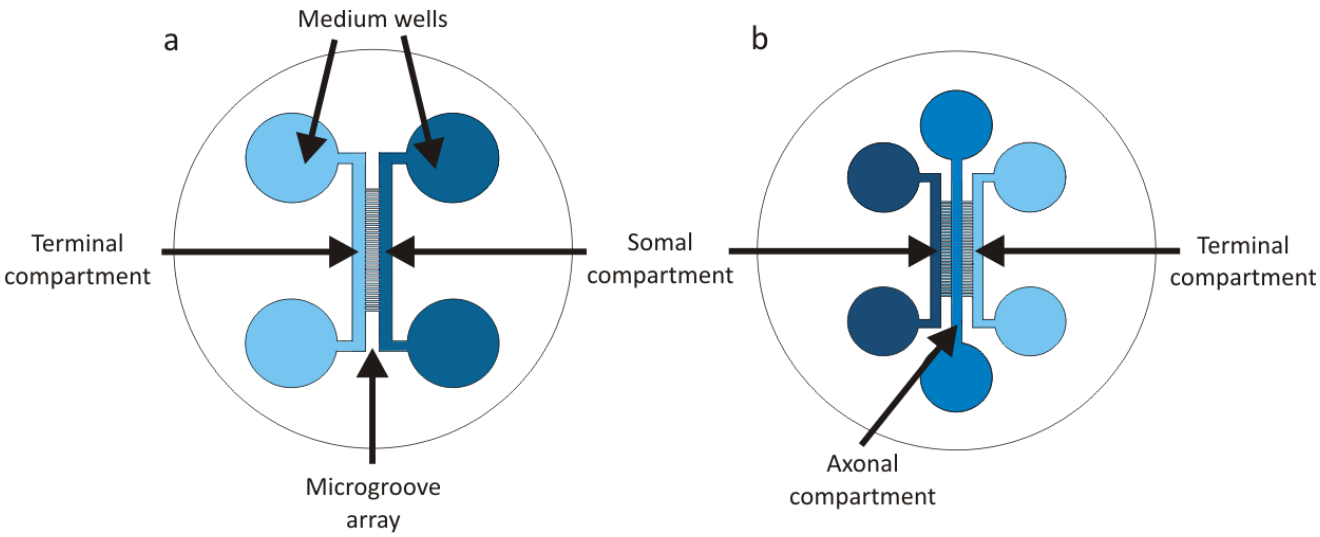

Figure 2.7.1
Schematic of the (a) 2 compartment and (b) 3 compartment microfluidic chambers showing the individual compartments and microgroove arrays.

2.8. Medium changes and chemo-attraction protocol

The microgroove array establishes a very high fluidic resistance between adjacent compartments. By maintaining a volume difference between compartments a hydrostatic pressure imbalance is created, resulting in a slow but steady flow from the compartment with the greater volume. In order to encourage axonal growth through the microgroove array the fluidic resistance is exploited to create a uni-directional NGF gradient across the array (Table 2.8.1). This encourages the growth of the axons from the somal compartment towards the higher concentration of NGF, through the microgrooves and into the terminal compartment (Figure 2.7.1a). In 3 compartment chambers the axons are encouraged to grow through two microgroove arrays. This is done by initially encouraging the growth into the middle axonal compartment (Figure 2.7.1b) using an NGF gradient, then switching the high concentration of NGF to the distal terminal compartment (Table 2.8.2). In the 3 compartment chambers, the soma, axon and sensory terminals are isolated in their own individual compartment.

2 Compartment protocol	Somal compartment	Terminal compartment
Day 0	200 ng/ml NGF in 200 µl	200 ng/ml NGF in 200 µl
Day 1	20 ng/ml NGF in 160 µl	200 ng/ml NGF in 200 µl
Day 3	0 ng/ml NGF in 160 µl	200 ng/ml NGF in 200 µl
Days 5, 7 and 9	0 ng/ml NGF in 200 µl	200 ng/ml NGF in 200 µl

Table 2.8.1
Chemo-attractant protocol for the 2 compartment chamber

3 Compartment protocol	Somal compartment	Axonal compartment	Terminal compartment
Day 0	200 ng/ml NGF in 100 µl	200 ng/ml NGF in 100 µl	200 ng/ml NGF in 100 µl
Day 1	20 ng/ml NGF in 80 µl	200 ng/ml NGF in 100 µl	200 ng/ml NGF in 100 µl
Day 2	0 ng/ml NGF in 80 µl	20 ng/ml NGF in 100 µl	200 ng/ml NGF in 120 µl
Day 3	0 ng/ml NGF in 80 µl	0 ng/ml NGF in 80 µl	200 ng/ml NGF in 100 µl
Days 5, 7 and 9	0 ng/ml NGF in 100 µl	0 ng/ml NGF in 100 µl	200 ng/ml NGF in 100 µl

Table 2.8.2
Chemo-attractant protocol for the 3 compartment chamber

The medium was changed on the indicated days by gently removing all fluid from the medium wells, without removing the medium in the channels. Medium is slowly applied first to the somal compartment followed by adjacent compartments. 5 µM Cytosine β-D-arabinofuranoside (ara-C, stock 5 mM dissolved in H_2O, Invitrogen, Paisley, UK) was added only to the complete Neurobasal medium being applied to the somal compartment between days 1 and 3 to inhibit DNA replication in dividing cells. After 2 to 3 days of ara-C treatment to the somal compartment, the resulting culture contained only DRG neurons and non-neuronal cells could no longer be observed.

2.9. Retrograde tracing in the compartmentalised chambers

In order to identify neurons that successfully projected from the somal compartment to the terminal compartment, 1,1'-dioctadecyl-3,3,3',3'-tetramethylindocarbocyanine perchlorate (DiI, Invitrogen, Paisley, UK, stock 2 mg/ml dissolved in Dimethyl sulfoxide (DMSO), used at 40 µg/ml in complete Neurobasal medium plus 200 ng/ml NGF) retrograde tracing is used. Medium was removed only from the terminal compartment and 50 µl of medium supplemented with DiI was added. The hydrostatic pressure imbalance corresponding to over a 100 µl volume difference across the microgrooves resulted in the terminal compartment being fluidically isolated. Therefore, only cells with axons projecting through the microgrooves come into contact with DiI. As a result only these cells will become DiI labelled in the cell soma as these will actively transport DiI in the retrograde direction. Cells without projecting axons are not exposed to DiI and therefore will not become labelled. Sensory terminals were incubated with DiI for 90 minutes at 37˚C, after which DiI was washed out with extracellular fluid (ECF). DiI labelled cell bodies were imaged with a 10 x FLUAR objective and SP 580 exciter filter, DCLP 595 dichroic mirror and BP 645/75 emitter filter, on a Zeiss

Axiovert 200 inverse microscope and an air-cooled CCD Imago Camera (TILL photonics, Germany). An excitation wavelength of 549 nm was produced using a Till Photonics *Polychrome IV* monochromator at 1000 ms exposure time.

Retrograde tracing in the 3 compartment chambers involved loading DiI in the terminal compartment, and 3,3'-Dioctadecyloxacarbocyanine Perchlorate (DiO, Invitrogen, Paisley, UK, stock 1 mg/ml dissolved in DMSO, used at 40 µg/ml in complete Neurobasal medium) into the middle axonal compartment. 50 µl of medium supplemented with DiO is added to the middle compartment and incubated for 90 minutes at 37˚C, DiI and DiO incubation was performed simultaneously. After the incubation, DiO was washed out with ECF. The different spectral properties of this tracer allow for the distinction between neurons that have projected through two microgroove arrays, and would therefore be positive for DiI and DiO in the soma, and neurons that have projected through one microgroove array, and would therefore only be positive for DiO. DiO labelled cell bodies were imaged with a 10 x FLUAR objective on a Zeiss Axiovert 200 inverse microscope and a DCLP 515 dichroic mirror with a BP 535/30 emitter filter. An excitation wavelength of 480 nm was produced using a Till Photonics *Polychrome IV* monochromator at 1000 ms exposure time.

2.10. Calcium imaging and visualisation of response

Usually 2 or 3 compartments were imaged after 7 or 8 days *in vitro* (DIV), to allow the establishment of a dense axonal network. The general exception to this are experiments in Chapters 3 and 6, where chambers are imaged at earlier and later time-points. Ratiometric calcium responses were always recorded from the cell bodies which were loaded with the calcium indicator Fura-2. To load the soma, 100 µl of complete Neurobasal medium containing 2 µM Fura-2 AM (derived from a stock solution of 2 mM dissolved in DMSO, Invitrogen, Paisley, UK) and 80 µM Pluronic acid (Invitrogen, Paisley, UK) is added to the somal compartment and incubated for 45 minutes at 37˚C. Fura-2 loading is done simultaneously with DiI loading. Therefore, 45 minutes after application of DiI, culture dishes are removed from the incubator, all medium in the wells of the somal compartment is removed and the Fura-2 AM supplemented medium is rapidly applied. The chamber is then immediately put back into the 37˚C incubator. Afterwards all compartments are washed with ECF and the culture chamber transferred to the recording stage mounted on a Zeiss Axiovert 200 inverse microscope and viewed with appropriate filters to view the fluorophores. A 10 x FLUAR objective and a DCLP 410 dichroic mirror and LP440 emitter filter were used for calcium imaging. Pairs of images at excitation wavelengths of 340 nm and 380 nm were captured every two seconds using a Till Photonics *Polychrome IV* monochromator at 200 - 400 ms exposure time. TILLvisION 4.0 software was used to analyse ratios of fluorescent images to give a time locked, pixel by pixel representation of intracellular calcium changes. Ratios are displayed as pseudocolour images representing the magnitude of each cellular calcium response. Stimuli are applied to the channel through a gravity-driven, time-linked application system (Dittert et al., 2006) with magnetic valves allowing for rapid fluid exchange rates. WAS97 software was used to programme the protocol, and

control the time locked release of solutions through the magnetic valves. Opening of a valve released the flow of stimulant or buffer through an applicator which was placed in one of the medium wells of the compartment to be stimulated. The applicator could easily be moved between different compartments whilst keeping the imaging area in exactly the same place (Figure 2.10.1 and Figure 2.10.2). This allowed the responses in the cell bodies of the same population to be analysed separately from either somal or terminal stimulation. A suction device was placed in the connected medium well of the same compartment, so that a steady and continuous flow was established through the channel of interest (Figure 2.10.1 and Figure 2.10.2).

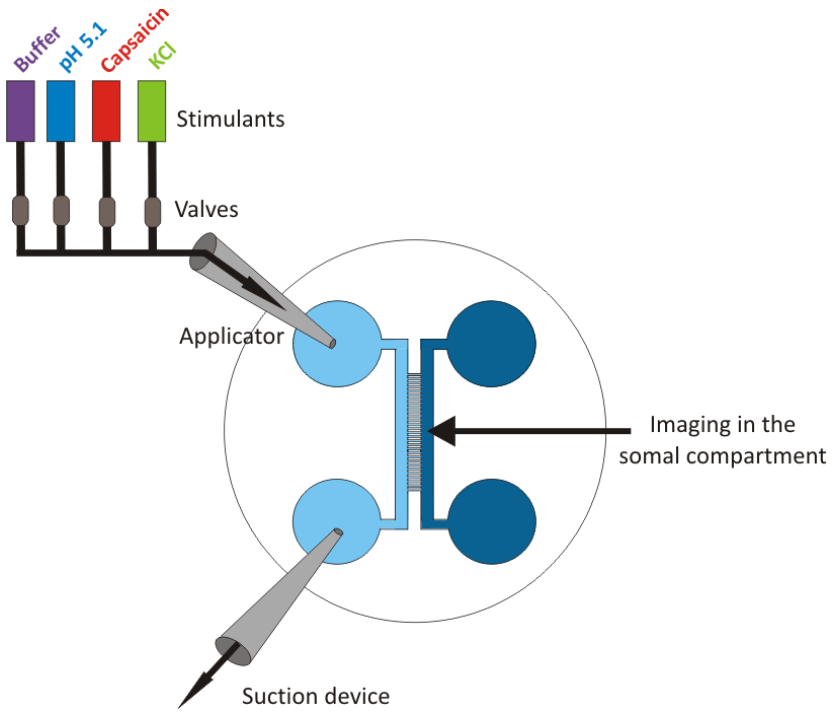

Figure 2.10.1
Schematic showing the imaging preparation in a 2 compartment system. Buffer or stimulants are continuously delivered to a specific compartment, the flow runs through the channel and is removed with a suction device placed in the connecting medium well of the same compartment.

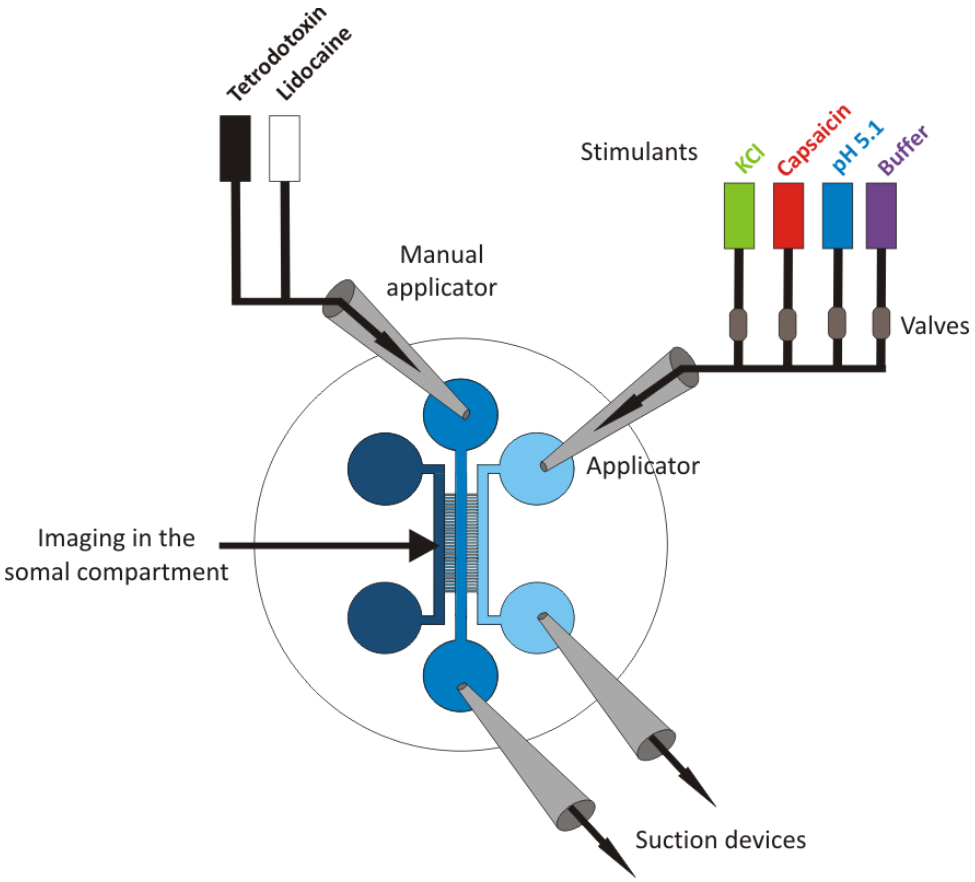

Figure 2.10.2
Schematic showing the imaging preparation in a 3 compartment system. Pharmacological agents can be delivered to the middle axonal compartment manually, whilst the terminals are separately stimulated.

All stimulants and pharmacological agents were made in ECF on the day of the experiment. ECF is composed of 145 mM NaCl, 5 mM KCl, 10 mM HEPES, 10 mM D-Glucose, 2 mM $CaCl_2$ and 1 mM $MgCl_2$ buffered to pH 7.4 with 1 M NaOH. ECF with high K^+ concentration was used as a neuronal depolarising agent (100 mM NaCl, 100 mM KCl, 10 mM HEPES, 10 mM D-Glucose, 2 mM $CaCl_2$ and 1 mM $MgCl_2$ buffered to pH 7.4 with 1 M NaOH). Pharmacological agents included Tetrodotoxin with citrate buffer (Tocris Biosciences, Bristol, UK) used at a range of concentrations from 10 nM to 10 µM (stock aliquot, 1 mM in H_20), Lidocaine Hydrochloride (Sigma, Gillingham, UK) used at a range of concentrations from 0.1 mM to 10 mM (stock aliquot, 1 M in H_20). Amiloride (Invitrogen, Paisley, UK) used at 100 µM (stock aliquot, 100 mM in DMSO). Stimulants included, Capsaicin (Invitrogen, Paisley, UK) used at a range of concentrations from 10 nM to 100 µM (stock aliquot, 20 mM dissolved in 100 % ethanol). Menthol used at 250 µM (stock aliquot, 2 M in 100 % ethanol), Mustard oil used at 100 µM (stock aliquot, 1 M in 100 % ethanol). For proton stimulation, the pH of ECF was modified with the addition of 1 M HCl to the required proton concentration. HEPES was used as a buffer in all pH solutions. All pH solutions were made fresh on the day of experimentation and pH was tested after experiments were completed. No change in pH was

detected at this second reading, indicating the pH remained constant throughout the experimental day.

At all times during the imaging protocol, the compartments not receiving the stimuli contained a greater volume of ECF than the compartment receiving the stimuli, ensuring stimulant did not diffuse into adjacent compartments. Stimulants or buffer were delivered by an applicator placed close to the channel entrance in a well in the compartment undergoing stimulation. In the adjoining well a suction device is placed close to the channel entrance, therefore the stimulant or buffer flows through the channel and is rapidly removed upon reaching the suction device in the connected well. This ensures that at any one point during the entire experiment there is only ever a small volume in the compartment undergoing stimulation. All other compartments are filled with approximately 200 µl of ECF, therefore the compartment being stimulated is fluidically isolated from other compartments ensuring stimulants do not diffuse through the microgrooves.

2.11. Data analysis and statistics

For each set of results, the number of neurons and experiments are displayed in text as ($n_{neurons}$= X, $n_{experiments}$= Y). $n_{neurons}$ refers to the total number of cells analysed. $n_{experiments}$ refers to the number of embryonic litters used. DRGs from one embryonic litter ($n_{experiments}$ = 1) were pooled and subsequently divided between chambers. For large litters, embryos were divided into 2 separate groups. DRGs from each group of embryos were dissected, pooled and during all steps were cultured separately. In these cases where embryonic litters were split and cultured separately $n_{experiments}$ = 2. All quantitative comparisons are presented as the arithmetic mean ± the standard error of the mean (SEM). Averages from one experiment were used to compute group means and measures of group variance. Statistical tests were performed using Statistica 6 software (Statsoft, Tulsa, OK, USA). Specific statistical tests are indicated in text.

Chapter 3:

Calcium imaging can be used to investigate the functional properties of sensory neurons *in vitro*

3.1. Introduction

Stimulus transduction and action potential propagation are fundamental to the mechanisms that underlie the detection of stimuli encountered in daily life. A range of techniques have been devised in an attempt to study these processes, including *in vivo*, *ex vivo* and *in vitro* methods, with each approach offering its own advantages and disadvantages. In theory, the ideal scenario would enable the study of human sensory neuron properties *in situ* where the natural environment of the cell is unaffected. The development of microneurography by Vallbo and Hagbarth in 1968, enabled just this, and provided fascinating insights into the excitability of sensory neurons. However, the requirement for molecular and genetic analysis of sensory neurons often requires the dissection of the soma, prohibiting the use of human subjects. Therefore, sensory neuron physiology is often investigated in anaesthetised animals, as first described by Adrian in 1926, and can be combined with post-recording immunocytochemistry by labelling the investigated cell by dye injection directly through the recording electrode, followed by perfusion of the animal and tissue processing (Fang et al., 2002). Alternatively, the whole peripheral sensory pathway including the skin, nerves, DRGs and spinal cord can be dissected intact and investigated in an *ex vivo* setup (Koerber and Woodbury, 2002). These techniques offer valuable information regarding neuronal excitability but often involve a demanding dissection or additional problems associated with maintaining the animal whilst performing the experiment. To circumvent these complications, *in vitro* experimentation is often used as a popular alternative. For example, *in vitro* heterologous expression experiments have proved to be successful in the detection of several molecules crucial for stimulus transduction, including the capsaicin receptor – TRPV1 (Caterina et al., 1997). Whilst heterologous expression allows the study of individual proteins, *in vitro* experiments using dissociated DRG neurons allow the entire molecular phenotype to be characterised in a more physiological context. This has helped to uncover the expression profile of many important sensory transduction proteins and determine distinct functional differences between DRG subpopulations. The feasibility of an *in vitro* approach has led to patch clamping and calcium imaging becoming indispensable tools in sensory physiology research.

In vitro methods often involve recording from, and directly stimulating, the cell body. This experimental approach is generally used to model the expression of transduction proteins and therefore the functional properties of the peripheral receptive terminals. However, responses recorded from the soma may not necessarily represent the functional expression of ion channels in the terminals and axon. Crucially, it is these peripheral structures which are primarily responsible for stimulus transduction in the intact neuron. Furthermore, the receptive terminals of sensory neurons can be located a vast distance away from the soma – in humans over 1 m, which raises the question how the sensitivity of the terminals is regulated at such distance. Conventional *in vitro* mass culture of DRG sensory neurons does not allow the neuronal microenvironments to be manipulated making it impossible to study differential mechanisms influencing distinct regions of the neuron. Additionally, whilst cellular transduction mechanisms can be studied using acutely dissociated

sensory somata, action potential propagation cannot be investigated as the axon is severed during dissection. Therefore, compartmentalised chambers have been developed in which axonal regrowth is directed into a separate compartment to the soma allowing the study of individual neuronal regions in isolation.

Compartmentalised chambers have improved significantly in recent years as a result of major advancements in the field of nanotechnology. This technology is now crucial for the accurate fabrication of compartmentalised microfluidic chambers, which provide a robust and reproducible method to study the properties of neuronal terminals and axons in isolation from the cell soma. Importantly, with intact axons, this *in vitro* system enables the study of sensory transduction at the terminals, and action potential propagation in the axon – providing a significantly more accurate representation of the neuron compared to studying the cell somata alone.

This chapter focuses on using this technology to investigate action potential propagation *in vitro.* First, I use a sensitive radioactive method to prove the individual compartments are fluidically isolated. Next, I show that neurites that have grown through the microgroove array can be retrogradely labelled and that these neurons can also propagate action potentials. I go on to use the compartmentalised chambers to accurately apply pharmacological agents at various concentrations to investigate the inhibitory effect on action potential propagation, and determine subpopulations based on single cell pharmacokinetics. Finally, I use movement of buffer flowing over discrete neuronal regions as a low-threshold mechanical stimuli to study if the sensory terminals and soma are mechano-sensitive.

3.2. Objectives

The initial aim of this set of experiments was to establish the novel use of functional calcium imaging within microfluidic chambers, by attempting to record somal calcium transients evoked by stimulation of the terminals. The second major objective was to detect projecting axons with retrograde tracing and measure the reproducibility of the somal depolarisation induced by stimulation of the terminals. The third major aim was to pharmacologically investigate action potential propagation in this *in vitro* preparation so that comparisons can be made with *in vivo* experiments.

3.3. Microgrooves create a fluidic barrier between compartments

In this study devices with one or two microgroove arrays were used (Figure 3.3.1a, b). In order to specifically stimulate the somata, axons or terminals of DRG neurons, the neurites were encouraged to grow through the microgroove array into a fluidically isolated compartment (Figure 3.3.1). Fluidic isolation occurs when there is a hydrostatic pressure imbalance, corresponding to a volume difference across compartments. To investigate the rate at which a 40 µl difference equilibrates across the microgroove array, a highly sensitive radioactive method was used. Radioactive ^{125}I solution was added to a single compartment in a 2 compartment chamber with PBS added to the adjacent compartment (Figure 3.3.2a, detailed description of quantification in Figure 2.5.3). The accumulation of radioactivity in the adjacent compartment was measured by placing the chamber on a phosphor screen, exposing for 1 hour, scanning the screen with a phosphorimager and quantifying the resulting signal. It was expected that no flow of radioactivity into the adjacent compartment would result in no visible pseudocolour signal (Figure 3.3.2 b). A small accumulation of radioactivity in the adjacent compartment was expected to be visualised as a faint accumulation of false colour signal (Figure 3.3.2c). As the pseudocolour signal is directly proportional to the amount of radioactivity, an increase in radioactive accumulation in the adjacent compartment was anticipated to result in an increase in pseudocolour intensity (Figure 3.3.2d). 3 volume differences were investigated as described in the Materials and Methods (Table 2.5.1), where the radioactive ^{125}I solution was in lower, equal and greater volume than the PBS in the adjacent compartment.

Immediately after addition of the solutions to the chambers no signal is observed in the adjacent compartment in all volume conditions tested (Figure 3.3.3a and Figure 3.3.4a) indicating the microgroove array provides an initial barrier to fluid flow between the 2 compartments. To investigate the extent to which this barrier inhibits the flow between compartments, measurements were taken on subsequent days. By 24 hours, a signal is detected in the adjacent compartment only when the radioactive volume difference is greater than the PBS volume (Figure 3.3.3b), this was quantified as 1.4 ± 0.2 % ($n_{experiments}$ = 4) of the total amount of radioactive signal (Figure 3.3.4). When the ^{125}I solution is added in a lower or equal volume no signal is detected in the adjacent compartment with -0.1 ± 0.2 % ($n_{experiments}$ = 4) and -0.2 ± 0.1 % ($n_{experiments}$ = 4) respectively, of total radioactive signal. These values for the lower and equal volume conditions were both significantly different ($p<0.001$, 2-way analysis of variance (ANOVA) with Bonferroni post hoc-test, Figure 3.3.4b) compared to the volume condition when the ^{125}I solution is in a greater volume. The slightly negative values at the 24 hour time point for the lower and equal volume conditions mean that the signal produced by radioactive shine is greater than the emitted activity of any radioactive solution that has travelled through the microgrooves, into the adjacent compartment, essentially meaning that there has been no detectable movement of radioactive solution from the radioactive loaded compartment A to the unloaded compartment B. The detected signal in chambers loaded with a greater volume of ^{125}I solution continued to increase over subsequent days reaching 2.1 ± 0.1 % ($n_{experiments}$ = 4) at 48 hours, 3.1 ± 0.1 % ($n_{experiments}$ = 4) at 72 hours and 4.2 ± 0.1 % ($n_{experiments}$ = 4) at

96 hours. When reversing the conditions, loading of ^{125}I in a lower volume resulted in an undetectable signal until 96 hours at which point, 0.6 ± 0.2 % ($n_{experiments}$ = 4) of total activity was detected in compartment B. In conditions in which ^{125}I solution and PBS were in equal volume 0.5 ± 0.1 % ($n_{experiments}$ = 4) was detected in the adjacent compartment at 48 hours, 1.1 ± 0.1 % ($n_{experiments}$ = 4) at 72 hours and 2.5 ± 0.2 % ($n_{experiments}$ = 4) at 96 hours. At 48, 72 and 96 hours, the accumulation of radioactivity in the unloaded compartment was significantly greater ($p<0.001$ for every time point, 2-way ANOVA with Bonferroni post hoc-test) when the ^{125}I solution was in a larger volume compared to equal and lower volume conditions (Figure 3.3.4b).

The relatively fast accumulation of detected signal in the adjacent compartment, at 24 hours, when ^{125}I solution was loaded in a greater volume reflects the flow of ^{125}I solution down the hydrostatic pressure gradient, through the microgroove array and into the adjacent compartment. The linear increase in accumulation after 24 hours suggests that the volumes have not equilibrated, and ^{125}I is continuing to move down a hydrostatic pressure imbalance into compartment B (Figure 3.3.4a). In the reverse condition, when ^{125}I solution is in a lower volume, accumulation of radioactive signal proceeds at a considerably slower rate due to the need to first equilibrate. After the volumes are equal which appears to occur between 72 and 96 hours (Figure 3.3.4a), radioactivity will be able to diffuse through the microgroove array by Brownian motion. This diffusion will occur at a considerably slower pace than movement down a pressure gradient, hence the small accumulation at 96 hours. In the final volume condition, when volumes are equal from the start, all movement of radioactivity will be due to diffusion; therefore this condition quantifies the movement that is entirely dependent on passive diffusion. In conclusion, fluidic isolation is maintained for up to 72 hours as long as a unidirectional hydrostatic pressure imbalance is maintained. Even in conditions with equal volume the microgroove array provides such a robust fluidic barrier that compartmental isolation is maintained up to 24 hours.

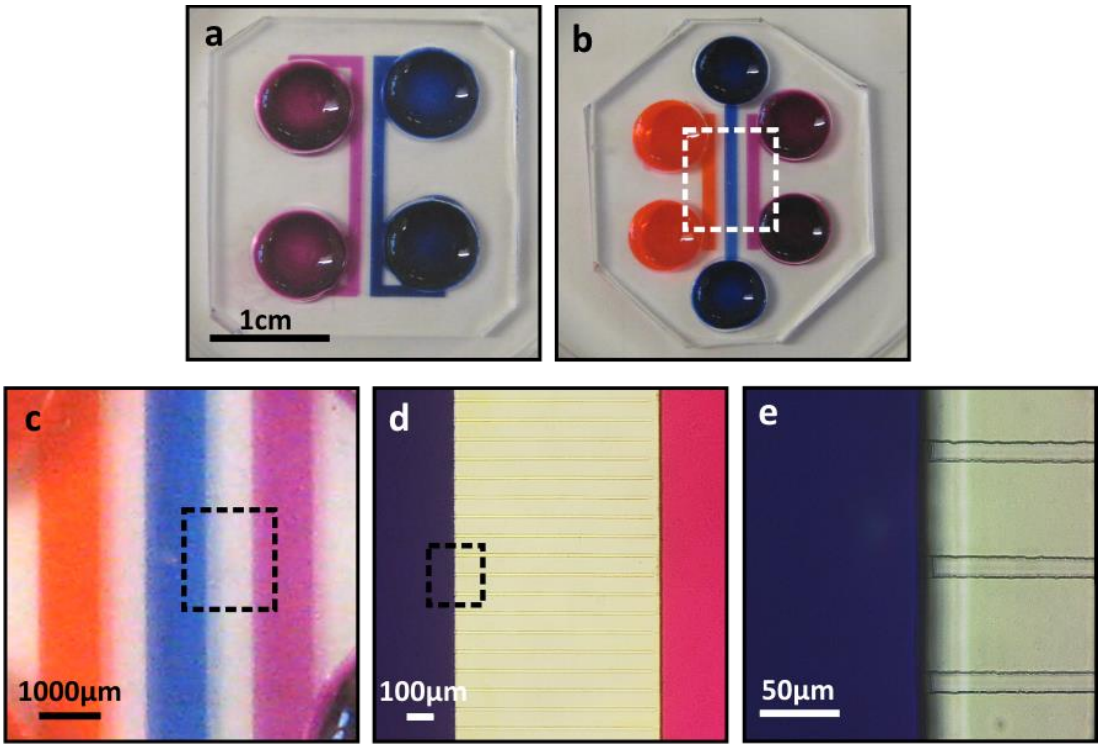

Figure 3.3.1
Microgrooves create a fluidically isolating barrier between compartments. (a), Image of a two compartment chamber, with dyes illustrating the fluidic isolation between the 2 compartments. (b), Image of the three compartment chamber. (c), Enlargement of the boxed area in (b) illustrating the separate compartments. (d), Enlargement of the boxed area in (c), showing a microscopic image of the microgrooves connecting a channel filled with ruthenium red with another filled with Evan's blue. (e), Enlargement of the boxed area in (d), showing a microscopic image of 3 individual microgrooves at the compartment border, each microgroove is 10 µm in width.

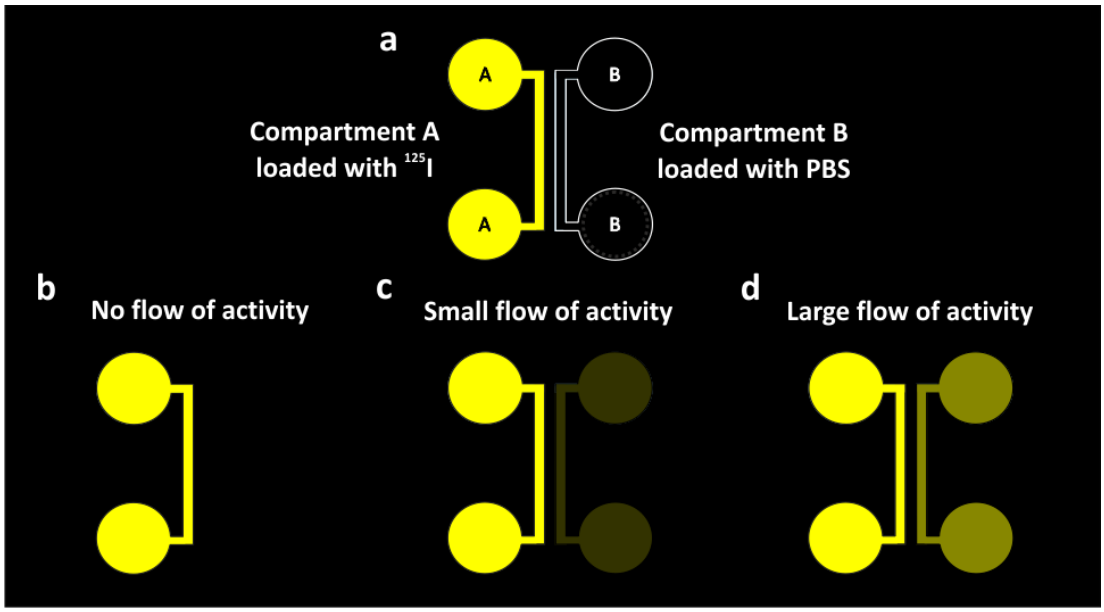

Figure 3.3.2
Schematic figure demonstrating the loading of radioactivity and PBS in separate compartments, and the anticipated results of radioactive flow. (a) Radioactive ^{125}I solution is loaded into compartment A, non-radioactive PBS solution is loaded into compartment B. Flow of radioactive solution into compartment B is detected by phosphorimaging and signal is displayed as a representative pseudocolour image. (b) If there is no flow of activity, only the compartment loaded with ^{125}I solution is visible upon imaging. (c) It is anticipated a small flow of radioactivity into compartment B will result in a low signal displayed as a faint accumulation of (false) colour. (d) Upon a larger accumulation of radioactivity in compartment B, the detectable signal is greater and therefore the false colour representation will appear brighter.

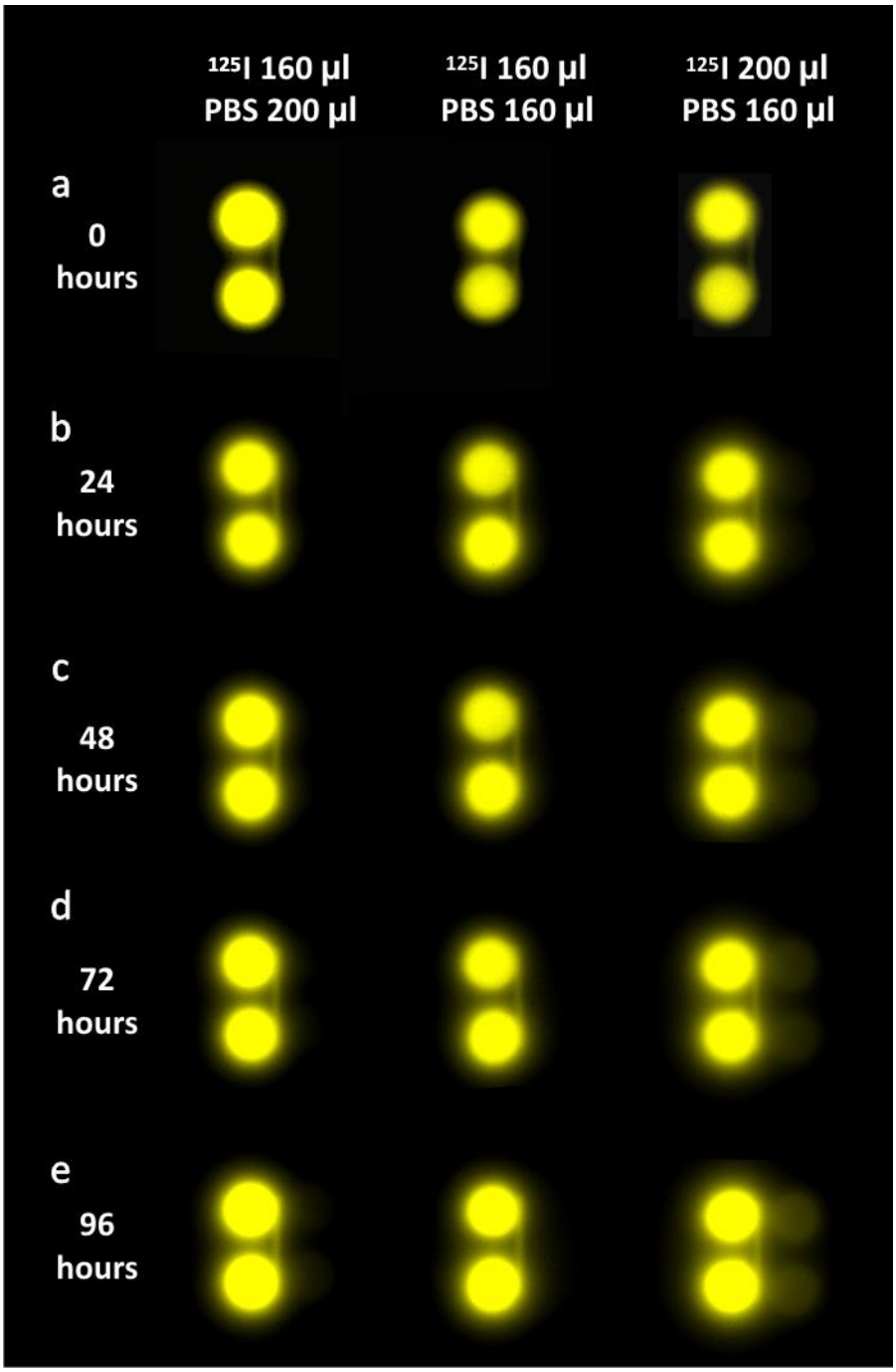

Figure 3.3.3
Fluidic isolation can be maintained with a hydrostatic pressure imbalance across the microgroove array. (a-e) Phosphorimaging pseudocolour images of radioactive signal when scanned at (a) 0 hours, (b) 24 hours, (c) 48 hours, (d) 72 hours and (e) 96 hours. The compartment loaded with radioactivity (left compartment) is clearly observed. Accumulation of activity on the unloaded compartment is seen over time when the radioactive solution is in a greater volume.

a

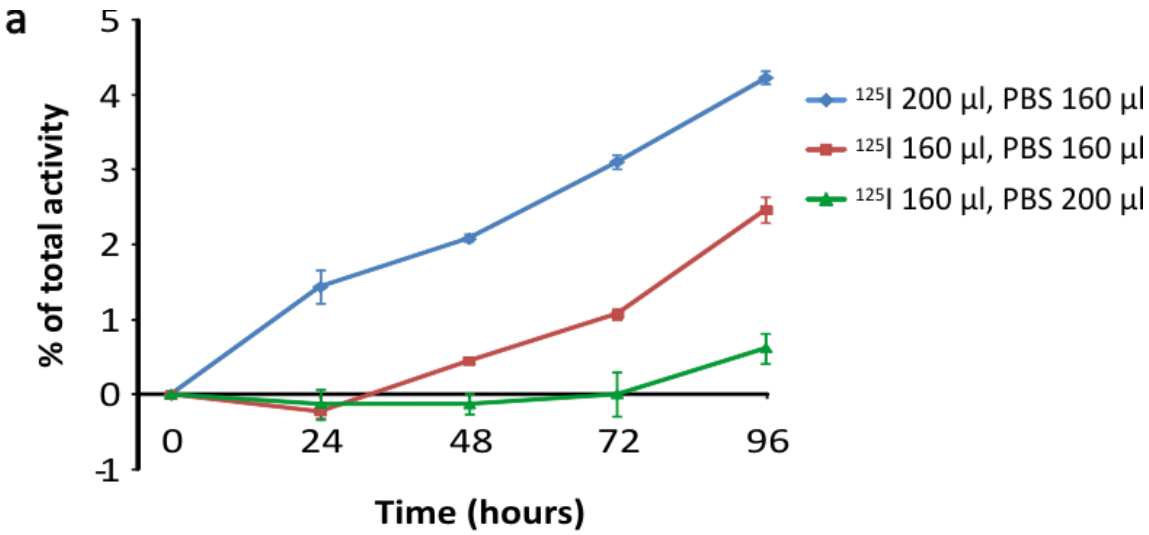

b

	24 hours	48 hours	72 hours	96 hours
^{125}I 200 µl, PBS 160 µl **vs** ^{125}I 160 µl, PBS 160 µl	***	***	***	***
^{125}I 200 µl, PBS 160 µl **vs** ^{125}I 160 µl, PBS 200 µl	***	***	***	***
^{125}I 160 µl, PBS 160 µl **vs** ^{125}I 160 µl, PBS 200 µl	ns	ns	***	***

Figure 3.3.4
*Quantification of radioactivity on unloaded side, as a percentage of total activity in the entire chamber. (b) Table showing the statistical significance when comparing between volume conditions at the different time points, (*** p<0.001, ** p<0.01, * p<0.05, ns - not significant, 2-way ANOVA with Bonferroni post-hoc test).*

3.4. Potassium Chloride application to the receptive terminals evokes a somal depolarisation

In order to examine the receptive properties of the sensory terminals in isolation a method to functionally detect all projecting axons was required. The non-selective neuronal depolarising agent of 100 mM KCl was applied exclusively to the terminals and then separately to the soma. Measurements of intracellular calcium concentration were performed by imaging the fura-2 loaded cell soma, whilst applying a time-locked stimulation protocol to a specific neuronal region (Figure 3.4.1a). In a single experiment, exactly the same field of cell somata are imaged during stimulation of the terminals and stimulation of the soma. Although the terminals of sensory neurons were exposed to KCl for a 30 second-long stimulus period the somal calcium response were transient in nature, rapidly peaking and returning to baseline in several seconds (Figure 3.4.1b). The baseline between KCl stimulation was stable, with very few fluctuations and no gradual incline which would indicate calcium accumulation in the somata (Figure 3.4.1b). Upon direct KCl stimulation of the soma, the baseline usually does not completely recover to pre-stimulus level with a 5 minute inter-stimulus period. Furthermore, the calcium peak usually lasted for longer than the 30 second stimulus period. In an average chamber, approximately 100 cells could be imaged using a x10 objective. Cells that were activated by KCl stimulation of the terminals responded with a rapid calcium influx in the soma (Figure 3.4.1c). Responses were scored as positive when the calcium peak is time-locked to the onset of the stimulus (Figure 3.4.1b). Furthermore the amplitude of the calcium peak must greatly exceed any baseline fluctuations. Cells are excluded from further analysis if fluctuations in calcium concentration occurring between stimuli are greater in amplitude than calcium peaks elicited by stimulation. The amplitude of a time-locked response must exceed 0.1 ΔF/F (delta ratio of 340nm fluorescence/380nm fluorescence) to be positively classified as a response. The amplitude of a calcium peak induced by stimulation of the terminals is generally smaller than that measured from direct stimulation of the soma. On average a peak from stimulation of the terminals is between 0.6 to 0.8 ΔF/F, whereas direct somal stimulation usually results in a peak between 0.8 to 1.0 ΔF/F.

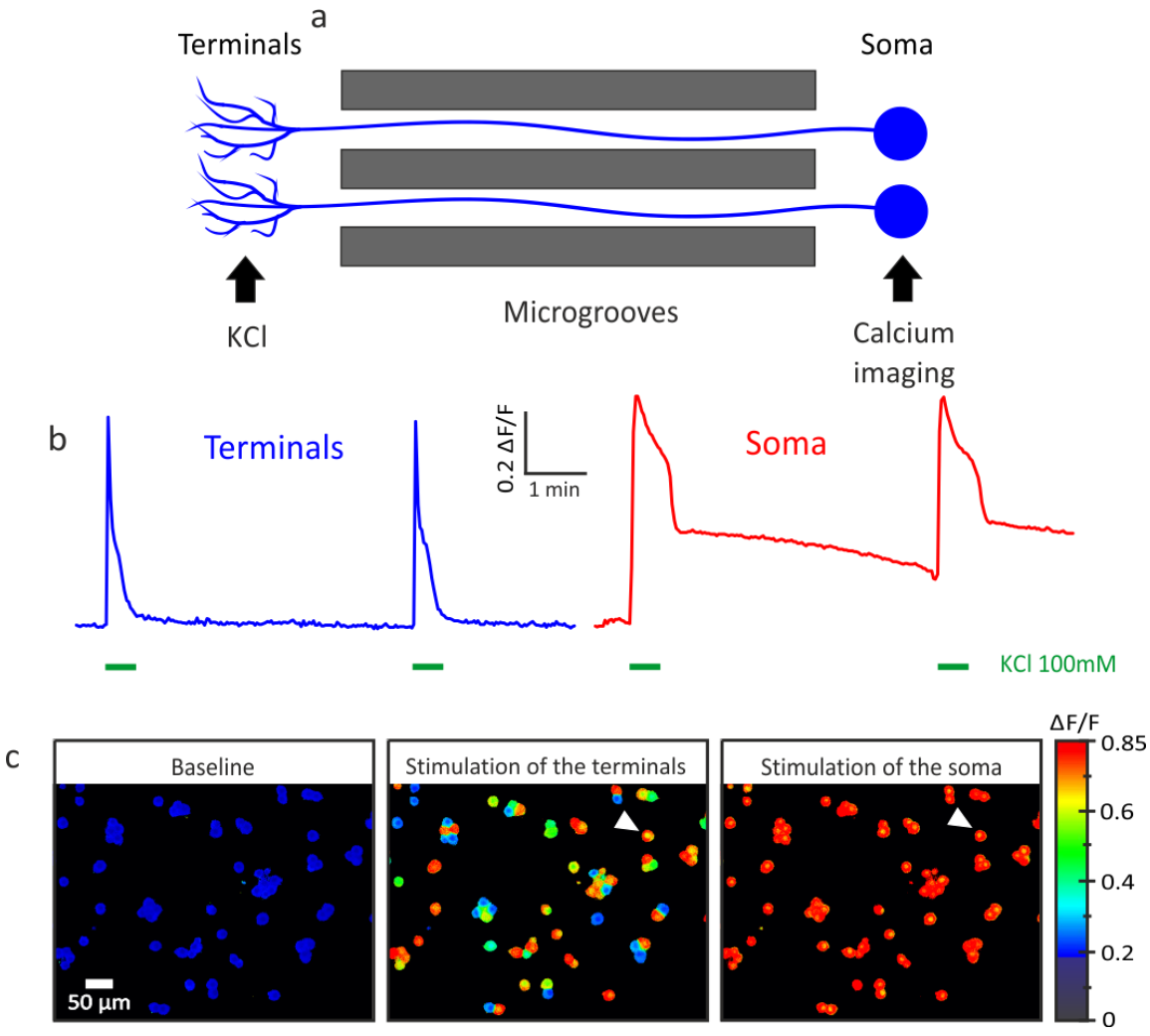

Figure 3.4.1
Stimulation of the terminals results in a somal calcium influx. (a), Schematic showing neurons growing through the microgrooves, the location of the KCl stimulus at the terminals and recording of calcium transients in the fura-2 loaded cell somata. (b), Representative calcium transients recorded from the cell soma (arrowhead in c) during a stimulation protocol of 2 KCl applications to the terminals and subsequently to the soma. (c), From left to right, representative field of fura-2 loaded cells at baseline, during the peak calcium response from stimulation of the terminals and the calcium response from stimulation of the soma.

3.5. Sensory neuron terminals can be repeatedly stimulated in rat DRG cultures

To test the reproducibility of the intracellular calcium change in response to repetitive stimulation of the terminals, I used a protocol with 9 consecutive KCl stimulations with an interstimulus period of 5 minutes. The repetitive stimulation protocol was applied to the terminal compartment of a 2 compartment system. Cultures were imaged at 7 DIV to allow sufficient time for neurons to grow a process into the adjacent compartment. In each culture, the number of neurons responding to the first KCl stimulation of the terminals (Figure 3.5.1b) was set as the 100 % value. Repeated stimulation of the sensory terminals resulted in a very reproducible calcium response in the cell soma (Figure 3.5.1c, d, e, f). After 4 stimulations 93 ± 2 % (n_{cells} = 555, $n_{experiments}$ = 8) (Fig 3.5.1e, f, g) of neurons continued to exhibit a robust calcium transient and only 27 ± 4 % (n_{cells} = 555, $n_{experiments}$ = 8) of neurons demonstrated tachyphylaxis after 8 stimuli (Figure 3.5.1g). All responding cells were always activated by the first KCl stimulus and cells were not recruited by later stimuli that did not respond to the first stimulation.

This demonstrates that the majority of neurons are able to repeatedly respond to stimuli applied to the terminals. The effect of tachyphylaxis over a repetitive stimulation protocol was important to know so that this could be taken into account when analysing the effect of inhibitory pharmacological compounds.

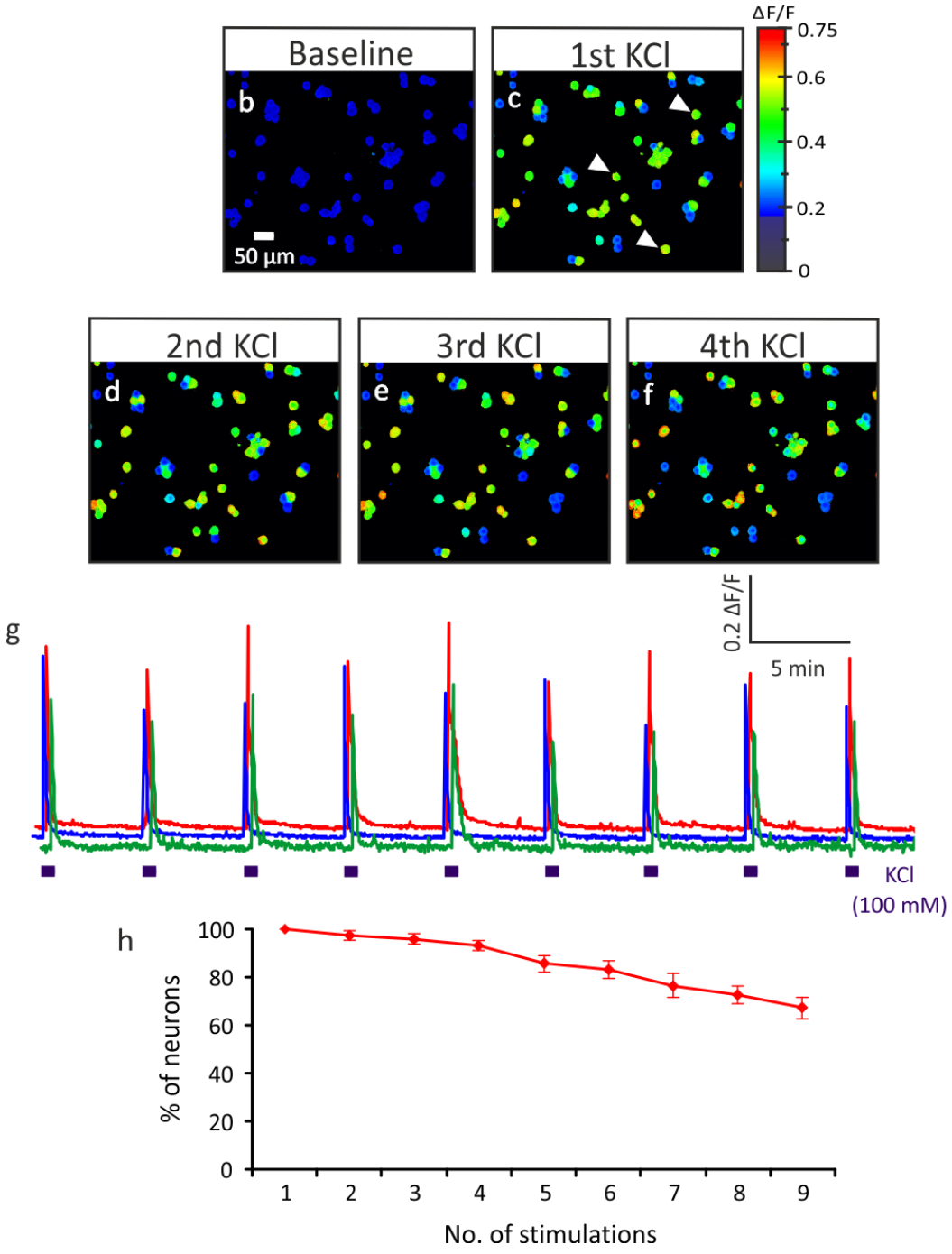

Figure 3.5.1

Neurons can reproducibly propagate action potentials in vitro. (a), Representative fura-2 loaded field of cells at baseline. (b-e), Fura-2 loaded cells at the peak calcium response for 1st, 2nd, 3rd and 4th consecutive KCl stimulation, respectively. (f), Representative calcium transients from the three cells depicted in (b), arrowheads, in response to 9 consecutive KCl stimulations to the terminals. (g), Quantification of the percentage of neurons responding to consecutive stimulation of the terminals.

3.6. Retrograde transport and functional development

It takes several days for neurons to grow neurites across the microgroove array and establish an axonal network in the adjacent compartment. To quantify this process, 2 compartment chambers were used and the non-selective retrograde tracer – DiI, was applied in the terminal chamber. The number of fluorescently labelled cell bodies was quantified 90 minutes after DiI application. This experiment was repeated on different cultures at 3, 5, 7 and 10 DIV in order to track the proportion of successfully projecting neurons. At 3 DIV axons are just beginning to emerge from the microgrooves. At this time point 31 ± 7% (n_{cells} = 762, $n_{experiments}$ = 8) were DiI labelled indicating the presence of a projecting neuron in the adjacent compartment (Figure 3.6.1b, e). By 5 DIV the percentage of neurons with a projecting axon had reached 55 ± 5% (n_{cells} = 510 , $n_{experiments}$ = 4) and increased to 76 ± 3% (n_{cells} = 898, $n_{experiments}$ = 7) at DIV 7 (Figure 3.6.1e). Further increasing the time in culture to 10 DIV did not result in the accumulation of DiI in any additional cells with 72 ± 11 % (n_{cells} = 318, $n_{experiments}$ = 5) of all cells labelled, suggesting that after a week in culture the large majority of neurons grow projecting neurites into the adjacent compartment. I next asked whether these cells are capable of propagating action potentials. The non-selective depolarising stimulus of 100 mM KCl was applied to the terminal compartment and the activation pattern of the somata was studied using ratiometric calcium imaging with Fura-2. At 3 DIV only 60 ± 11 % (n_{cells} = 762, $n_{experiments}$ = 8) (Figure 3.6.1c, d, e) of those with a projecting axon were activated by KCl, suggesting that the axons were capable of active transport, but the mechanisms to propagate action potentials in a large proportion (40%) of cells were not present. However, during the 10 days in culture, the proportion of cells that were DiI labelled increased to 55 ± 5 % at 5 DIV, and was significantly greater by 7 DIV and 10 DIV (76 ± 3 % and 72 ± 9 %, respectively, $p<0.001$, 2-way ANOVA with Bonferroni post-hoc test). Furthermore, the overlap of functionally excitable cells with DiI labelling also steadily increased, with 60 ± 11 % at 3 DIV (n_{cells} = 762, $n_{experiments}$ = 8), 82 ± 8 % at 5 DIV (n_{cells} = 510, $n_{experiments}$ = 4) (Figure 3.6.1e), 90 ± 2 % at 7 DIV (n_{cells} = 898, $n_{experiments}$ = 7) and 95 ± 2 % at 10 DIV (n_{cells} = 318, $n_{experiments}$ = 5) (Figure 3.6.1e). Statistical comparisons revealed there was a significant increase in the proportion of DiI labelled cells that could also be excited from stimulation of the terminals over time in culture (3 DIV vs 7 DIV, $p<0.05$, 3 DIV vs 10 DIV, $p<0.05$, 2-way ANOVA with Bonferroni post-hoc test). Therefore, whilst some cells which have a projecting axon are unable to transduce or propagate action potentials at early time points, by 7 and 10 DIV the neurons have matured and the majority now express the machinery required for transduction and propagation.

No significant increase (2-way ANOVA with Bonferroni post-hoc test) was observed from 7 DIV to 10 DIV in either the DiI labelled population or functionally responding cells from stimulation of the terminals, therefore 7DIV was chosen as the optimum time to functionally investigate sensory terminals in subsequent experiments.

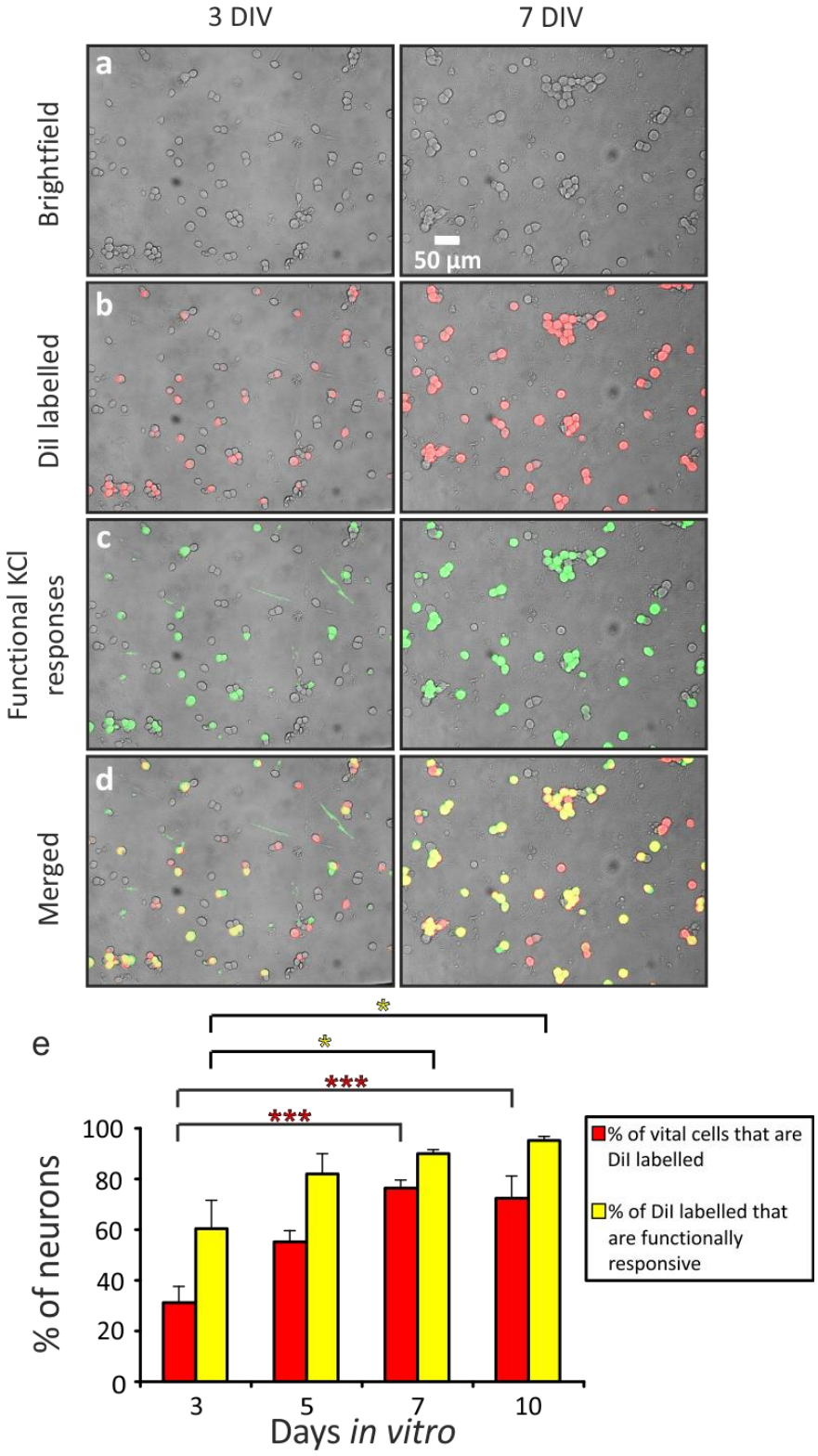

Figure 3.6.1

*Number of neurons with axons that transport DiI and propagate action potential increases over time in culture. (a) Brightfield image of DRG cell soma at 3 or 7 days in vitro. (b) Pseudocolour image of DiI labelled cell soma and brightfield. (c) Pseudocolour representation of cells with a functional response to stimulation of the sensory terminals. (d) Merged image of DiI labelled cells and those with functional responses. Yellow cells display both a functional response and DiI labelling. (e) Quantification of cells with functional responses to stimulation of the terminals, DiI labelling and the overlap between these populations over time in culture (*p <0.05, **p <0.01, 2-way ANOVA with Bonferroni post-hoc).*

3.7. DRG sensory neurons can be cultured in a 3 compartment system to fluidically isolate the terminals, axon and soma.

In order to further compartmentalise the sensory neuron and study specific neuronal regions in isolation the 3 compartment system with 2 separate microgroove arrays was used. This also allows the application of pharmacological agents to the fluidically isolated middle axonal compartment. To investigate the growth of the axons in a 3 compartment system, DiO was applied to the middle axonal compartment, and DiI applied to the most distal terminal compartment. With their differing excitation wavelengths, neurons that projected through the 2 microgroove arrays could readily be detected by the somal accumulation of both DiO and DiI (Figure 3.7.1d,f). Neurons that projected only into the middle axonal compartment would only transport DiO as these would not come into contact with DiI (Figure 3.7.1h). 72 ± 6 % of all neurons, detected by a brightfield cell count, projected into the middle compartment, and were therefore positive for DiO (Figure 3.7.1e) (n_{cells} = 426, $n_{experiments}$ = 5). Of the DiO positive cells, 77 ± 3 % were also positive for DiI (Figure 3.7.1e), demonstrating that the majority of axons but not all, continue to grow into the most distal terminal compartment. These percentages equate to 55 % ± 4 % of the total cell population that grow through the 2 microgroove arrays. As can be seen in Figure 3.7.1h and j the axons and terminals are easily detected by DiO or DiI imaging, respectively. Only 5 ± 2 % of total cells were positive for DiI and negative for DiO (Figure 3.7.1e). Whilst it is impossible for an axon to project into the terminal compartment without first passing through the axonal compartment, this small discrepancy is likely to be due to the DiO accumulation falling just below the set detection threshold. Despite this very small anomaly, DiO and DiI staining provided a powerful technique to prove that that the majority of neurons grow through the 2 microgroove barriers, therefore allowing experiments to be conducted on the soma, axon or terminals in isolation.

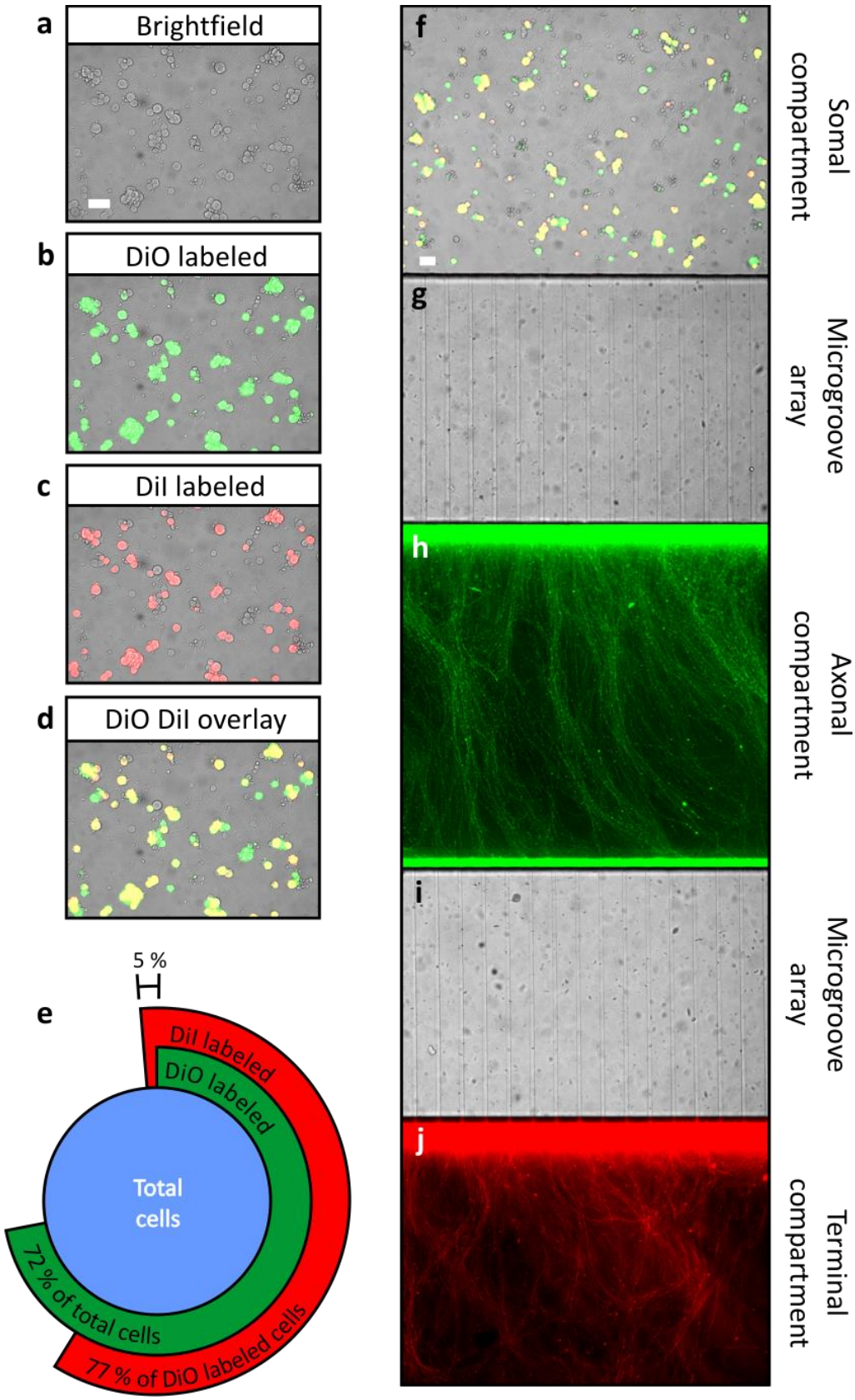

Figure 3.7.1
In a 3 compartment system the majority of axons continue to grow into the most distal terminal compartment. (a), Brightfield image of a field of cells. (b), DiO labelled cells from application to the axons. (c) DiI labelled cells from application to the terminals. (d) Overlay of the DiO and DiI labelled cells, yellow cells are dual labelled whereas green cells have not projected into the terminal compartment. (e) Quantification of the DiO and DiI labelled cells. (f) Brightfield image of a pseudocolour DiO and DiI overlay. (g) Microgroove barrier separating the somal and axonal compartments. (h) DiO labelled axons. (i) Microgroove barrier separating the axonal and terminal compartments. (j) DiI labelled terminals. Scale bars refer to 50 µm.

3.8. Somal calcium transients induced by stimulation of the terminals require action potential propagation

Following on from the retrograde transport experiments, the mechanisms responsible for the somal calcium transients after terminal stimulation were investigated in the 3 compartment chambers. Due to the fluidic isolation of the microgroove array (Figure 3.3.1) calcium transients induced by stimulation of the terminals cannot be attributed to stimulant diffusion through the microgrooves. I therefore tested the hypothesis that the sensory terminals transduce the depolarising stimuli, and the axons propagate action potentials back to the cell soma, resulting in the observable calcium response. Therefore, using the 3 compartment chamber the distal terminal compartment was exposed to an excitatory stimulus whilst drugs were applied in a time locked manner to the middle axonal compartment. Action potential propagation relies on VGSCs, and these can be separated into TTX-s and TTX-r subtypes (Catterall et al., 2003). The application of TTX resulted in an overall highly significant effect compared to control experiments ($F_{1, 49}$ =1187.3, $p<0.001$, 2-way ANOVA). Upon application of 1 µM TTX to the axonal compartment, 72 % ± 5 % (n_{cells} = 237, $n_{experiments}$ = 4) of neurons were blocked and therefore did not respond with a calcium influx in the cell body. Prolonged application of TTX did not result in the blockade of additional cells, demonstrated by the plateau of responding cells in the drug treated group. The TTX treated group showed a greatly reduced percentage of responding cells, a Bonferroni post-hoc test revealed that at each consecutive KCl stimulation, the difference between test and control conditions was highly significant ($p<0.001$, 2-way ANOVA with Bonferroni post-hoc test) demonstrating tachyphylaxis is not responsible for the dramatic reduction in responding cells. Instead, these cells were unable to produce a calcium response with the TTX block applied to their axons (Figure 3.8.1b, d) suggesting that the large majority of neurons in this *in vitro* preparation require TTX-sensitive ion channels for action potential propagation. Importantly, the TTX-resistant responses were immediately and completely abolished by application of the non-selective sodium channel blocker lidocaine (10 mM) (Figure 3.8.1c, d). Ultimately this demonstrates that the calcium response induced in the somal compartment upon peripheral stimulation is entirely dependent on action potential propagation through VGSCs. This has therefore provided convincing proof of concept that the pharmacology of action potential propagation in sensory neurons can be pharmacologically investigated *in vitro* using functional calcium imaging in microfluidic chambers.

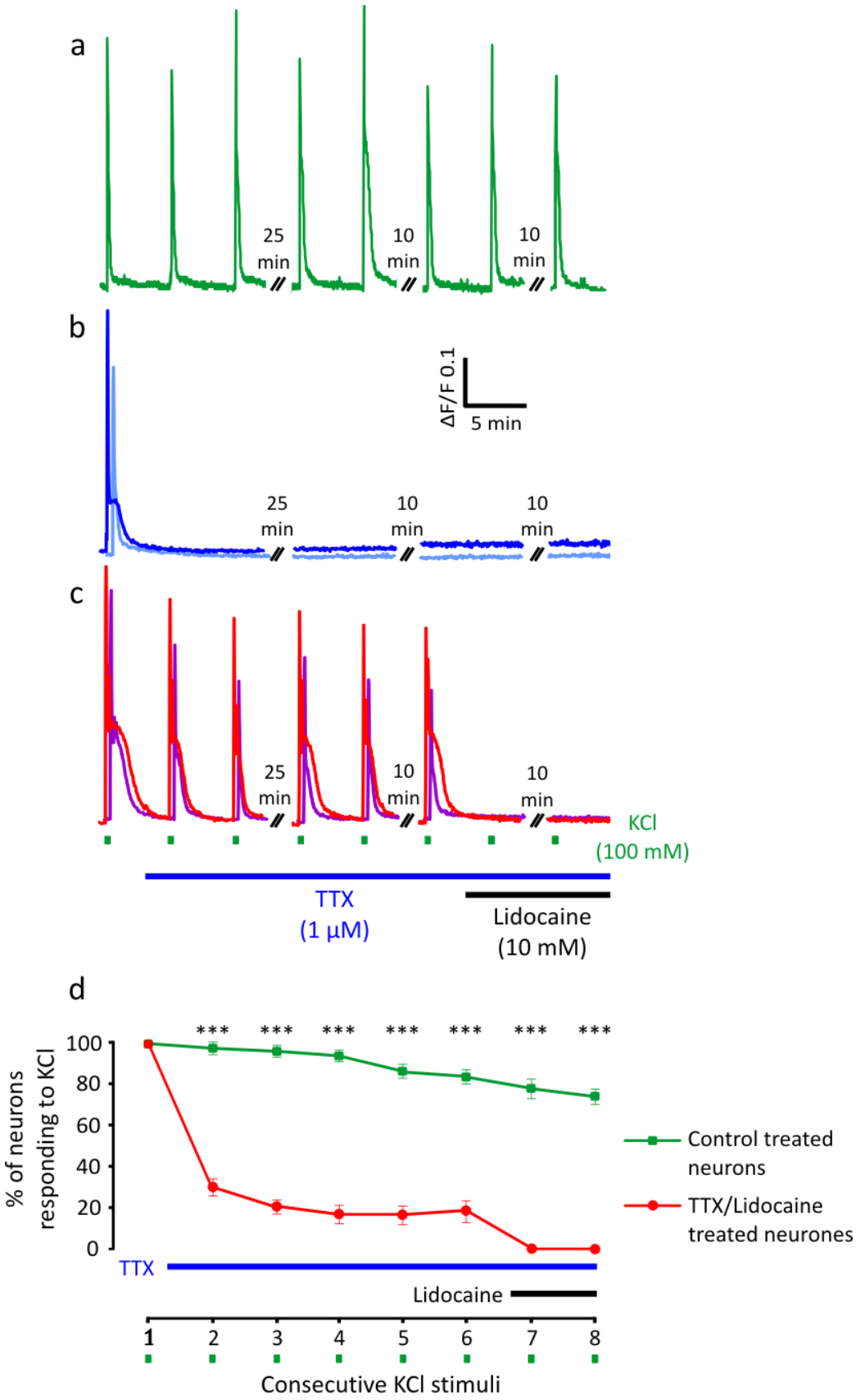

Figure 3.8.1

*Action potential propagation depends upon TTX-s and TTX-r VGSCs. (a-c) Representative calcium transients from single DRG neurons recorded whilst repetitively stimulating the sensory terminals. (a) Calcium transient during a control experiment, demonstrating the reproducibility of the evoked calcium response. (b-c) Evoked calcium response during TTX and Lidocaine application to the axons. (b) Calcium transients from 2 cells demonstrating TTX-sensitive properties. (c) Calcium transients from 2 cells demonstrating TTX-resistant properties. (d) Quantification of the percentage of neurons in treated and untreated cultures responding to consecutive KCl stimulation. (***p<0.001, 2-way ANOVA with Bonferroni post-hoc test).*

3.9. Dose response functions can be performed in the 3 compartment system to determine the IC50 of pharmacological blockers of VGSCs.

Using 3 compartment chambers, the dose response function of TTX and Lidocaine was investigated to examine the range of inhibition on voltage gated sodium channels in DRG neurons in culture. The terminals were first stimulated with KCl to acquire the maximal responding population. Between each subsequent KCl stimulation either TTX or lidocaine was washed into the middle axonal compartment in ascending concentration. The response at each concentration is displayed as a percentage of the responding neurons in the absence of any drug. Confirming the previous identification of a TTX-r sub-population, the prevalence of TTX-r neurons at 1 µM in this experiment is 17 ± 5 % (Figure 3.9.1d) (n_{cells} = 148, $n_{experiments}$ = 4), which is almost identical to the 18 ± 5 % previously detected (Fig 3.8.1 d). The percentage of responding cells at 300 nM TTX was also very similar at 20 ± 5 % (Figure 3.9.1d). At 10 µM TTX there is a complete abolition of all responses indicating that even the TTX-r channels can be blocked if the concentration of TTX is high enough. The half-maximal inhibitory concentration (IC50) for TTX obtained from this *in vitro* dose response experiment is approximately 100 nM at which 48 ± 15 % of all vital cell continue to respond. Figure 3.8 suggests that DRG neurons in culture can be divided into two subpopulations based on individual TTX sensitivity. 1 µM TTX was sufficient to inactivate the TTX-sensitive neurons whilst approximately 20 % of neurons displayed TTX-resistant characteristics. Therefore, an IC50 for these respective populations can be derived from Figure 3.9.1d. Taking 1 µM as the dividing concentration between TTX-sensitive and TTX-resistant, at which, 17 % ± 5 % of cell remained active, the TTX-sensitive IC50 was determined at 58.5 % (the half way value between 100 % and 17 %). This resulted in a TTX-sensitive IC50 of approximately 55 nM. The TTX-resistant IC50 was determined between 1 µM (17 ± 5 % of cells remain active) and 10 µM (0 % of cells remain active), and therefore taken at 8.5 % (the half way value between 17 % and 0 %). This resulted in a TTX-resistant IC50 of approximately 25 µM.

Using the same experimental set up and stimulus protocol, Lidocaine was investigated in a similar manner. Previous experiments demonstrated that 10 mM was sufficient to block all responses (Figure 3.8.1d), however in this experiment the lower concentration of 3 mM resulted in a 100% block (Figure 3.9.2c). At the lowest concentration of 0.1 mM, 85 ± 10 % continued to respond, reducing to 65 ± 16 % at 0.3 mM and 20 ± 11 % at 1mM (Figure 3.9.2c) (n_{cells} = 165, $n_{experiments}$ = 4). The IC50 as determined in these experiments was therefore approximately 450 µM.

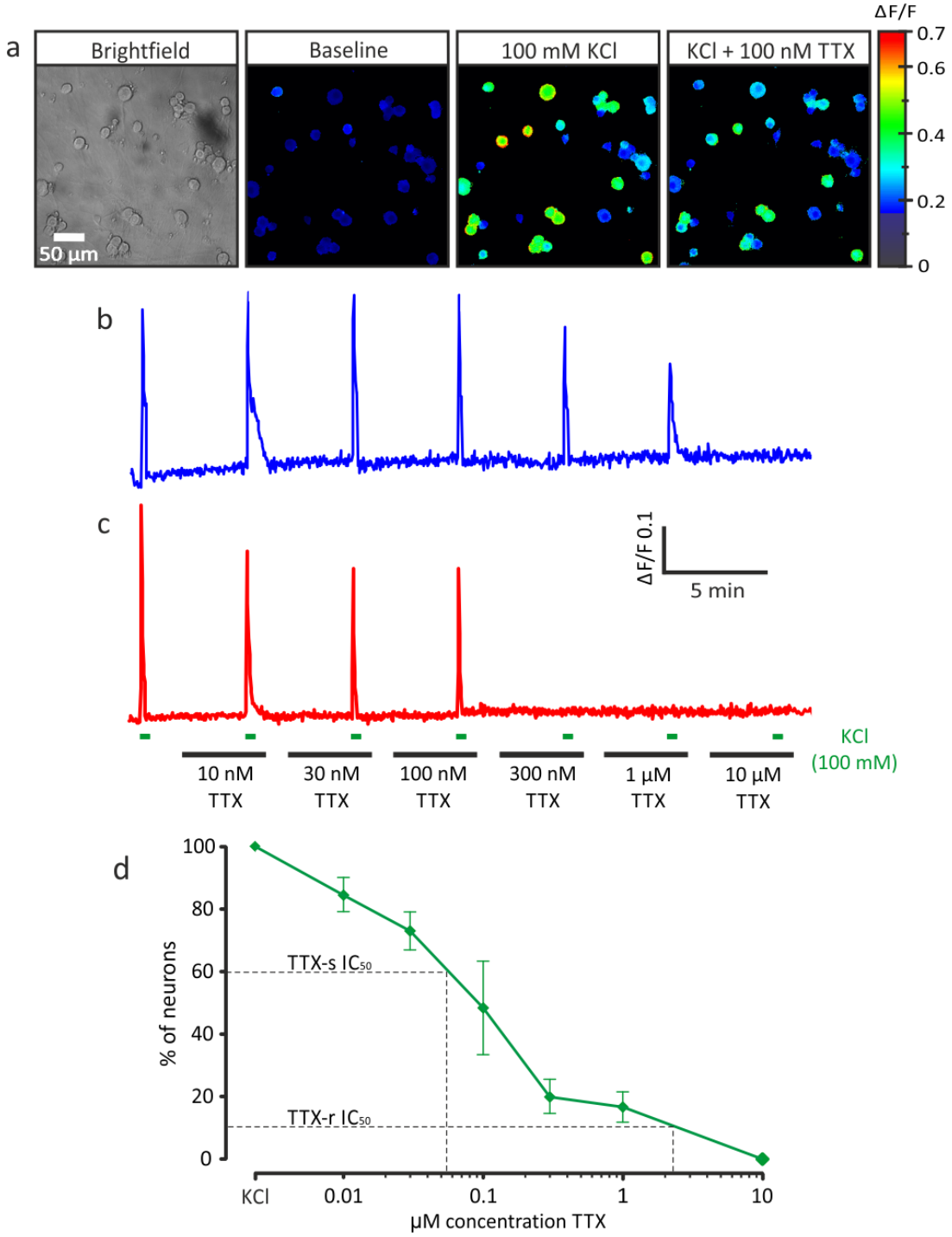

Figure 3.9.1

TTX dose response function performed in a 3 compartment system. (a) From left to right, brightfield image of a field of cells, baseline calcium level in fura-2 loaded cells, peak calcium response from KCl stimulation of the terminals and responding cells to KCl stimulation of the terminals in the presence of 100 nM TTX. (b) Representative calcium transient from a TTX-r neuron. (c) Representative calcium transient from a neuron that is blocked at 300 nM TTX. (d) Dose response curve demonstrating an IC50 of approximately 100 nM. All cells including TTX-r neurons are blocked with 10 µM TTX.

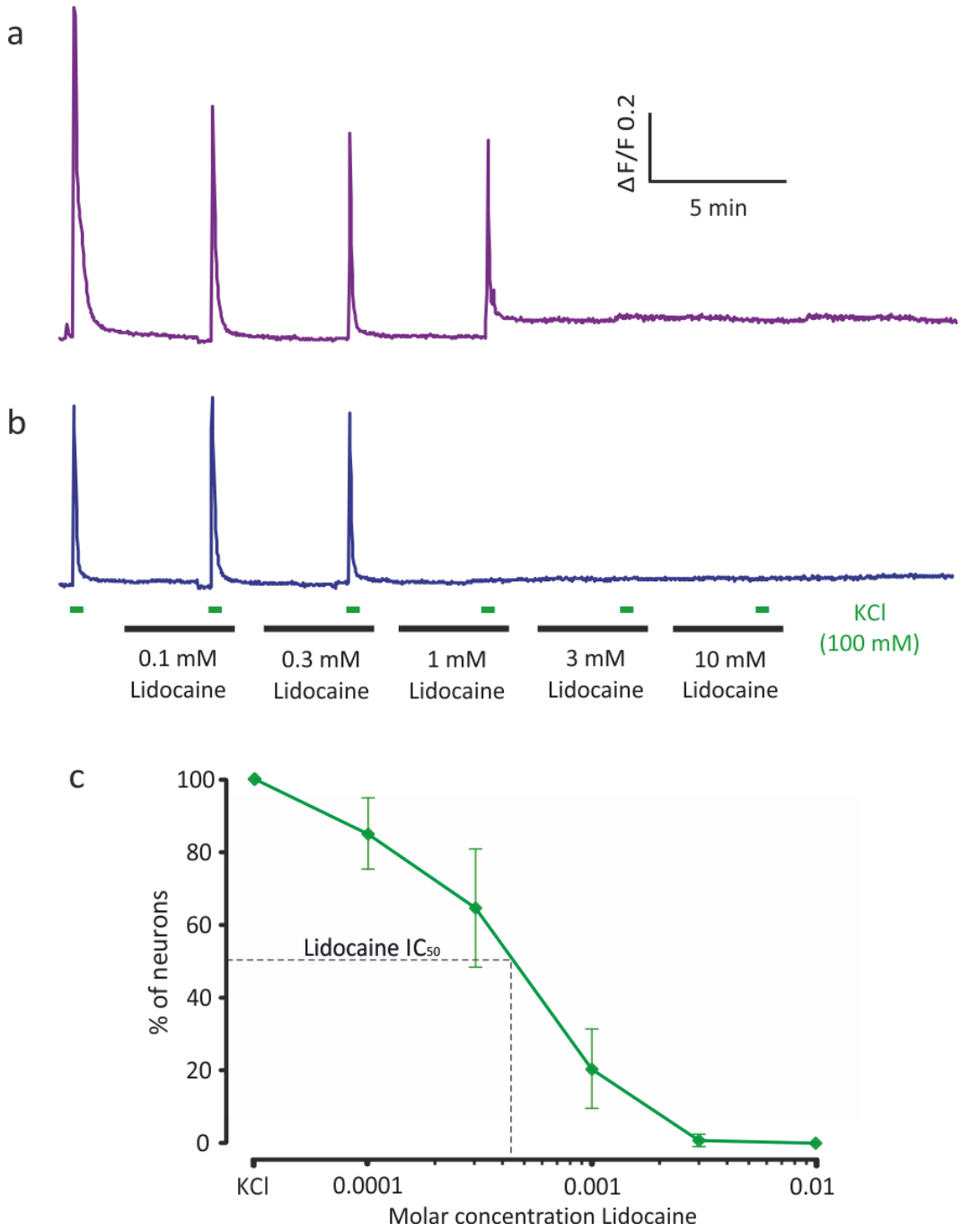

Figure 3.9.2
Lidocaine dose response function performed in a 3 compartment system. (a) Representative calcium transient from a neuron that is blocked by 3mM Lidocaine. (b) Representative calcium transient from a neuron that is blocked by 1 mM Lidocaine. (c) Dose response curve demonstrating an IC50 of between 0.3 mM and 1 mM.

3.10. A subpopulation of mouse DRG neurons are sensitive to mechanical stimulation of their receptive terminals.

The terminals and somata were investigated for their sensitivity to low threshold mechanical stimulation. In previous experiments a continuous flow of either ECF or stimulant is applied to the stimulating compartment. In these experiments, the flow of ECF itself was applied to act as a low threshold mechanical stimulation. Any detectable time-locked calcium peaks in response to the fluid flow are likely to represent mechanical sensitivity as no other stimulant is applied at the same time, and any peaks are only counted if substantially greater than baseline fluctuations. Therefore, during the 30 second mechanical stimulation, ECF was allowed to flow through the compartment, whereas during the 5 minute inter-stimulus period the ECF was stationary in all compartments. Three mechanical stimuli were followed by a capsaicin and KCl stimulation, between these stimuli and after KCl, ECF continually flowed to wash out the stimulants.

The first mechanical stimulation applied to the terminals in a 2 compartment system at 7 DIV elicited a response in 32 ± 11 % (Figure 3.10.1a, c) (n_{cells} = 309, $n_{experiments}$ = 9) neurons. Mechanical stimulation of the soma resulted in 12 ± 3 % (Figure 3.10.1c) (n_{cells} = 309, $n_{experiments}$ = 9) of cells activated. This difference was not significant ($p > 0.1$, t-test), which probably reflects the large variation in the proportion of neurons that could be activated by mechanical stimulation applied to the terminals. It is presently unclear what caused this large range, which varied from 100 % to just 2 % of cells between experiments. All experiments were conducted at the same *in vitro* time point and all mice were dissected at E15.5. Therefore it is unlikely this variation is due to embryonic development. Variations in the length of the axon that has grown into the terminal compartment may influence the sensitivity, although again this is unlikely as each culture was imaged at the same *in vitro* time point meaning axonal growth should be similar between cultures.

Sensitivity to consecutive mechanical stimuli rapidly declined at the terminals, with 10 ± 4 % (n_{cells} = 309, $n_{experiments}$ = 9) and 4 ± 2 % (n_{cells} = 309, $n_{experiments}$ = 9) responding to the second and third stimuli, respectively (Figure 3.10.1c). Similarly, the sensitivity to mechanical stimuli at the soma also declined with repetitive stimulation so that 8 ± 2 % (n_{cells} = 309, $n_{experiments}$ = 9) responded to the second and 3 ± 1 % (n_{cells} = 309, $n_{experiments}$ = 9) responded to the third mechanical stimulation (Figure 3.10.1c). Therefore the mechanisms that govern mechanical sensitivity appear to be sensitive to tachyphylaxis in this preparation.

Capsaicin sensitivity was tested alongside mechanical sensitivity to provide an insight into whether small-diameter, TRPV1 expressing nociceptors can be activated by low-threshold mechanical stimuli. Due to the rapid decline in fluid-flow induced responses with subsequent applications, it is practical to only assess those responding to the first stimulation. Of the neurons that responded to mechanical stimulation applied to the terminals, 40 ± 12 % (n_{cells} = 309, $n_{experiments}$ = 9) functionally expressed TRPV1 at the terminals. Of the neurons that responded to mechanical stimulation applied to the soma, 67 ± 11 % (n_{cells} = 309, $n_{experiments}$ = 9) were capsaicin sensitive at the

soma. Therefore, in the soma, the majority of neurons that respond to mechanical stimulation are capsaicin sensitive, whereas in the terminals this pattern is reversed, with most being capsaicin insensitive. This is likely to simply be due to the increased mechanical responsiveness of the terminals compared to the soma.

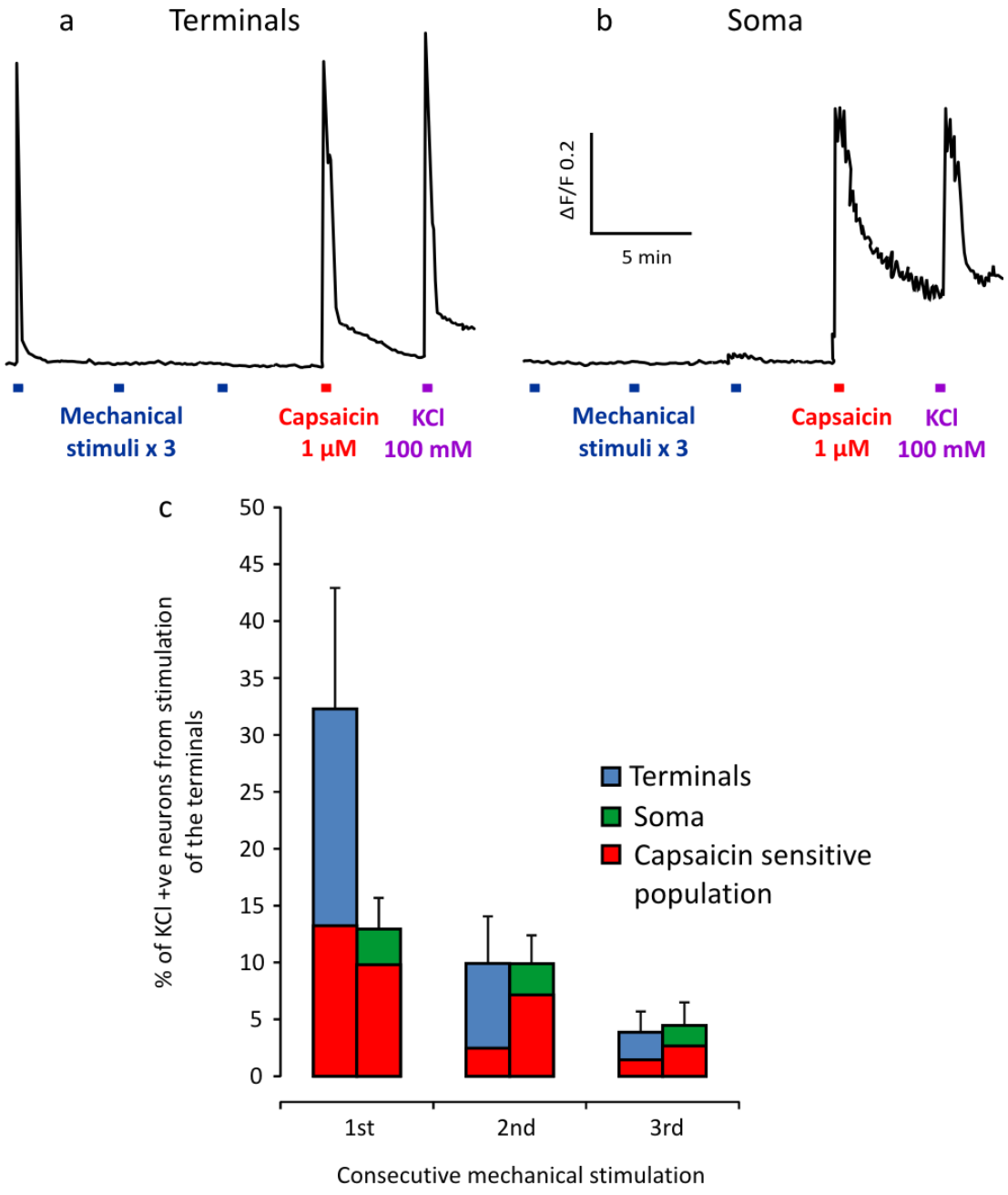

Figure 3.10.1
Receptive terminals are initially more sensitive to mechanical stimulation than the cell soma. (a) Representative calcium transient displaying a neuron sensitive to mechanical and capsaicin stimulation on the terminals. (b) Representative calcium transient displaying a neuron that is mechanically insensitive, and capsaicin sensitive on the cell soma. (c) Quantification of the neuronal populations responding to 3 consecutive mechanical stimulations, and the proportion that are capsaicin sensitive.

3.11. Discussion

The principle finding of this study is that calcium imaging can be used in combination with compartmentalised DRG cultures to investigate action potential propagation *in vitro*. I demonstrate that stimulation of peripheral neuronal regions results in a robust increase in the intracellular calcium levels of the soma. Pharmacological experiments indicate that the somal calcium response is due to the propagation of action potentials from the peripheral regions to the cell soma, and that this propagation relies on voltage gated sodium channels that are expressed in the projecting neurite. Furthermore, the somata that are activated by peripheral stimulation can be labelled using retrograde tracing, proving that the machinery required for energy dependent axonal transport is expressed in this *in vitro* culture system.

Phenotype of embryonic DRG neurons in vitro

In vivo, the majority of embryonic DRG neurons express TrkA and require NGF for survival. Knockout of NGF using homologous recombination results in approximately a 70 % loss of neurons in the lumbar DRGs (Crowley et al., 1994). Similarly, *in vitro* culture of embryonic DRG neurons require NGF supplement for survival, and this dependence in culture conditions mimics that of *in vivo* neurons and lessens as the neurons mature in culture (Tong et al., 1996). Here, NGF has been used simultaneously as a survival factor and a chemo-attractant. Despite the majority of neurons depending on NGF at the time of dissection in these experiments, a subpopulation of TrkA negative, TrkB/C positive neurons that constitute the early mechano- and proprio-ceptors will be lost due to the absence of their required neurotrophins. In addition, the absence of Schwann cells in the culture means these neurons are unmyelinated. Therefore, the phenotype of the neurons selected for with the use of NGF is likely to predominantly represent the unmyelinated population, many of which develop into nociceptors *in vivo*.

Somal calcium transients evoked by peripheral stimulation are due to action potential propagation

The initial objective of these experiments was to record calcium transients in the cell soma evoked by stimulation of the terminals. Figure 3.4.1 illustrates that application of the neuronal depolarising agent, KCl, to the terminal compartment, results in a robust peak in intracellular somal calcium concentration. A crucial step was to prove that this response was not evoked by direct stimulation of the soma due to KCl diffusion through the microgrooves into the somal compartment. Rigorous radiochemistry experiments were performed to investigate the flow rate through the microgroove array at various hydrostatic pressure imbalances. Figure 3.3.4 shows that a compartment containing 40 µl more in volume than the adjacent compartment remains fluidically isolated for up to 72 hours. Even if the compartments are filled with an equal volume, the fluidic isolation remains for up to 24 hours. Therefore, during all imaging experiments a volume difference of approximately 100 µl was maintained between the stimulation and recording compartments at all

times. Consequently this maintained a fluidic isolation meaning any stimulant or drug applied in a lower volume to that in adjacent compartments was fluidically isolated in that single compartment.

The microgroove array therefore provides an excellent fluidically isolating barrier. Consequently, somal calcium peaks in response to stimulation of the terminals with high K^+ concentration cannot be attributed to stimulant diffusion and direct activation of the soma. Therefore, a physiological propagation of the signal from the terminals to the soma must be responsible for the calcium peak measured in the soma.

Calcium signalling is indispensable for neurons, and functions in many cellular processes, from regulation of gene expression by the second messenger actions of calcium, to calcium mediated apoptosis (Augustine et al., 2003) and as a result, neurons are highly adapted at calcium regulation. Extracellular calcium rapidly enters neurons in response to membrane depolarisation through voltage-gated calcium channels (VGCC's) or ionotropic glutamate receptors (William A. Catterall et al., 2009), which is exploited by calcium imaging to detect functional responses of neurons *in vitro*. In addition to calcium influx from extracellular sources through voltage gated- and ligand gated channels, calcium is also released from intracellular stores (Watanabe et al., 2006). The two distinct calcium transients observable in neurons are calcium spikes and calcium waves, which differ in their temporal kinetics, spatial distribution and effects they exert. These different calcium transients were important to consider in terms of the measurable calcium response in the microfluidic chambers. Calcium spikes are generated by action potentials and calcium-induced calcium release that result in rapid increases in cytosolic calcium concentration. Calcium imaging experiments using Fura-2 loaded neurons have demonstrated calcium spikes raise intracellular calcium concentration to maximal levels in less than 5 seconds (Gu et al., 1994). Calcium spikes are readily generated by depolarisation and are rapidly and bidirectionally propagated in neuronal processes (Rosenberg and Spitzer, 2011). Contrary to the rapid kinetics of calcium spikes, calcium waves display rise and decay times in the order of several minutes, and when assessed with calcium imaging induce a much more modest increase in intracellular calcium levels (Rosenberg and Spitzer, 2011). These slow moving changes in calcium concentration are most commonly found in the growth cone of developing neurons and have been demonstrated to regulate axon extension (Lautermilch and Spitzer, 2000).

The temporal kinetics of calcium spikes, their propagating ability and the generation by focal depolarisation suggest action potentials are required for their initiation. This was confirmed in my experiments in which somal calcium spikes were blocked in 82 ± 5 % of all cells by TTX. Consequently, voltage dependent calcium entry into cells predominantly expressing TTX-s VGSCs will be abolished by the TTX-induced blockade of the VGSC dependent action potential. Therefore, depolarisation of peripheral neuronal regions induce action potentials that propagate to the cell soma to rapidly increase intracellular calcium concentration, which is detected in this system by Fura-2 dependent calcium imaging. Whilst calcium waves are still present in cultured neurons, these

are unlikely to contribute to the somal calcium response recorded in this preparation for several reasons. Firstly, calcium waves are not elicited by depolarisation, meaning it would be improbable that they contribute to the time locked calcium peaks in this preparation. Secondly, calcium waves are propagated at a rate consistent with calcium diffusion (Gu et al., 1994), these slow kinetics suggest they are not implicated in the somal response observed here which is rapidly elicited after stimulation of the receptive terminals. Finally, calcium waves are generated by release of calcium from intracellular stores (Lorenzon et al., 1995) and therefore would be able to continue propagating even in the presence of TTX. Correspondingly, if calcium waves were responsible for the calcium response in the microfluidic chambers, TTX would be entirely ineffective at producing a conduction block which as demonstrated in Figure 3.9.1 is clearly not the case.

In conclusion, microfluidic chambers create fluidically isolated microenvironments, where stimulants are unable to freely pass from the one compartment to another if a hydrostatic pressure imbalance is established. Peripheral stimulation of the receptive terminals with KCl induces VGSC dependent action potentials that rapidly propagate to the cell soma. The induced action potential propagation exhibits a TTX-s and TTX-r component, with the majority of cells depending on TTX-s VGSCs for propagation.

The contribution of TTX-s and TTX-r voltage gated sodium channels

Voltage gated sodium channels are extensively expressed in DRG neurons and are essential for normal nerve conduction. The VGSC family is divided into two subgroups based on their sensitivity to TTX. Extensive studies have determined the IC50 for each individual sodium channel. These experiments usually involved cloning the rodent channel and heterologously expressing it in a donor such as HEK cells. Such studies reveal that the TTX-s are consistently blocked in the low nanomolar range, for example, rat $Na_v1.6$, preferentially expressed at the node of Ranvier has an IC50 of approximately 1 nM (Dietrich et al., 1998) and rat $Na_v1.7$, expressed in nociceptors, has an IC50 of 4.3 nM (Sangameswaran et al., 1997). TTX-r channels have undergone similar scrutiny in heterologous expression studies. The IC50 of the cardiac sodium channel - $Na_v1.5$, was 0.74 µM (Zeng et al., 1996), $Na_v1.8$ was measured to be 60 µM (Akopian et al., 1996) whilst $Na_v1.9$ was found to be 47 µM (Renganathan et al., 2002). Although it is useful to know specific TTX sensitivities for individual channels, the TTX-s and TTX-r currents are formed by the contribution of multiple types of sodium channel each with distinct electrophysiological properties. Studies have investigated the expression of sodium channels at the cell soma, and the density of TTX-r channels in some small DRG neurons of both Aδ and C type has been found to be sufficient to generate an action potential at the soma (Villière and McLachlan, 1996). However, it is more unclear whether the expression of TTX-r and TTX-s sodium channels are expressed at a sufficient density to conduct action potentials in the central and peripheral branches of DRG neurons. In order to assess this, Pinto and colleagues have studied the peripheral and central branches of C and Aδ fibres in an *ex vivo* preparation. Interestingly, conduction in Aδ fibres was entirely inhibited with 30 nM TTX (IC50 of 5 – 7 nM)

suggesting that in these lightly myelinated axons the TTX-s sodium channels are entirely responsible for action potential conduction (Pinto et al., 2008). The C-fibre responses were blocked by 85 – 89 % in the peripheral branch by a concentration range between 1 and 100 nM. The IC50 of the TTX-s component was determined as between 14 – 33 nM (Pinto et al., 2008). These concentration ranges are typical for the block of TTX-s VGSC (Ogata and Tatebayashi, 1993; Sangameswaran et al., 1997; Dietrich et al., 1998). Therefore TTX-s VGSC dominates conduction in these unmyelinated axons.

The microfluidic chambers have provided an excellent opportunity to investigate the expression of TTX-s and TTX-r channels along the axon in an *in vitro* preparation. I have demonstrated that TTX produced a dose dependent block of action potential propagation with complete inhibition at 10 µM and an IC50 of approximately 100 nM when all cells are analysed as a whole. The percentage of cells responding to KCl stimuli in the presence of 300 nM and 1 µM TTX plateaus at 20 % and 17 %, respectively. The block of TTX-s VGSC with a low nanomolar TTX concentration suggests that this population of cells are relying entirely on TTX-r VGSC for action potential propagation. The IC50 of the TTX-s component as determined by the half inhibitory concentration between 10 nM and 1 µM (by which all TTX-s VGSC should be blocked) is approximately 55 nM, which is in good agreement with that determined by Pinto et al., 2008 for unmyelinated C-fibres.

A subpopulation of neurons determined as 17 % of the total responding population appear to express a sufficient density of TTX-r channels in the length of axon present in the middle axonal compartment to propagate through this TTX filled compartment. The finding that a subpopulation of neurons in these experiments are able to propagate in the presence of 1 µM TTX adds to the ongoing debate regarding the expression of TTX-r VGSC on the peripheral axons of C-fibres. There is a suggestion that 1 µM TTX completely inhibits C-fibre evoked action potentials in small diameter DRG neurons if TTX is applied to the axons (Yoshida and Matsuda, 1979). On the other hand, changes to the C-fibre compound action potential upon TTX application have been described such as an increase in stimulus to peak latency, yet a complete block was not observed (Quasthoff et al., 1995). Steffens and colleagues recorded cord dorsum potentials from the dorsal root entry zone of the L4 ganglia and observed that local application of 1 µM TTX to the primary afferents reduced the first part of the A-fibre compound action potential yet the second C-fibre component, was maintained (Steffens et al., 2001). Furthermore a slowing of nerve conduction velocity to 0.16 m/sec within the TTX application site was measured. The maintenance of the second component of the evoked potential suggests that TTX-r VGSC may be expressed at a sufficient density to provide a slowly propagating spike that is able to cross the TTX application region. Upon reaching the site proximal to TTX application, TTX-s VGSC may be able to restore spike amplitude to normal levels. Similar to the report by Steffens et al., 2001, a population of neurons that are able to propagate a pure TTX-r sodium current through 1 µM TTX have been detected in the microfluidic chambers (Figure 3.8.1). The density of TTX-r channel expression in these neurons appear to be sufficient to propagate a sodium current across the 1 mm axonal compartment that is filled with TTX. It is currently unclear

whether the current recruits TTX-s sodium channels upon reaching the microgroove in which TTX-free ECF resides (Figure 3.11.1). TTX-s VGSC may be required to increase the current density and amplitude to a level that is sufficient to depolarise the cell somata. An interesting development to the current experimental protocol would be to apply 1 µM TTX to the cell soma compartment in order to investigate whether the TTX-r current only, is sufficient for somal depolarisation. These *in vitro* results are in agreement with those recorded from the *ex vivo* preparation by Steffens et al., 2001 which suggest TTX-r channels are expressed at an adequate density in the primary afferent of a subpopulation of unmyelinated C-fibres to propagate action potentials.

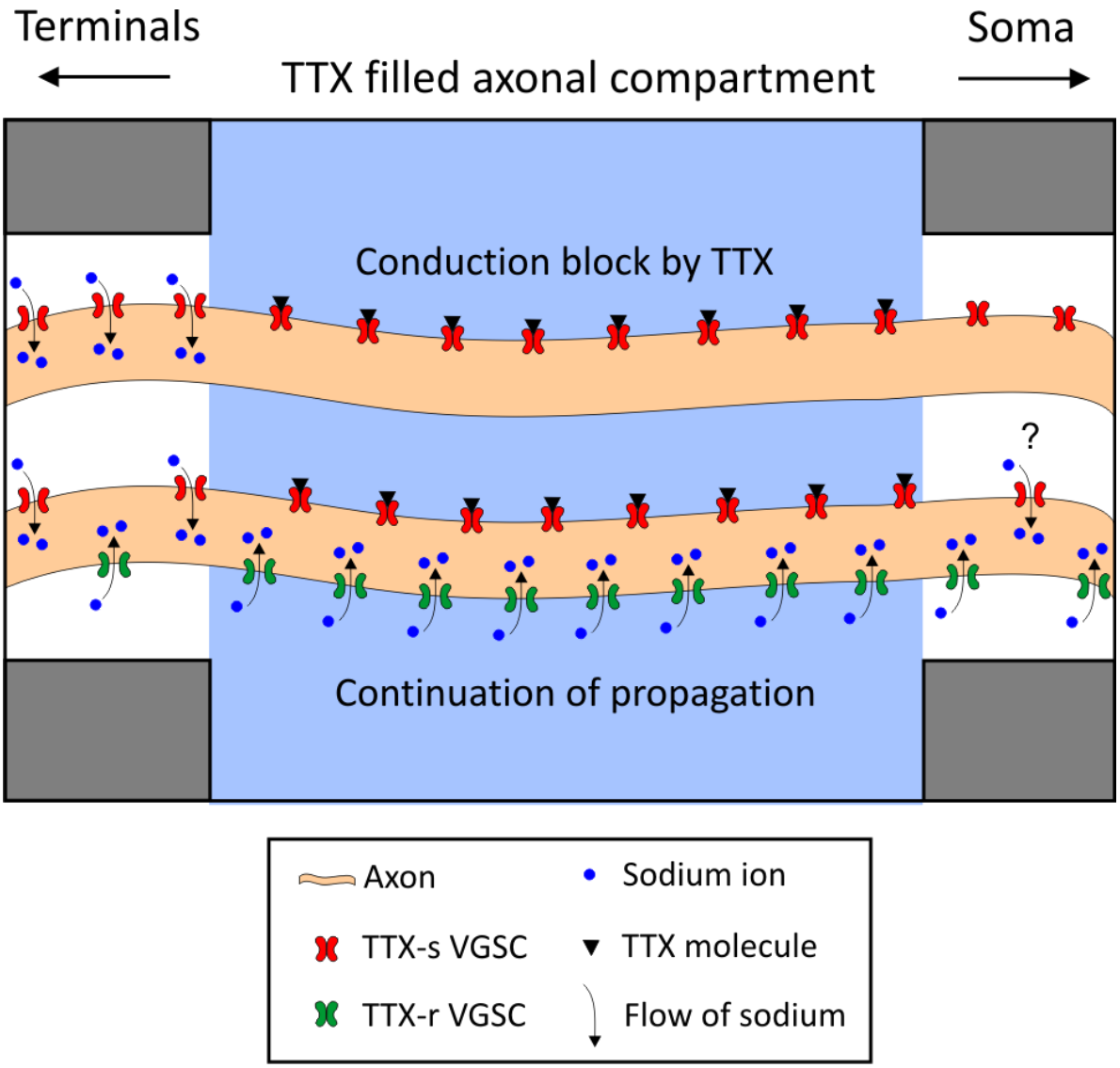

Figure 3.11.1
Schematic showing a TTX-s axon (top) and a TTX-r axon (bottom) growing through the axonal compartment. Action potential propagation is inhibited by TTX in axons expressing only TTX-s VGSCs. In axons which may express a combination of TTX-s and TTX-r VGSCs, or only TTX-r VGSCs action potential propagation continues through the TTX filled compartment to reach the soma. It is presently unknown if TTX-s VGSCs are recruited in axons expressing both sodium channel subtypes once the action potential reaches the TTX-free environment of the microgroove.

In terms of the TTX-r current, $Na_v1.8$ and $Na_v1.9$ are the two VGSCs that display TTX-r characteristics and are predominantly expressed in nociceptive DRG neurons. In these small, slower conducting neurons, TTX-r and TTX-s sodium channels both contribute to the production of the action potential (Blair and Bean, 2002). The quickly activating TTX-r channels carry the largest proportion of the inward charge during the upstroke phase, contributing to approximately 58 % of the total inward current (Blair and Bean, 2002). The TTX-r mediated current was found to be carried almost entirely through $Na_v1.8$ with a very small contribution from $Na_v1.9$. Both these channels are abundantly expressed in adult DRG neurons, however, the expression during embryonic development should be considered due to the use of embryonic cultures in this study. $Na_v1.8$ is first expressed at E15, with $Na_v1.9$ becoming detectable at E17 (Benn et al., 2001). These TTX-r sodium channels have been shown to contribute towards action potential initiation in immature neurons (Orozco et al., 1988), whereas in the adult, TTX-r sodium currents modulate the excitability in the peripheral terminals (Tanaka et al., 1998). DRG neurons that were investigated in Figure 3.8.1, were dissected from E15 rat embryos, therefore the dissection coincided with the onset of $Na_v1.8$ expression (Benn et al., 2001). Neurons were subsequently cultured for 7 DIV, which would correspond to approximately P0 – P1 in the rat, a time point where both $Na_v1.8$ and $Na_v1.9$ are reaching near maximum expression (Benn et al., 2001). Therefore, it seems likely that the TTX-r population, defined as those continuing to respond in the presence of 1 µM TTX, are expressing a high proportion of $Na_v1.8$ and $Na_v1.9$, and it is these channels that are responsible for the propagation of the action potential from the terminals to the soma.

TTX-r sodium currents were entirely abolished by the application of lidocaine at 10 mM (Figure 3.8.1). A dose response study performed in the 3 compartment chambers demonstrated that the IC_{50} of lidocaine in the microfluidic *in vitro* preparation was between 0.3 and 1 mM (Figure 3.9.2). Interestingly, when lidocaine is used as a local anaesthetic a clinically observed phenomenon of differential anaesthesia is observed, where the suppression of motor and sensory functions has a differential onset. Scholz and colleagues investigated the lidocaine induced block on DRG neurons and found that the sensitivity of TTX-s sodium channels to lidocaine blockade was 5 fold greater than TTX-r channels. The IC50 of lidocaine for TTX-s VGSCs was determined to be 42 µM, whereas for TTXr channels the IC50 was 210 µM (Scholz et al., 1998). These large differences in the IC50 between subpopulations of sodium channels can explain the onset of anaesthesia in fast conducting sensory fibres before the slower unmyelinated fibres. The almost exclusive expression of TTX-s channels on larger fibres, and the selective expression of the TTX-r channels - $Na_v1.8$ and $Na_v1.9$ on predominantly nociceptive, slowly conducting fibres would result in a conduction block in the larger fibres first. Therefore, the presence of TTX-r sodium channels which may underlie action potential propagation in a subpopulation of small fibres means these would require a higher concentration for them to block. Indeed, an earlier paper has confirmed this effect; the IC50 of lidocaine was determined to be 85 µM for A-fibres, whereas for C-fibres it was measured to be 724 µM (Gissen et al., 1980). Consequently it is plausible that in the microfluidic system, the neurons blocked with 0.1

mM constitute those predominantly expressing TTX-s VGSC, whereas those which are still responding at 1 mM lidocaine may comprise neurons with TTX-r properties. In the separate TTX and lidocaine dose response experiments, approximately 20 % of all responding neurons continue to propagate at 1 µM TTX and 1 mM lidocaine, respectively. It seems likely that this 20 % of neurons are in fact the same population that display TTX-r characteristics and therefore require a greater concentration of lidocaine for conduction block.

DiI retrograde transport and the maturation of functional responses

Carbocyanine dyes, including DiI and DiO are regularly used to label neuronal projections, and have been shown to provide intense, long-lasting staining for neurons, both *in vivo* and *in vitro* (Godement et al., 1987). These dyes are highly lipophilic, enabling their efficient insertion into the outer leaflet of the plasma membrane. In fixed tissues, the carbocyanine dyes laterally diffuse along the lipid membrane, producing detailed labelling of neuronal projections both in the anterograde and retrograde directions. Application of DiI crystals to fixed tissue requires many weeks of incubation for staining of long neuronal projections, due to the slow diffusion rates (Lukas et al., 1998). However, application to live cells results in considerably faster staining of neuronal processes and must therefore rely on mechanisms other than diffusion for movement throughout the cell. Upon insertion into the outer leaflet of the plasma membrane, labelled membrane fragments become packaged into vesicles as part of lipid turnover, and as a result are transported in vesicular dependent processes (Köbbert et al., 2000). Vesicular transport proceeds at rates of approximately 1 µm/s (Cui et al., 2007), therefore in relation to the microfluidic chambers, and taking into account the rapid insertion into the lipid membrane, loading of the terminal compartment could potentially result in DiI positive vesicles reaching the somal compartment in approximately 15 minutes – based on the 800 µm long microgrooves in the 2 compartment chambers. The 90 minutes incubation time performed in these experiments therefore allows for abundant accumulation in the cell somata.

DiI retrograde tracing was used to visualise cells with projecting axons, and at 7 DIV approximately 80 % of all vital cells display robust DiI labelling. 90 % of these cells displayed somal calcium responses to KCl stimulation of the terminals, which increased to 95 % at 10 DIV. Therefore, at later stages in the embryonic culture of DRG neurons, the vast majority of cells that are detected with DiI tracing are also able to propagate action potentials in the retrograde direction towards the cells somata. The small population of cells that are DiI labelled but display no functional responses to peripheral stimulation may arise due to DiI transfer between a projecting axon and a non-projecting axon which are in close contact. This would result in the false classification of a non-projecting neuron as having a projecting process. However, the vesicular active transport of DiI in live cells means that it is internalised and is not available to transfer between axons, even if in very close proximity (Köbbert et al., 2000). Membrane transfer of DiI from labelled to unlabelled neurons may occur in fixed tissues which are incubated for weeks or months. Over these prolonged periods, the diffusion of DiI, limited to the plasma membrane can be incorporated into other touching lipid

membranes. However the present incubation period of only 90 minutes, combined with the imaging in live cells, which internalise and actively transport DiI, suggests that DiI is not transported between cells.

An interesting pattern was observed by analysing DiI labelled cells and those with a functional response to KCl applied to the terminals. During the in vitro culture period from 0 to 7 DIV the number of neurons that are DiI labelled increases over time as more neurites grow through the microgrooves. However, the relative proportion of DiI labelled neurons that are able to propagate action potentials at each time point is initially lower than at later time points (Figure 3.6.1). At 3 DIV, 40 % of neurons that are labelled by DiI tracing are unable to propagate action potentials, suggesting these cells have regrown a process that has successfully projected into the adjacent compartment yet is unable to functionally propagate an action potential. Over time in culture, the proportion of DiI labelled cells which lack functional responses greatly reduces to less than 5 % at 10 DIV. The acquisition of functional responses in a relatively large proportion of cells from stimulation of the terminals, suggests that these neurons undergo a period of maturation. Whole-cell patch clamp recordings from acutely dissociated embryonic DRG cultures reveal a period from E11.5 to E15.5 in which large proportions of DRG neurons exhibited immature action potential characteristics such as a failure to repolarise and a slow upstroke (Lechner et al., 2009). Immature neurons also lacked a sufficient density of VGSC as inward current amplitudes were significantly smaller in neurons with immature action potential characteristics (Lechner et al., 2009). Whilst these immature characteristics are measured in the DRG somata, it is conceivable that a similar maturation period occurs in the axon during its regrowth *in vitro*.

Embryonic onset of DRG excitability will undoubtedly be influenced by the expression of VGSCs. $Na_v1.3$ is characteristically expressed at high levels during DRG embryonic development peaking at approximately E17 in the rat, before being downregulated so that it is undetectable in normal conditions in the adult (Waxman et al., 1994). Prior to this embryonic peak in $Na_v1.3$ expression, during the time in which extensive neurite outgrowth is occurring, DRG neurons are unable to be excited by natural stimuli at E16 when recorded from *in vivo*, although spontaneous activity could still be detected (Fitzgerald, 1987). Therefore embryonic maturation of the neuron *in vivo* encompasses a period from approximately E15 to E18 during which they develop electrical excitability and expression of the embryonic $Na_v1.3$ channel is upregulated. At 3 DIV, a subset of neurons cultured in the microfluidic chambers appear to be electrically inexcitable and may therefore still be in an immature state, yet these cells appear to still possess the machinery required for axonal transport. By 5 DIV and 7 DIV, the large proportion of neurons are functionally responsive, suggesting they have matured and now express the required VGSCs necessary for action potential propagation. In terms of neuronal maturation *in vivo*, early pathfinding neurons must have appropriate mechanisms to detect and respond to guidance cues (Raper and Mason, 2010), in DRG neurons, these cues are often target derived neurotrophins. Therefore, *in vivo*, neurotrophin receptors and axonal transport proteins are absolutely essential for survival and to establish early

neuronal tracts, and it is only later that these neurons develop electrical excitability. It is conceivable that during the regrowth of the neurite in the microfluidic chambers, the ability to propagate action potentials lags slightly behind the establishment of axonal transport mechanisms, hence why a maturation period is observed during the first 3 – 5 DIV.

By 7 DIV the majority of cells are able to transport DiI from the terminals to the soma. However, there is a population of approximately 20 % that remain DiI negative (Figure 3.6.1). These neurons are also functionally unresponsive to stimulation of the terminals, but all display robust calcium transients in response to stimulation of the soma. It is unlikely that these neurons grow a projecting axon that does not transport DiI. DiI is a carbocyanine dye that is highly lipophilic meaning it readily incorporates into all plasma membranes that it is applied to and is not selective for specific neuronal subpopulations. Furthermore, the observation that DiI negative cells are also unresponsive to KCl stimulation at the terminals, simply suggests that a neurite has not grown through the microgrooves into the adjacent compartment. These DiI negative cells remain phase bright and are still activated by direct stimulation of the somata demonstrating they are alive and vital. To survive for approximately a week *in vitro*, these embryonic cells must have been signalling through TrkA to remain alive. However, without a projecting process how do they come into contact with NGF which after 3 DIV is only applied to the terminal compartment? At all medium changes, the established concentration and volume gradient means the unidirectional flow of NGF supplemented media is towards the somal compartment. The data I have collected by using a sensitive radioactive technique, suggests that over 24 hours there is a movement of approximately 1.5 % from the compartment with the greater volume to the compartment with a lower volume. A movement of only 1.5 % of 200 ng/ml NGF supplemented media would result in the NGF concentration in the somal compartment reaching approximately 3 ng/ml. A report by Lee and colleagues suggest that mouse DRG neurons dissected at E15 only need approximately 300 pg/ml NGF to survive (Lee et al., 1994) therefore these neurons are able to remain alive without projecting an axon into the terminal compartment. The proportion of cells that do not project into the terminal compartment is however always in the minority. I find that in an average culture at 7 DIV approximately 80 % of neurons actively seek the high concentration of NGF by growing a axon through the microgroove array into the adjacent compartment.

DiI and DiO double retrograde tracing was used to identify projecting neurons in the 3 compartment system. The lipophilic nature of both of these dyes lends them perfectly to this task. Both will permeate into the plasma membrane and will be incorporated into vesicles as part of lipid turnover, therefore uptake of the dye is not dependent on neuronal region, and will proceed in the axon, axonal collaterals and sensory terminals. Double tracing provides a reliable method to identify cells projecting into the distal terminal compartment as the soma of these cells will be positive for both DiI and DiO. These cells can confidently be labelled as having grown a process through the 2 microgroove arrays into the terminal compartment. However, from this technique alone, it is not possible to deduce if the cell has many projecting processes or if the processes themselves have

sprouting collaterals, as the use of lipophilic dyes does not differentiate between axonal uptake and uptake at any collaterals that may sprout from the axon. Despite this limitation, double retrograde tracing was perfectly suitable for the purposes of these studies due to the differences in the spectral properties of each dye, and the need for an accurate system to quantify neurons with a projecting process.

In the 3 compartment system, less than a quarter of cells that project into the middle compartment fail to project into the distal terminal compartment. In the same way that a small proportion of cells fail to project in the 2 compartment system but remain vital, these neurons will still receive NGF due to the hydrostatic pressure imbalance and therefore remain alive. Personal observations of projecting neurites in the middle compartment sometimes show that the neurites begin to grow perpendicular to the microgrooves once they have projected through the first microgroove array. These neurons when emerging from the microgroove pore, immediately turn either right or left and appear to remain tight against the PDMS mould. This may represent the preference for neuronal growth cones to grow adhered to surfaces, *in vivo*, these surfaces are formed by adjoined cells which form small openings that are thought to create tracts through which early neurons grow (Raper and Mason, 2010). The neurons that remain tight against the PDMS appear to continue growing and are not inhibited by this close contact, however this direction of growth, perpendicular to the microgrooves means they are unlikely to traverse the channel to the next microgroove array. Despite these cells that do not grow in a straight line after emerging from a microgroove, the majority of neurons do continue to grow a straight axon, with over 75 % successfully reaching the distal terminal compartment.

Mechanical sensitivity

To investigate the mechanical sensitivity, a very low-intensity mechanical stimulus was applied to both the somal and terminal compartment. This consisted of stopping and starting the flow of ECF in the respective compartments to induce membrane deformation. Mechanical stimulation is thought to be transduced by ion channels that are responsive to stretch or pressure, however the molecular identity of these channels has remained unclear. Mechanical force applied to the sensory terminals is suggested to activate mechano-transducers, through which ions influx and cause a local depolarisation, that may bring the membrane potential above the threshold for action potential triggering (Delmas et al., 2011). ASICs are suggested to play a role in mechanosensation. In animals with a knockout of ASIC2, firing frequencies in rapidly adapting fibres are reduced in response to mechanical stimulation (Price et al., 2000). Knockout of ASIC3 also resulted in a reduction of A-fibre mechanosensitivity (Price et al., 2001). However, in cultured DRG neurons derived from ASIC2 and ASIC3 double knockout, no difference in mechanical sensitivity was observed in large neurons, and mechanical currents evoked in medium and small diameter neurons were no different to wildtype controls (Drew et al., 2004). Therefore there is some discrepancy between the

involvement of the ASIC channels in mechanosensation, Delmas and colleagues suggest that ASICs do not function as direct mechano-transducers, but may modulate mechanical sensitivity.

The application of a low-intensity mechanical stimulus to the sensory terminals excited approximately 30 % of all cells, whilst stimulation of the soma excited less than 10 %. The difference in mechanical sensitivity may result from a differential expression of mechano-sensitive channels. Later studies suggest that the sensory terminals are significantly more sensitive to pH than the somata (Figure 4.3.1) which may result from a preferential transport of ASICs to the periphery (see Chapter 4 discussion). Therefore the heightened sensitivity of the terminals may result from a greater expression of ASICs in the periphery compared to the soma. *In vivo*, the large non-nociceptive are predominantly responsible for the detection of many forms of pressure change, and are characterised by their low threshold to mechanical stimulation. Alternatively, nociceptive neurons have a higher threshold of activation (Lewin and Stucky, 2000). Therefore, the use of NGF as a chemo-attractant may select predominantly for the nociceptive population. This, in addition to the low threshold stimulus, may account for the relatively low mechanical sensitivity observed in the soma compared to the terminals.

In summary, the novel combination of microfluidic chambers and functional calcium imaging provide an *in vitro* system in which action potential propagation can be investigated. Cultured DRG sensory neurons can be encouraged to regrow their axons in a unidirectional manner through 1 or 2 fluidically isolating microgroove arrays, which are readily detected using retrograde tracing. Furthermore, this technique is highly adaptable to discrete pharmacological treatments on the terminals, axon and soma.

Chapter 4

The receptive terminals of DRG sensory neurons can be investigated for proton sensitivity in microfluidic chambers

4.1. Introduction

Protons evoke a sustained activation of small, nociceptive sensory neurons, resulting in sharp, stinging pain in humans (Reeh and Steen, 1996). The molecular transduction mechanism of proton stimulation has been suggested to rely on distinct mechanisms, chiefly activation of TRPV1 (Bevan and Yeats, 1991; Caterina et al., 2000) and members of the ASICs (Price et al., 2001). The functional expression of two molecular proton transducers is thought to underlie the heterogeneous activation kinetics upon DRG stimulation with acid. Fast activated currents which are fully inactivated within 3 seconds are suggested to be mediated by the ASIC subunits that are heteromerically assembled (Benson et al., 2002), as these transients currents can be blocked by amiloride (Leffler et al., 2006). In contrast, sustained currents have been demonstrated to be maintained during a 10 second acid stimuli (Leffler et al., 2006), or even for minutes with continued acid stimulation (Bevan and Yeats, 1991). This second type of current is activated at a lower pH (pH < 6.2) than the transient current (activated with a step to pH < 6.8) and is shown to be almost exclusively restricted to capsaicin sensitive cells (Bevan and Yeats, 1991) suggesting TRPV1 is mediating the sustained acid-evoked current.

Over the past two decades a multitude of research has implicated TRPV1 and ASICs in the detection of H^+-ions. However, these reports often provide contradictory evidence as to the contribution of each transduction mechanism. In dissociated DRG cultures, Caterina et al., 2000, report an almost complete abolition of pH 5 evoked calcium transients in *Trpv1 -/-* mice, similarly in the *ex vivo* skin nerve preparation the same study also reports an almost complete elimination of acid evoked responses in C-fibres. This was confirmed in a later study by Leffler et al., 2006 in which disruption of the mouse *Trpv1* gene also led to a significant reduction of proton induced current in unmyelinated C-fibres detected by using the *ex vivo* skin-nerve preparation. Interestingly, proton responses were unaffected among the thin myelinated nociceptive population. These knockout studies suggest an almost complete reliance on TRPV1 for the detection of pH 5 in unmyelinated C-fibres.

Conversely, ASICs have been demonstrated to also play a significant role in acid transduction. Human transcutaneous acid iontophoresis evoked pain could be reduced by amilorde – a blocker of ASICs (Jones et al., 2004). In a similar psychophysical study, pain evoked from direct infusion of pH ≥ 6 into the forearm was significantly blocked by amiloride, whereas capsazepine, a blocker of TRPV1 had no effect (Ugawa et al., 2002). However, at pH 5, amiloride was less effective at blocking acid induced pain (Ugawa et al., 2002), suggesting ASICs play a major role in acid detection on nociceptors at moderately acidic pHs. In a separate study, repeated capsaicin application, which would temporarily desensitise TRPV1, did not reduce acid-induced pain, suggesting nociceptive proton detection is not through TRPV1 (Jones et al., 2004). Despite the evidence presented, experiments in ASIC knockout animals produce unclear results. One study in which ASIC3 was knocked out, report heightened pain behaviour to strong acid injection, and increased sensitivity to noxious thermal stimuli in the mutant animals (Chen et al., 2002). This unexpected phenotype was

suggested to result from a reduction in modulating activity due to loss of ASIC3, in response to high- but not low-intensity stimuli. Interestingly, this knockout mouse developed inflammation induced hyperalgesia and allodynia at the same level to wild-type controls, suggesting ASIC3 does not contribute to inflammatory induced pain. However, ASIC3 was shown to be essential for the development of mechanical hyperalgesia produced by repeated intramuscular acid injection (Sluka et al., 2003). Another ASIC3 knockout study demonstrated that the mutant mice show a reduction in mechanosensitivity to noxious pinch, but no behavioural differences compared to controls after acid injection in the paw (Price et al., 2001). The ASIC3 knockout studies tell a disparate story, which is likely to be further complicated by the fact ASICs are able to form heteromultimers (Benson et al., 2002).

In conclusion, there is a wealth of literature implicating both TRPV1 and ASICs as proton transducers, but the actual contribution of each channel to the overall detection of acid remains unclear. There seems to be some level of agreement that TRPV1 is involved with the transduction of stronger acids, whereas ASICs transduce moderate acidic stimuli (Tominaga et al., 1998), although even this is contradicted by *in vivo* ASIC3 knockout studies (Chen et al., 2002). In the reported literature acid sensitivity is usually only investigated in a single neuronal region. Transduction in the soma for example, is selectively studied in mass culture calcium imaging or patch clamp experiments, whereas the terminals are investigated in the skin nerve preparation and in acid application to the skin in human psychophysical experiments. Microfluidic chambers combined with calcium imaging allow a novel *in vitro* approach, in which functional investigations of spatial proton sensitivity in the terminals, axon and soma can be simultaneously examined. Furthermore, sensitivity differences can be studied by performing dose response experiments on separate neuronal regions, allowing the novel study of functional expression of acid transducers in the soma versus the peripheral neurites. This approach also lends itself to studying the contribution of specific transducers, by pharmacologically manipulating neuronal microenvironments, furthermore co-expression of acid transducers with other sensory ion channels can readily be investigated.

4.2. Objectives

The primary focus of these experiments was to investigate the proton sensitivity differences between peripheral terminals and the soma. The second aim was to explore the peripheral transduction mechanism of proton stimulation in the receptive terminals by using pharmacological blockers.

4.3. Proton sensitivity is differentially regulated in cell bodies and terminals of rat DRG sensory neurons *in vitro*

To investigate the sensitivity of the terminals and soma in isolation the 2 compartment microfluidic chambers were used. A pH dose response protocol was applied in ascending proton concentration first to the terminal compartment then to the somal compartment whilst imaging exactly the same field of cells. A range of pH solutions were investigated, beginning with pH 6.9 and finishing with pH 5.1. All percentages are expressed as a function of cells responding to KCl from stimulation of the terminals. The overall percentage of responding cells to stimulation of the terminals was significantly different compared to that of the terminals ($F_{1, 90}$ = 121.4, p<0.001, 2-way ANOVA). A Bonferroni post-hoc test revealed that at every pH level investigated, stimulation of the terminals resulted in a greater number of responding cells when compared with somal stimulation. For example, application of pH 6.9 (n_{cells} = 440, $n_{experiments}$ = 7) to the terminals activated 21 ± 5 % of cells, compared to only 3 ± 2 % when the soma was stimulated (Figure 4.3.1a, Figure 4.3.2a) (p<0.01). Further increasing the proton concentration to pH 6.6 (n_{cells} = 600, $n_{experiments}$ = 9) depolarised 74 ± 6 % of neurons when applied to the terminals, and only 26 ± 7 % responded to direct somal stimulation (Figure 4.3.1b, Figure 4.3.2a) (p<0.001). The increased sensitivity of the terminals compared to the soma continued to be observed at all subsequent pH levels. Application of pH 6.3 (n_{cells} = 781, $n_{experiments}$ = 12) excited 87 ± 2 % of neurons when applied to the terminals, and only 33 ± 7 % when applied to the soma (Figure 4.3.1c, Figure 4.3.2a) (p<0.001). Similarly, pH 5.7 (n_{cells} = 781, $n_{experiments}$ = 12) depolarised 92 ± 2 % of terminals, whereas somal stimulation activated only 49 ± 6 % of neurons (Figure 4.3.1d, Figure 4.3.2a) (p<0.001). Finally, at the most acidic pH used, pH 5.1 (n_{cells} = 571, $n_{experiments}$ = 10) depolarised 96 ± 2 % of cells when applied to the terminals, with only 62 ± 9 % activated at the soma (Figure 4.3.1e, Figure 4.3.2a) (p<0.01). KCl stimulation of the terminals is used to functionally identify all neurons with a projecting axon. When the terminal KCl pseudocolour image is overlaid with the pH 5.1 pseudocolour it is clear that there is almost a complete overlap of functional responses, indicating that the huge majority of receptive terminals express proton transducing proteins (Figure 4.3.1g). On the contrary, there is a profound reduction in neurons responding to pH 5.1 when assessing the somal pseudocolour overlay. The significantly increased sensitivity of the terminals was observed at all pH levels tested, and provides compelling evidence that proton sensitivity is differentially regulated between peripheral regions and the cell body in cultured DRG neurons.

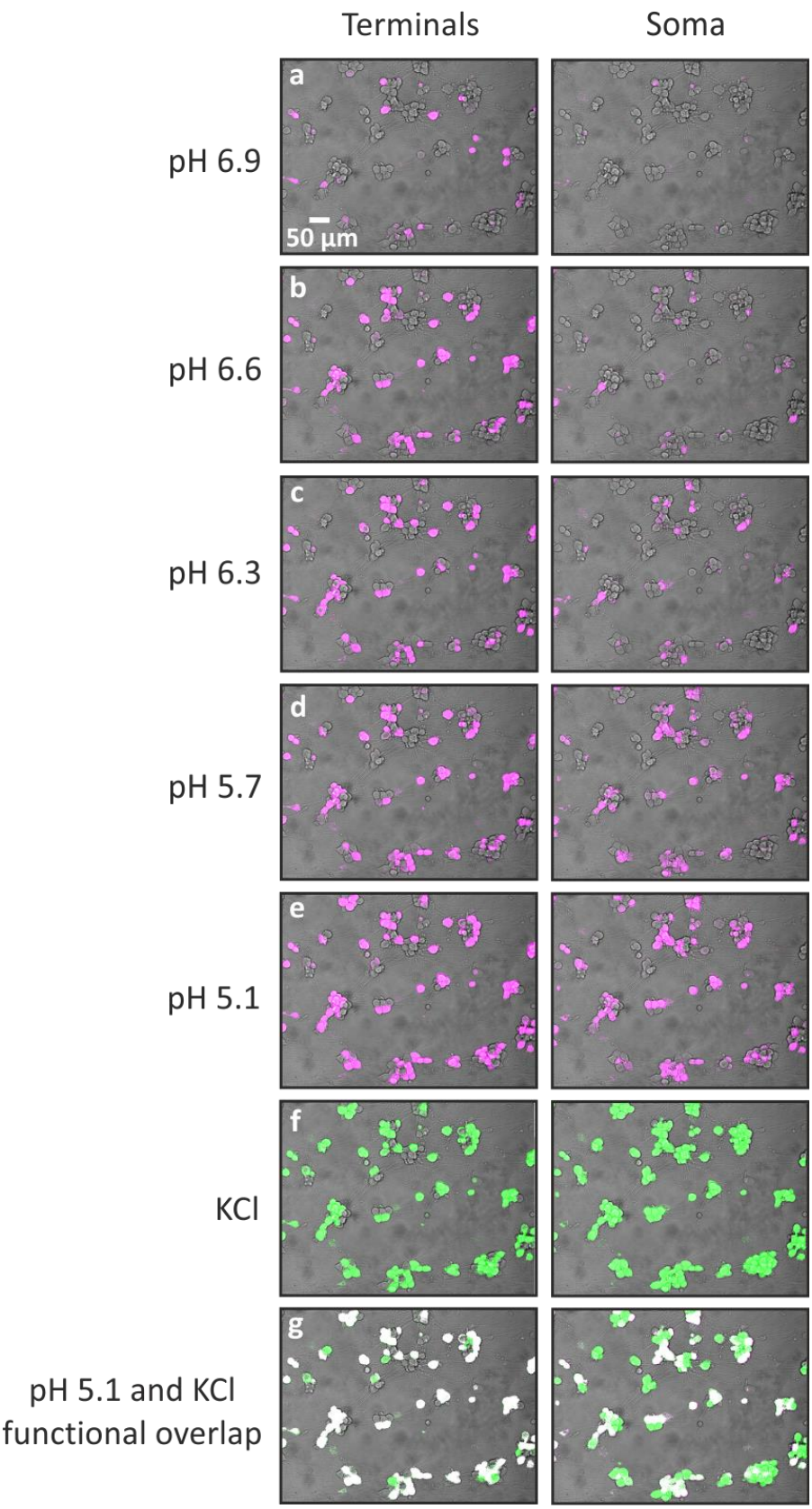

Figure 4.3.1
Receptive terminals exhibit an increased sensitivity to proton stimulation than the cell soma. Representative pseudocolour image of cells responding to (a) pH 6.9, (b) 6.6, (c) 6.3, (d) 5.7, (e) 5.1, (f) KCl, when applied to the terminals or the soma. (g) Representative pseudocolour overlay of cells responding to pH 5.1 and KCl, for terminal and somal stimulation, white cells respond to both stimuli, whereas green cells only respond to KCl.

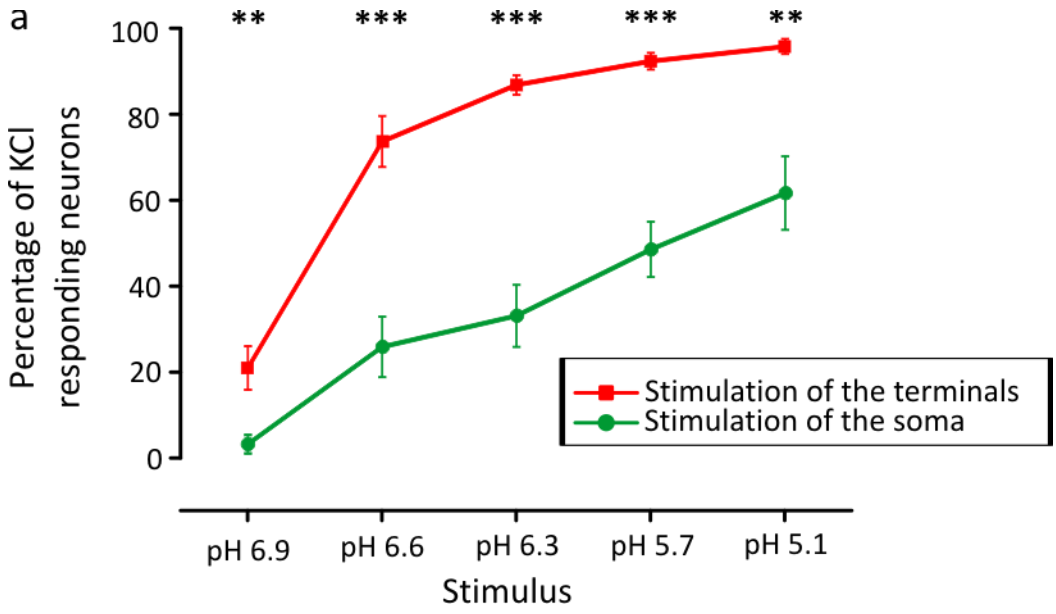

Figure 4.3.2
*(a) Quantification of responding cells to proton stimulation applied to the terminals and soma, expressed as a percentage of KCl responding neurons from stimulation of the terminals. In the same population of cells, pH stimulation of the terminals always results in a greater percentage of responding neurons compared to direct stimulation of the somata. (***p<0.001, **p<0.01, 2-way ANOVA with Bonferroni post-hoc).*

4.4. The terminals and axon both display a greater sensitivity to protons than the soma *in vitro*

To study functional proton sensitivity across regions of a rat DRG neuron the 3 compartment chamber was used. Acidic solution of pH 5.1 was first applied to the terminals, then to the axons and finally to the soma, whilst recording the calcium responses from the same population of cell soma. All percentages are expressed as a function of cells responding to KCl from stimulation of the terminals. Of these cells, 91 ± 2 % (n_{cells} = 687, $n_{experiments}$ = 6) also responded to proton stimulation applied to the terminals (Figure 4.4.1a, d). Moreover, 95 ± 2 % (n_{cells} = 687, $n_{experiments}$ = 6) of the same population of cells also responded to the proton stimuli applied to the axonal compartment (Figure 4.4.1b, d) indicating an almost complete overlap in functional responsiveness. This suggests that almost all neurons have proton sensitivity in both the terminals and axon *in vitro*. As previously demonstrated, the somal sensitivity was lower, with only 49 ± 12 % (n_{cells} = 687, $n_{experiments}$ = 6) of cells responding (Figure 4.4.1c, d). Comparisons of the differences between neuronal regions, revealed that the proton sensitivity of the soma was significantly different to the terminals ($p<0.01$, Mann-Whitney *U* test) and the axon ($p<0.01$, Mann-Whitney *U* test), there was no significant difference between the terminal and axonal populations ($p>0.3$, Mann-Whitney *U* test). This therefore suggests that both the terminals and axons express proton transducing proteins in DRG neurons in culture. This confirms the previous result that the terminals have a heightened sensitivity to protons compared to the soma. Furthermore, these results suggest that this heightened sensitivity extends to the axons of DRG neurons *in vitro*.

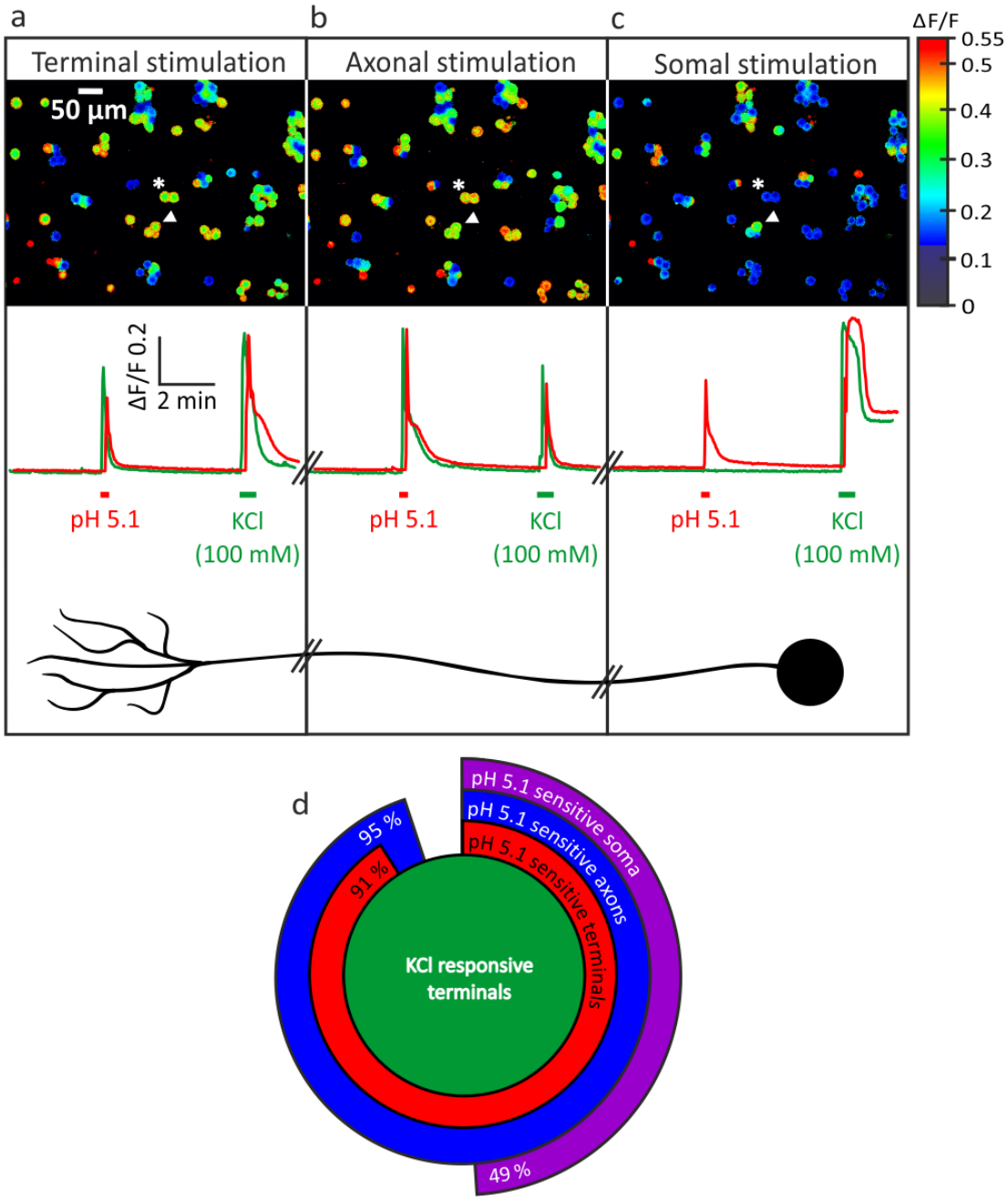

Figure 4.4.1

Terminals and axons show a high degree of proton sensitivity overlap. (a-c) Fluorescent images and representative calcium transients during regional stimulation of DRG sensory neurons. (a) Peak calcium response and transients showing stimulation of the terminals by pH 5.1 results in the depolarisation of the majority of cells. (b) Peak calcium response and transients showing stimulation of the axons by pH 5.1 also activates many of the cells. (c) Peak calcium response and transients showing direct stimulation of the soma results in activation of only a subset of cells. Green trace illustrates the calcium response of a neuron that is activated by pH 5.1 in the terminals and axon, but is proton insensitive at the soma (asterisk). The red trace illustrates the calcium response of a neuron that is activated by protons in all 3 neuronal regions (arrowhead). (d) Quantification of cells responding to pH 5.1 stimulation of the terminals, axons and soma. Values are expressed as a percentage of cells activated by KCl stimulation of the sensory terminals.

4.5. Proton responses are primarily transduced by acid-sensing ion channels

Proton stimulation can be transduced by both the ASICs and TRPV1. To assess the contribution of each molecular transducer in rat DRG cells cultured in the compartmentalised chambers, acid stimuli were applied in the presence of the ASIC blocker – amiloride. pH 5.7 was chosen as the test stimulus, as this evoked a somal depolarisation in over 90 % of KCl responsive cells when applied to the terminals (Figure 4.3.2a). In order to calculate the contribution of ASICs, the population of cells responding to pH 5.7 were set as the 100 % value. After an initial pH 5.7 test stimuli, 100 µM amiloride was continuously washed into the terminal compartment of a 2 compartment system during the 5 minute interstimulus interval (Figure 4.5.1e). This was followed by a second pH 5.7 stimulus that also contained 100 µM amiloride, so that the test stimulus did not wash out the drug. Responses in the presence of amiloride were significantly reduced to only 21 ± 4 % ($p<0.001$, paired t-test) (n_{cells} = 412, $n_{experiments}$ = 6) of neurons that were previously responsive to pH 5.7 (Figure 4.5.1c, e, Figure 4.5.2a). Furthermore, after a subsequent 5 minute drug washout period with ECF, the large majority of cells (91 ± 4 %) were depolarised again by a third pH 5.7 test stimuli (Figure 4.5.1d, e, Figure 4.5.2a). The difference between the cellular populations that responded with amiloride and after amiloride wash-out proved to be highly significant ($p<0.001$, paired t-test) (Figure 4.5.2a). The use of a specific ASIC blocker has revealed that these channels are primarily responsible for the transduction of a pH 5.7 stimulus in vitro. There is however a population of cells that are insensitive to amiloride and continue to respond despite its application (Figure 4.5.1c, e, Figure 4.5.2a). This suggests that another proton transducing mechanism must contribute to the proton induced excitability at pH 5.7.

To investigate the proton transduction mechanisms at a less acidic pH, the same experiment was repeated with a test stimulus of pH 6.6. At this pH there was a complete elimination of all responses when amiloride was washed in (Figure 4.5.2b) which was significant when compared to the percentage of cells responding to pH 6.6 before and after amiloride treatment (Figure 4.5.2b). This indicates that ASICs are entirely responsible for the transduction of a pH 6.6 stimulus when applied to the sensory terminals.

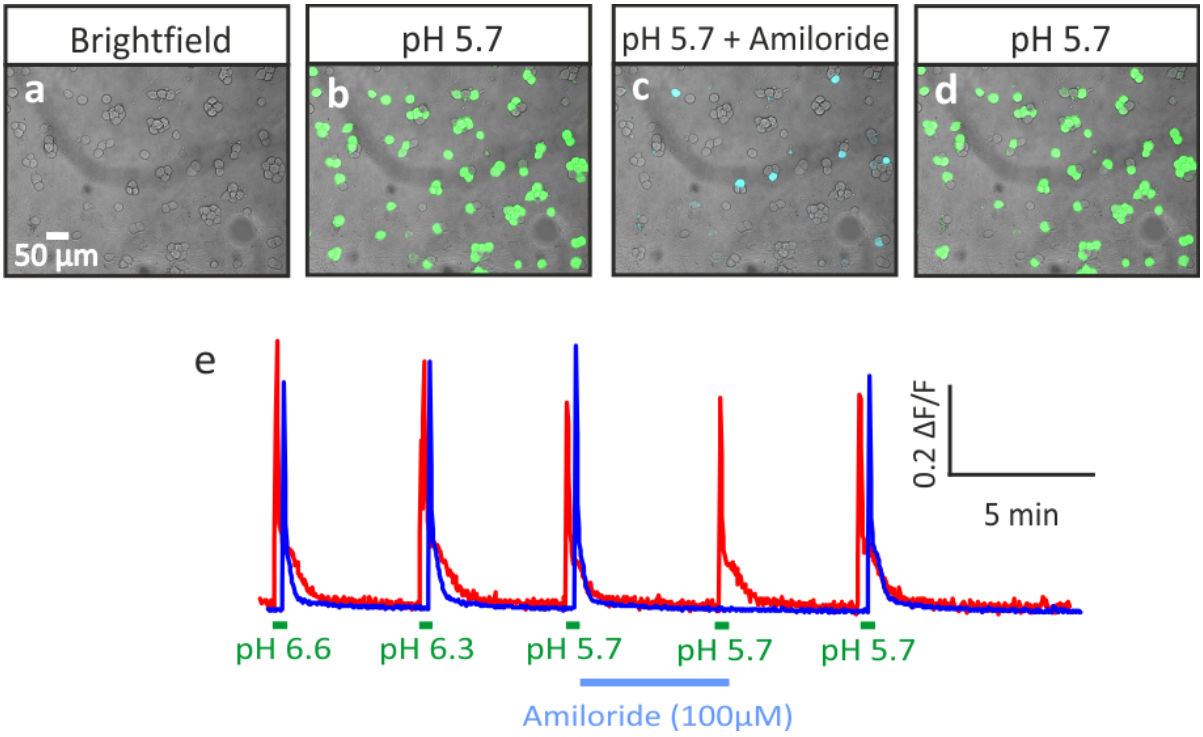

Figure 4.5.1
Proton transduction is mediated primarily through acid sensing ion channels. (a) Brightfield image of a field of cells. (b) Representative pseudocolour image of the cells that are depolarised by pH 5.7 applied to the terminals. (c) Representative pseudocolour image of the cells that continue to be activated by pH 5.7 in the presence of amiloride. (d) Representative pseudocolour image of the cells that are depolarised by pH 5.7 after amiloride washout. (e) The red trace illustrates the calcium response of an amiloride insensitive cell. The blue trace illustrates the calcium response of an amiloride sensitive cell.

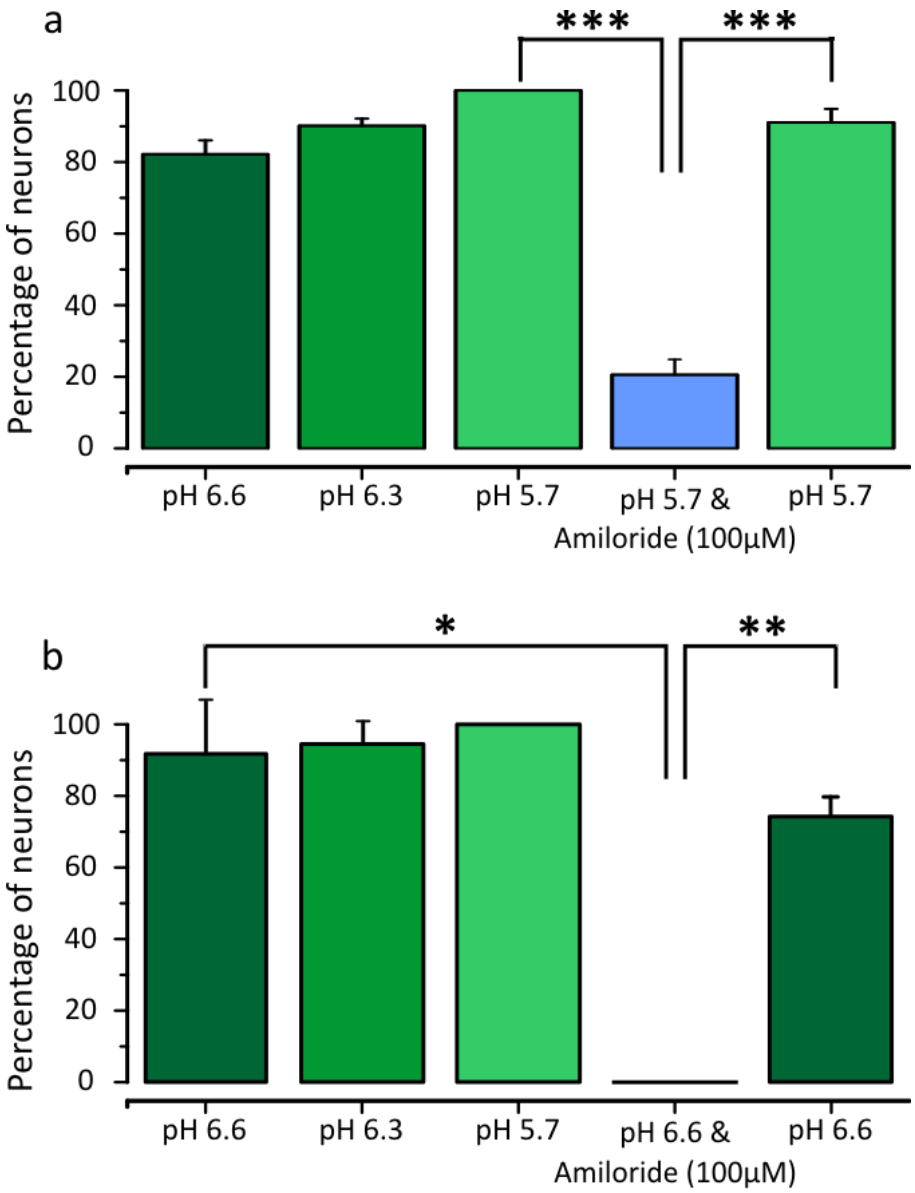

Figure 4.5.2
*(a) Quantification of responding cells to pH 5.7 in the presence of amiloride. (b) Quantification of responding cells to pH 6.6 in the presence of amiloride. (*p<0.05, **p<0.01, ***p<0.001, paired t-test).*

4.6. The majority of amiloride resistant neurons express TRPV1

Approximately 20 % of neurons rely on ASIC-independent mechanisms for proton transduction demonstrated by their insensitivity to amiloride. Therefore at least one other mechanism should exist in these cells that are responsible for proton induced excitation. To address this question, additional experiments were conducted repeating the pH 5.7 test stimuli in the presence of amiloride, with an additional stimulus of the TRPV1 receptor agonist, capsaicin, applied to the terminals. The percentage of amiloride resistant cells observed in this set of experiments was 17 ± 6 % (Figure 4.6.1a) (n_{cells} = 239, $n_{experiments}$ = 5) which was very similar to that observed in the previous experiment. As depicted in Figure 4.6.1a, 50 ± 5 % of the cells excited by pH 5.7 applied to the terminals also displayed a robust depolarisation by peripheral application of 1 µM capsaicin (n_{cells} = 239, $n_{experiments}$ = 5). Of the amiloride resistant neurons, 72 ± 8 % were activated by capsaicin, indicating that TRPV1 is the likely candidate for proton transduction in these neurons. Of the neurons that were blocked by amiloride, 35 ± 6 % (n_{cells} = 239, $n_{experiments}$ = 5) also displayed capsaicin sensitivity. This suggests that these neurons functionally expressed both TRPV1 and ASICs, yet upon amiloride induced blockade of the ASICs, TRPV1 was unable to transduce any acid-evoked excitation, indicating that these neurons relied entirely upon ASICs for proton transduction. Interestingly, 28 ± 8 % of the amiloride resistant neurons, equating to 5 % of the total pH 5.7 responsive population, were also unresponsive to capsaicin (Figure 4.6.1a). This intriguing result hints at the possibility of an additional, TRPV1 and ASIC independent mechanism for proton transduction that is expressed in the terminals of DRG sensory neurons in culture.

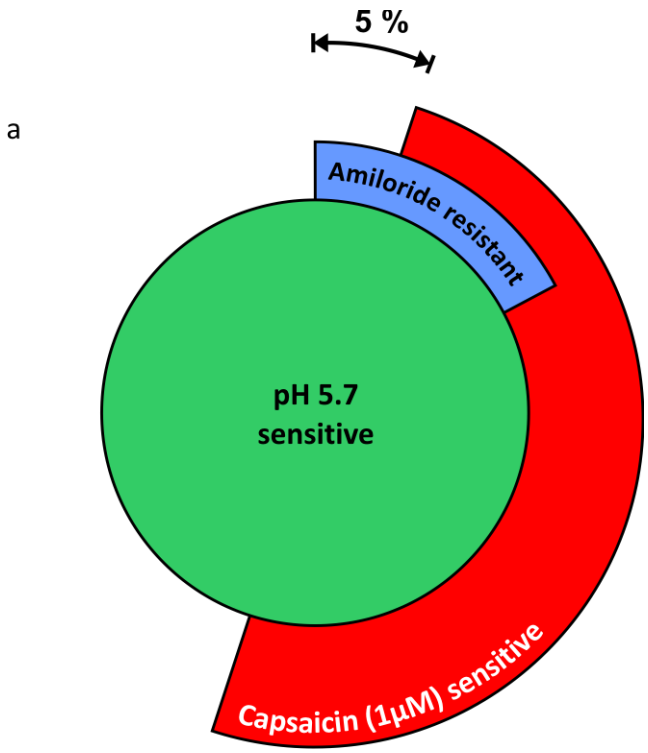

Figure 4.6.1
The majority of neurons with ASIC independent proton responses express TRPV1. (a) Quantification of the amiloride resistant population to pH 5.7 stimulation, and the functional overlap with TRPV1 expressing neurons.

4.7. Amiloride does not induce a conduction block when applied to the axons

In order to investigate how and where amiloride binds to produce a significant inhibition of pH 5.7 induced excitation, the 3 compartment chamber was employed. The terminal compartment was stimulated with a pH 5.7 buffered solution, whilst amiloride was washed into the middle compartment before the second stimuli. This experimental protocol enabled investigations into whether amiloride produced a conduction block in a similar manner to TTX and Lidocaine. In two separate experiments (n_{cells} = 73, $n_{experiments}$ = 2), 98 % and 93 % of cells continued to respond to acid stimulation of the terminals when the axon was exposed to amiloride (Figure 4.7.1a, b, c, d). Figure 4.7.1c displays a calcium transient for a single cell that was representative of the majority. The cell continued to respond with a robust calcium peak in response to a pH 5.7 stimulus to the terminals, even when amiloride was applied to the axonal compartment, suggesting stimulus transduction rather than action potential propagation is blocked by amiloride.

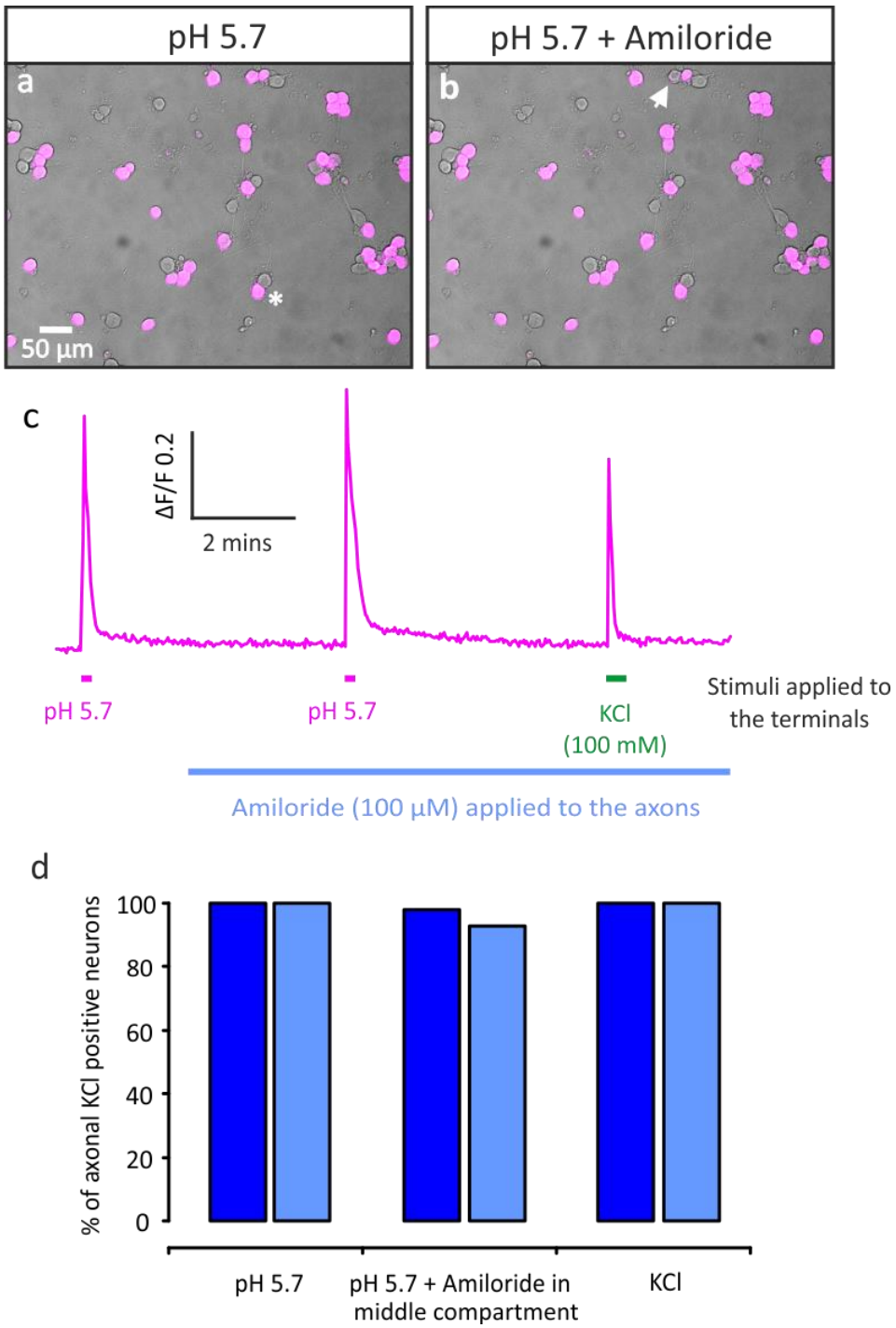

Figure 4.7.1
Amiloride does not cause a conduction block when applied to the middle axonal compartment of a 3 compartment chamber when the terminals are stimulated with pH 5.7. (a) Representative pseudocolour image showing all neurons that are depolarised by pH 5.7 application to the terminals. (b) Representative pseudocolour image showing neurons that continue to respond to pH 5.7 stimulation, when amiloride is applied to the axons. Arrow illustrates one neuron that does not respond to the second pH 5.7 stimulation. (c) Calcium transient of the cell highlighted with an asterisk in (a) demonstrating amiloride does not induce a conduction block when applied to the axons. (d) Quantification of 2 separate experiments showing almost no reduction in responses when terminals are stimulated with pH 5.7 and amiloride is applied to the axons.

4.8. Discussion

The principle finding of these experiments is that there is a significant differential regulation of proton sensitivity between peripheral neuronal regions and the cell soma *in vitro*. Furthermore, neurons depend entirely upon ASICs for proton transduction at pH 6.6, and these channels constitute the major transduction mechanism for a pH 5.7 stimulus. The majority of amiloride insensitive neurons are capsaicin sensitive, suggesting TRPV1 is implicated in proton transduction in these neurons. A small population of cells are both amiloride resistant and capsaicin insensitive indicating the possible presence of an additional transduction mechanism other than ASICs and TRPV1.

Differential proton sensitivity may be caused by a preferential transport of ASICs to the periphery

The profound differences in proton sensitivity between peripheral regions and the soma, observed in Figure 4.3.2, suggest that there is a differential regulation of sensitivity between these neuronal regions. This differential regulation was manifested as a significant increase in the responding population when stimulated in the periphery compared to the soma, and was also observed across a range of pH test stimuli. There are several mechanisms which could result in a heightened peripheral sensitivity. Firstly, mechanisms may be in place to preferentially associate newly translated proton transducers in the cell body with the axonal transport machinery. This would favour the functional expression of the transducing molecules in the periphery rather than in the somal membrane, and as a result influence the regional sensitivity to H^+. Secondly, ion channels and sensory receptors are heavily modulated by intracellular mechanisms such as phosphorylation. Rather than a physical increase in the expression of proton transducers in the periphery, these may be more highly 'tuned' to detect protons compared to those in the soma. Membrane bound proton transducers are gated by H^+ ions, intracellular signalling may influence the kinetics of the transducing proteins so that channel opening is kinetically easier.

ASICs are proton-gated, voltage insensitive, sodium permeable channels, which are expressed in nociceptors where they participate in detecting acidosis. A report by Garcia-Anoveros and colleagues in 2001, thoroughly investigated the subcellular localisation of BNaC1α (García-Añoveros et al., 2001), which is now referred to as ASIC2. Within the cell bodies of DRG neurons, the protein was not uniformly expressed throughout the membrane, but was accumulated in the cytoplasm near the axon hillock, suggesting that it is being prepared for peripheral transport (García-Añoveros et al., 2001). Axonal transport analysis using ligatures applied to the central and peripheral axon demonstrated that ASIC2 was not undergoing transport to the central synaptic terminals or the processes leading up them, but instead the large proportion is transported in the anterograde direction towards the sensory terminals (García-Añoveros et al., 2001). Detection of the ASIC2 protein using immunohistochemistry in skin sections revealed that it was heavily associated with a variety of mechanosensory terminals, including Meisner corpuscles, Merkel cells and myelinated intra-epidermal free nerve endings (García-Añoveros et al., 2001; Cabo et al., 2012). The location of

ASIC2 in specialised mechanoreceptor end organs is consistent with the view that this channel is implicated in mechanosensation (Price et al., 2000), however, this channel has also been shown to be gated by protons (Lingueglia et al., 1997), and therefore may have an additional role in the periphery as an acid sensor. The unidirectional transport of ASIC2 suggests that this protein must be sorted before the branching of the central and peripheral process so that it is targeted to the correct destination. The preferential transport in the anterograde direction suggests ASIC2 has a function exclusive to the periphery.

Other structurally related ASICs have also been demonstrated to be proton gated. A rapid drop of pH from 7.4 to 4 induced a fast rising, amiloride sensitive sodium current in cells heterologously expressing ASIC3 (Waldmann, 1997). ASIC3 was detected in most large and small diameter neurons, suggesting widespread expression amongst all sensory neuron subtypes. A large overlap in expression between ASIC3 and substance P, a marker of the peptidergic nociceptors, has been observed (Price et al., 2001). Furthermore, ASIC3 colocalised with neuronal markers of Meisner corpuscles, lanceolate nerve endings and in some free nerve endings in the epidermal layer (Price et al., 2001). The same study also demonstrated that ASIC3 knockout mice displayed a reduced number of withdrawals to mechanical stimulation after intra-muscular acid injection. These data suggest ASIC3 is expressed in the peripheral terminals of nociceptors innervating both muscle and skin, indicating mechanisms are present to control the peripheral expression or to transport ASIC3 to the sensory terminals. Furthermore, in response to NGF application to the skin, ASIC3 axonal transport has been demonstrated to increase the sensitivity to proton stimulation (Rukwied et al., 2010), confirming mechanisms exist to translocate acid sensors.

The peripheral localisation of ASICs, and the preferential transport to the sensory terminals therefore makes them well placed to function as proton detectors. It is conceivable that the mechanisms involved in the transport of ASICs *in vivo* also influence the localisation of these channels *in vitro*. Stomatin-like protein 3 (SLP3) and stomatin, are both proteins that colocalise with microtubule associated vesicles distributed throughout the cytoplasm and axon in DRG neurons (Lapatsina et al., 2012). Recently, SLP3 has been shown to strongly interact with ASIC2 and ASIC3, and that these protein complexes were localised to vesicular compartments (Lapatsina et al., 2012). The vesicle marker – Rab11 also colocalised with these vesicles, and previous work has demonstrated that Rab11 positive vesicles in vesicles are implicated in the transport of important signalling proteins to the plasma membrane (Eva et al., 2010), and that these are predominantly transported in the anterograde direction (Ascaño et al., 2009). It therefore seems likely that Rab11/SLP3-positive vesicles in DRG neurons transport ASICs to peripheral neuronal regions. Lapatsina and colleagues further demonstrate that acid-gated currents are substantially increased in amplitude at the same time SLP3 positive vesicles fuse with the plasma membrane, which incorporates more ASIC subunits into the membrane making them available for proton gating (Lapatsina et al., 2012).

The preferred anterograde transport of Rab11 positive vesicles and their association with ASICs make these an attractive option for the sorting process which results in the preferential anterograde transport of some ASICs. The increased proton sensitivity of peripheral neuronal regions observed in the microfluidic chambers may reflect the preferred localisation of ASICs to the sensory terminals. Greater expression of ASICs in the periphery would increase the evoked sodium current upon proton stimulation, and increase the probability of action potential propagation. Furthermore, if functional expression is greater in the periphery due to the preferential transport of ASICs, a greater proportion of neurons would respond upon peripheral acid stimulation, which could explain the differential regulation of sensitivity observed in the microfluidic chambers.

Does local axonal translation influence proton sensitivity?

In recent years there has been a growing appreciation for the role of local protein synthesis in regulating neuronal function. Mechanisms in which mRNAs are transported, localised and translated are emerging, and these processes have been shown to heavily contribute to the regenerative capacity of sensory neurons after axotomy by promoting the synthesis of growth cone proteins (Verma et al., 2005). When DRG neurons are dissected for *in vitro* culture, only the soma is removed therefore meaning both the peripheral and central processes are axotomised during the dissection. Consequently, regeneration of the growth cone is essential for the regrowth of axons (Verma et al., 2005) and this is especially important in the microfluidic chambers which depend upon the regrowth of the axon into adjacent compartments. Clearly, the development of the growth cone during embryogenesis and regeneration after nerve injury are fundamental for DRG development and repair. The regrowth of the axon *in vitro* demonstrates the growth cone is regenerated when the cell is removed from its natural environment. A recent study has used microfluidic chambers to isolate the mRNA transcripts localised specifically in sensory axons from both embryonic and adult neurons (Gumy et al., 2011). This system provides an excellent method for harvesting axonal specific transcripts due to the isolated microenvironments, this also ensuring samples are free of somal transcript contamination. One of the most important findings of this study revealed that synthesis of some proteins in embryonic DRG axons rely heavily on local translation rather than axonal transport from the cell soma, this included TUBB3, a cytoskeletal protein, which is likely to be required during axonal growth (Gumy et al., 2011).

In terms of sensory neurons, and the considerable distance between soma and terminals, it is conceivable that local translation in the periphery would enable a much more rapid response to the local environment rather than relying on axonal transport alone. Translation takes place in three stages, initiation, where the ribosome is correctly assembled around the initiation codon of the mRNA, elongation, where the transfer RNA binds to the corresponding sequence on the mRNA, resulting in the formation of a peptide bond between amino acids, and finally, termination, where a stop codon is encountered and the finished peptide is released from the ribosome (Kapp and Lorsch, 2004). Translation of mRNA is tightly regulated by a large number of kinases, with initiation largely

controlled by the protein kinase, mammalian target of rapamycin (mTOR). Extracellular regulated kinase (ERK) can also control the initiation of translation by phosphorylating the eukaryotic initiation factor 4E (eIF4E).

Both mTOR and ERK pathways are activated in sensory afferents after noxious stimuli and are critical for neuronal plasticity following such insults. Interestingly, these protein kinases are thought to act through different mechanisms and in different subpopulations of sensory neurons (Obara et al., 2012). These separate mechanisms have been investigated using the algogens, interleukin (IL)-6 and NGF as both induce long-lasting hyperalgesia in rodents, and both are heavily linked to inflammatory and neuropathic pain (Lewin et al., 1994; Dina et al., 2008). Sensitisation of DRG neurons by intraplantar injection of IL-6 or a combination of IL-6 and NGF induced a long-lasting mechanical hypersensitivity which could be reduced by inhibition of the ERK pathway using U0126 (Melemedjian et al., 2010). In the same study, cultured DRG neurons were shown to be activated by NGF, and this could be blocked by the mTOR inhibitor rapamycin. Further studies have demonstrated that the inhibition of mTOR by local injection of rapamycin into the hind paw of rodents, reduced the mechanical hyperalgesia around the capsaicin injection site (mediated by A-fibre nociceptors) (Jiménez-Díaz et al., 2008). Therefore, local translation appears to play a significant role in regulating the sensitivity of the sensory terminals in a subset of nociceptive neurons. The current thinking is that in response to tissue injury, the inflammatory factors released in the periphery increase the sensitivity of a subpopulation of C-fibres resulting in primary hyperalgesia, which can be attenuated by blockade of the ERK pathway. mTOR has not been detected in afferents penetrating into the epidermal layer (Jiménez-Díaz et al., 2008), suggesting this member of the translation apparatus is not expressed in unmyelinated C-fibres. In agreement, primary hyperalgesia cannot be attenuated by mTOR inhibitors (Obara et al., 2011). The area surrounding the injury site is sensitised to mechanical stimuli that results from central processing acting predominantly on a subset of A-fibres. Rapamycin can reduce mechanical sensitivity implying mTOR mediated translation contributes to secondary hyperalgesia (Obara et al., 2011).

TRPV1 is a well-established proton sensor (Figure 4.8.2) and anterograde transport of the capsaicin receptor in a form capable of ligand binding has been reported (Szallasi et al., 1995). However, in addition to the transport of the TRPV1 protein to the periphery, an increase in the transport of TRPV1 mRNA has also been observed under inflammatory conditions, which may contribute to the hypersensitivity to primary afferents (Tohda et al., 2001). In addition, changes in TRPV1 receptor expression and threshold are well documented after inflammation (Caterina and Julius, 2001). Important protein synthesis sites in the form of ribosomes, have also been found to be distributed in clusters along myelinated axons (Koenig et al., 2000), demonstrating the machinery required for local translation is present in some peripheral sensory axons. mTOR however is not found in the peripheral terminals of unmyelinated C-fibres (Jiménez-Díaz et al., 2008) suggesting the enhanced expression of proton transducers observed in the periphery of unmyelinated cultured neurons is not regulated by mTOR mediated local translation. Whilst mTOR appears not to be

involved, the ERK protein kinases may play a role. Peripheral sensitisation results from heightened thermal sensitivity as a result of increased TRPV1 receptor expression in the peripheral terminals. It is thought that ERK activation at the cell body results in increased TRPV1 synthesis and its transport to the peripheral terminals (Zhuang et al., 2004), suggesting increased axonal transport rather than local translation may play a greater role in regulating the acid sensitivity in the peripheral terminals of cultured neruons. The detailed genome wide microarray expression analysis of embryonic and adult sensory axons grown in compartmentalised chambers also failed to detect mRNA of the classical proton transducers – TRPV1 and ASICs (Gumy et al., 2011). With these studies in mind, it seems more likely that the preferential transport of acid sensors to the peripheral terminals is responsible for their enhanced sensitivity.

Distal and proximal neurites display a similar acid sensitivity

The axonal transport of proton transducing proteins may be responsible for the heightened proton sensitivity in the peripheral regions of cultured DRG neurons. If this is the case, it is clear that the mechanisms involved in localising and depositing the proteins is not restricted to the extreme distal regions of the neuron. Functional identification of proton transducers in the 3 compartment chamber demonstrates an almost complete overlap in expression of the distal terminals with the more proximal axon. Whilst this system does not allow discrete identification between the axon and axon collaterals, it is clear that the functional insertion of acid sensors is occurring at more than one distal axonal region, due to the dual sensitivity when tested in the terminal and axonal compartment. Axonal transport can deposit proteins into the plasma membrane in two ways which would result in functional sensitivity when tested in the middle axonal compartment. Firstly, if sprouting collaterals terminate in the middle compartment, the fusion of transport vesicles containing newly synthesised proteins can occur at the growth cone meaning the collaterals would be sensitive to proton stimulation. On the other hand, membrane insertion could occur at all points along the axon, including the collaterals, so that the entire axolemma has the potential to detect protons. During development, transporting proteins to the growth cone appears to take precedence over insertion into the axolemma (Vogt et al., 1996). The preferential insertion of membrane proteins at the tip is crucial for the growth of the axon, and during development, key signalling molecules located in the growth cone such as neurotrophin receptors are crucial for guiding the axon to its target (Gallo et al., 1997). However, capsaicin sensitivity has been demonstrated along the entire extent of sensory neurons, including the central and peripheral fibres and their respective endings (Holzer, 1991), suggesting that TRPV1 is not only inserted at the growth cone, but along the entire axolemma. Functional data alone is unable to pinpoint the exact location of acid sensors whether specifically at the growth cone or more widely distributed, but these data presented here do confirm the functional expression of these sensors at several peripheral regions – the distal receptive terminals, and either or both the proximal axon and axon collaterals.

ASICs account for the major acid detectors in vitro

Due to the disparity in the literature regarding the contribution of TRPV1 and ASICs to acid sensitivity, one of the objectives of these experiments was to investigate the mechanisms by which proton stimuli are transduced in the compartmentalised in vitro system. Data presented here suggest that ASICs transduce the entire proton response in the terminals when stimulated with pH 6.6, due to the complete block of all pH 6.6-evoked responses by amiloride. This role of the ASICs to transduce relatively weak acidic stimuli, is in good agreement with early work in which transient currents, now thought to be mediated through ASICs, are evoked by a pH 6.8 stimulus in DRG neurons (Bevan and Yeats, 1991) (Figure 4.8.2). The acid detection threshold of ASICs is somewhat dependant on the heteromeric arrangement of subunits, which can be difficult to measure, however homomeric arrangements have been well studied and the half maximal effective pH has been determined as 6.2-6.8 (ASIC1a), 5.1-6.2 (ASIC1b), 4.1-5 (ASIC2) and 6.2-6.7 (ASIC3) (Waldmann et al., 1997; Chen et al., 1998; Benson et al., 2002). These activation values suggest ASIC1a and ASIC3 are well placed as the likely transducers for pH 6.6 as tested in Figure 4.5.2.

The role of ASICs in transducing stronger acidic stimuli is however more controversial. The results presented in this thesis suggest that ASICs transduce the majority of the response at pH 5.7. However, analysis of the capsaicin knockout animal show strongly reduced inward currents with a pH 5 stimulus, suggesting that TRPV1 is primarily responsible for transduction at this acidity (Caterina et al., 2000; Davis et al., 2000). Despite the suggestion that TRPV1 transduces stronger acidic stimuli, amiloride sensitive, transient, sodium currents were found to have a considerably increased prevalence at pH 4 than pH 5 and 6, when tested in wildtype mouse DRG neurons (Leffler et al., 2006). Similarly, when the TRPV1 knockout mouse was examined, the detection of ASIC mediated proton currents was found to be 7 % with a pH 5 stimuli, and 42 % with pH 4 (Leffler et al., 2006). This suggests that in mouse DRG somata, ASICs show a greater sensitivity to low (pH 4) over moderate (pH 5 and 6) acidic stimuli. Despite this finding, my results suggest ASICs are vital for the detection of moderate (pH 5.7 – pH 6.6) acidic stimuli. The reason for this discrepancy is likely to be due to inter-species variation and there are two possible reasons for this discrepancy. Firstly, all the experiments discussed in this chapter were performed using embryonic rat cultures. The prevalence of ASIC mediated sodium currents are considerably greater in rat compared to mouse. For example, Leffler et al., 2006 report that in wildtype rat DRG neurons tested *in vitro*, 61 % and 45 % of pH 6 and pH 5 evoked current, respectively, displayed a transient, ASIC-like current. This compares with only 18 % and 12 % of pH 6 and pH 5 evoked currents, respectively, in wildtype mouse cultures (Leffler et al., 2006). Therefore, the 80 % inhibition of pH 5.7 evoked responses by amiloride, as measured in the microfluidic cultures most likely represents the greater expression of ASICs in rat DRG neurons compared to mouse.

The test stimulus of pH 5.7 in combination with amiloride did not result in a complete block as exhibited by pH 6.6. Instead, 21 % of pH 5.7 sensitive cells continued to respond to a stimulation

in the presence of amiloride, indicating the presence of an additional transduction mechanism. To investigate this, experiments were carried out in which a pH 5.7 and capsaicin stimulus were applied to detect the functional expression of TRPV1. Of the pH 5.7 responsive neurons, four subpopulations were detected in terms of ASIC and TRPV1 expression. 45 % expressed only ASICs which were solely responsible for pH 5.7 detection as they were blocked by amiloride. 38 % functionally expressed both ASICs and TRPV1, but only ASICs transduce the acid response as all these neurons were blocked by amiloride. 12 % were amiloride resistant and capsaicin sensitive, suggesting TRPV1 is the likely candidate for acid detection in this subpopulation. Finally, 5 % were amiloride resistant and capsaicin insensitive suggesting neither of these channels were responsible for acid detection in these neurons. The finding that TRPV1 plays a role in acid transduction at pH 5.7, but not at pH 6.6, corresponds well with the proton activation threshold of TRPV1. At room temperature, TRPV1 exhibited an activation threshold of ≤ pH 5.9 (Tominaga et al., 1998), meaning the evoked response in amiloride resistant, capsaicin sensitive cells is likely to be transduced by TRPV1. Figure 4.6.1 demonstrates that 76 % of TRPV1 positive neurons also express ASICs, as determined by the functional block with amiloride, this is in line with a previous report, which suggested that nearly 60 % of TRPV1 positive neurons coexpress ASICs (Ugawa et al., 2005). The coexpression of TRPV1 and ASICs would likely confer a broad range of acid sensitivity, and indeed, some nociceptors have been shown to respond from pH 4 to pH 6.8. It is still evident however, that even with the stronger acidic stimulus of pH 5.7, ASICs still account for the majority of the proton evoked response in this *in vitro* preparation.

An important consideration in these experiments was the concentration of amiloride. The concentration had to be chosen so as to to maximally block ASICs without interfering with TRPV1. Firstly, amiloride has been determined to have half maximal inhibitory concentrations for ASIC1a, ASIC2 and ASIC3 of 10 µM, 28 µM and 16-63 µM, respectively (Alexander, 2009). Therefore, 100 µM should represent a maximal inhibitory concentration and as a result, the neurons with amiloride resistant proton evoked responses are very unlikely to rely on ASICs as their acid detector. Secondly, heterologous expression of TRPV1 in Xenopus oocytes resulted in a capsaicin half-maximal effective concentration (EC50) of 111 nM, and at 1 µM capsaicin effectively produces a maximal response (Tominaga et al., 1998). Furthermore, in the next chapter I go on to demonstrate that 92 % of capsaicin sensitive neurons are activated by 1 µM capsaicin applied to the somata of DRG neurons in culture (Figure 5.5.1). Therefore, it seems logical to suggest that 1 µM capsaicin is activating essentially the entire population of TRPV1 expressing neurons.

ASIC and TRPV1 independent acid sensors

With respect to the complete block with 100 µM amiloride, and the full activation of all TRPV1 expressing neurons with 1 µM capsaicin, it is likely that the small population of neurons demonstrated to be amiloride resistant and capsaicin insensitive, represent a subset that transduce proton stimulation in an ASIC- and TRPV1- independent mechanism. One such alternative

mechanism is the ovarian cancer G-protein coupled receptor (GPCR) 1 (OGR1) family. However, the activation threshold of these channels lies between pH 6.4 and pH 6.8 (Huang et al., 2007), which would be too weak for activation at the test stimulus of pH 5.7 used here. Furthermore, these are predominantly implicated in the modulation of channels following inflammation by activation of protein kinases (Chen et al., 2009). Therefore, it seems likely an alternative mechanism is functioning *in vitro* to contribute to acid detection.

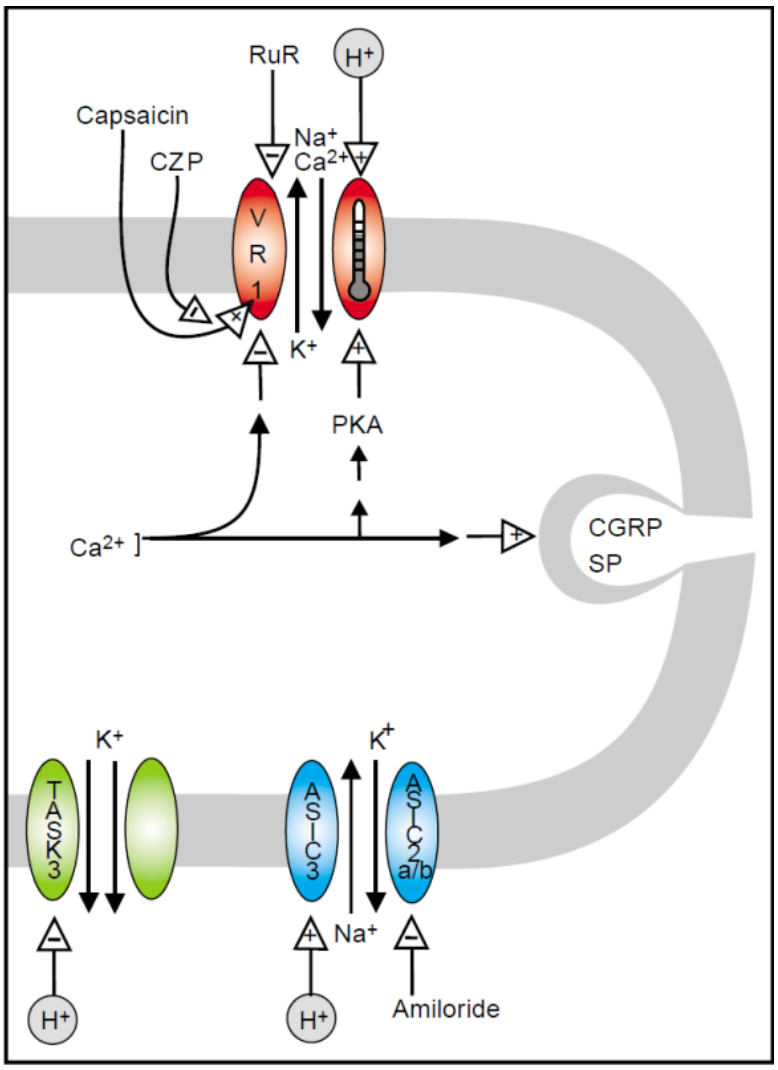

Figure 4.8.2
Ion channels involved in proton transduction in sensory nerve endings. TRPV1 (VR1) shown in red is activated by heat, capsaicin and protons, and is a non-selective cation channel. Ruthenium red (RuR) and capsazapine (CZP) are both potent inhibitors of TRPV1 activation. Intracellular calcium can desensitise the channel, whereas calcium induced activation of protein kinase A (PKA) can increase capsaicin responses. Calcium can also activate cellular exocytosis, liberating the neuropeptides CGRP and substance P. ASICs are depicted in blue as a hetero-dimer of ASIC2 and 3, and are also implicated in the detection of protons. Upon acid stimulation, the ASICs open allowing an influx of sodium ions. The activation of these cation channels can be blocked by amiloride. TASK-3 is a tandem-pore K^+ channel, open at resting membrane potential, but closed by extracellular protons which can lead to a depolarisation of the membrane. Adapted from Reeh and Kress, 2001.

The two pore K^+ channel family (K2p) are known to be gated by extracellular protons, these include the TASK (TWIK (tandem of P domains in a weak inwardly rectifying K^+ channel) -related acid sensing K^+ channel) family. TASK channels are acid sensing, K^+ selective channels that are ordinarily open at resting membrane potential, but close in the presence in extracellular protons (Duprat et al., 1997) (Figure 4.8.2). Therefore, due to the relative potassium concentration gradient, inhibiting the flow of K^+ ions can depolarise the membrane potential resulting in neuronal excitability. With regards to proton detection, interest into the TASK channels began with the finding that stimulation of human DRG neurons with pH 6 caused a decrease in membrane potential in many cells, rather than an increase associated with TRPV1 activation (Baumann et al., 1996). This reversal of membrane potential can be accounted for by a reduction in outward K^+ current. mRNA transcripts for TASK-1 and TASK-3 have both been detected in human DRG tissue (Baumann et al., 2004) and TASK-3 has been demonstrated to be particularly sensitive to extracellular proton levels, with a reduction in TASK-3 K^+ current by 96 % when pH was dropped from 7.2 to 6 (Kim et al., 2000). The TASK-3 channel is an alternative, ASIC and TRPV1 independent mechanism for proton transduction. The large inhibition of this channel at pH 6, is close to the test stimulus of pH 5.7 used in this protocol, and may be responsible for the small population of cells that demonstrate amiloride resistant, capsaicin independent characteristics.

In conclusion, the results presented here demonstrate a clear difference in the proton sensitivity between the soma and peripheral neuronal regions and this may be due to a preferential transport of proton transducers out of the soma to these distal regions. In this culture system, ASICs are indispensable for the transduction of weak acidic stimuli, whereas at pH 5.7 additional transduction mechanisms are utilised. These results are in agreement with published literature, in which TRPV1 is implicated in the detection of stronger stimuli. These data suggest the presence of an ASIC- and TRPV1- independent mechanism for proton transduction, which may represent the peripheral expression of potassium channels that are inhibited by extracellular protons.

Chapter 5

The functional expression of TRPV1 can be investigated using microfluidic technology

5.1. Introduction

Peripheral transduction is the mechanism whereby sensory stimuli are converted into action potentials. The specific mechanism of transduction is unique for each modality and often many cellular proteins are involved in the process. The previous chapter was concerned with the transduction of proton stimuli, with TRPV1 and ASICs demonstrated to be key molecules in this process. However TRPV1 has additional important roles in thermo- and chemo-sensation, and indeed, the TRP channels in general are recognised as principal transducers of thermal stimuli (Clapham, 2003; Tominaga and Caterina, 2004).

TRPV1 is a ligand gated ion channel activated by the plant derived irritant, capsaicin. TRPV1 is also gated by heat, with an activation temperature of approximately 43˚C (Caterina et al., 1997; Tominaga et al., 1998). The TRPV1 knockout animal has provided a wealth of information regarding the role of TRPV1 in both thermal and proton-detection (Caterina et al., 2000; Davis et al., 2000). One of the most profound discoveries in the *Trpv1* (-/-) mouse, includes the absence or significantly reduced heat current in DRG neurons *in vitro* (Caterina et al., 2000; Davis et al., 2000). These results observed in single cells were confirmed with recordings from the primary afferent fibre and dorsal horn, which showed reduced thermal nociceptive properties and impaired thermal coding, respectively (Caterina et al., 2000). The skin nerve and cultured DRG preparations therefore agree that TRPV1 function is abolished in this knockout mouse. However, analysis of temperature evoked behaviour revealed that TRPV1 knockout mice displayed only a comparatively mild deficit in detecting and reacting to temperature stimuli that has previously been demonstrated to activate TRPV1 (Caterina et al., 2000).

The discrepancy between the virtually absent heat-evoked responses in cultured DRG neurons and in terminals of *ex vivo* preparations and the moderately altered behavioural phenotype has so far not been adequately explained. One possible explanation is that the molecular and cellular mechanisms of heat sensitivity and TRP channel responses differ between soma and terminals. If it were the case that the heat sensitivity of soma and terminals are differentially controlled then the possibility exists that this may extend to other modalities as well.

Microfluidic culture chambers provide an opportunity to study the functional expression of transduction molecules expressed on the axon and terminals of sensory neurons *in vitro*. Therefore, in this chapter, the focus is directed towards TRPV1 in a bid to understand if the expression of the capsaicin receptor differs between the soma and peripheral neuronal regions in neurons cultured in compartmentalised chambers.

5.2. Objectives

The primary objective of this set of experiments was to investigate stimulation by capsaicin and understand the differences in expression between the soma and peripheral neuronal regions.

5.3. TRPV1 expression is differentially regulated in the terminals and cell bodies of rat DRG sensory neurons *in vitro.*

Using microfluidic chambers, the peripheral regions of cultured DRG neurons have been demonstrated to possess profound sensitivity differences to proton stimulation. With this in mind, the expression of the capsaicin receptor – TRPV1, was investigated in a similar manner to reveal any differences in expression. KCl stimulation of the terminals was used to detect all cells with a functionally intact projecting axon (Figure 5.3.1a). Using this population as the baseline, 54 ± 4 % (Figure 5.3.1b) (n_{cells} = 1312, $n_{experiments}$ = 12) were depolarised by capsaicin stimulation applied to the terminals, and in the same population of cells, 41 ± 5 % (Figure 5.3.1c) were depolarised when the capsaicin stimulation was switched to the cell body. This resulted in a significant difference ($p<0.05$, paired t-test) between the sensitivity of the terminals compared to the soma, showing that in this *in vitro* preparation the terminals have a greater sensitivity to capsaicin than the soma.

Within the neuronal population activated by capsaicin at the terminals, 63 ± 6 % (Figure 5.3.1b) were also positive for a capsaicin response at the soma. In addition, of the neurons expressing TRPV1 in the soma, 83 ± 4 % (Figure 5.3.1c) also expressed the capsaicin receptor in the terminals. Focussing on the neurons that were capsaicin insensitive at the terminals, these studies reveal only 10 ± 3 % (Figure 5.3.1d) of this population were activated by capsaicin stimulation to the terminals. On the other hand, when analysing those cells that are capsaicin insensitive at the soma, 38 ± 4 % (Figure 5.3.1e) displayed a capsaicin response to stimulation of the terminals. Collectively, these studies suggest that there is a greater population of neurons with TRPV1 expression at the terminals, compared with the cell body. However, cells with capsaicin sensitivity in the soma are very likely to express TRPV1 in the terminals, with 83 ± 4 % of cells demonstrating this expression pattern. Conversely, capsaicin sensitivity in the terminals, does not accurately predict functional TRPV1 expression in the soma, with only 63 ± 6 % of these cells positive for a capsaicin response in the soma.

Therefore, unlike the compelling differences observed in proton sensitivity, functional analysis of TRPV1 expression has uncovered subtle, but nevertheless important differences in capsaicin sensitivity between neuronal regions. Interestingly, this reveals a considerable population in which functional expression of TRPV1 is limited to the terminals and does not extend back to the soma, conversely, the majority of cells expressing TRPV1 in the soma are also capsaicin sensitive in the terminals.

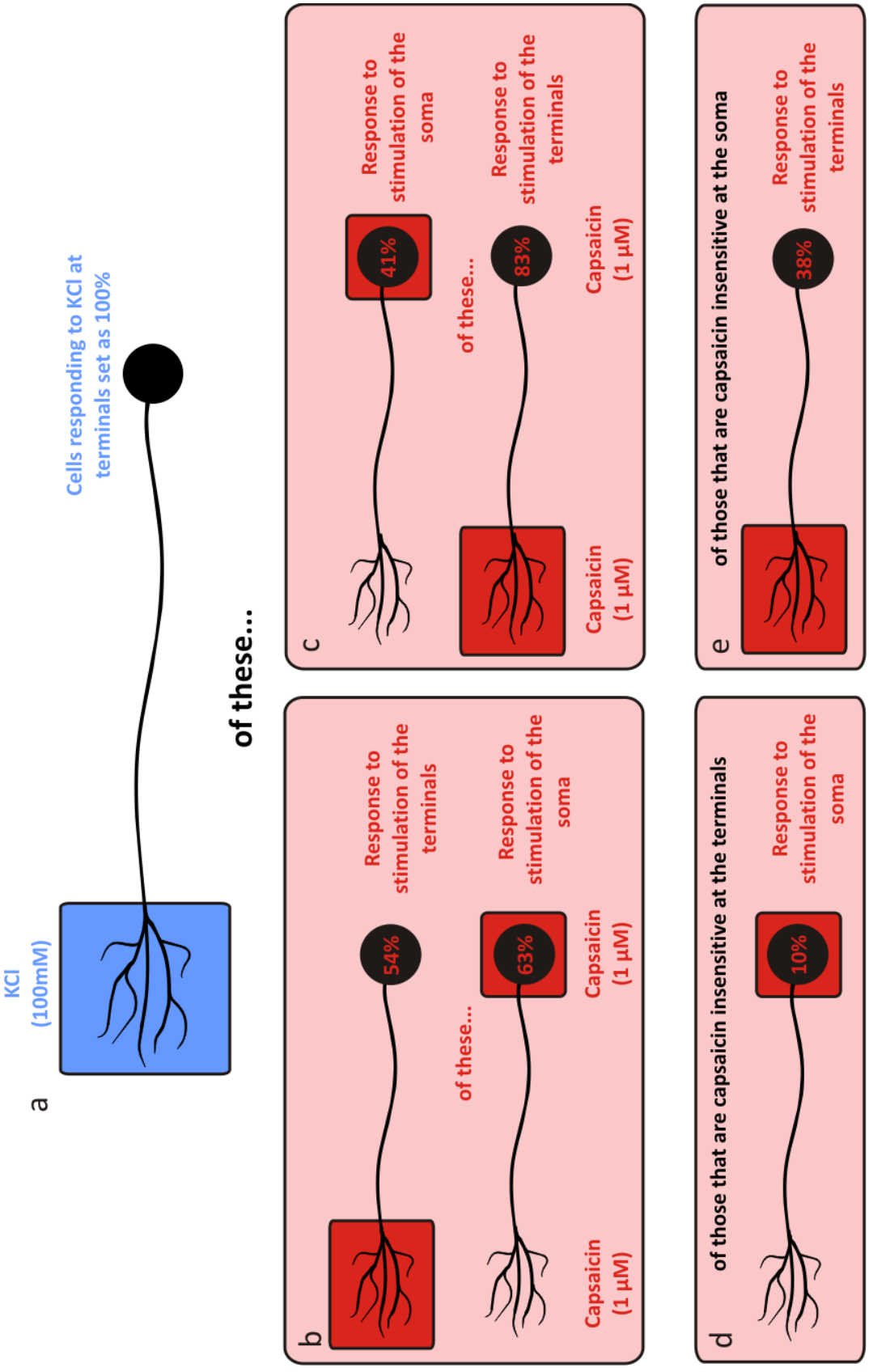

Figure 5.3.1
Schematic representation of neuronal population responding to KCl and capsaicin. (a) All cells responding to KCl applied to the terminals is set as the 100 % level. (b) Percentage breakdown of TRPV1 expression in cells responding to capsaicin application to the terminals. (c) Percentage breakdown of TRPV1 expression in cells responding to capsaicin application to the soma. (d) Somal capsaicin sensitivity in cells that are unresponsive to capsaicin at the terminals. (e) Capsaicin sensitivity at the terminals, in cells that are unresponsive to capsaicin at the soma.

5.4. TRPV1 expression can be investigated in the terminals, axon and cell body in isolation.

In this set of experiments, the 3 compartment system was used to investigate the functional expression of TRPV1 in the terminals, axon and soma, to understand if the axon or axonal collaterals can also be activated by capsaicin. Figure 5.4.1a displays a pseudocolour image of all capsaicin sensitive cells when the terminals, axons and soma are separately stimulated. Approximately 60 % of all neurons grow through the two microgroove arrays (Figure 3.7.1e) and it is these neurons which are used for the capsaicin sensitivity comparisons and are detected with a KCl test stimulus applied to the terminals. Neurons that do not respond to this test stimulus have failed to grow a process through the 2 microgroove arrays. A pseudocolour representation of the responding cells from KCl stimulation of the terminals can be overlaid with the capsaicin response from stimulation of the terminals (Figure 5.4.1b). It is possible to observe that all capsaicin sensitive cells are activated by KCl, indicating the KCl detection stimulus is sufficient to stimulate all neurons with terminals that grow into the distal terminal compartment. Furthermore, when the same KCl response from the terminals is overlaid with the axonal capsaicin response, there is a large overlap of functional responses (Figure 5.4.1b). The small number of cells illustrated in red depicts those that have grown a capsaicin sensitive process into the middle compartment, which has subsequently failed to grow into the terminal compartment (Figure 5.4.1b - asterisks). Similarly, when the terminal KCl and somal capsaicin pseudocolour responses are overlaid, the cells illustrated in red depict those that are capsaicin sensitive at the soma, and have not grown a process into the axonal or terminal compartment (Figure 5.4.1b - arrow). However, the majority of cells that are capsaicin sensitive at the terminals, also display capsaicin sensitivity in axonal and somal regions (Figure 5.4.1b - arrowhead).

Individual capsaicin stimulation of the terminals, axon and soma resulted in activation of 53 ± 5 %, 50 ± 4 % and 48 ± 6 % of neurons that were activated by KCl stimulation of the terminals, respectively (n_{cells} = 575, $n_{experiments}$ = 6) (Figure 5.4.1a, c, d). A high degree of overlap in capsaicin sensitivity was observed between neuronal regions, of the neurons that displayed capsaicin sensitivity in the soma, 87 ± 3 % (Figure 5.4.1c) and 92 ± 3 % (Figure 5.4.1d) were also positive for a capsaicin response in the axon and terminals, respectively. Reassuringly, the percentage of neurons that display capsaicin sensitivity in the soma and are capsaicin sensitive in the terminals in the 3 compartment system, is similar to the percentage observed in the 2 compartment chambers (Figure 5.3.1c).

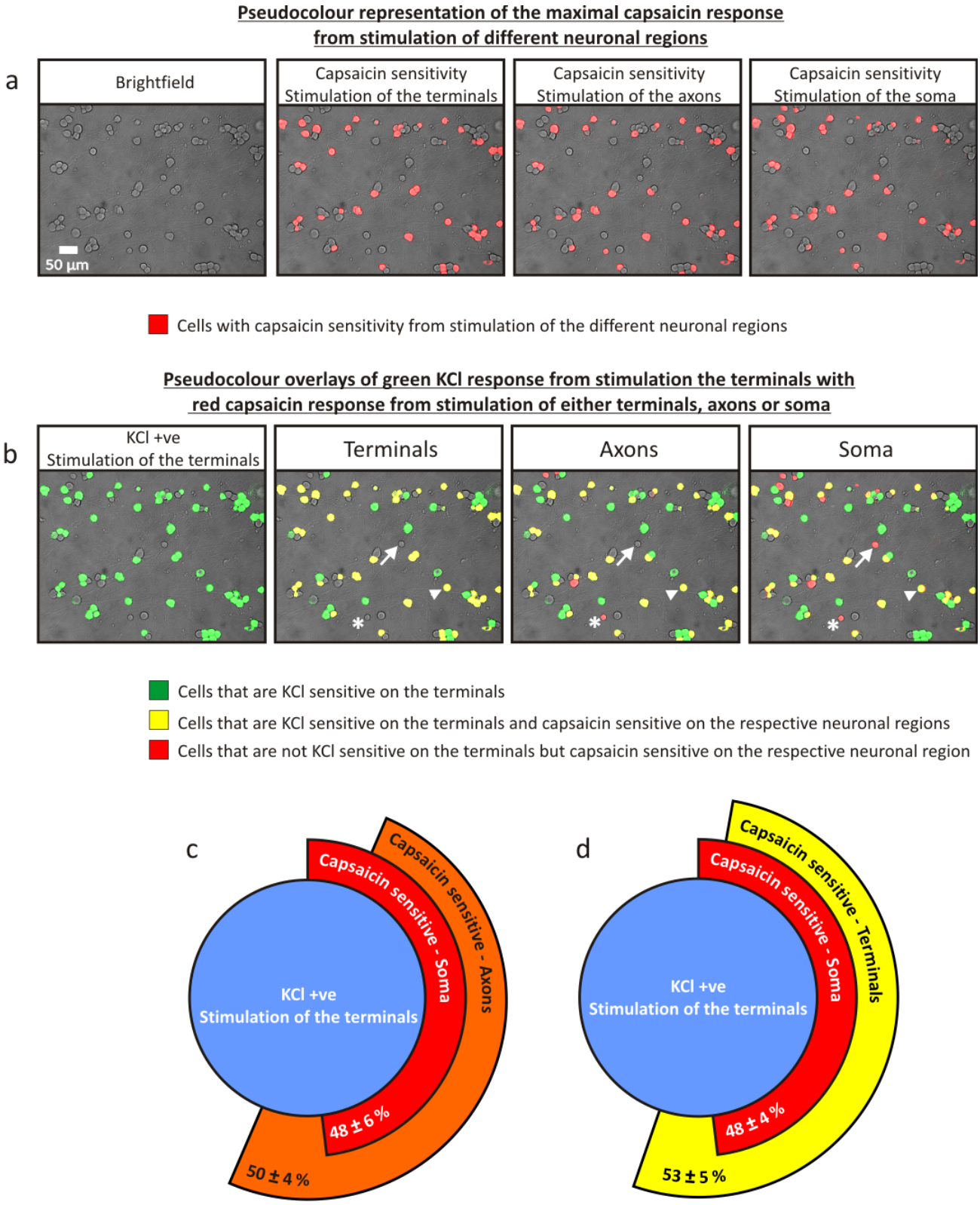

Figure 5.4.1
Capsaicin is expressed across all neuronal regions with some degree of overlap. (a) From left to right, brightfield and pseudocolour overlays of cells responding to capsaicin when applied to the terminals, axons and somata. (b) From left to right, pseudocolour of cells responding to KCl when applied to the terminals, and overlays of this response with capsaicin responses from stimulation of the terminals, axons and somata. Arrowhead, depicts a cell that has grown into the terminal compartment and is capsaicin sensitive at the terminals, axon and soma. Asterisks, depicts a cell that has failed to grow into the terminal compartment, but is capsaicin sensitive at the axon and soma. Arrow, depicts a cell that has failed to grow into the terminal compartment, but is capsaicin sensitive on the soma only. (c,d) Quantification and overlapping populations of cells responding to capsaicin stimulation of the (c) soma and axons and (d) soma and terminals.

5.5. Sensory terminals have a greater sensitivity to low concentration capsaicin than the cell somata in mouse E15.5 DRG neurons

In order to investigate the differential regulation of capsaicin sensitivity over a range of capsaicin concentrations, dose response experiments were performed in the two compartment chambers. Ascending capsaicin concentrations were applied first to the terminal compartment then to the soma compartment. Responses were classified as positive if a time locked calcium peak was detected in the soma, or, due to capsaicin-induced desensitisation of TRPV1, if they had previously responded to a lower concentration of capsaicin. Previous work has demonstrated that at physiological pH, 10 µM capsaicin elicits a maximal current, with 1 µM virtually producing an equal sized current (Tominaga et al., 1998). This data was collected in whole cell patch clamp of TRPV1 expressing HEK293 cells. Therefore, 10 µM was the highest concentration that was used in this set of experiments.

The data is presented in two ways. Firstly, in Figure 5.5.1a I have discarded any cells that are unresponsive to KCl applied to the terminals, and plotted capsaicin sensitive cells as a percentage of those responding to 10 µM capsaicin. The two curves show the responding populations when the terminals and soma are separately stimulated. This enables comparisons of responding cells at each capsaicin concentration against the total capsaicin sensitive population (determined by the responding population to 10 µM capsaicin). 0.01 µM capsaicin stimulation of the terminals excited 9 ± 3 % (n_{cells} = 199, $n_{experiments}$ = 4) of the total capsaicin sensitive population whereas 2 ± 2 % responded upon somal application. Stimulation with 0.1 µM capsaicin excited 25 ± 6 % in the terminals, whereas only 10 ± 3 % responded upon direct somal stimulation. Similarly at 0.3 µM capsaicin stimulation, a greater proportion of the terminals were sensitive than the soma. This trend reversed at 1 µM stimulation, at which 80 ± 6 % of the terminals displayed capsaicin sensitivity, yet 92 ± 4 % were excited by somal stimulation. Application of 3 µM capsaicin activated 91 ± 4 % in the terminals and 98 ± 2 % in the soma. Therefore at lower concentrations the terminals display a greater sensitivity than the soma, whereas at concentrations of 1 µM and higher, a greater proportion of the soma are activated by capsaicin. The dose response curve of somal sensitivity is in strong agreement with previously published data (Tominaga et al., 1998), demonstrating that 1 µM capsaicin elicits a response in nearly all cells that respond to 10 µM. The dose response curve for the terminals is interesting in that it does not mirror the sensitivity of the soma and has a shallower slope. At lower concentrations proportionally more cells are sensitive to capsaicin at the terminals compared to the soma. The important finding is that at 1 µM, the large majority of capsaicin sensitive cells are activated.

The second method in which the data is presented, expresses the capsaicin sensitive populations as a percentage of cells responding to KCl application to the soma (Figure 5.5.1b). Therefore, the capsaicin sensitive cells can be seen as a percentage of the total population which includes both capsaicin sensitive and insensitive cells. As previously observed (Figure 5.3.1), the

terminals display a slightly greater sensitivity to capsaicin than the soma at 1 μM with 55 ± 12 % responding from stimulation of the terminals and 47 ± 12 % responding at the soma. There was an overall statistically significant difference between the terminals and soma ($F_{1, 42}$ =4.9, $p<0.05$, 2-way ANOVA), Bonferroni post-hoc test revealed that at 0.1 μM the difference between percentage of cells responding to stimulation of the terminals compared to the soma was significantly different ($p<0.05$). The difference at 1 μM did not reach significance as in previous experiments (Figure 5.3.1) probably due to the smaller number of experiments and therefore larger errors. There is a clear trend at all concentrations which suggest a greater proportion of all responsive cells are capsaicin sensitive in the terminals compared to the soma, which would likely become significant upon increasing the experimental number. A stimulation of 0.1 μM capsaicin applied to the terminals activated 17 ± 4 %, whereas when applied to the soma, only 6 ± 2 % responded. Similarly, 0.3 μM capsaicin activated 31 ± 8 % in the terminals and 18 ± 4 % in the soma. At higher concentrations, 3 and 10 μM applied to the terminals excited 62 ± 12 % and 67 ± 11 %, respectively, and 48 ± 12 % and 50 ± 12 % in the soma.

In order to see specific differences in sensitivity at different capsaicin concentrations, graphs have been drawn showing the proportional sensitivity of the soma (Figure 5.5.2). Therefore, each graph shows the entire population of cells that respond to a specific capsaicin stimulus applied to the terminals, and the subsequent sensitivity in the same group of cells when the soma is stimulated. Of all the cells that are activated by 0.01 μM applied to the terminals, 41 % are also activated by the same concentration at the soma, whilst 25 % are capsaicin insensitive at the soma (Figure 5.5.2a). At higher concentrations of 0.1, 0.3, 1 and 3 μM, the general trend is that the soma requires a higher concentration of capsaicin for activation. For example, not a single cell that responded to 0.1 μM applied to the terminals responded to 0.01 μM at the soma (Figure 5.5.2b). Similarly, only 8 % of all cells that responded to 0.3 μM at the terminals were activated by 0.1 μM at the soma (Figure 5.5.2c) and only 11 % of all cells that were excited by 1 μM at the terminals were activated by a lower concentration at the soma (Figure 5.5.2d). This again suggests that the terminals have an overall higher sensitivity than the cell soma in cultured DRG neurons.

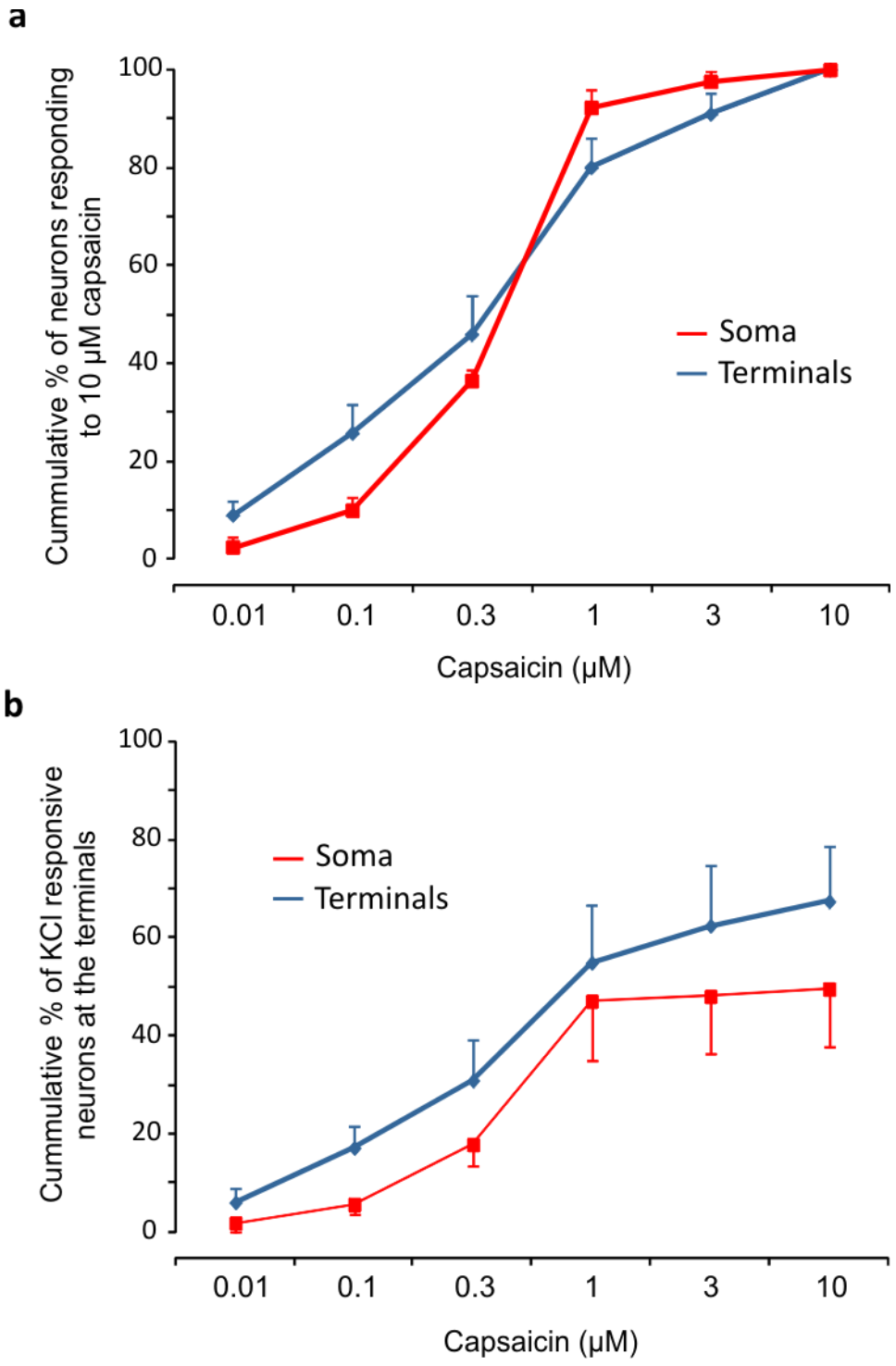

Figure 5.5.1
Dose response curves of capsaicin induced activation when applied to the terminals and soma. (a) Responding populations are expressed as a percentage of cells that respond to 10 µM capsaicin applied either to the terminals or the soma. Cells that were unresponsive to KCl applied to the terminals were discarded from the analysis. (b) Responding populations are expressed as a percentage of cells that respond to 100 mM KCl applied to the terminals.

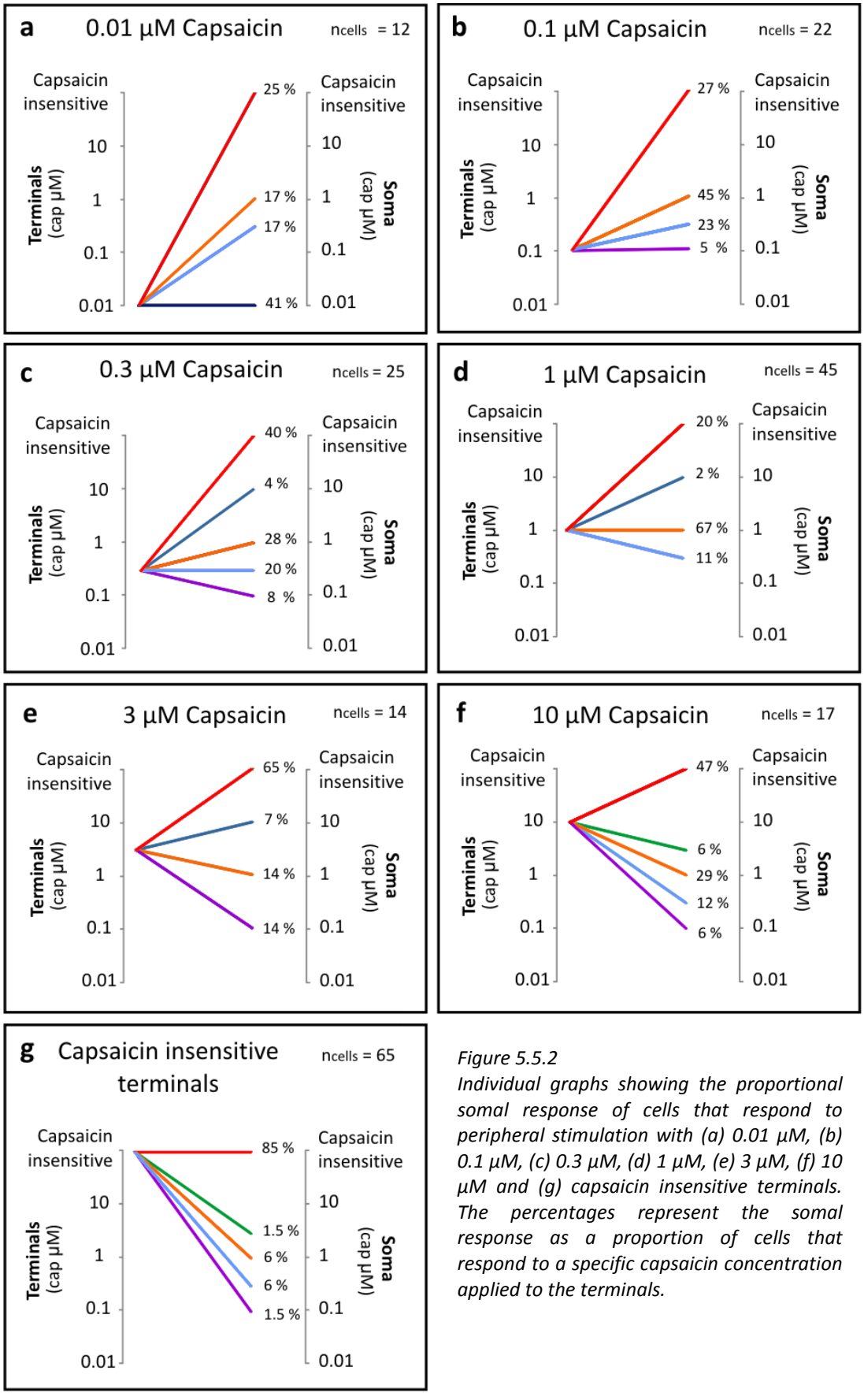

Figure 5.5.2
Individual graphs showing the proportional somal response of cells that respond to peripheral stimulation with (a) 0.01 µM, (b) 0.1 µM, (c) 0.3 µM, (d) 1 µM, (e) 3 µM, (f) 10 µM and (g) capsaicin insensitive terminals. The percentages represent the somal response as a proportion of cells that respond to a specific capsaicin concentration applied to the terminals.

5.6. High concentration capsaicin produces a conduction block in neurons that are capsaicin sensitive at the terminals.

With the previous experiment demonstrating TRPV1 is functionally expressed along the length of the axon, experiments were conducted to investigate if action potential propagation could be blocked with the use of capsaicin. 3 compartment chambers were used in which a 1 µM capsaicin and KCl stimuli were applied to the terminals to detect the total population of neurons with a projecting process and the percentage that displayed capsaicin sensitivity at the terminals. Subsequently, 100 µM capsaicin was applied to the axonal compartment in a low volume so that this compartment was fluidically isolated from the others. The high concentration capsaicin remained in the axonal compartment for the rest of the experiment, whilst the terminals were stimulated with consecutive applications of KCl (Figure 5.6.1a).

Upon application of 100 µM capsaicin to the middle axonal compartment, 96 ± 3% (n_{cells} = 323, $n_{experiments}$ = 6) of neurons functionally expressing TRPV1 in the terminals responded to axonal capsaicin stimulation, demonstrating that TRPV1 is functionally expressed along the entire length of the axon. I next asked whether high concentration capsaicin applied to the middle axonal compartment would affect action potential propagation from the terminals to the soma. Using this paradigm of selectively applying high concentration capsaicin to the axonal compartment, action potential propagation continued in 94 ± 2 % (n_{cells} = 323, $n_{experiments}$ = 6) of neurons with capsaicin insensitive terminals (Figure 5.6.1a, c). Conversely, of those neurons that display capsaicin sensitivity in the terminals, only 6 ± 3 % (n_{cells} = 323, $n_{experiments}$ = 6) continue to propagate action potentials through the capsaicin filled compartment, back to the soma (Figure 5.6.1b, d). A comparison of the percentage of cells that continue to propagate, between capsaicin sensitive and insensitive was highly significant ($p<0.001$, unpaired t-test). This therefore demonstrates that in the large majority of neurons that can be functionally excited by capsaicin application to the terminals also express TRPV1 along the length of the axon, and high concentration capsaicin can be used as a specific blocker of action potential propagation in these TRPV1-expressing neurons. The 6 % of cells that are capsaicin sensitive at the terminals yet continue to respond to KCl with 100 µM capsaicin applied to the axon are primarily comprised of neurons that display no functional response to the high concentration capsaicin applied to the axon. This implies that a small number of cells functionally express TRPV1 at the terminals yet do not express TRPV1 at the level of the axon, and therefore the conduction is unaffected by application of high concentration capsaicin.

In each culture tested, application of 100 µM capsaicin to the axonal compartment routinely activated neurons that did not respond to KCl stimulation of the terminals. 20 ± 6 % of all cells that were activated by 100 µM capsaicin applied to the axon were not activated by any stimulation in the terminals. These cells are likely to comprise a population that have grown a process into the middle axonal compartment, but do not grow through the second microgroove array into the distal terminal compartment.

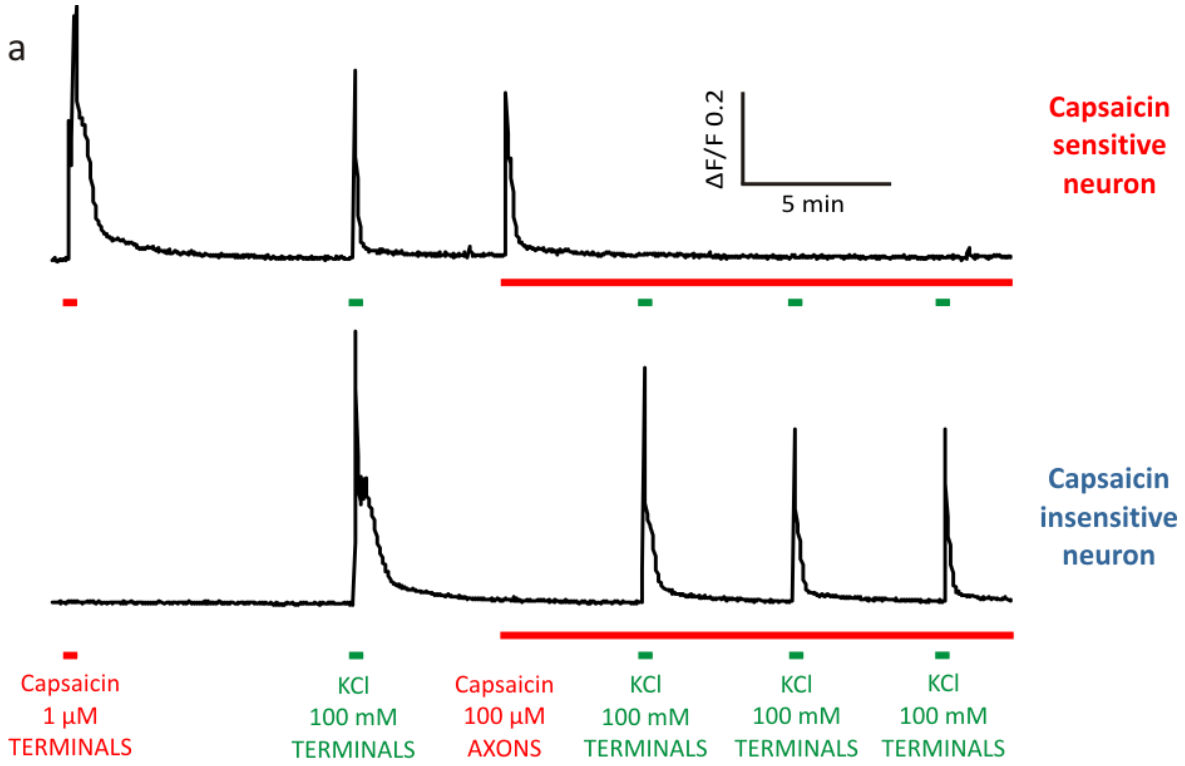

Figure 5.6.1
High concentration capsaicin induces a conduction block in TRPV1 expressing neurons. (a) Two example traces of a cell that is capsaicin sensitive in the terminals (top trace) and a cell that is capsaicin insensitive (bottom trace). Action potential propagation is blocked in the capsaicin sensitive cell by application of high concentration capsaicin to the axonal compartment. Whereas action potential propagation in the cell displaying capsaicin insensitive properties is unaffected by application of high concentration capsaicin.

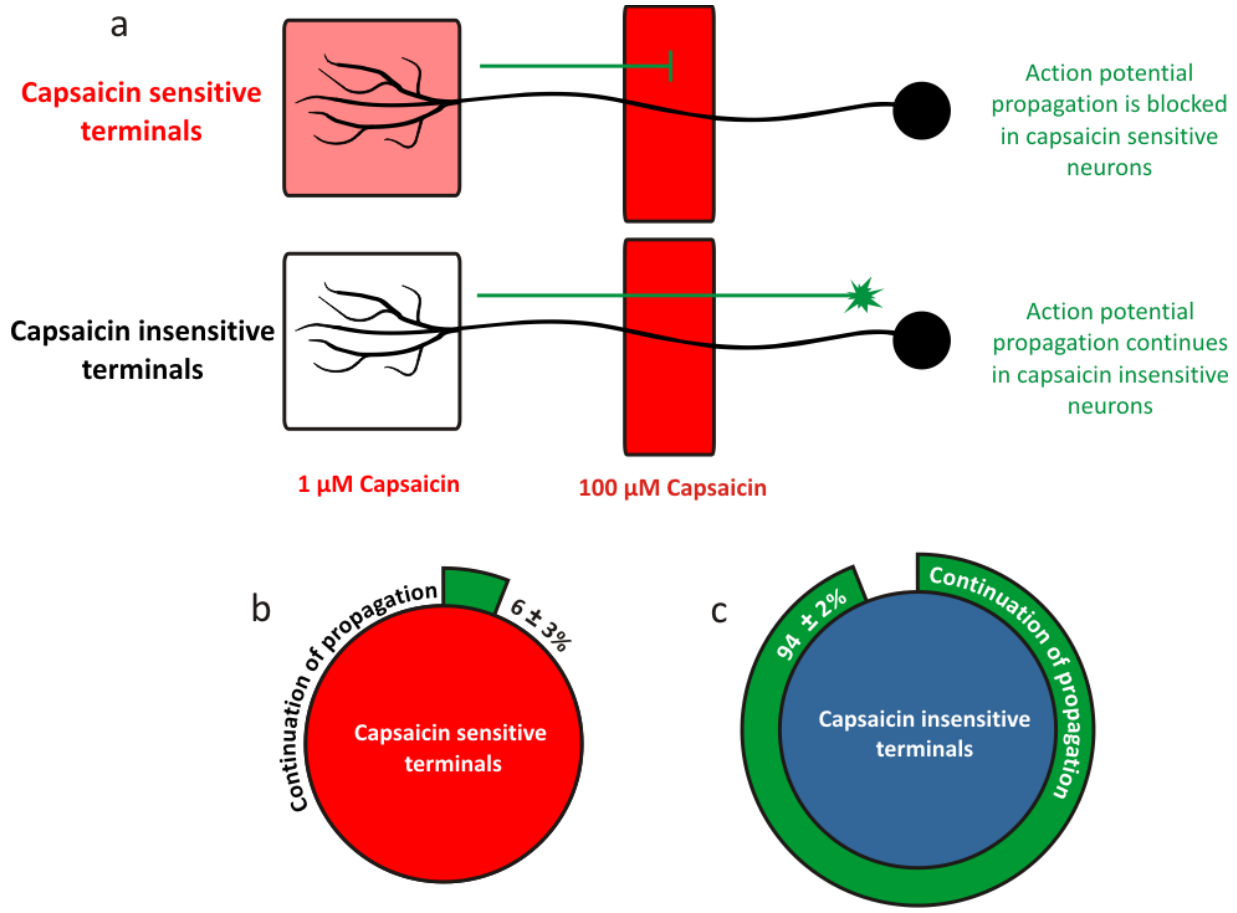

Figure 5.6.2
(a) Schematic representation of the three compartment experimental set up, showing location of capsaicin test stimulus to the terminals and location of high concentration capsaicin to the axons. (a,b) Cells that are capsaicin sensitive in the terminals are unable to propagate action potentials through the high concentration capsaicin compartment. (a,c) Cells that are capsaicin insensitive in the terminals are able to propagate action potentials through the high concentration capsaicin compartment.

5.7. The average cell size increases over time in culture, whilst TRPV1 is expressed in a population of cells with a smaller cell body size.

DRG neurons can be classified into subpopulations according to the size of their cell body. The nociceptive subpopulation can be further divided into subclasses based on their molecular properties, but usually share the same characteristic of an inherently small diameter cell body. Sensitivity to capsaicin is a major defining factor for nociceptors (Jancsó et al., 1977). Therefore, the *in vitro* development of cultured nociceptors has been investigated by tracking the cell size over time, in order to examine if the capsaicin sensitive and therefore nociceptive population occupy the lower end of the total cell size profile. The cell size of all dissociated mouse DRG neurons in the microscopic field of view was measured. Embryos were dissected at E15.5 (0 DIV) (Figure 5.7.1) and cultured to 10 DIV (Figure 5.7.2), during which the average size significantly increased from 100 μm^2 ± 2 (n_{cells} = 302, $n_{experiments}$ = 6) to 249 μm^2 ± 19 (n_{cells} = 79, $n_{experiments}$ = 3) ($p<0.001$, unpaired t-test) (Figure 5.7.3).

At all times *in vitro*, capsaicin insensitive cells were larger than capsaicin sensitive cells (Figure 5.7.3). A small difference in cell size was detected between the capsaicin sensitive 98 μm^2 ± 2 (n_{cells} = 210, $n_{experiments}$ = 6) and insensitive populations 104 μm^2 ± 4 (n_{cells} = 92, $n_{experiments}$ = 6) at 0 DIV although this was not significantly different (Figure 5.7.1a, Figure 5.7.3). By 2 DIV (Figure 5.7.1a, Figure 5.7.3), the difference was highly statistically significant with the capsaicin sensitive cells measuring an average of 132 μm^2 ± 3 (n_{cells} = 100, $n_{experiments}$ = 3) and the capsaicin insensitive an average of 145 μm^2 ± 3 (n_{cells} = 128, $n_{experiments}$ = 3) ($p<0.001$, unpaired t-test). At 7 DIV the capsaicin sensitive and insensitive populations measured an average of 201 μm^2 ± 6 (n_{cells} = 128, $n_{experiments}$ = 3) and 254 μm^2 ± 11 (n_{cells} = 128, $n_{experiments}$ = 3), resulting in a highly significant difference (Figure 5.7.2c, Figure 5.7.3) ($p<0.001$, unpaired t-test).

In order to investigate the cell size profile of neurons with a projecting axon, Figure 5.7.2a-d display the peripherally activated cells in green as a percentage of the total cells. Neurons with a projecting axon that also display capsaicin sensitivity are then plotted as a percentage of the neurons activated by KCl stimulation of the terminals.

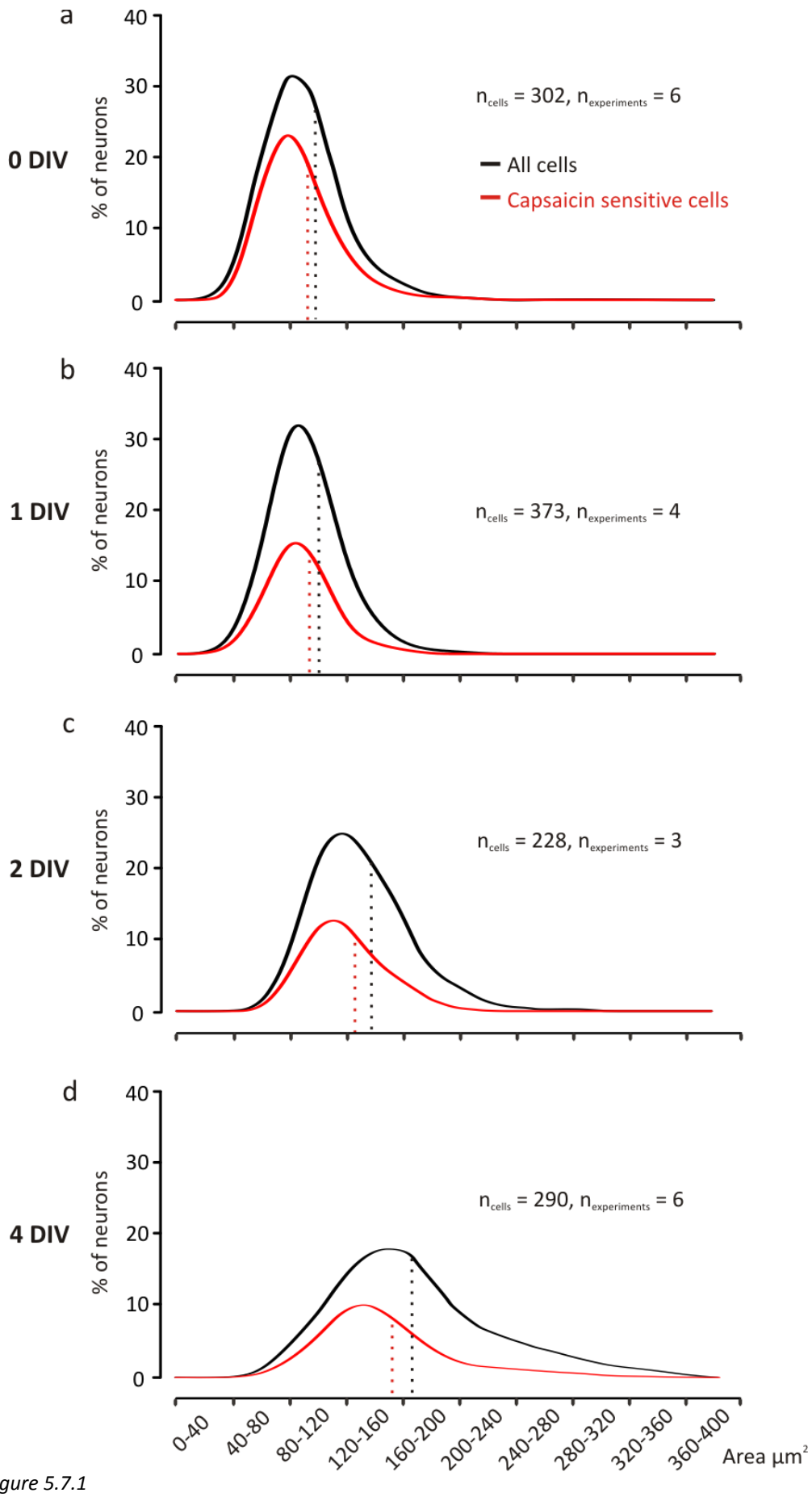

Figure 5.7.1
Cell size profile for all cells and capsaicin sensitive cells. (a-d) Average cell size increases over the first 4 days in culture. Dotted lines illustrate the mean for each population.

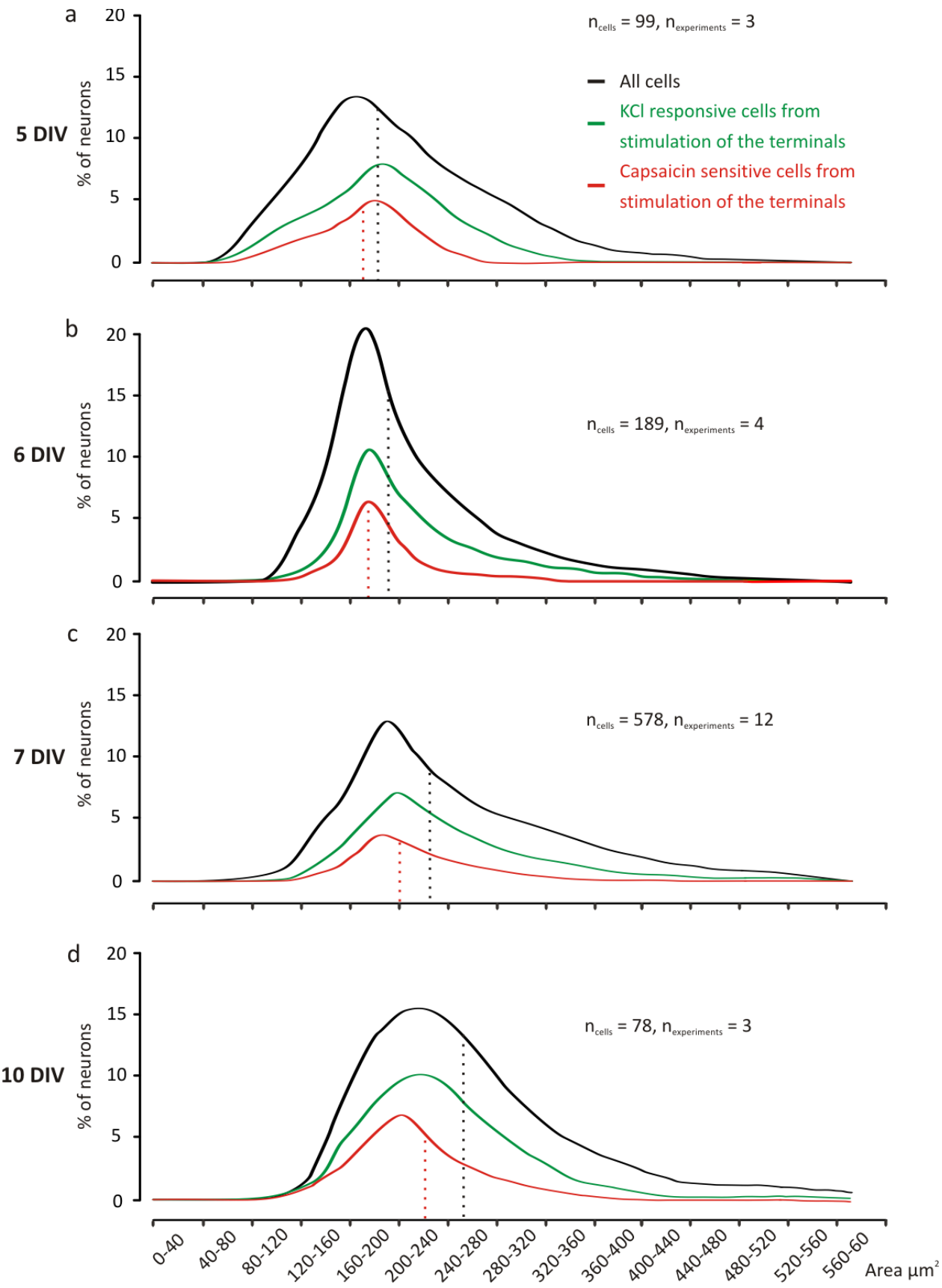

Figure 5.7.2
Size profile for all cells, cells with a projecting process, and capsaicin sensitive cells. (a-d) Average cell size further increases from 5 to 10 DIV. Dotted lines illustrate the mean for each population. Dotted lines illustrate the mean.

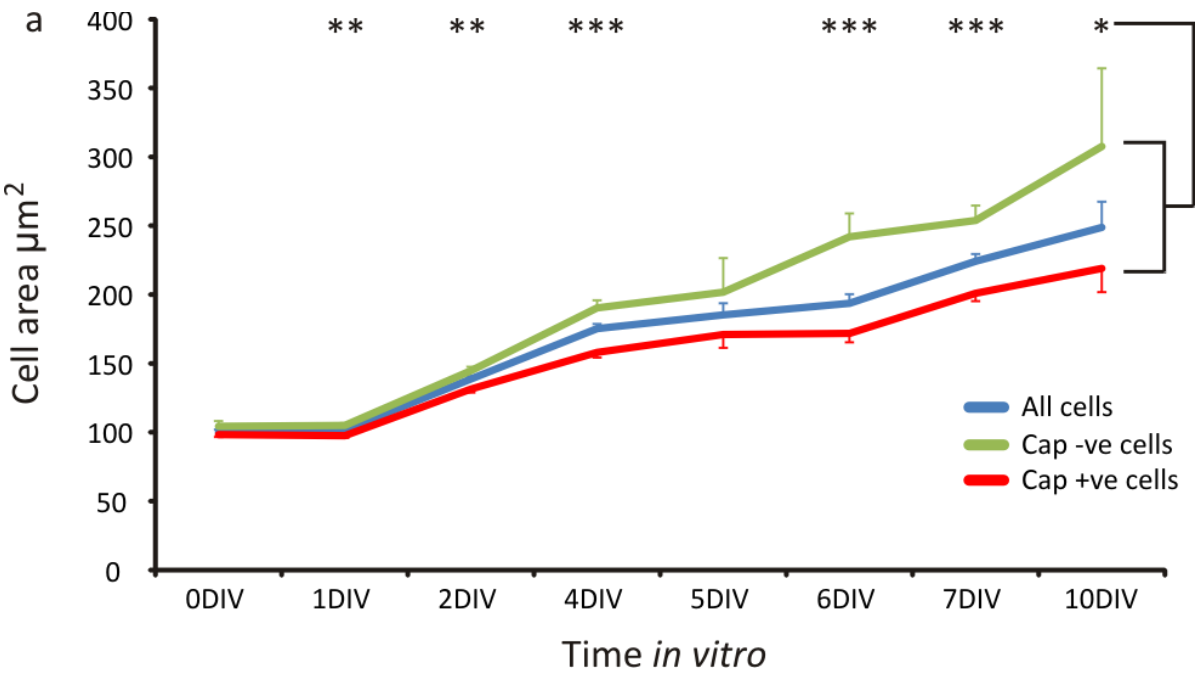

Figure 5.7.3
*Average cell size increases over time in culture and TRPV1 expressing cells are significantly smaller than non-TRPV1 expressing. (a) Cell size profile graphs for 0, 1, 2 and 4 DIV, showing the total neuronal population in blue, and the capsaicin sensitive population in red. (e-h) Cell size profile graphs for 5, 6, 7 and 10 DIV, showing the total neuronal population in blue, the cells which grow an axon into the adjacent compartment and respond to KCl stimulation of the terminals in green, and the cells that respond to capsaicin in both the terminals and soma in red. (i) Average cell size over time in culture for all cells (blue), capsaicin negative cells (green) and, capsaicin positive cells (red). (*p<0.05, **p<0.01, ***p<0.001, ANOVA with Bonferroni post-hoc test)*

5.8. Discussion

The principle findings in these experiments demonstrate that TRPV1 is largely, but not always evenly expressed throughout all neuronal regions *in vitro*. In regards to capsaicin sensitivity, there are distinct subpopulations of neurons which include those that functionally express the capsaicin receptor in the soma, peripheral axons and terminals, those that only express TRPV1 in the soma, and those that only express TRPV1 on the axons and terminals and are capsaicin insensitive at the soma. To investigate the functional expression of TRPV1 in the axon, I have used a high concentration capsaicin stimulus applied specifically to the axonal compartment, to induce a selective conduction block in capsaicin sensitive neurons. Expression of TRPV1 is observed in a population of neurons that are significantly smaller in cell body area.

TRPV1 expression is differentially regulated throughout neuronal regions in vitro

The data presented here suggest that in the same population of cells, a significantly greater proportion of cells are capsaicin sensitive in the terminals compared to the soma (54 ± 4 % at the terminals vs 41 ± 5 % at the soma, $p<0.05$, paired t-test), indicating there is a greater functional expression of TRPV1 in the periphery than in the cell soma of cultured rat DRG neurons. Therefore, mechanisms must be in place to efficiently transport either the TRPV1 protein or TRPV1 mRNA from the cell soma to these peripheral regions. However, despite this differential regulation of capsaicin sensitivity, the large majority of neurons that are excited by capsaicin applied to the soma were also activated in the periphery.

Before the cloning and characterisation of TRPV1, capsaicin sensitivity was demonstrated not only in the soma, but along the entire length of the neuron, including both peripheral and central terminals (Holzer, 1991). A few years later, Szallasi and colleagues used radioactively tagged Resiniferatoxin (RTX), a potent agonist of TRPV1 that similar to capsaicin also contains a homovanillyl moiety. They were able to demonstrate that after sciatic nerve ligation, an accumulation of RTX binding sites proximal to the ligation site were detected (Szallasi et al., 1995). This suggests that TRPV1 is transported in the anterograde direction in a form that is capable of ligand binding thereby providing a mechanism by which the terminals are able to respond to capsaicin.

An interesting finding of the experiments performed in this chapter is that the huge majority of neurons that express TRPV1 in the peripheral terminals are also capsaicin sensitive on the axon (Figure 5.4.1a and Figure 5.6.2). Consistent with these studies, Tominaga and colleagues used immunohistochemistry to analyse the expression of the capsaicin receptor and demonstrated that TRPV1 expression could be detected along the length of the axon in addition to the peripheral terminals (Tominaga et al., 1998). This study was unable to differentiate whether the detected immunofluorescence was due to TRPV1 insertion in the peripheral axonal membrane or large quantities of the TRPV1 protein were in the process of being transported intra-axonally. My studies

argue that the axon is responsive to capsaicin suggesting TRPV1 receptors are functionally inserted into the axolemma.

An early study by Hayes et al., investigated the depolarising effect of capsaicin on the axon using an isolated rat sciatic nerve preparation. Upon separate capsaicin applications of 1 µM, 3 µM and 10 µM to a discrete section of the nerve, depolarisations were recorded in adjacent segments (Hayes et al., 1984). This suggests that the axon expresses TRPV1 which upon binding capsaicin depolarises fibres resulting in action potential propagation. A study in the late 90's by Peter Reeh's group demonstrated that stimulation of isolated axons with 1 µM capsaicin led to a dramatic increase in the release of CGRP, again providing evidence for the expression of TRPV1 along the axon (Sauer et al., 1999). More recent work has studied TRPV1 receptor immunolocalisation using electron microscopy. The immunoreaction product (directed against TRPV1) was present in vesicles throughout the axoplasm, and along the axonal plasma membrane where immunopositive regions formed an almost gap-free lining (Bernardini et al., 2004). Therefore, there is considerable evidence suggesting TRPV1 is functionally inserted into the axolemma and that upon binding to capsaicin can trigger action potential propagation and release of CGRP at a site considerable distance from any specialised synaptic zones (Figure 5.8.1). In addition, the detection of TRPV1 immunoreaction product in vesicles (Bernardini et al., 2004) suggests the TRPV1 protein undergoes vesicular transport from the cell soma and is translocated into the axonal membrane of unmyelinated primary afferent axons (Figure 5.8.1). Localisation of TRPV1 along neurites and to specific areas of embryonic DRG growth cones has also been demonstrated (Goswami et al., 2007). Activation of TRPV1 expressed at the growth cone is suggested to play an important role in growth cone motility during DRG embryogenesis (Goswami et al., 2007). There is therefore considerable evidence that TRPV1 is abundantly expressed in distal and proximal axons, which is in strong agreement with the results presented in this chapter.

In addition to the transport of the TRPV1 protein, transport of TRPV1 mRNA and local axonal translation may play a key role in regulating the sensitivity of peripheral neuronal regions. Peripheral inflammation robustly increased the bidirectional transport of TRPV1 mRNA in primary afferents, where it was shown to be locally translated in the nerve terminals (Tohda et al., 2001). Intrathecal pretreatment with the axonal transport inhibitor – colchicine, prevented the transport of TRPV1 mRNA after carrageenan induced peripheral inflammation. Furthermore, ligation of the sciatic nerve after peripheral inflammation resulted in an accumulation of TRPV1 mRNA proximal to the ligation site, demonstrating the anterograde transport of TRPV1 mRNA (Tohda et al., 2001). In the same study, inhibition of local translation with cycloheximide in dorsal horn slices prepared from animals with peripheral inflammation, suppressed the increase of capsaicin evoked release of glutamate from the primary afferent central terminals (Tohda et al., 2001). In non-inflamed conditions, inhibition of axonal transport did not result in an accumulation of TRPV1 mRNA in the DRG soma, as it did during inflamed conditions. In addition, depletion of TRPV1 mRNA by antisense oligodeoxynucleotide did not affect capsaicin-evoked release of glutamate in the dorsal horn.

Therefore, these results suggest that during normal conditions, local translation of transported TRPV1 mRNA contributes little to TRPV1 expression in peripheral regions. Consequently, in normal conditions, transport of the protein seems to play a greater role in equipping the axon and terminals with capsaicin sensitivity than local translation of TRPV1 mRNA (Figure 5.8.1).

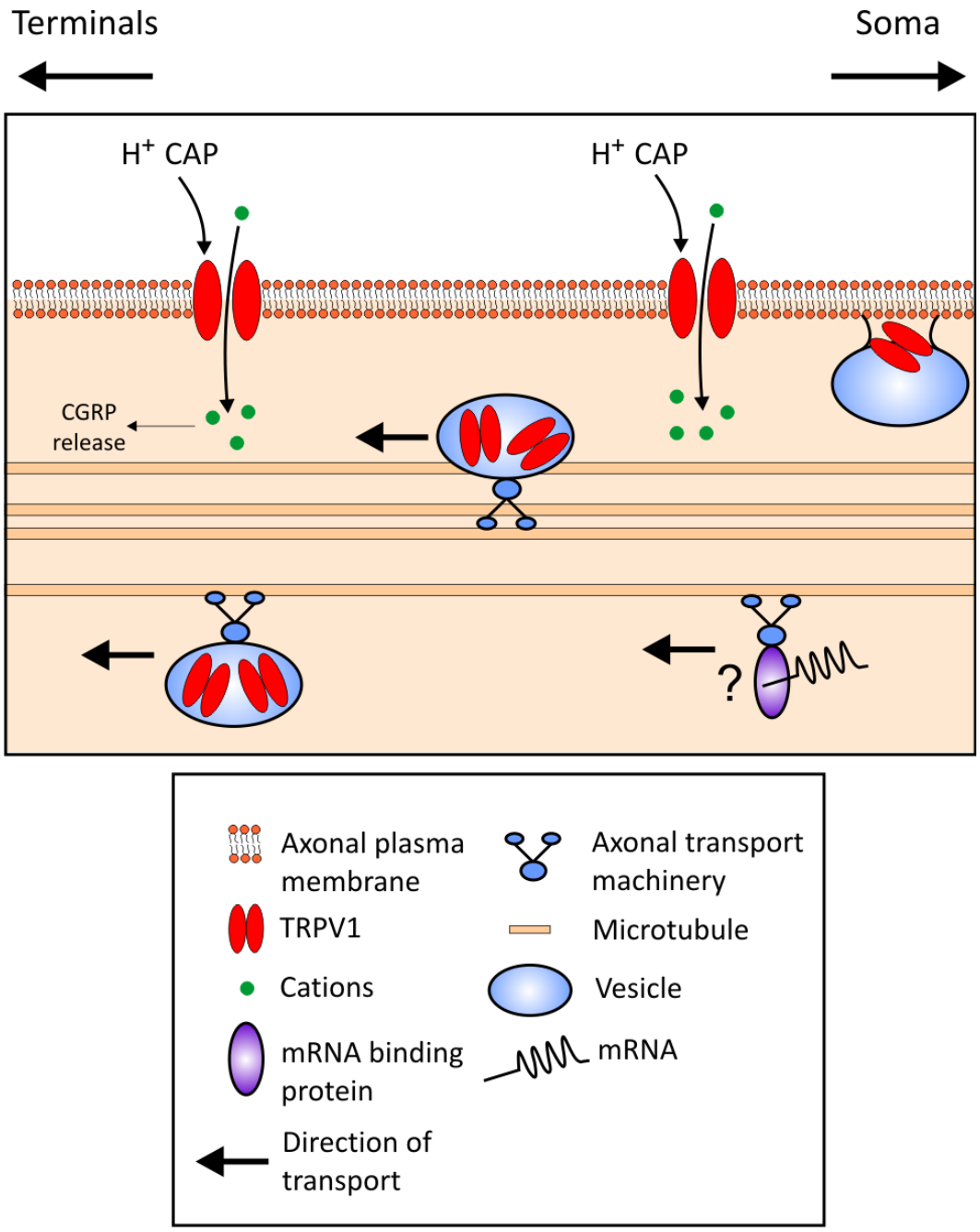

Figure 5.8.1
Schematic of the plasma membrane in a DRG neuron axon. TRPV1 is functionally inserted into the axolemma. Both protons and capsaicin can activate TRPV1 resulting in an influx of cations that can depolarise the axon resulting in action potential propagation. CGRP release has been shown to result from axonal stimulation with capsaicin. The TRPV1 protein is transported in vesicles from the cell soma to peripheral neuronal regions. The vesicles can fuse with the axonal plasma membrane enabling TRPV1 incorporation into the axolemma. TRPV1 mRNA may also be transported by binding to proteins that associate with transport proteins such as the kinesins. The local translation of TRPV1 in peripheral regions is thought to occur during peripheral inflammation but appears not to have a major role during normal conditions.

With regard to functional TRPV1 expression, three subpopulations were detected by using the microfluidic chambers. The majority of neurons displayed capsaicin sensitivity in both the soma and peripheral axons and terminals. These neurons likely depend upon vesicular axonal transport to ship the TRPV1 protein from the soma to peripheral regions, whilst mechanisms within the soma directly deliver TRPV1 to the somal membrane. The remaining two subpopulations identified here are interesting in that their TRPV1 expression is limited either to the soma or the periphery. 38 % of neurons that are capsaicin unresponsive when tested on the soma are activated by capsaicin when applied to the neurites. Conversely, 10 % of neurons that are capsaicin insensitive at the terminals functionally express TRPV1 on the soma. Therefore, whilst the majority of cells functionally express TRPV1 throughout the neuron, TRPV1 is preferentially being expressed in the periphery or the soma in these subpopulations. It is presently unclear whether this is an artefact of the culturing process. However, the density of TRPV1 expression in the DRG cell soma determined by immunohistochemistry has been shown to be highly variable. High expression of TRPV1 in mouse DRGs is dependent on the transcription factors - Runx1 and T-cell leukemia homeobox 3 (Tlx3), both of which regulate the expression of many sensory receptors and ion channels (Lopes et al., 2012). Recently, analysis of a complete Tlx3 knockout mouse showed that high expression of TRPV1 was abolished, with low and medium expression remaining (Lopes et al., 2012). High expression of TRPV1 has also been shown to be absent when Runx1 was conditionally knocked out in early embryonic development (Chen et al., 2006). Therefore it is clear that high expression of TRPV1 relies on Runx1 and Tlx3-dependent programmes, whilst low to medium expression appears to be regulated by Runx1-independent mechanisms. One possibility that may account for the peripherally capsaicin sensitive, yet somal insensitive population as detected in these functional experiments (Figure 5.3.1), is that these represent a population that express TRPV1 at a very low level in the soma which is insufficient for functional activation. The majority of the work profiling the low, medium and high TRPV1 expressing neurons has been carried out by immunohistochemistry on the cell soma. Therefore, the extent of TRPV1 expression in the periphery of these neurons is unknown. The level of expression in the soma may not necessarily correlate with that in the terminals and axons, therefore, a low TRPV1 expressing soma may project neurites that abundantly express the capsaicin receptor, and conversely, high TRPV1 expressing somata may have neurites that are very low in TRPV1 expression. A regional difference in TRPV1 expression may manifest as distinct functional differences in capsaicin sensitivity of somal compared to peripheral regions. It is clear that the differential regulation of TRPV1 detected using compartmentalised chambers represents a potentially interesting functional characteristic of DRG neurons *in vitro*, and once again highlights the need to study all neuronal regions.

High concentration capsaicin produces a conduction block in capsaicin sensitive neurons

The 3 compartment chamber provides a comprehensive method to further compartmentalise neuronal cultures. To study TRPV1 expression in the middle compartment containing the axon and potential axon collaterals, high concentration capsaicin was applied, whilst

the terminals were stimulated with KCl. Action potential propagation in neurons with capsaicin sensitivity in the terminals was blocked with high concentration capsaicin whilst capsaicin insensitive neurons were unaffected. Capsaicin is a strong activator of a subpopulation of primary afferents which experience profound tachyphylaxis and desensitisation in response to a high concentration or repeated capsaicin stimulus. For example, repeated subcutaneous capsaicin injection induced desensitisation of neurons *in vivo* when recorded from the saphenous nerve (Jancsó et al., 1967). Furthermore, the local application of capsaicin to an isolated section of the saphenous nerve blocked nociceptive C-fibre conduction in response to mechanical and heat stimuli applied to the receptive field (Petsche et al., 1983). The desensitisation of neurons by capsaicin has been shown to be calcium dependent, repeated application of capsaicin to TRPV1 expressing HEK293 cells resulted in almost complete desensitisation by the third application of 1 µM capsaicin (Caterina et al., 1997). However, consecutive capsaicin stimulation of neurons in calcium-free bathing solution did not result in any desensitisation by the third capsaicin stimulus (Caterina et al., 1997). Calcineurin is a phosphatase regulated by intracellular calcium, and is part of the calcium, calcineurin/nuclear factor of activated T cells (NF-AT) signalling pathway bridging the membrane and soma (Crabtree, 2001). Calcineurin can dephosphorylate TRPV1 resulting in a profound desensitisation to subsequent capsaicin stimuli (Docherty et al., 1996). Inhibition of calcineurin with cyclosporin A-cyclophilin strongly inhibited desensitisation of cultured DRG neurons to consecutive capsaicin application (Docherty et al., 1996). Furthermore, calcineurin is a calcium dependent enzyme, therefore, the removal of calcium can inhibit TRPV1 desensitisation as demonstrated by Caterina et al., 1997.

The desensitisation of TRPV1 by capsaicin is a physiologically important mechanism to prevent calcium-induced excitotoxicity, however it does not explain the conduction block observed in Figure 5.6.1 and Figure 5.6.2 for two reasons. Firstly, high concentration capsaicin would induce desensitisation of TRPV1 to capsaicin. However the test stimulus in Figure 5.6.1 and Figure 5.6.2 is KCl which activates neurons in a TRPV1-independent mechanism, therefore desensitisation of TRPV1 would not necessarily desensitise the whole neuron to stimuli other than capsaicin. Secondly, discrete application of high concentration capsaicin to the axon and axonal collaterals in the middle compartment would desensitise TRPV1 in this region, but calcineurin dependent dephosphorylation of TRPV1 may not extend out of this immediate region to the test location in the distal terminal compartment. Therefore, whilst capsaicin produces a classical pharmacological desensitisation of TRPV1, the conduction block observed in Figure 5.6.1 and Figure 5.6.2 is due to a more global 'functional desensitisation' (Winter et al., 1995), where TRPV1 expressing neurons fail to respond to other depolarising stimuli such as KCl.

The desensitisation of capsaicin sensitive nociceptors has been previously exploited to treat a range of pathologies such as arthritis and trigeminal neuralgia (Szallasi and Blumberg, 1999). The mechanisms responsible for the desensitisation of nociceptors in human patients could also be acting to specifically desensitise the TRPV1 expressing neurons in the microfluidic culture system. Calcium responses recorded from the soma show that in response to 100 µM capsaicin application to

the axonal compartment there is an initial depolarisation and generation of action potentials (Figure 5.6.1). However, a subsequent desensitisation and conduction block then occurs in capsaicin sensitive neurons, where they become unresponsive to KCl stimulation of the terminals. In a study by Su and colleagues, *in vitro* investigations of capsaicin sensitive DRG neurons that innervated the colon of the rat, demonstrated that capsaicin virtually abolished voltage gated sodium currents. This effect was prevented with the application of the TRPV1 antagonist capsazepine, suggesting that activation of TRPV1 by capsaicin modulates the activity of VGSCs (Su et al., 1999). Liu and colleagues have also investigated the relationship between capsaicin sensitivity and the modulation of VGSCs in TG neurons. Initial results confirmed earlier studies that application of capsaicin to TG somata inhibits the generation of action potentials which was dependent upon activation of TRPV1. They went on to show that capsaicin stimulation resulted in an increase in cAMP levels, which was blocked by capsazepine, again illustrating the need for TRPV1 activation (Liu et al., 2001). This study therefore suggests that activation of TRPV1 triggers second messenger pathways, including cAMP that indirectly modulate VGSCs. Several studies have implicated second messenger pathways and the activation of protein kinases A and C in modulating various subtypes of VGSCs (England et al., 1996; Gold et al., 1998; Fitzgerald et al., 1999).

A recent study has also investigated the capsaicin evoked effect on sodium current. Onizuka and colleagues suggest that the initial increase in intracellular sodium concentration due to the opening of TRPV1 would decrease the chemical driving force for sodium across the cell membrane. Furthermore, the increase in intracellular sodium concentration by capsaicin also produced a hyperpolarising shift in the steady state inactivation curve of the sodium current, meaning at a specific membrane potential there is more inactivation and therefore less sodium current. In addition, capsaicin was shown to inhibit both TTX-s and TTX-r VGSC to an almost identical degree in neurons that initially responded to capsaicin, whereas sodium currents were entirely unaffected in capsaicin insensitive neurons (Onizuka et al., 2011). This study has therefore characterised the responses to capsaicin in DRG neurons and suggested another mechanism by which capsaicin can desensitise VGSCs. Onizuka and colleagues show that similar to the results presented in Figure 5.6.1, capsaicin sensitive neurons are initially depolarised by capsaicin stimuli which then results in a conduction block due to the indirect blockade of sodium current.

To induce a specific conduction block in capsaicin sensitive neurons I have used 100 µM capsaicin. High concentrations of capsaicin have been suggested to have non-specific effects on voltage gated ion channels, for example, Kuenzi and Dale, demonstrate that 150 – 200 µM capsaicin blocked potassium and calcium currents in spinal neurons of *Xenopus* embryos (Kuenzi and Dale, 1996), and Docherty and colleagues, show that in rat DRG neurons, 20 µM capsaicin greatly inhibited the calcium current (Docherty et al., 1991). In my experiments inhibition of conduction was only observed in capsaicin sensitive neurons arguing that in this experimental preparation capsaicin induces a conduction block by acting specifically through TRPV1. Capsaicin administered in very high concentration has also been demonstrated to produce degeneration of primary afferents or cells

heterologously expressing TRPV1 which was accompanied by cell swelling (Caterina et al., 1997). In these experiments no histological feature in the somata or axons were observed that would suggest the cells were stressed or undergoing excitotoxicity. This implies that the conduction block was due to the modulation of VGSCs rather than deterioration of the primary afferent itself.

Collectively, two mechanisms of desensitisation may occur in response to high concentration capsaicin. The first is a calcium dependent desensitisation of TRPV1 itself, and the second is the capsaicin evoked inhibition of action potential generation through the indirect blockade of VGSC. The data presented in this chapter here is in strong agreement with studies by Su et al., 1999; Liu et al., 2001 and Onizuka et al., 2011, who report capsaicin produces an initial depolarisation followed by a subsequent current blockade in capsaicin sensitive neurons.

Capsaicin sensitivity is restricted to DRGs with small soma during in vitro culture

DRG cell size has been used for years as a feature to distinguish subpopulations of sensory neurons, Harper and Lawson, 1985, were among the first to correlate conduction velocity with neuronal soma size. The restriction of TRPV1 expression to the smaller neuronal population has been investigated by using high concentration capsaicin administration into neonatal rats. Subcutaneous capsaicin injection into 2-day old rats resulted in an exclusive damage to the small type 'B-neurons' (Jancsó et al., 1977), (this study was performed before the nomenclature of Aβ, Aδ and C was adopted). The large A-type neurons were unaffected by capsaicin treatment in this study. Consistent with the capsaicin mediated damage in small neurons, TRPV1 mRNA transcripts are localised to small and medium diameter nociceptors (Michael and Priestley, 1999). Recently, Cavanaugh and colleagues have used an elegant method to study TRPV1 lineage neurons through embryonic development into adulthood. Confirming earlier studies (Hjerling-Leffler et al., 2007), this study demonstrates that TRPV1 is transiently expressed in an extensive population of DRG neurons during development and later becomes largely restricted to the peptidergic population of unmyelinated C-fibre nociceptors in the mouse (Cavanaugh et al., 2011a). In agreement with the expression of TRPV1 in the smaller nociceptive population, Figure 5.7.3 demonstrates that even when DRG neurons are dissected at an early age (E15.5) and cultured for 10 days *in* vitro the restriction of expression to the neurons with smaller cell bodies remain.

In conclusion, these results discussed in this chaper illustrate that functional TRPV1 expression is common in the soma and peripheral neurites of DRG neurons in compartmentalised cultures. However, there are some cells that show a restricted expression either to the cell body or the peripheral neurites. The ability of high concentration capsaicin to selectively block TRPV1 expressing neurons demonstrates the functional expression of TRPV1 along the axon and/or axonal collaterals. Finally, as observed *in vivo,* capsaicin sensitivity is restricted to a neuronal population with significantly smaller cell somata from 1 to 10 days *in vitro*; suggesting that at least in terms of TRPV1 expression, DRG neurons in culture resemble their *in vivo* counterpart.

Chapter 6

The role of embryonic development in functional TRP channel expression *in vitro*

6.1. Introduction

TRPV1 is expressed in somatosensory neurons, and its expression is commonly used as a classical marker to identify nociceptors (Jancsó et al., 1977). Nociceptors are predominantly dependent on NGF during early embryonic development (Ruit et al., 1992). These embryonically TrkA expressing neurons later divide into two separate subpopulations as their dependence on neurotrophins changes. It is therefore clear that during development NGF has a great influence on TRPV1 expression; however, until only recently, the exact selectivity of TRPV1 expression among these nociceptor subpopulations was unknown. Cavanaugh and colleagues used a sensitive method to accurately study TRPV1 expression throughout development. Two reporter mice strains were used, which were generated by the same group (Cavanaugh et al., 2011c); in the first, Cre recombinase was expressed under the control of the TRPV1 promoter ($TRPV1^{Cre}$) and these were bred with a reporter strain in which lacZ is expressed in a cre dependent manner. As Cre is turned on when the TRPV1 promoter is first active, a floxed stop region is removed allowing expression of lacZ, generating a 'fate map' of TRPV1-expressing cells (Cavanaugh et al., 2011a). In the second mouse strain, placental alkaline phosphatase (PLAP) and nuclear lacZ are expressed under the control of the endogenous TRPV1 promoter ($TRPV1^{PLAP\text{-}nlacZ}$), the expression of these reporter molecules is driven by transcription at the *Trpv1* locus, and therefore is only observed in cells in which TRPV1 is expressed at the time of analysis (Cavanaugh et al., 2011a). Analysis of TRPV1 expression using the $TRPV1^{Cre}$ mice demonstrated that in the adult almost half of the cells that have at some point expressed TRPV1 are no longer TRPV1 positive (Cavanaugh et al., 2011a). The cells that no longer expressed TRPV1 were largely restricted to the nonpeptidergic population, suggesting a developmental downregulation of TRPV1 expression in this C-fibre subpopulation. This was confirmed with the $TRPV1^{PLAP\text{-}nlacZ}$ mice which showed a preferential TRPV1 expression in the peptidergic population (Cavanaugh et al., 2011a). These studies agree with earlier work which has demonstrated a developmental reduction in functional capsaicin sensitive cells (Hjerling-Leffler et al., 2007). Therefore, with the use of reporter mice Cavanaugh and colleagues provide a convincing argument that a large population of cells developmentally expressing TRPV1 do not die, but instead downregulate TRPV1 and constitute a significant proportion of the unmyelinated, nonpeptidergic nociceptors in the adult. As TRPV1 is predominantly expressed in the subset of neurons that continue to express TrkA and form the peptidergic population, NGF may be crucial for the regulation of TRPV1 expression.

In another recent paper, Mishra and colleagues studied the TRPV1 lineage in an attempt to address the very mild behavioural phenotype of the TRPV1 knockout, despite the fact that TRPV1 is a major noxious heat sensor when tested in *in vitro* conditions. A cre-mediated expression of diphtheria toxin under the control of the TRPV1 promoter allowed the ablation of the entire TRPV1 lineage. This resulted in a mouse line that was entirely insensitive to noxious heat and cold, but with normal mechanosensory responses (Mishra et al., 2011). This data implies that embryonic expression of TRPV1 marks the majority of nociceptors and all the prospective TRPA1 and TRPM8

expressing neurons, required for cold thermo-sensation. The mild behavioural phenotype of the TRPV1 knockout therefore suggests the presence of additional thermo-sensors, such as TRPV3 and TRPV4, however sensory input through these receptors are absent in the TRPV1-diptheria toxin animals. The potentially large population of thermo-sensors, suggests there is some redundancy when an individual receptor is genetically knocked out, however the complete loss of hot and cold sensation in the diphtheria toxin animals suggest that a limited neuronal population, all of which express TRPV1 embryonically, are responsible for thermal transduction in the adult.

These developmental studies have accurately traced the development of the TRPV1 lineage neurons, and have demonstrated that embryonic expression of TRPV1 is present in the majority of nociceptors, before a subsequent downregulation of expression and restriction to the peptidergic subpopulation. In order to understand the effects that *in vitro* culture of embryonic DRG neurons has on the expression of TRP channels a series of experiments were conducted analysing the functional expression over time *in vitro* in cultures prepared from a range of embryonic ages.

6.2. Objectives

The primary aim of these experiments was to examine if TRP channel expression is affected by removing DRG neurons from their natural environment and placing them in artificial culture conditions. These experiments were conducted to ultimately understand if TRP channel expression is regulated by external factors, which control the onset and/or maintenance of expression. Neurotrophin signalling is one example known to be crucial for the development of DRG neurons, therefore a secondary aim was to investigate a range of neurotrophins, for their ability to induce expression of functional TRP channels in culture conditions.

6.3. Functional expression of TRPV1 in mouse DRG somata is heavily dependent on embryonic dissection age whereas onset of TRPM8 expression is detected at all ages

A central question in embryonic primary cell culture is whether the normal development and maturation of cells continue uninterrupted when the cell is removed from its natural environment and cultured *in vitro*. The onset of TRPV1 expression *in vivo* has a well defined time course; TRPV1 protein expression is first detected at E12.5 in the mouse, and robust functional expression is observed in the cell soma at E13.5 (Hjerling-Leffler et al., 2007). To address the effect of *in vitro* culture on TRPV1 expression, DRG cultures were prepared from E13.5, E14.5 and E15.5 mouse embryos. Capsaicin sensitivity was assessed in each of these cultures at various time points throughout the culture period with the aim of quantifying the functional expression of TRPV1 in the soma over time in culture. All capsaicin percentages are expressed as a function of somal KCl responding neurons

Figure 6.3.1a demonstrates that in E13.5 mouse cultures, acutely dissociated DRG neurons initially have 47 ± 4 % (n_{cells} = 209, $n_{experiments}$ = 3) capsaicin sensitivity which rapidly declines so that at later time points, the functional TRPV1 expression is never greater than 10 % in the soma, for example at 4, 5 and 7 DIV only 5 ± 1 % (n_{cells} = 267, $n_{experiments}$ = 3), 3 ± 1 % (n_{cells} = 286, $n_{experiments}$ = 3), and 6 ± 2 % (n_{cells} = 257, $n_{experiments}$ = 4) are capsaicin sensitive, respectively.

Measurements of capsaicin sensitivity in acutely dissociated E14.5 mouse DRG neurons (DIV 0) reveal 55 ± 8 % (n_{cells} = 225, $n_{experiments}$ = 3) of the total population functionally express TRPV1 in the soma, this drops to 38 ± 4 % at 1 DIV (n_{cells} = 274, $n_{experiments}$ = 4), 35 ± 8 % at 2 DIV (n_{cells} = 272, $n_{experiments}$ = 4) and 13 ± 2 % at 3 DIV (n_{cells} = 198, $n_{experiments}$ = 3) (Figure 6.3.1b). After 3 days in culture, the capsaicin sensitive population remains relatively stable, with 14 ± 4 % positive at 5 DIV (n_{cells} = 467, $n_{experiments}$ = 6), and 9 ± 3 % positive at 7 DIV (n_{cells} = 584, $n_{experiments}$ = 7) (Figure 6.3.1b).

At E15.5, 68 ± 4 % of acutely dissociated (DIV 0) DRG neurons functionally expressed TRPV1 (n_{cells} = 615, $n_{experiments}$ = 11) (Figure 6.3.1c), which is comparable to the levels seen at the same time point in E14.5 cultures. However, unlike E14.5 cultures, the capsaicin sensitivity does not rapidly decline; instead, functional expression of TRPV1 was maintained at approximately 50 % throughout all time points in culture. At 2, 4 and 7 DIV, TRPV1 expression is observed in 50 ± 6 % (n_{cells} = 268, $n_{experiments}$ = 4), 44 ± 7 % (n_{cells} = 319, $n_{experiments}$ = 7) and 65 ± 5 % (n_{cells} = 549, $n_{experiments}$ = 9) (Figure 6.3.1c) respectively.

Comparison between embryonic ages reveal that at 1 DIV, E13.5 cultures are significantly different from both E14.5 and E15.5, yet later in culture E13.5 and E14.5 capsaicin sensitivity are no longer different, as the capsaicin sensitive population reduces during the first 3 culture days (Figure 6.3.1d). E15.5 cultures have a significantly greater sensitivity to capsaicin than E13.5 cultures at all tested DIV, and apart from 1 DIV are also significantly greater than E14.5 (Figure 6.3.1d).

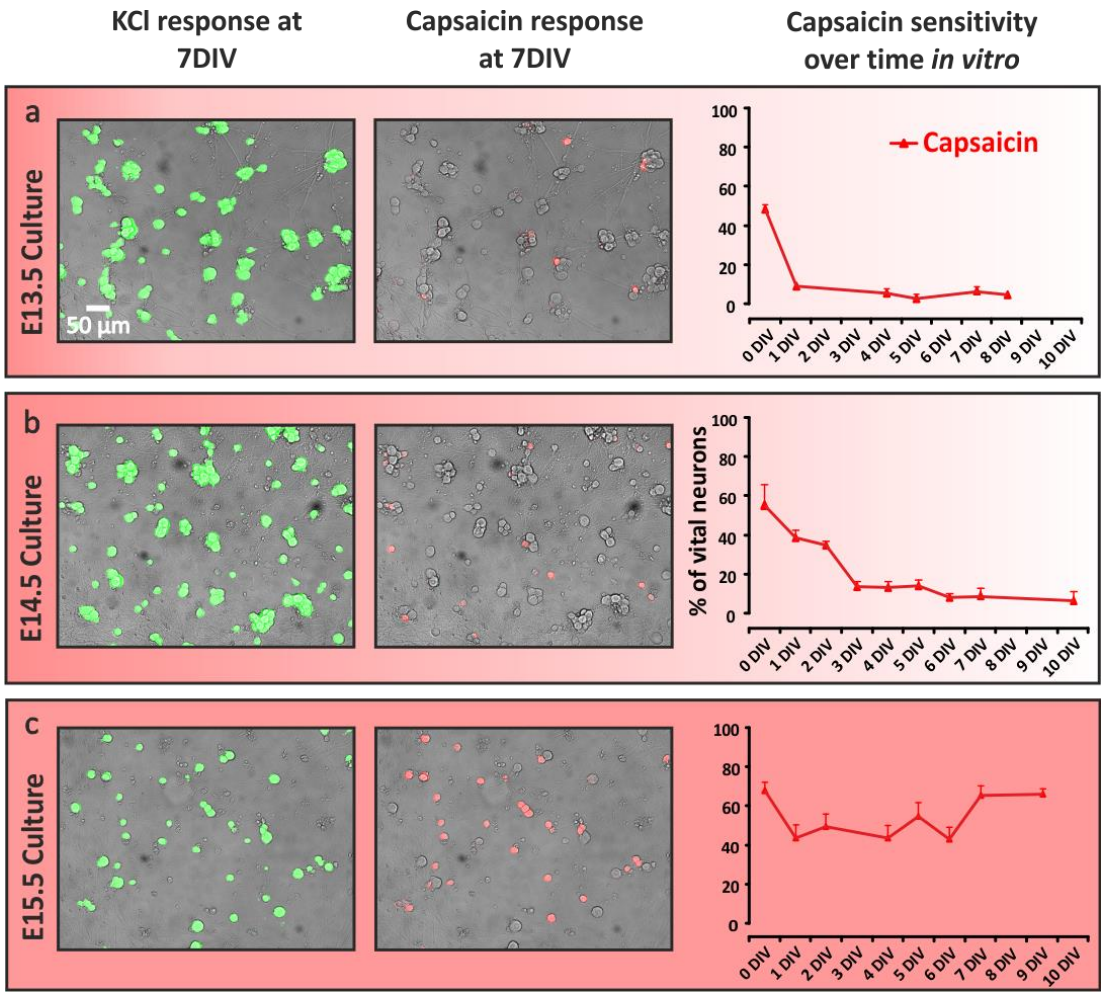

d

	0 DIV	1 DIV	4 DIV	5 DIV	7 DIV
E13.5 vs E14.5	ns	*	ns	ns	ns
E13.5 vs E15.5	ns	**	**	***	***
E14.5 vs E15.5	ns	ns	*	***	***

Figure 6.3.1
*Functional expression of TRPV1 in mouse DRG neurons is only maintained in vitro if embryos are dissected after E14.5. (a-c) Representative pseudocolour images of cells responding to KCl somal stimulation, representative pseudocolour images of cells responding to somal capsaicin stimulation and quantification over time in vitro for (a) E13.5 cultures, (b) E14.5 cultures and (c) E15.5 cultures. (d) Statistics table showing the statistical significance of comparing capsaicin sensitivity at the same DIV between embryonic ages. (ns – not significant, *p<0.05, **p<0.01, ***p<0.001 one-way ANOVA with Bonferroni post-hoc test).*

TRPM8 is robustly activated by the cooling compounds menthol and icilin (Peier et al., 2002a) and its initiation of expression *in vivo* begins approximately 4 – 6 days later than TRPV1 (Hjerling-Leffler et al., 2007). Therefore, to examine if embryonic age of dissection affects TRPM8 expression in the same way as TRPV1, menthol sensitivity was studied over time in culture and at different embryonic ages. A subpopulation of DRG neurons from E13.5, E14.5 and E15.5 embryonic cultures displayed robust calcium transients from somal menthol stimulation. The first detectable menthol induced calcium transient in the soma was recorded at 5 DIV, 4 DIV and 3 DIV for E13.5, E14.5 and E15.5, respectively (Figure 6.3.2a, b, c). At these time points menthol sensitivity in the soma measured 2 ± 1 % in E13.5 cultures at 5 DIV (n_{cells} = 286, $n_{experiments}$ = 3) (Figure 6.3.2a), 1 ± 1 % in E14.5 cultures at 4 DIV (n_{cells} = 264, $n_{experiments}$ = 4) (Fig 6.3.2b), and 6 ± 4 % in E15.5 cultures at 3 DIV (n_{cells} = 319, $n_{experiments}$ = 7) (Figure 6.3.2c).

Once in culture, neuronal age is referred to as 'days *in vitro* (DIV)', rather than continuation of the embryonic and postnatal nomenclature. However, if DIV is converted to the relevant projected embryonic/postnatal age for each culture, the onset of menthol expression is well conserved at approximately E18.5, despite the dissection taking place at different embryonic ages (Figure 6.3.2d). The population of neurons functionally expressing TRPM8 steadily increases from the first detection time point. At 7DIV, 7 ± 2 % (n_{cells} = 257, $n_{experiments}$ = 4) (Figure 6.3.2a), 8 ± 2 % (n_{cells} = 584, $n_{experiments}$ = 7) (Figure 6.3.2b) and 8 ± 2 % (n_{cells} = 549, $n_{experiments}$ = 9) (Figure 6.3.2c) of all vital cells display menthol sensitivity in E13.5, E14.5 and E15.5 cultures, respectively. In the three different embryonic cultures, this population increases further to approximately 20 % at the latest recorded *in vitro* time point. Therefore, unlike functional TRPV1 expression, the onset and maintenance of TRPM8 expression in the soma is not affected by the embryonic age of dissection.

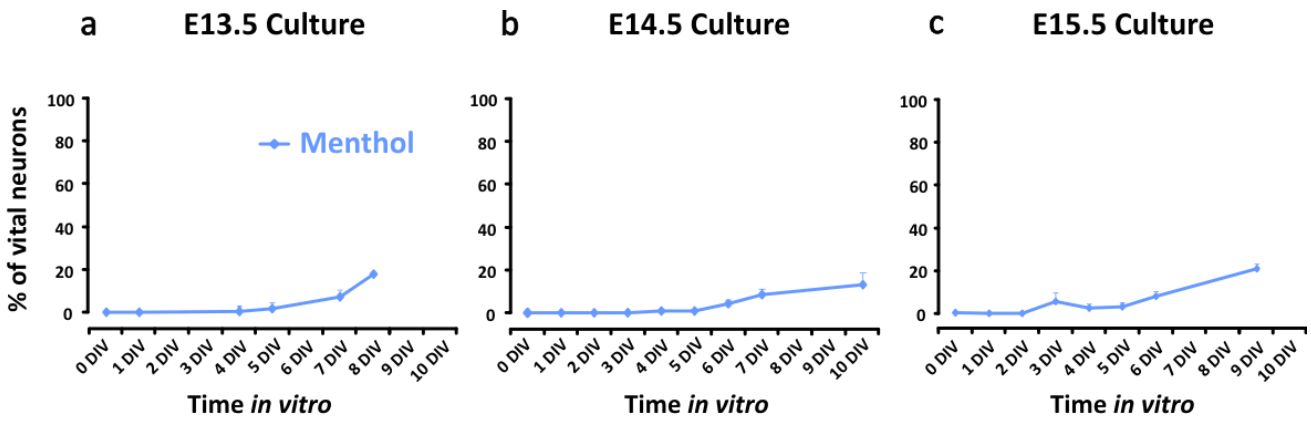

d

Projected developmental age compared to DIV

Embryonic dissection age	E13.5	E14.5	E15.5	E16.6	E17.5	E18.5	P0	P1	P2	P3	P4	P5	P6
E13.5	0	1	2	3	4	5	6	7	8	9	10	11	12
E14.5		0	1	2	3	4	5	6	7	8	9	10	11
E15.5			0	1	2	3	4	5	6	7	8	9	10

Figure 6.3.2
Functional expression of TRPM8 in mouse DRG neurons is observed in cultures prepared from E13.5, E14.5 and E15.5 embryos. (a-c) Quantification of menthol sensitivity over time in vitro in cultures prepared from (a) E13.5 embryos, (b) E14.5 embryos and (c) E15.5 embryos. (d) Table displaying the projected developmental age and onset of menthol sensitivity at each embryonic age. Arrow refers to the developmental age at which menthol sensitivity begins in each culture.

6.4. Functional TRPV1 expression is only maintained in the terminals and soma of mouse DRG neurons when embryos are dissected at E15.5

Previous chapters have demonstrated that somal expression of key transducing molecules is not necessarily replicated in peripheral regions of DRG sensory neurons *in vitro.* Therefore, in order to investigate if TRPV1 expression in the terminals is dependent on embryonic age as it is in the soma, peripheral capsaicin sensitivity was also examined. Once the DRG neurons are dissected and seeded into the compartmentalised chamber they begin to regrow neuronal processes which are then directed to grow through the 800 µm long microgrooves into the adjacent compartment. The time taken for this regrowth means early time points in the culture period cannot be tested. Capsaicin values for both the terminals and soma are represented as a percentage of KCl responding cells from stimulation of the terminals, therefore, only cells with a projecting axon are included in the analysis.

The test stimuli of menthol, mustard oil, capsaicin and KCl were applied in that order to the terminal compartment followed by application to the soma. Observations showed that at 10 DIV, in the terminals, capsaicin sensitivity was very low in E14.5 cultures (Figure 6.4.1a, b) and relatively common in E15.5 cultures (Figure 6.4.1c, d) which coincided with the previous pattern detected in the soma. In E13.5 embryonic cultures at 7 DIV (n_{cells} = 102, $n_{experiments}$ = 4) the capsaicin sensitivity remained consistently low, with 15 ± 6 % and 6 ± 3 % responding to stimulation of the terminals and soma, respectively (Figure 6.4.2a, b). Similarly, capsaicin stimulation of the terminals and soma at 7 DIV, in cultures from E14.5 embryonic mice resulted in 23 ± 5 % (n_{cells} = 284, $n_{experiments}$ = 7), and 10 ± 3 % activation (Figure 6.4.2c, d). As previously established, slightly greater capsaicin sensitivity is observed at the terminals compared to the soma, a pattern that has now been shown to be conserved across species, embryonic ages and time *in vitro*. The functional expression of TRPV1 at a level comparable to expression in adult mice is only observed in cultures dissected at E15.5. The critical developmental time point for TRPV1 expression in the mouse therefore appears to be between E14.5 and E15.5, after which DRG neurons *in vitro* are able to maintain functional expression of the capsaicin receptor. In E15.5 cultures, at 4 DIV only a relatively small number of cells have grown a projecting axon, however, of this population, capsaicin sensitivity is already prevalent in 63 ± 6 % of the terminals and 68 ± 11 % of the soma (n_{cells} = 31, $n_{experiments}$ = 5) (Figure 6.4.2e, f). The number of projecting neurons rapidly increases over the next 2 - 3 days in culture, yet capsaicin sensitivity remains stable throughout all times *in vitro,* for example at 7 DIV, 62 ± 7 % and 65 ± 6 % (n_{cells} = 158, $n_{experiments}$ = 5) (Figure 6.4.2e, f) of the terminals and soma, respectively, are activated. Functional expression of TRPM8 at the receptive terminals was also detected in cultures prepared from all embryonic ages, indicating the menthol receptor is expressed in the periphery in addition to the soma in this *in vitro* preparation. Across each embryonic time point, the percentage of neurons expressing TRPM8 in the terminals was slightly greater than those expressing it in the soma. In E13.5 cultures at 7 DIV, 5 ± 4 % responded to stimulation of the terminals, compared to 3 ± 2 % at the soma (Figure 6.4.2a, b). Similarly, in E14.5 cultures at 5 DIV, 3 ± 1 % and 1 ± 1 % were menthol

responsive in the terminals and soma, with this increasing to 13 ± 4 % and 8 ± 2 % at 7 DIV (Figure 6.4.2c, d). In E15.5 cultures at 7DIV, the percentage of menthol sensitive neurons was very similar, with 14 ± 5 % and 8 ± 3 % detected in the terminals and soma, respectively (Figure 6.4.2e, f). Therefore, as detected in the soma, menthol sensitivity is observed in the receptive terminals in cultures prepared from all three embryonic ages, and the functional expression of TRPM8 gradually increases throughout the *in vitro* culture period. E15.5 cultures were investigated for the functional coexpression of TRPV1 and TRPM8. At 7 DIV, 85 ± 10 % of menthol sensitive soma were capsaicin sensitive, and 64 ± 11 % of terminals with menthol sensitivity were activated by capsaicin.

The TRPA1 agonist - mustard oil, was also included in the stimulation protocol for both the terminals and soma. E13.5 (Figure 6.4.2a, b) and E14.5 (Figure 6.4.2c, d) embryonic cultures were completely insensitive to mustard oil at all time points. Furthermore, mustard oil stimulation of the soma in E15.5 cultures was also unable to evoke a calcium influx at all *in vitro* time points tested (up to 10 DIV) (Figure 6.4.1d). However, mustard oil stimulation of the terminals at 10 DIV, depolarised 6 ± 4 % of neurons (Figure 6.4.1c and Figure 6.4.2e). At this time point, peripheral sensitivity to mustard oil overlapped entirely with peripheral sensitivity to capsaicin, demonstrating a complete functional coexpression of TRPA1 and TRPV1. At 10 DIV, only a single neuron functionally responded to both menthol and mustard oil, essentially indicating that TRPM8 and TRPA1 are expressed in non-overlapping subpopulations.

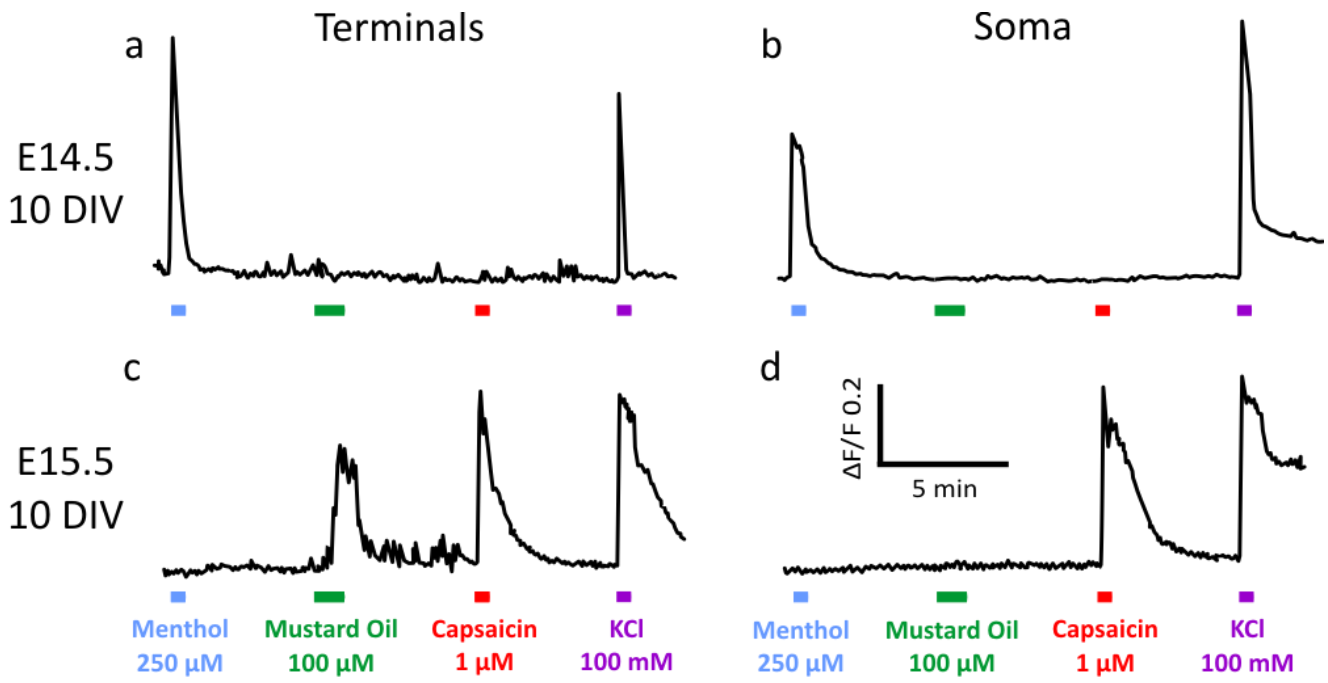

Figure 6.4.1
TRP channel expression is differentially regulated in vitro at different embryonic ages. (a-b) Representative calcium transients from a single cell at 10 DIV from an E14.5 mouse culture which is menthol sensitive, capsaicin insensitive. (c-d) Representative calcium transients from a single cell at 10 DIV from an E15.5 mouse culture which is sensitive to mustard oil when applied to the terminals and capsaicin sensitive when applied to the terminals and soma.

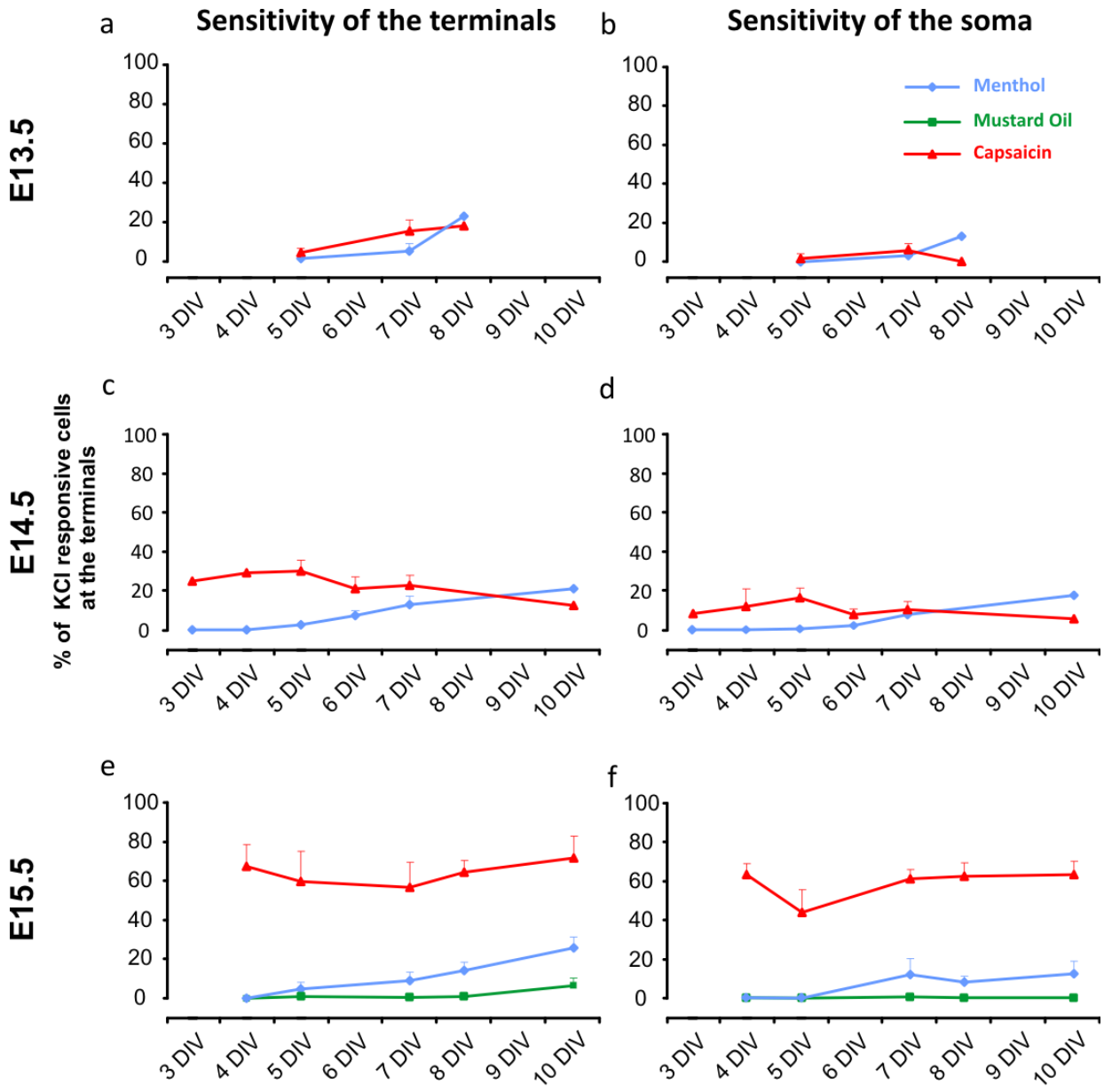

Figure 6.4.2
Quantification of neurons responding to capsaicin, menthol and mustard oil from stimulation of the terminals (a, c, e) and soma (b, d, f), expressed as a percentage of cells responding to KCl application to the terminals. Functional TRP channel expression in the terminals and soma is displayed over time in vitro at E13.5 (a, b), E14.5 (c, d) and E15.5 (e, f).

6.5. Functional expression of TRPV1 in the soma of rat DRG cultures is also influenced by embryonic dissection age

In mice, embryonic dissection age has a major influence on TRPV1 expression. Therefore, in order to ascertain whether a separate species also displays a similar pattern of capsaicin sensitivity, rat cultures were investigated. According to the Carnegie staging of mice and rats (Butler and Juurlink, 1987), E13.5 in the mouse corresponds to E15 in rat development. Therefore, two embryonic ages of E15.5 and E16.5 were investigated in the rat, which correspond to the mouse ages during which capsaicin sensitivity is low or downregulated during culture.

As expected, acutely dissociated DRG neurons from E15.5 rat embryos displayed capsaicin sensitivity, with 35 ± 8 % (n_{cells} = 316, $n_{experiments}$ = 4) of KCl positive neurons positive in the soma (Figure 6.5.1e). However, in the presence of NGF, the capsaicin sensitivity began to decrease over time in culture, with 23 ± 4 % activated at 1 DIV (n_{cells} = 770, $n_{experiments}$ = 6) and only 6 ± 2 % at DIV 2 (n_{cells} = 400, $n_{experiments}$ = 6) (Figure 6.5.1e). The capsaicin sensitive population remained very low for the rest of time in culture, with 11 ± 6 % at 6 DIV (n_{cells} = 587, $n_{experiments}$ = 6) and 6 ± 3 % at 7 DIV (n_{cells} = 366, $n_{experiments}$ = 4) (Fig 6.5.1b e). Similar to mice cultures, a different pattern of TRPV1 expression was observed in cultures dissected from older embryos. At E16.5, capsaicin sensitivity was considerably greater in acutely dissociated cells, with 75 ± 1 % (n_{cells} = 485, $n_{experiments}$ = 5) activated by the TRPV1 agonist (Figure 6.5.1e). Instead of the rapid decline as observed in E15.5 cultures, TRPV1 expression reduced only slightly in the first few days, with 65 ± 4 % at 1 DIV (n_{cells} = 753, $n_{experiments}$ = 6) and 53 ± 5 % at 2 DIV (n_{cells} = 307, $n_{experiments}$ = 4). Capsaicin sensitivity then plateaued for the remaining time in culture with 47 ± 4 % positive at 3 DIV (n_{cells} = 521, $n_{experiments}$ = 6), 46 ± 9 % at 5 DIV (n_{cells} = 354, $n_{experiments}$ = 5) and 45 ± 5 % at 7 DIV (n_{cells} = 563, $n_{experiments}$ = 7) (Figure 6.5.1d, e). A slight increase to 58 ± 6 % was observed at 10 DIV (n_{cells} = 248, $n_{experiments}$ = 3). The overall difference in capsaicin sensitivity between E15.5 and E16.5 cultures was significantly different ($F_{1, 61}$ = 242.4, $p<0.001$, 2-way ANOVA). The stark difference in TRPV1 expression at DIV 7 is clearly illustrated in Figure 6.5.1b and d where significantly more cells display a calcium response to capsaicin in the E16.5 culture compared with the same time point in an E15.5 culture ($p<0.01$, 2-way ANOVA with Bonferroni post-hoc test). At every DIV, capsaicin sensitivity was significantly greater in E15.5 cultures than E14.5 (Figure 6.5.1e).

Consequently, an almost identical pattern of capsaicin sensitivity is detected during culture of embryonic neurons in the rat and mouse. In both species, dissection after a specific embryonic time point – between E15.5 and E16.5 in the rat, and between E14.5 and E15.5 in the mouse, enables the cells to maintain capsaicin sensitivity throughout the entire culture period. Intriguingly, capsaicin sensitivity rapidly declines over the first few days *in vitro* if DRGs are dissected prior to this time point, as observed in both rat and mouse cultures. In the mouse, if dissection takes place even earlier in embryogenesis, TRPV1 expression remains especially low and never reaches the levels commonly detected in the adult mouse.

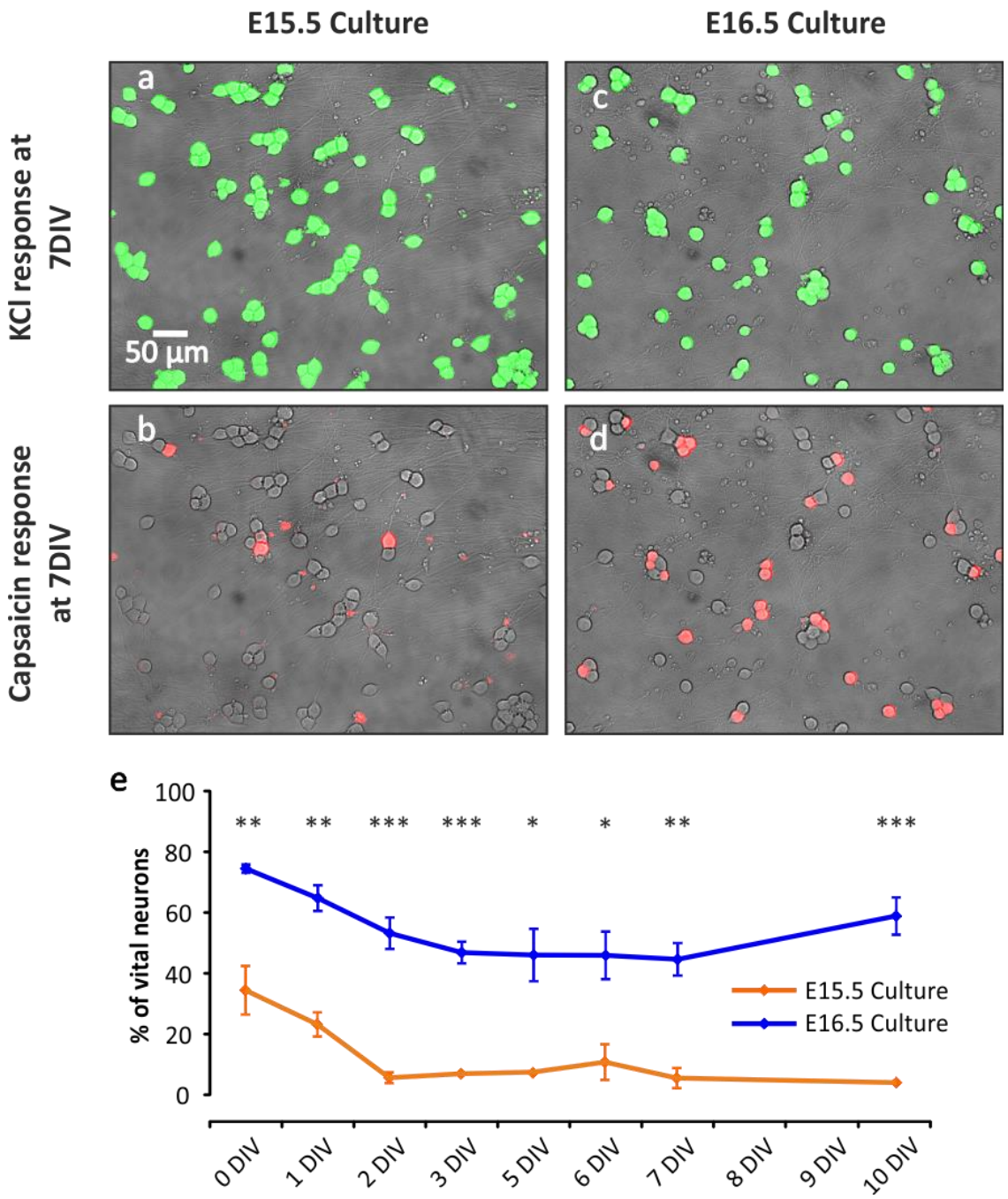

Figure 6.5.1
*Rat DRG neurons only maintain a substantial TRPV1 expression when cultured after E16.5. (a) Pseudocolour image of a representative field of cells responding to somal KCl stimulation at 7 DIV from an E15.5 culture. (b) Pseudocolour image of the same field of cells in (a) showing the capsaicin sensitive population. (c) Pseudocolour image of a representative field of cells responding to somal KCl stimulation at 7 DIV from an E16.5 culture. (d) Pseudocolour image of the same field of cells in (c) showing the capsaicin sensitive populations. (e) Quantification of TRPV1 positive cells in E15.5 and E16.5 cultures over 10 days in vitro. (*p<0.05, **p<0.01, ***p<0.001, 2-way ANOVA with Bonferroni post-hoc test).*

6.6. The terminals display a similar level of functional TRPV1 expression to the cell soma in rat cultures harvested at different embryonic ages.

Somal capsaicin sensitivity in rat cultures was only maintained *in vitro* if embryos were dissected at E16.5. Preparation of cultures from E15.5 embryos resulted in a rapid downregulation of capsaicin sensitivity within the first 3 days *in vitro*. To investigate the functional expression of TRPV1 at the terminals, stimulation of the peripheral regions was initiated upon the first visual observation that neuronal processes were present in the terminal compartment, usually occurring at 4 DIV.

In both the terminals and soma, the capsaicin sensitive populations were dramatically reduced in cultures from E15.5 embryos (Figure 6.6.1b and Figure 6.6.2a), whereas cultures dissected only a day later result in relatively stable TRPV1 expression in both the terminals and soma across all tested time points (Figure 6.6.1b and Figure 6.6.2b). In E15.5 cultures at 7 DIV, the percentage of capsaicin sensitive neurons in the terminals and soma was 7 ± 3 % and 5 ± 2 %, respectively (Figure 6.6.2a) (n_{cells} = 194, $n_{experiments}$ = 4). In comparison, E16.5 cultures at the same time point display 60 ± 4 % (Fig 6.6.1d, f) and 40 ± 7 % (Figure 6.6.2b) for the terminals and soma, respectively (Fig 6.6.1h) (n_{cells} = 531, $n_{experiments}$ = 12). As previously demonstrated, in both the E15.5 and E16.5 cultures the terminals display a greater sensitivity to capsaicin than the cell soma across all time points tested.

These results show that during embryonic rat development there is a critical time point between E15.5 and E16.5. Dissection of the DRG neurons before this time point results in a rapid down-regulation of capsaicin sensitivity in the cell soma, and by the time the terminals can be tested these are largely insensitive to the TRPV1 agonist.

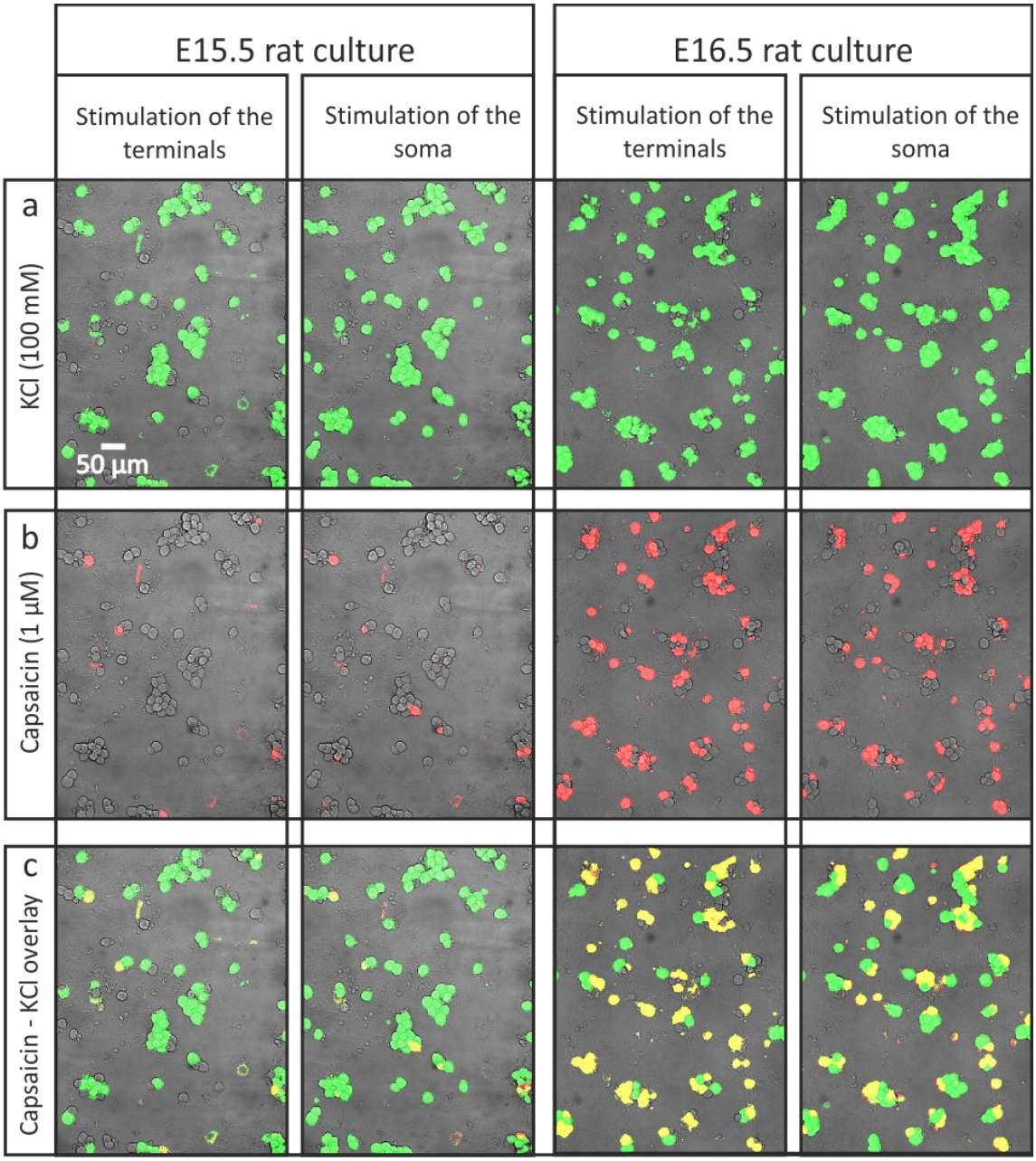

Figure 6.6.1
TRPV1 expression in the terminals and soma is very low in E15.5 cultures at 7 DIV, whereas many neurons display capsaicin sensitivity at 7 DIV in E16.5 cultures. (a-c) Representative pseudocolour images from an E15.5 or E16.5 culture at 7DIV, showing cells responding to (a) KCl stimulation of the terminals or soma, (b) capsaicin stimulation of the terminals or soma, (c) overlay of capsaicin and KCl responding neurons.

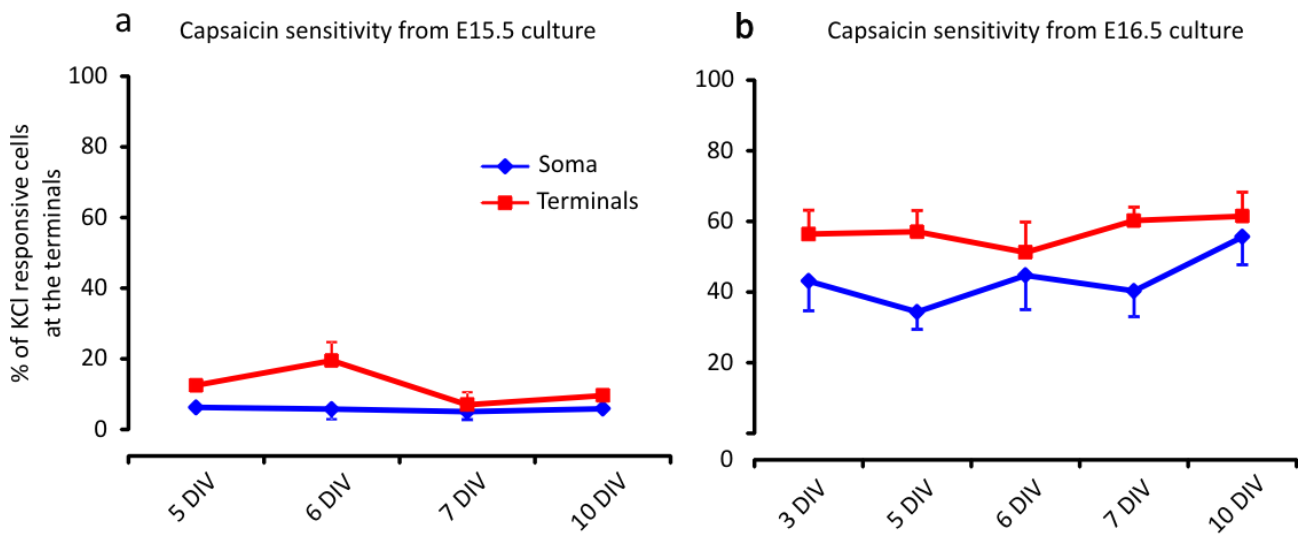

Figure 6.6.2
Quantification of capsaicin sensitivity over time in vitro in cultures prepared from (a) E15.5 or (b) E16.5 rat embryos.

6.7. Addition of neurotrophin-3 to a mouse E14.5 culture does not influence TRPV1 expression.

In vitro culture conditions are designed to model the *in vivo* culture conditions, however they are unable to directly replicate them. It is therefore likely that the down regulation in capsaicin sensitivity in E14.5 mouse cultures is due to the absence of a regulatory factor required for the maintenance of TRPV1 expression during DRG embryogenesis. Neurotrophins play an essential role in DRG neuronal development, therefore, as the culture medium in previous experiments only contained NGF, additional neurotrophins were added to the culture medium in order to establish if TRPV1 expression could be influenced. E14.5 mouse embryos were used, as these initially expressed a substantial TRPV1 positive population early in the culture time course. Choosing E14.5 over E13.5 embryos meant that the maintenance of TRPV1 instead of expression initiation was being investigated. The focus was primarily concentrated at 7DIV, as by this time point in E14.5 cultures, somal capsaicin sensitivity was very low, and additionally most of the previous capsaicin experiments were carried out at this time point.

Studies began with NT3 supplement of the culture medium. NT3 (10 ng/ml) was added to both the somal and terminal compartment, in addition to the standard NGF chemo-attractant protocol. This meant that at all time during the *in vitro* culture, NT3 was freely available to all neuronal regions. In control cultures, the standard NGF medium protocol was adhered to.

Previous experiments have demonstrated that somal capsaicin sensitivity in E14.5 cultures is almost absent when cultured only with NGF and tested at 7DIV, with the terminals displaying a slightly greater sensitivity. At 7 DIV in the control conditions (n_{cells} = 222, $n_{experiments}$ = 4), the same pattern of expression is repeated, with 17 ± 6 % sensitive in the terminals and only 2 ± 1 % in the soma (Figure 6.7.1a, c). In the cultures supplemented with NT3 at 7 DIV (n_{cells} = 217, $n_{experiments}$ = 4), TRPV1 expression is very similar to control conditions, with 22 ± 6 % and 4 ± 1 % sensitivity in the terminals and soma, respectively. Statistical comparisons of somal capsaicin sensitivity in control conditions (only NGF) and test conditions (NGF and NT3) revealed no significant difference (p=0.25, unpaired T-test). Similarly, comparisons of capsaicin sensitivity in the terminals between control and test conditions also revealed no significant difference (p=0.95, unpaired T-test). Overall this indicates that NT3 has no influence on TRPV1 expression in vitro (Figure 6.7.1b, c).

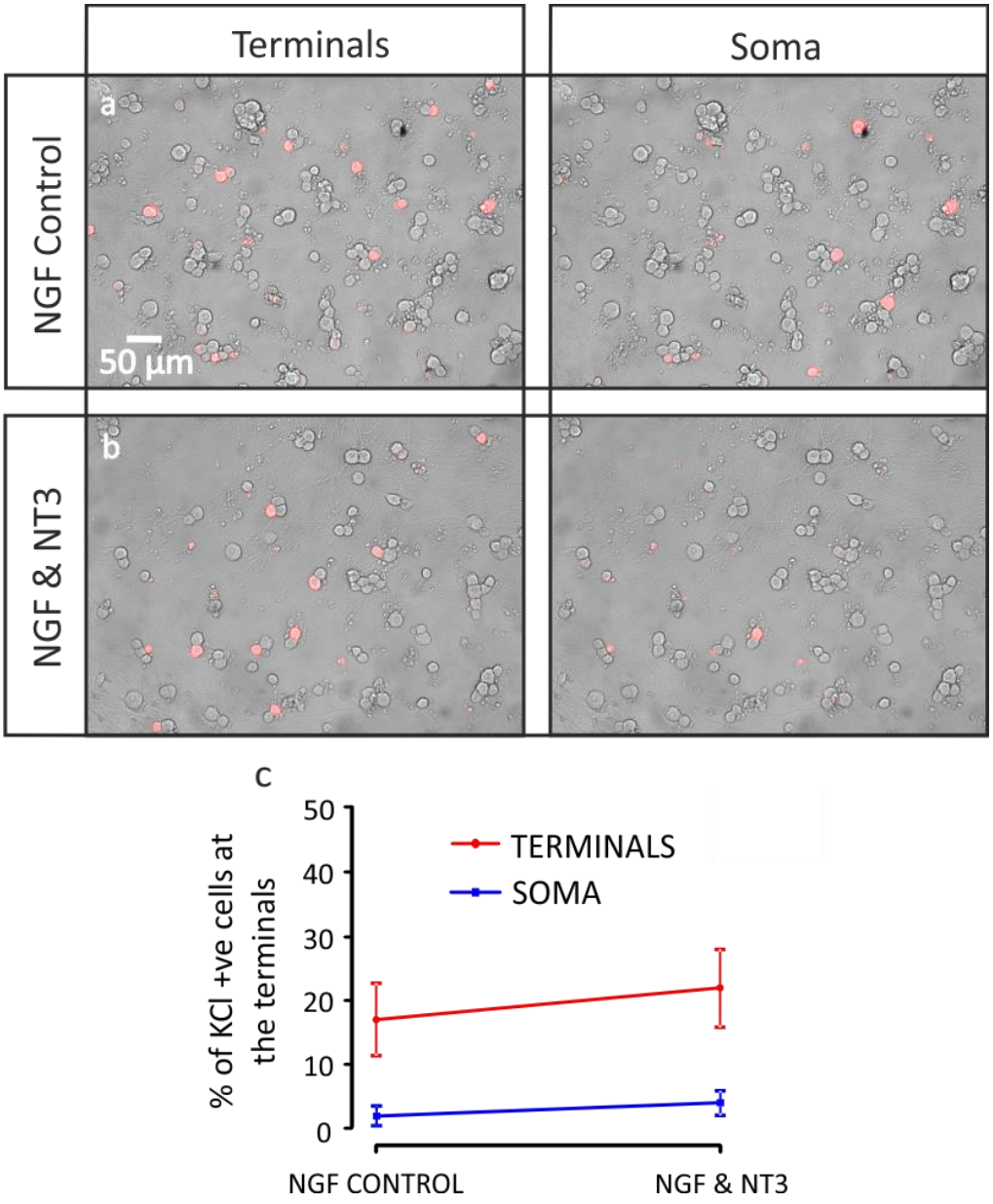

Figure 6.7.1
NT3 medium supplement does not influence TRPV1 expression. (a) Representative pseudocolour images showing cells responding to capsaicin stimulation applied to the soma and the terminals when cultured in control NGF medium. (b) Representative pseudocolour images showing cells responding to capsaicin stimulation applied to the soma and the terminals when cultured in NT3 supplemented medium. (c) Quantification of capsaicin positive cells expressed as a percentage of cells responding to KCl from stimulation of the terminals. Capsaicin sensitivity of the terminals or soma does not significantly increase when medium is supplemented with NT3.

6.8. Addition of retinoic acid increases the expression of TRPV1 in both the terminals and soma of mouse DRG neurons.

DRG neurons are a heterogeneous population consisting of several subpopulations. In general DRG neurons can be classified according to their neurotrophic factor dependence during embryogenesis (Marmigère and Ernfors, 2007). Therefore in an attempt to provide additional neurotrophic cues and study the effect on capsaicin sensitivity, three separate medium conditions were tested, these consisted of an NGF control, medium containing NGF, NT3, GDNF and BDNF and medium containing NGF, NT3, GDNF, BDNF and retinoic acid. All percentages are expressed as a function of cells responding to KCl application to the terminals.

As previously observed, culture in NGF alone resulted in low functional expression of TRPV1. At 7 DIV (n_{cells} = 179, $n_{experiments}$ = 4), somal capsaicin sensitivity was measured at 4 ± 1 %, and 20 ± 5 % of neurons were excited by capsaicin application to the terminals (Figure 6.8.1a, d, e). Supplement of DRG neurons with NGF, NT3, GDNF and BDNF (n_{cells} = 281, $n_{experiments}$ = 6) did not increase either the somal capsaicin sensitivity which was measured at 6 ± 2 %, or the sensitivity of the terminals which was quantified as 27 ± 4 % of neurons (Figure 6.8.1b, d, e). Statistical tests revealed this medium condition did not significantly increase capsaicin sensitivity in either the terminals or soma ($p>0.05$, t-test). This suggests that NT3, GDNF and BDNF do not act to regulate functional expression of TRPV1 *in vitro*.

In addition to neurotrophins, retinoids including retinoic acid are also reported to be involved in the survival and development of DRG neurons (Corcoran et al., 2000). Therefore, the third culture condition contained NGF, NT3, GDNF, BDNF and retinoic acid. In these conditions, at 7 DIV (n_{cells} = 411, $n_{experiments}$ = 10), functional TRPV1 expression in the soma of these cultures was measured at 24 ± 4 %, a significant increase of over 15 % from control conditions ($p<0.05$, unpaired t-test) (Figure 6.8.1c, e). Furthermore, sensitivity in the terminals also increased to 37 ± 3 %, which also proved to be a significant increase compared to control cultures ($p<0.05$, unpaired t-test) (Figure 6.8.1c, d). Figure 6.8.1c illustrates a representative field of cells that have been cultured with NGF, NT3, GDNF, BDNF and retinoic acid with a pseudocolour overlay of capsaicin sensitive cells, it is possible to observe there are significantly more cells functionally expressing TRPV1 when compared to the NGF controls. Therefore, retinoic acid appears to be acting either alone or in combination with other neurotrophins to upregulate the functional expression of TRPV1 in embryonic cultures *in vitro.*

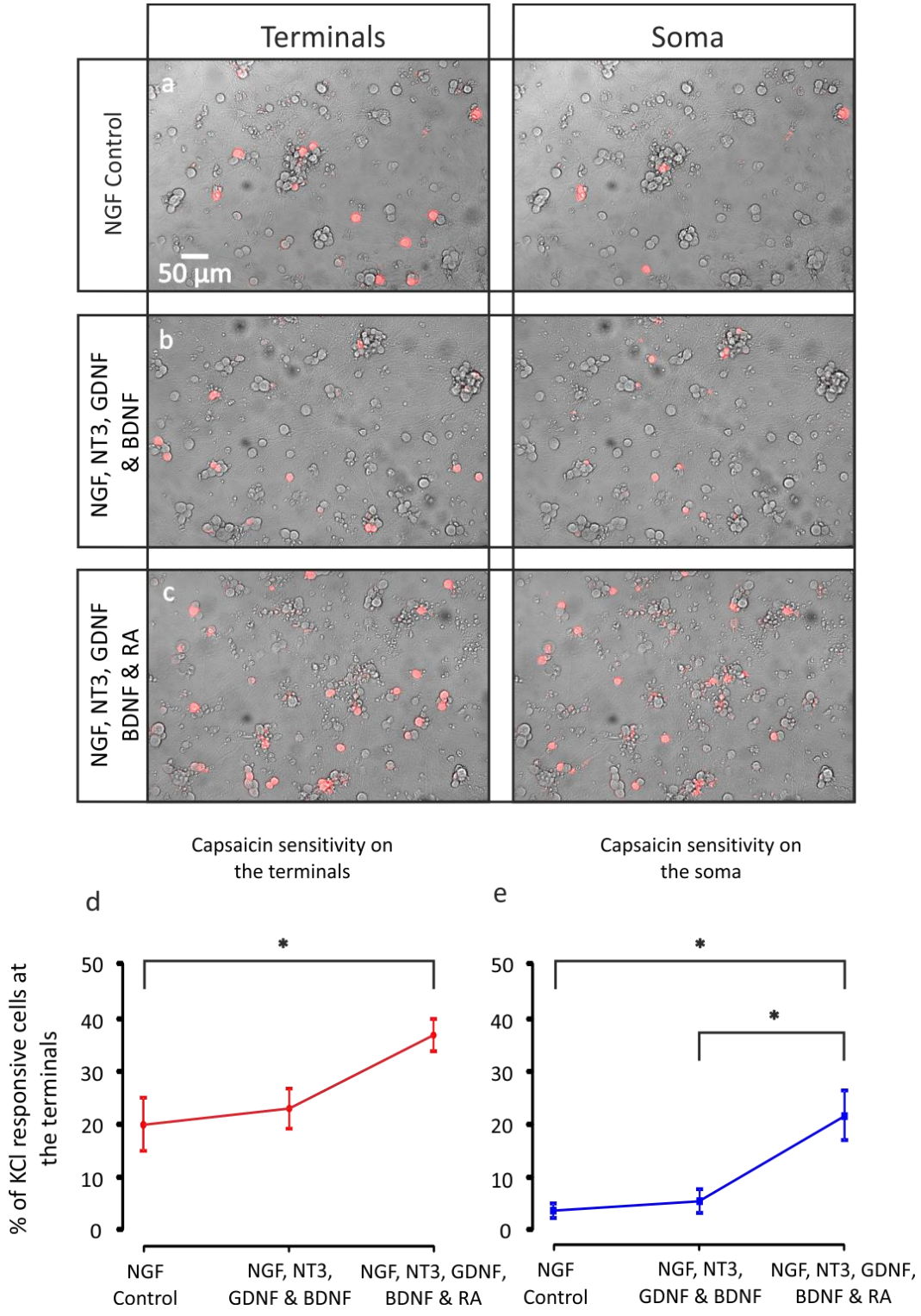

Figure 6.8.1
*Medium supplement with a neurotrophin cocktail and retinoic acid significantly increases capsaicin sensitivity. Representative pseudocolour images showing cells responding to capsaicin stimulation applied to the terminals and soma when cultured in (a) NGF medium, (b) NGF, NT3, GDNF and BDNF, (c) NGF, NT3, GDNF BDNF and retinoic acid. (d,e) Quantification of capsaicin responsive cells expressed as a percentage of cells responding to KCl at the terminals. (d) Capsaicin sensitivity of the terminals, (e) capsaicin sensitivity of the soma. (*p<0.05, unpaired t-test).*

6.9. Supplement of retinoic acid and NGF increases the functional expression of TRPV1 at 7 and 10 DIV in mouse DRG neurons.

Retinoic acid significantly increased capsaicin sensitivity in both the terminals and soma when supplemented in combination with a host of neurotrophins. To investigate whether retinoic acid was acting synergistically with the other neurotrophins present to increase functional TRPV1 expression, cultures were supplemented with only NGF and retinoic acid, and tested for their capsaicin sensitivity. Cultures containing retinoic acid again proved to have a greater TRPV1 sensitivity than the NGF control. In control cultures at 7 DIV (n_{cells} = 109, $n_{experiments}$ = 3) the terminals and soma were measured to have 12 ± 7 % and 6 ± 3 %, whilst retinoic acid supplemented cultures at 7 DIV (n_{cells} = 230, $n_{experiments}$ = 5) were significantly more sensitive at 30 ± 2 % and 16 ± 2 % capsaicin sensitive in the terminals ($p<0.05$, unpaired t-test) and soma ($p<0.05$, unpaired t-test), respectively (Figure 6.9.1a).

Additional cultures were tested at the later time point of 10 DIV for their capsaicin sensitivity. Interestingly, the cells supplemented with retinoic acid showed considerably greater sensitivity to capsaicin at this later time point with 45 ± 8 % and 48 ± 12 % (n_{cells} = 86, $n_{experiments}$ = 3) of neurons sensitive for capsaicin in the terminals and soma. At the same time point, NGF controls measured 23 ± 6 % and 9 ± 3 % (n_{cells} = 111, $n_{experiments}$ = 4) in the terminals and soma. Retinoic acid significantly increased somal TRPV1 functional expression compared to DIV and litter matched NGF controls ($p<0.05$, unpaired t-test), furthermore, the somal expression was significantly increased compared to the 7 DIV time point for cultures in the presence of retinoic acid ($p<0.05$, unpaired t-test). The significant increase of functional TRPV1 expression in cells cultured in the prolonged presence of retinoic acid suggests that the effect retinoic acid is producing may be cumulative, ultimately leading to a considerably greater proportion of capsaicin sensitive cells in E14.5 cultures.

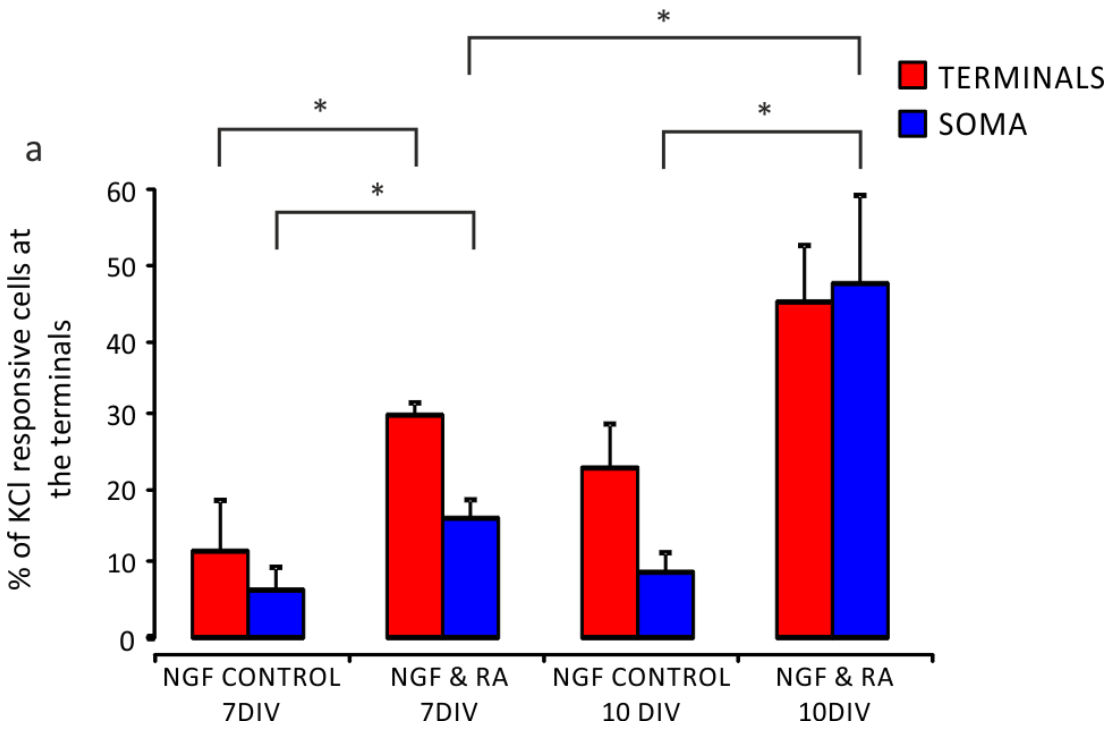

Figure 6.9.1
*Retinoic acid supplement increases TRPV1 expression at 7 and 10 DIV. (a) Quantification of capsaicin positive cells expressed as a percentage of cells responding to KCl from stimulation of the terminals. Bar graphs show percentage of TRPV1 expressing cells at 7 and 10 DIV, when stimulated on the terminals and soma, for cells cultured in control NGF medium or NGF and RA supplemented medium. (*p<0.05, unpaired t-test).*

6.10. TRPM8 expression is not affected by neurotrophin supplement at 7DIV in E14.5 mouse cultures.

TRPV1 appears to be heavily influenced by the embryonic age at which DRG dissection took place. A substantial population of neurons from E14.5 cultures initially were capsaicin sensitive, before the overall capsaicin sensitivity dramatically declined to less than 10 % of the population. Retinoic acid was shown to significantly increase the proportion of capsaicin sensitive cells at 7DIV and 10 DIV in E14.5 cultures. In addition to a capsaicin stimulus, these experiments also included stimulation with the TRPM8 receptor agonist, menthol. This enabled investigations into whether the functional expression of TRPM8 was influenced by the supplement of retinoic acid or neurotrophins.

In all experiments with different neurotrophin combinations, the percentage of menthol sensitive neurons was quantified from stimulation of the terminals and soma at 7 DIV. Menthol sensitive neurons in all experiments with different neurotrophin combinations were quantified. The pseudocolour representation of each medium condition (Figure 6.10.1a-e) suggests that menthol sensitivity does not significantly change between each medium condition. Indeed, the quantification (Figure 6.10.2a-c) demonstrates a constant level of menthol sensitivity between each medium condition. In the NT3 supplemented cultures, 16 ± 2 % and 8 ± 2 % (n_{cells} = 217, $n_{experiments}$ = 4) of neurons were menthol sensitive in the terminals and soma, and 12 ± 1 % and 8 ± 2 % (n_{cells} = 222, $n_{experiments}$ = 4) measured in the NGF control experiments (Figure 6.10.1b, Figure 6.10.2a). An NGF control accompanied each different medium condition, in those supplemented with NT3, GDNF, BDNF with and without retinoic acid, the control measured 13 ± 6 % and 7 ± 5 % (n_{cells} = 179, $n_{experiments}$ = 4), with retinoic acid measured 14 ± 3 % and 9 ± 3 % (n_{cells} = 411, $n_{experiments}$ = 10) and without retinoic acid measured 15 ± 3 % and 7 ± 2 % (n_{cells} = 281, $n_{experiments}$ = 6) in the terminals and soma respectively (Figure 6.10.1c, d and Figure 6.10.2b). In the cultures that contained only NGF and retinoic acid, unlike TRPV1, functional TRPM8 expression did not significantly change from control, with 12 ± 5 % and 9 ± 2 % (n_{cells} = 109, $n_{experiments}$ = 3) measured in the control cultures, and 17 ± 4 % and 11 ± 4 % (n_{cells} = 230, $n_{experiments}$ = 5) measured in the cultures supplemented with retinoic acid (Figure 6.10.1e and Figure 6.10.2c).

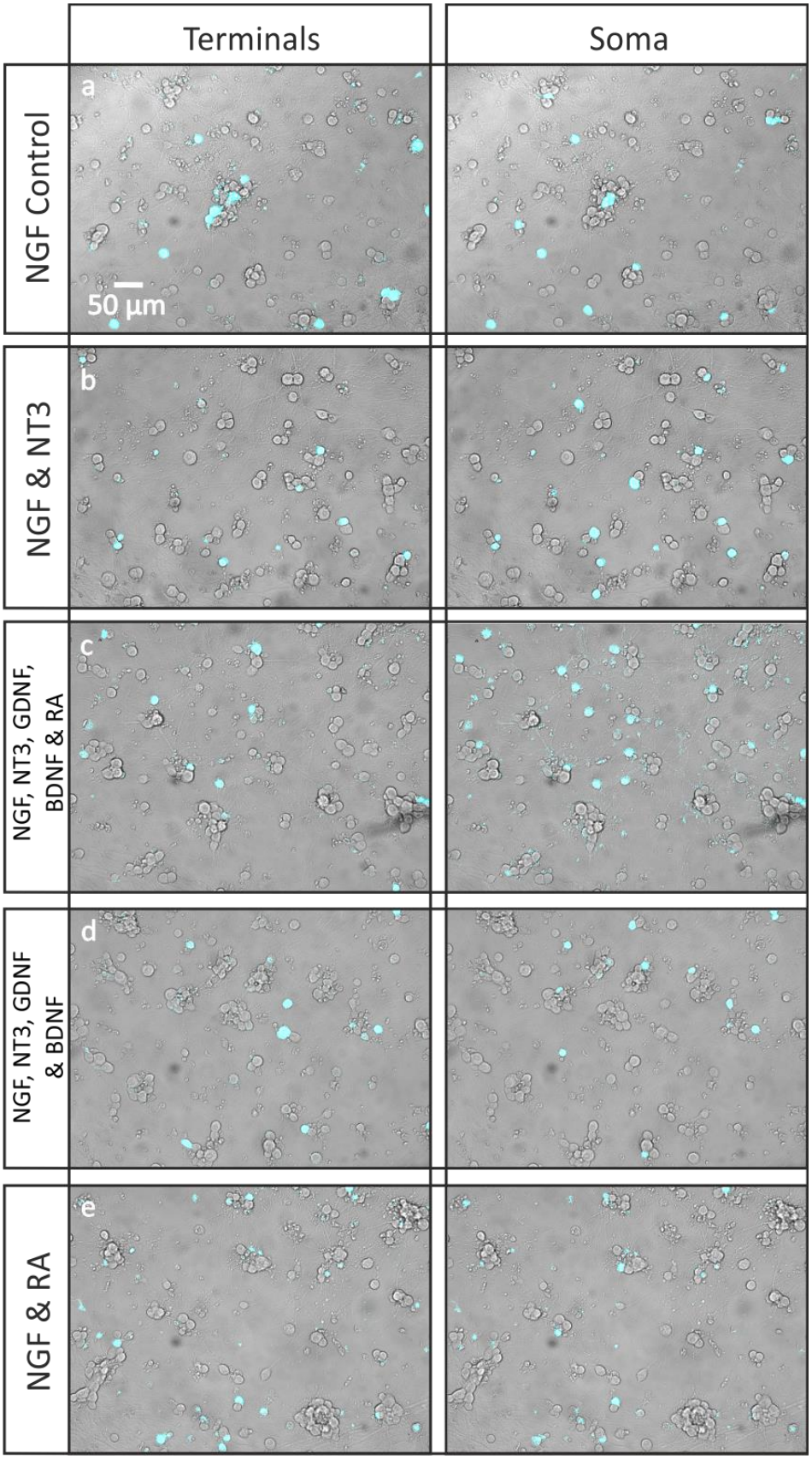

Figure 6.10.1
Menthol sensitivity on the terminals and soma is unaffected by neurotrophin supplement. (a-e) Representative pseudocolour images showing cells responding to menthol stimulation applied to the terminals and soma when cultured in (a) NGF, (b) NGF and NT3, (c) NGF, NT3, GDNF, BDNF and RA, (d) NGF, NT3, GDNF and BDNF, (e) NGF and RA.

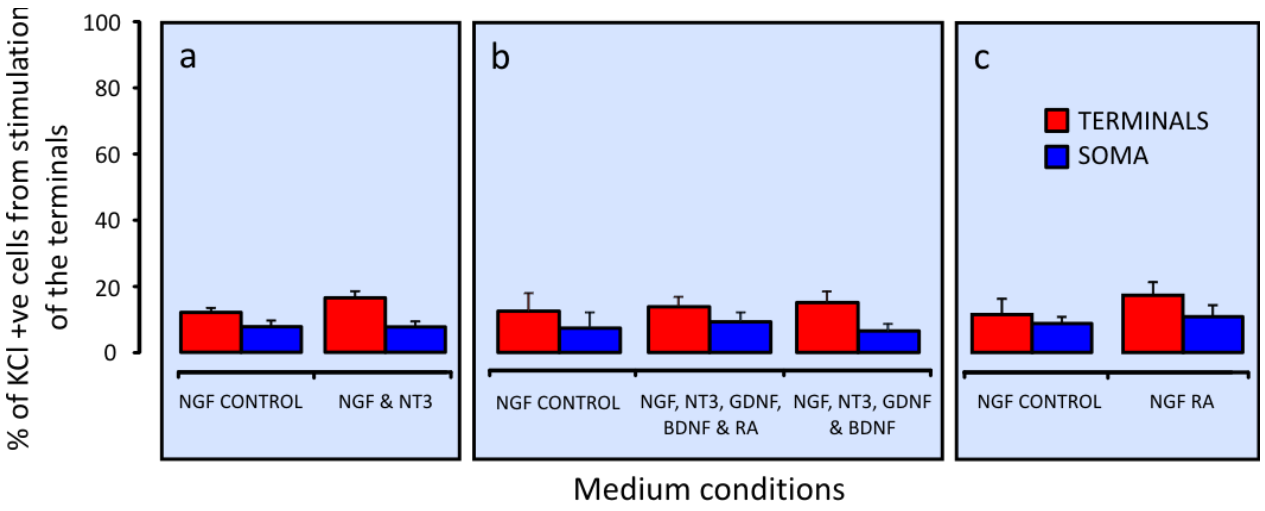

Figure 6.10.2
(a-c) Quantification of menthol sensitive neurons from stimulation of the terminals and soma in different culture conditions.

6.11. Discussion

The principle findings of these experiments are as follows. Maintenance of TRPV1 expression *in vitro* is highly dependent on the embryonic age at which the dissection takes place. These results suggest that in both rat and mouse, there is a critical developmental time point which marks the age after which TRPV1 expression is maintained in DRG neurons. If cultures are prepared from embryos before this time point, capsaicin sensitivity rapidly declines in the first 1 – 3 days *in vitro.* Supplement of retinoic acid in the culture medium can rescue the expression of TRPV1 in cultures prepared before this time point. However, the onset of menthol sensitivity is independent of embryonic dissection age, and functional expression of TRPM8 is not modulated by NT3, BDNF, GDNF or retinoic acid.

The maintenance of TRPV1 expression and regulation of capsaicin sensitivity

In the present investigations, functional expression of TRPV1 was investigated in mouse cultures prepared from E13.5, E14.5 and E15.5 embryos. At these ages *in vivo* TRPV1 expression is abundant, in fact, the maximum level of capsaicin sensitivity at any developmental time point has been reported to be E14.5 (Hjerling-Leffler et al., 2007). Therefore, the detected capsaicin sensitivity of approximately 50 % in acutely dissociated E13.5 neurons is in agreement with the reported literature. Cultures prepared from E14.5 cultures and tested acutely also displayed robust capsaicin sensitivity of approximately 60 %, which was very similar to the 64 % previously published (Hjerling-Leffler et al., 2007). However, it was surprising that the proportion of capsaicin sensitive cells rapidly declined in both E13.5 and E14.5 cultures during the first 3 days *in vitro* (summarised in Figure 6.11.1). Cultures prepared from E15.5 embryos maintained their capsaicin sensitivity throughout all time points tested (Figure 6.11.1).

Projected developmental age

Capsaicin sensitivity

	E13.5	E14.5	E15.5	E16.6	E17.5	E18.5	P0	P1	P2	P3	P4	P5	P6
E13.5	0	1	2	3	4	5	6	7	8	9	10	11	12
E14.5		0	1	2	3	4	5	6	7	8	9	10	11
E15.5			0	1	2	3	4	5	6	7	8	9	10

Figure 6.11.1
Table demonstrating the capsaicin sensitivity of cultures prepared from E13.5, E14.5 and E15.5 mouse embryos. E13.5 cultures display consistently low expression, E14.5 cultures initially display high capsaicin sensitivity which is rapidly downregulated over time in culture, and E15.5 cultures maintain the functional expression of TRPV1 throughout time in vitro.

Collectively these results suggest that the introduction of DRG neurons at E13.5 and E14.5 to culture conditions affects the functional expression of TRPV1. Developmental cues that regulate the expression of TRP channels may be lost *in vitro*, which may result in the reduction of capsaicin sensitivity observed in E13.5 and E14.5 cultures. However, a critical period occurs between E14.5 and E15.5 in the mouse, after which neurons are capable of maintaining the expression of TRPV1 when cultured only with NGF. The observation that the downregulation of TRPV1 expression was not species specific, and also occurs in E15.5 rat cultures confirms that DRG neurons in two rodent species pass through a developmental period. Before this critical time point, factors that are required for the maintenance of TRPV1 may be absent.

During mouse embryogenesis, TRPV1 expression is initially expressed in a large population of DRG neurons, peaking at E14.5, and declining to approximately 40 % at adulthood (Hjerling-Leffler et al., 2007). Until recently it was unclear whether this decline in functional capsaicin sensitivity was due to downregulation of TRPV1 or the selective death of some cells expressing the capsaicin receptor. Recently, Cavanaugh and colleagues used knock-in mice to generate a fate map if TRPV1 expressing cells. They showed that the reduction of capsaicin sensitivity was due to a downregulation of TRPV1 expression in many neurons that develop into the non-peptidergic unmyelinated nociceptors, rather than a wave of cell death occurring in late embryonic development (Cavanaugh et al., 2011a). They go on to illustrate that TRPV1 is largely restricted to the peptidergic population following the downregulation in Ret expressing cells (Cavanaugh et al., 2011a). Similarly, the loss of capsaicin sensitivity observed in E13.5 and E14.5 mouse, and E15.5 rat cultures in the experiments presented in this chapter, cannot be attributed to the death of capsaicin sensitive neurons as no loss of neurons was observed over time in culture. Therefore, neurons that are vital and respond to potassium chloride, downregulate capsaicin sensitivity over time in culture.

Despite the progressive loss of capsaicin sensitivity in E13.5 and E14.5 cultures, this may not necessarily mean that the TRPV1 protein is not expressed. An increase in the desensitisation of TRPV1 or translocation of TRPV1 from the membrane to cytoplasmic or vesicular stores may also be responsible for these results. For example, autophosphorylation of a TrkA site can activate phosphatidylinositide 3-kinase (PI3-k), inducing Src kinase mediated phosphorylation of TRPV1, leading to the translocation of cytoplasmic TRPV1 and functional insertion into the membrane (Zhang et al., 2005). It may be possible that earlier in culture, there is a decline in similar signalling pathways leading to a reduction in membrane expression of TRPV1 manifesting as a reduction in capsaicin sensitivity. Due to the role of phosporylating and dephosphorylating enzymes in regulating the sensitivity of TRPV1 it would be informative to study the levels of the TRPV1 protein expressed on the membrane and in cytoplasmic strores, to understand if the loss in capsaicin responses is due to desensitisation of the receptor, reduced translocation to the membrane or simply an overall reduction in protein expression.

These experiments do clearly show however, that NGF alone, is unable to maintain TRPV1 expression in embryonic rat and mouse DRG neurons in culture prior to a critical time point. Interestingly, NGF does modulate capsaicin sensitivity in adult DRG neurons. Only 8 % of adult rat DRG neurons grown in the absence of exogenous NGF could be excited with capsaicin, compared to 47 % when NGF was present (Winter et al., 1988). Similarly, removal of NGF from cultured DRG neurons for 7 days reduced capsaicin sensitive neurons from 48 % to 14 %. Neurons subsequently regained capsaicin sensitivity when NGF was added back into the cultures (Bevan and Winter, 1995). Inflammation upregulates NGF which has also been shown to increase capsaicin sensitivity in the rat, this increase could be abolished with an anti-NGF antibody (Nicholas et al., 1999), suggesting NGF plays an important role in regulating TRPV1 expression during inflammation. Clearly, NGF has an important function in TRPV1 regulation in the adult, yet in the results presented here it is unable to influence TRPV1 expression in E13.5 and E14.5 mouse, and E15.5 rat cultures. The role of adult NGF signalling is therefore clearly different to that in the embryo; NGF is a potent inflammatory agent that can also maintain TRPV1 expression in the adult, whereas embryonically, it is essential for the survival of many DRG neurons.

The embryonic dependence on NGF goes through an important transition in the mouse which coincides with some of the embryonic ages tested in these experiments. At E12, the survival of most mouse DRG neurons is dependent on NGF signalling through both TrkA and $p75^{NTR}$, demonstrated by the 70 % loss of neurons if the expression of $p75^{NTR}$ is downregulated by an antisense oligonucleotide directed against the low-affinity neurotrophin receptor (Barrett and Bartlett, 1994). However, the dependence on $p75^{NTR}$ signalling rapidly diminishes, whereby at E19, less than 10 % of neurons are lost if $p75^{NTR}$ signalling is inhibited. This finding suggests that early on in embryogenesis, both TrkA and $p75^{NTR}$ are required for survival, yet $p75^{NTR}$ signalling becomes superfluous for survival in later embryonic periods, and TrkA signalling alone can maintain neuronal survival (Barrett and Bartlett, 1994). This change in signalling may influence TRPV1 expression if embryos are dissected through this transition period. Earlier dissection at a time when both receptors are required for survival may indicate that throughout the *in vitro* culture, dual TrkA and $p75^{NTR}$ signalling is dedicated to promoting survival, rather than regulating the expression of TRPV1. However, at E15.5, considerably less neurons depend on the dual signalling by TrkA and $p75^{NTR}$ for survival, the 'uncoupling' of these neurotrophic receptors may enable NGF signalling to promote both survival and maintain the functional expression of TRPV1.

In conclusion, it is difficult at the present moment to definitively pinpoint a specific mechanism responsible for the downregulation of capsaicin sensitivity observed both in embryonic mouse and rat cultures. This interesting observation, may result from an increase in desensitisation of the capsaicin receptor or simply a reduction in the TRPV1 protein. The loss of dependence on $p75^{NTR}$ signalling seems to coincide with the embryonic ages at which capsaicin sensitivity is not maintained *in vitro*. Therefore, TRPV1 expression could be influenced by the interaction between TrkA and $p75^{NTR}$.

NT3 signalling and capsaicin sensitivity

NGF signalling alone is insufficient to maintain functional expression of TRPV1 in E13.5 and E14.5 embryonic mouse DRG neurons *in vitro*. Therefore, to examine if neurotrophin signalling through other Trk receptors influenced capsaicin sensitivity, NT3 was added to the culture medium of E14.5 cultures. During DRG embryogenesis, neurons expressing TrkB and TrkC are born in a separate and earlier wave to TrkA expressing neurons (Frank and Sanes, 1991) and by late embryonic ages are essentially expressed in non-overlapping populations in the trigeminal ganglia (Huang et al., 1999). Interestingly, knockout of NT3 results in a 50 % loss of TrkA positive neurons between E12.5 and E13.5 in the mouse trigeminal ganglia, therefore suggesting NT3 directly supports the survival of some TrkA expressing neurons (Huang et al., 1999). Deficits in TrkA expressing neurons are not observed in TrkC mutants (Piñon et al., 1996) indicating NT3 can activate the TrkA receptor to mediate survival. Furthermore, findings have indicated that virtually all neuronal precursors and early postmitotic neurons express TrkC, and therefore may require NT3/TrkC signalling for survival during the period when neurogenesis is most active (E10.5 – E12.5) (White et al., 1996). Whilst many cells express TrkA at E11.5, there is little dependence on TrkA signalling at this time point, whereas by E13.5, axons of TrkA expressing neurons are beginning to innervate NGF rich areas, and this coincides with a downregulation of TrkC in all but the large proprioceptive neurons (White et al., 1996). Therefore whilst TRPV1 is expressed in TrkA lineage neurons, at E13.5 a dependence on NT3 may still be crucial for the survival of many sensory neurons. Hence, E13.5 and E14.5 cultures supplemented only with NGF may select only for the DRGs that have fully transitioned from NT3 to NGF dependence, which may exclude a population of capsaicin sensitive neurons, accounting for the very low functional expression of TRPV1. A wave of *in vitro* cell death is not observed that coincides with the reduction in functional capsaicin sensitivity, suggesting neurons downregulate TRPV1 expression. A residual dependence on NT3 may therefore remain at E13.5 and E14.5 in the mouse, which may signal through TrkA to regulate TRPV1 expression. At E15.5, apart from proprioceptive neurons, cells are independent of NT3 signalling, which may then allow the stable expression of TRPV1 over time *in vitro*. NT3 was therefore investigated in the microfluidic chambers as a potential regulator of TRPV1 expression in E14.5 mouse DRG neurons. However, no increase in functional capsaicin sensitivity was observed in cultures supplemented with NT3, suggesting that at least in E14.5 mouse cultures NT3 signalling through TrkA or TrkC does not play a role in maintaining the functional expression of TRPV1.

Retinoic acid is a factor that can increase capsaicin sensitivity in vitro

In light of this result, an approach was designed to supplement E14.5 mouse DRG neurons with a range of neurotrophins including NGF, NT3, GDNF, BDNF and retinoic acid to replicate a differentiation medium that has been used for E11 DRG culture (Hjerling-Leffler et al., 2007). This differentiation medium was used in studies that were investigating boundary cap derived sensory neurons. Boundary cap cells of the dorsal root entry zone (DREZ) appear in the mouse at E10.5

(Topilko et al., 1994), yet unlike DRG progenitor cells, continue to proliferate throughout embryogenesis. 5 % of DRG neurons are derived from boundary cap cells that migrate into the DRG at E11.5 and continue to generate sensory neurons up to E13 (Hjerling-Leffler et al., 2005). These neurons constitute a late, third wave of neurogenesis. When cultured in differentiation medium, boundary cap derived sensory neurons form heterogenous subpopulations some of which display cold, capsaicin and/or mechanical sensitivity, suggesting thermoreceptors, nociceptors and mechanoreceptors are born from boundary cap derived stem cells (Hjerling-Leffler et al., 2005). The development of capsaicin sensitivity and the continued generation of neurons up to E13 in boundary cap derived neurons may consequently influence total DRG capsaicin sensitivity. Therefore two culture conditions were investigated, in the first, NGF, NT3, BDNF and GDNF was added, and in the second, NGF, NT3, BDNF GDNF and retinoic acid was added. Interestingly, the latter condition containing retinoic acid significantly increased capsaicin sensitivity in both the terminals and soma (Figure 6.8.1). The functional increase in TRPV1 expression was only observed in cultures which contained retinoic acid, and despite the extra supplement of NGF, NT3, BDNF and GDNF in the first culture condition, there were no more capsaicin sensitive cells than in cultures supplemented only with NGF. In agreement with earlier studies (Corcoran et al., 2000) no difference in the number of surviving neurons in cultures with and without retinoic acid were observed suggesting retinoic acid is mediating functional TRPV1 expression rather than the selective survival of neuronal subpopulations.

Retinoic acid is a metabolic product of vitamin A (retinol). Retinol is taken up by cells and emzymatically metabolised to retinoic acid. In the nucleus retinoic acid binds to a transcription complex, either retinoic acid receptors (RARs) or retinoid X receptors (RXRs) (Maden, 2007). The ligand receptor complex can then bind to a sequence of DNA known as the retinoic acid-response element (RARE), which activates the transcription of the target gene (Maden, 2007). In the central nervous system, retinoic acid appears to have a profound influence on the differentiation of stem cells. For example, retinoic acid enhanced the response to neurotrophic factors in cultured hippocampal derived stem cells mediated by maintaining or increasing the levels of TrkA, B, C and $p75^{NTR}$ mRNA (Takahashi et al., 1999). Similarly, retinoic acid treatment of sympathetic chick neurons increased the expression of TrkA mRNA and protein (von Holst et al., 1995). Therefore to determine if retinoic acid acts synergistically with either NT3, BDNF and/or GDNF to regulate TRPV1 functional expression, cultures were prepared which only contained NGF and retinoic acid (Figure 6.9.1). Interestingly, at 7 DIV capsaicin sensitivity remained greater in cultures containing NGF and retinoic acid compared to cultures only containing NGF, suggesting NT3, BDNF and GDNF are redundant for the induction of retinoic acid induced-increases in capsaicin sensitivity. Furthermore, capsaicin sensitivity was further increased in the soma at 10 DIV compared to the same culture condition at 7 DIV. This suggests retinoic acid may induce a cumulative effect on functional TRPV1 expression, meaning capsaicin sensitivity increases with exposure time to retinoic acid.

The increase in retinoic acid induced capsaicin sensitivity may be due to a direct effect on TRPV1, or alternatively, a synergistic effect with NGF. NGF is essential for the survival of embryonic

DRGs, meaning in these experiments, retinoic acid alone could not be tested in embryonic cultures. A study by El Andaloussi-Lilja and colleagues has studied TRPV1 expression during retinoic acid-induced neuronal differentiation. The differentiation of TRPV1 expressing neuroblastoma cells into a neuronal phenotype using retinoic acid resulted in a large upregulation of total and cell surface TRPV1 expression compared to cells cultured without retinoic acid (El Andaloussi-Lilja et al., 2009). They demonstrated the upregulated TRPV1 protein was localised both to the cell body and developing neurites, resulting in an increase in the capsaicin-induced calcium influx in the soma. Interestingly, this study also revealed, that similar to my functional experiments (Figure 6.9.1), an increase in TRPV1 protein levels was observed with prolonged exposure to retinoic acid (El Andaloussi-Lilja et al., 2009).

How retinoic acid induces the upregulation of capsaicin sensitivity is presently unknown. In 2002, Balmer and Blomhoff screened over 500 genes that according to the literature at the time were suggested to be regulated by retinoids. They determined whether each gene was likely to be directly or indirectly regulated by retinoic acid by analysing the presence of a RARE sequence (Balmer and Blomhoff, 2002). The TRPV1 gene was not included in the screening because at the time it was not suggested to be regulated by retinoic acid. However, the genes encoding $p75^{NTR}$, TrkA, TrkB, TrkC and Ret are all directly upregulated or induced by retinoic acid (Balmer and Blomhoff, 2002). The sheer number of genes that are positively regulated by retinoic acid make it difficult to ascertain the exact mechanism of how capsaicin sensitivity is upregulated. It is possible that whilst the *in vitro* concentrations of NGF are well above physiological levels the membrane expression and therefore the availability of the TrkA receptor may limit NGF signalling. It may be possible that in earlier embryonic cultures that are supplemented only with NGF, the membrane expression of TrkA is sufficient for survival yet insufficient to mediate robust TRPV1 expression. Retinoic acid may increase the expression of both TrkA and $p75^{NTR}$ in the DRG; coexpression of which greatly increases the affinity of TrkA for NGF thereby increasing the selectivity of NGF (Hempstead et al., 1991; Barker and Shooter, 1994). The intimate link between NGF signalling and capsaicin sensitivity has been well documented; *in vitro,* NGF potentiates the responses of DRG neurons to capsaicin (Shu and Mendell, 1999), and *in vivo,* knock out of TRPV1 attenuates NGF-induced thermal hypersensitivity (Chuang et al., 2001). Therefore, increased TrkA signalling promoted by heightened expression of TrkA and $p75^{NTR}$ may maintain or even upregulate TRPV1 expression during time *in vitro*. Furthermore co-immunoprecipitation studies have suggested TRPV1 can associate with TrkA and PLC-γ to form a protein complex (Chuang et al., 2001). In *Xenopus* oocytes that heterologously coexpressed both TrkA and TRPV1, NGF produced almost a 30-fold increase in proton-evoked currents through TRPV1 (Chuang et al., 2001). Therefore, TRPV1 appears to be potentiated when expressed with TrkA by an NGF mediated phosphorylation cascade that involves PLC-γ. Consequently, retinoic acid-induced upregulation of TrkA expression may lead not only to increased expression of TRPV1 but also a sensitisation of the capsaicin receptor.

Collectively, retinoic acid induces a significant increase in capsaicin sensitivity in E14.5 cultures at 7 and 10 DIV through a NT3, BDNF and GDNF-independent mechanism. It seems likely that TRPV1 is either upregulated or sensitised by one or several of the many genes modulated by retinoic acid. Specifically, both TrkA and $p75^{NTR}$ have been reported to be directed upregulated by retinoic acid, and NGF signalling is known to increase capsaicin responses. Finally, TrkA can directly associate with TRPV1 to modulate its activity, increased expression of both TrkA and TRPV1 by retinoic acid mediated transcription may lead to an increase in complex formation which can sensitise the channel to capsaicin induced activation.

The onset of menthol sensitivity begins in culture and is unaffected by additional neurotrophin supplement

In terms of functional TRPM8 expression, a striking finding of these studies was that at all embryonic ages tested in the mouse (E13.5, E14.5 and E15.5) DRG neurons early in culture were entirely menthol insensitive yet developed sensitivity during time in culture. This finding suggests that the onset of functional TRPM8 expression proceeds *in vitro* regardless of the embryonic dissection age, meaning that unlike capsaicin sensitivity, developmental cues are present in culture conditions that are required to initiate the functional expression of TRPM8. Furthermore, the supplement of the culture medium with a range of neurotrophins or retinoic acid did not influence menthol sensitivity. This stands in stark contrast to the *in vitro* capsaicin sensitivity which is highly dependent on embryonic age of dissection and can be induced with the addition of retinoic acid.

One similarity of TRPM8 expression with TRPV1 expression remains, the peripheral terminals show a greater sensitivity to menthol than the cell soma. Therefore, mechanisms may be in place to transport the synthesised protein out of the soma to the peripheral axons and terminals and/or machinery to translate TRPM8 mRNA is present in peripheral regions. An important finding of this study is there is a high functional co-expression of TRPM8 and TRPV1 in both the terminals and soma. 85 % of menthol sensitive soma at 7 DIV were also activated by capsaicin, which is in strong agreement with previous reports, Hjerling-Leffler and colleagues reported that 93 % and 86 % of menthol sensitive neurons at E18.5 and P0, respectively, were functionally activated by capsaicin (Hjerling-Leffler et al., 2007). The same study demonstrated that the percentage of overlap between menthol and capsaicin sensitive neurons decreased in early post-natal development to reach less than 60 % in the adult. If days *in vitro* (DIV) are related to the *in vivo* age, mouse embryos dissected at E15.5 and cultured for 7 DIV would correspond to P3, therefore the 85 % functional overlap measured in my experiments at this time point, is almost identical to the 86 % observed in acutely dissociated P0 neurons (Hjerling-Leffler et al., 2007). Furthermore, in terms of functional TRPM8 and TRPV1 coexpression, mice and rats appear to be very similar; 60 % of menthol sensitive DRG neurons harvested from P7 mouse pups express TRPV1 (Hjerling-Leffler et al., 2007), which is comparable to the 55 % of menthol sensitive trigeminal ganglia neurons from newborn rats that are also sensitive to capsaicin (McKemy et al., 2002). Therefore, the data reported in this chapter is in good agreement

with previous published reports and demonstrates a high functional coexpression of TRPM8 and TRPV1 in cultured DRG neurons and supports the concept that there is a substantial overlap in menthol and capsaicin sensitivity. Therefore, the high coexpression with TRPV1 at the onset of TRPM8 sensitivity suggests TRPM8 expressing neurons develop from a population of TRPV1 positive neurons.

The onset of menthol sensitivity in E13.5, E14.5 and E15.5 cultures occurs between 4 – 5 DIV. Therefore, the projected developmental age at which menthol sensitivity is first detected corresponds to between E18.5 and P0. This is in strong agreement with published literature which report that TRPM8 mRNA is first detected at E16.5 at low levels, followed by a large increase at E18.5 and P0, which corresponds to the first detectable functional responses at E18.5 (Hjerling-Leffler et al., 2007). A more recent study has investigated the differential onset of TRPM8 expression in lumbar and thoracic mouse DRGs; lumbar DRGs were negative for TRPM8 mRNA at E14, yet displayed high levels at E18 (Staaf et al., 2010). Thoracic DRGs displayed a slightly later and more gradual onset of TRPM8 mRNA expression, which could be first detected at P0 (Staaf et al., 2010). Therefore, due to the dissection of DRGs at all spinal levels, the onset of menthol sensitivity reported here agrees with these published figures.

The present functional data suggest that TRPM8 expression begins at the projected ages of E18.5 to P0 in TRPV1-positive neurons. Hjerling-Leffler and colleagues found menthol sensitivity to be entirely absent from the IB4 positive, nonpeptidergic population (Hjerling-Leffler et al., 2007). In a Wnt1-cre mediated knockout of Ret, TRPM8 expression was unaffected, whereas TRPA1 expression was completely absent (Luo et al., 2007), suggesting TRPM8 is not dependent on GDNF signalling through Ret for expression. Conversely, the expression of TRPM8 was abolished when Runx1 was knocked out by Wnt1-cre mediated recombination in embryonic, post-natal and adult mice (Chen et al., 2006). The early expression of Runx1 in TrkA lineage neurons is crucial for the expression of many ion channels and receptors in thermoreceptive and nociceptive neurons which can explain the absence of TRPM8 in Runx1 conditional knockout mice. The independence on Ret signalling suggest menthol sensitive neurons remain reliant on NGF signalling through TrkA. The results presented here confirm that NGF signalling alone is sufficient as a development cue to induce TRPM8 functional expression *in vitro*. Supplement of culture medium with retinoic acid had no effect on TRPM8 expression as it did with TRPV1 nor did NT3, GDNF or BDNF upregulate menthol sensitivity. Furthermore, the onset of menthol sensitivity several days after dissection suggests the expression of TRPM8 is not interrupted by the dissection and culturing process and that in terms of menthol sensitivity, DRG neurons continue to develop as they would *in vivo*.

Mustard oil sensitivity develops in vitro in capsaicin sensitive neurons

Functional expression of TRPA1 was only detected in E15.5 cultures at 10 DIV. Again, if the projected developmental age is calculated, 10 DIV would correspond to P6. Hjerling-Leffler and colleagues first detected very low levels of TRPA1 mRNA at P0 which quadrupled by P7, this

coincided with the first consistent functional responses to cinnamaldehyde (a TRPA1 agonist) at P7 (Hjerling-Leffler et al., 2007). Therefore, the onset of functional TRPA1 expression in the experiments presented in this chapter are in agreement with the published observations. An interesting result was that mustard oil sensitivity was only detected in peripheral neuronal regions, with the soma completely insensitive at all ages and days tested, suggesting that the mustard oil receptor may be preferentially transported to the periphery.

Cinnamaldehyde sensitivity develops to a greater extent in the IB4 positive populations, reaching approximately 25 % of the nonpeptidergic population in the adult (Hjerling-Leffler et al., 2007). This is consistent with the absence of TRPA1 mRNA in a Ret conditional knockout, which is crucial for the development of GDNF dependent, IB4 positive neurons (Luo et al., 2007). However a small group of cells do develop cinnamaldehyde sensitivity in the non-IB4 positive population (Hjerling-Leffler et al., 2007), suggesting NGF may be able to induce TRPA1 expression in a small subset of Ret independent, NGF dependent neurons. Therefore the limited expression observed in my cultures containing only NGF may reflect the small population in which TRPA1 can be induced by NGF signalling. No functional overlap of TRPA1 with TRPM8 expression was observed in E15.5 cultures at 10 DIV suggesting these channels are expressed by different subpopulations. A complete overlap in capsaicin sensitivity was however observed in mustard oil sensitive cells, suggesting TRPA1 expression begins in TRPV1 expressing cells. In agreement, in situ hybridisation studies have shown all neurons expressing TRPA1 mRNA also express TRPV1 in the adult rat (Kobayashi et al., 2005).

Collectively, the experiments discussed in this chapter suggest that age of embryonic dissection and neurotrophin supplement can greatly influence TRPV1 channel expression. TRPV1 expression has been demonstrated to be highly dependent on dissection age, and retinoic acid was able to upregulate capsaicin sensitivity. Onset of menthol sensitivity was detected in E13.5, E14.5 and E15.5 embryonic cultures at 4 to 5 DIV, corresponding to approximately E18.5 to P0. The projected age of onset was in agreement with reported literature, and NGF alone was sufficient to induce TRPM8 expression.

Chapter 7:

Discussion

In terms of size, neurons are the largest cell in the mammalian body. The somata measures in the range of tens of micrometres, which is comparable to most other cells. However, some neurons, such as motor and sensory subtypes, can extend an axon over a large distance to innervate specific targets, in the human this distance can be over 1 metre in length. The innervation of peripheral targets that are often a considerable distance from the cell soma makes the study of these peripheral neuronal regions critical to understanding the neuron in its entirety. Compartmentalised chambers are highly compatible for the *in vitro* study of receptive terminals, however until fairly recently the technology to produce high quality, compartmentalised chambers at micrometre precision has not been available. The description of using soft lithography by Park and colleagues in 2006 has overcome previous limitations to produce leak-free, fluidically isolating microfluidic chambers. This thesis is the first description of using these chambers in combination with functional calcium imaging to investigate the properties of peripheral DRG terminals *in vitro* and compare these with the cell somata.

7.1. Initial investigations

As this was a novel combination of technologies, initial proof of concept experiments were undertaken which constitute some of the results in chapter 3. This included determining the flow rate across the microgrooves, correlating retrograde tracing with functional responses, determining the effect of consecutive stimulation and pharmacologically characterising the evoked-action potential. The initial Nature Protocols paper describing the fabrication of the microfluidic chambers suggests that a 30 µl volume difference across the microgroove barrier will take more than 24 hours to equilibrate (Park et al., 2006). I have extended these findings by thoroughly investigating the flow rate in 3 different volume conditions over a 96 hour period. I have found that a volume difference of 40 µl takes greater than 72 hours to equilibrate, essentially providing an entirely fluidically isolated environment in the compartment with the greater volume for this time period. This was important to ascertain for two reasons. Firstly, the NGF chemo-attraction protocol relies on a volume and concentration difference to encourage the growth of the neurites into the adjacent compartment. Therefore, knowing the flow rate was vital to maintaining a volume and concentration difference and establishing the medium change protocol. Consequently, the large majority of DRG neurons seeded into the compartmentalised cultures successfully grew neuronal processes through the microgroove array. Secondly, during the imaging experiments it was absolutely vital to establish a fluidically isolated environment for the compartment undergoing stimulation. This was to ensure any calcium response recorded from the somata was not evoked by the diffusion of stimulants through the microgroove array. The isolation up to 72 hours with a 40 µl volume difference ensured that during the course of all imaging experiments lasting approximately 1 – 2 hours, the stimulated compartment was entirely isolated.

7.2. Neuronal polarity and axonal regrowth *in vitro*

Neuronal morphology and function fundamentally relies on the correct orientation of axons and dendrites. These structures can be differentiated by their composition of proteins and organelles; axons are typically long and thin, with a uniform width. Dendrites are usually shorter, and often appear thick upon emerging from the cell soma, before tapering with distance (Arimura and Kaibuchi, 2007). Axons contain the synaptic machinery required for neurotransmitter release, whereas dendrites typically contain neurotransmitter receptors, this organisation allows neurons to receive and transmit electrical signals.

Formation of a functional neuron involves the polarisation of distinct regions which is crucial in the selection of a single neurite to form the axon and all other neurites becoming dendrites. Cell polarity is determined by the cytoskeleton, which organises in such a way to polarise the cell interior whilst maintaining the structural scaffold of the cell. During this process, one of the minor neurites rapidly elongates to form the axon, which is predominantly brought about by stabilisation of the microtubules in the shaft of the future axon, and enlargement of the growth cone in that neurite (Stiess and Bradke, 2011). In contrast, the microtubules in minor neurites are not stabilised, and dynamic microtubules are blocked from entering the growth cone, meaning these processes do not elongate, and will eventually develop into dendrites (Stiess and Bradke, 2011). The formation of the asymmetrical axon and dendrites *in vivo* is unlikely to be a random process, since the trajectory of both axon and dendrites is directed toward their targets (Adler et al., 2006). For example, DRG neurons initially develop a bipolar morphology, with one neurite projecting toward the periphery and the second growing toward the spinal cord (Jackman and Fitzgerald, 2000). Slightly later in development, at approximately E14-E15 in the mouse, the base of these two projections fuse, forming a single pseudounipolar axon, with a peripherally projecting dendritic structure, and an axon-like projection into the spinal cord. Therefore, the *in vivo* development of DRG neurons relies on neuronal polarisation to determine the functionally distinct axon and dendrite branches.

During *in vivo* development the cell detects a number of biological inputs which affect neurite outgrowth; however, when neurons are maintained in culture they still proceed through a similar developmental process resulting in the establishment of a polarised cell and the formation of an electrically excitable axon and dendrites. Hippocampal neurons have predominantly been used to study polarisation of cultured cells, which have been shown to pass through 5 stages. In stage 1, filopodia are formed shortly after plating the cells *in vitro*, which after several hours form minor, immature processes during stage 2. After approximately 12 hours in culture, stage 3 is characterised by the elongation of a single neurite which will become the axon. During stage 4, both this axon and the dendrites mature over the next week in culture. Finally in stage 5, all neurites become electrically and synaptically functional (Dotti et al., 1988).

Despite the similarities in the development of polarisation *in vivo* and in cultured cells, there are obviously distinct differences arising from environmental influences. Cultured cells are maintained in an artificial environment comprising of a flat substrate that is usually rich in laminin, and are generally cultured as a homogeneous population. Neurons *in vivo* however, are completely surrounded by a heterogeneous population of cells which they have extensive contact with. The cues released from neighbouring cells in this 3-dimensional matrix can have profound positional influences during differentiation and development, which is likely to impact on which neurite is selected to become the axon (Zolessi et al., 2006). Indeed, retinal ganglion cells *in vitro* are round and during initial stages of differentiation extend filopodia at all points around its surface, these go on to develop into short neurites before one of them elongates in an axon-like manner. In contrast, retinal ganglion cells *in vivo* first extend from the apical to basal surface assuming a spindle shape, and filopodial activity is only seen at the basal surface (Zolessi et al., 2006). Despite these differences, the commonality of *in vitro* and *in vivo* polarisation is the breaking of symmetry, which eventually leads to the formation of the molecularly and morphologically distinct axon and dendrite (Arimura and Kaibuchi, 2007).

The use of microfluidic chambers to study the properties of peripheral neurites depends entirely on the growth of these neurites through the microgroove array into the adjacent compartment. Therefore these neurons must undergo polarisation in order to grow an axon and dendrites. The axon and dendrites of hippocampal neurons can be detected *in vitro* using tau1 (an axon marker) and MAP2 (a dendrite marker), also the axon is usually easily recognised based on its length and speed of growth. For example, using the same microfluidic design as that used in this thesis, Taylor and colleagues demonstrate that a microgroove distance of 450 µm resulted in no detectable MAP2 positive dendrites in the adjacent compartment of hippocampal cultures. Only tau1 positive axons were able to grow this full distance through the microgroove array (Taylor et al., 2005). However, in DRG neurons, all neurites are positive for tau1 and MAP2, and due to their unusual characteristic that *in vivo* the dendrite can often be longer than the axon, length of the neurite cannot be used to distinguish between these structures when in culture. Experiments have not been carried out to trace individual neurites from single DRG cell bodies cultured in the microfluidic chambers, therefore it is not possible to definitively say whether the projecting neurites in the adjacent compartment are axons, dendrites or a combination of both. It is also not possible to know how many neurites from each cell somata grow through the microgroove array. As neurons in culture grow multiple dendrites and these can characteristically be very long in DRG neurons, it is possible that each somata has multiple projecting neurites in this system. Therefore, in terms of the interpretation in this thesis, I have observed a difference in sensitivity between the peripheral neurite and the soma when testing with algogenic compounds such as acid and capsaicin. These peripheral neurites could be an axon, dendrite or a mixture of both. Therefore the characteristics observed in these neurites *in vitro* cannot directly be correlated to the peripheral terminal of the dendritic branch, or the central terminal of the axonal branch as they are orientated *in vivo*.

Furthermore, the distribution of the receptor proteins may also influence the interpretation of the results observed in the compartmentalised chambers. TRPV1 for example is not only expressed at the peripheral dendritic terminal *in vivo*, but is also highly localised in the central axonal terminals of the primary afferent (Pabbidi et al., 2008). This is particularly evidenced by the ablation of TRPV1 positive central nerve terminals by intrathecal injection of capsaicin or RTX, which has been shown to profoundly reduce inflammation-induced thermal hypersensitivity (Jeffry et al., 2009). Therefore, both the axonal and dendritic terminals are capsaicin sensitive *in vivo* and it is assumed that these characteristics would be preserved *in vitro*, as such, the compartmentalised chambers may model both peripheral and central terminals. The question then arises that if a soma has multiple neurites (consisting of a capsaicin sensitive axon and several capsaicin sensitive dendrites) this may increase the probability of detecting a functional response to peripheral stimulation with capsaicin. Despite the possibility that there may be several projecting neurites from a single cell soma, the fact remains that these as a group still display different sensitivity profiles when compared to the cell body. This is most evident when acidic stimuli is used, which results in a far greater activation of cells when applied to the terminals compared to the cell body. Whether these terminals are dendritic, axonal or a combination of both remains to be answered. Many mouse lines are now available in which specific subpopulations of somatosensory neurons are fluorescently labelled. Preparation of DRG cultures from such a mouse would firstly enable the analysis of how many neurites from a single cell body project through the microgroove array, and secondly, detailed microscopy over time *in vitro* could allow the identification of the axon as opposed to the dendrites as the cell polarises and the neurites begin to emerge. Patch clamp recordings of single neurites from cells cultured in the compartmentalised chambers would enable the electrophysiological characterisation of the axon and dendrites helping to understand how their properties are influenced by *in vitro* culture. Therefore, with slight modifications microfluidic chambers hold great potential to investigate neuronal polarisation and the individual characteristics of the axon and dendrites of sensory primary afferents.

7.3. Pharmacological investigations of DRG neurons *in vitro* using microfluidic chambers

The successful culture and compartmentalisation of DRG neurons *in vitro* allowed functional investigations to begin. A major objective early on in my PhD project was to establish that the somal calcium response evoked by peripheral stimulation was due to action potential propagation. The radiochemistry experiments proved that the stimulation compartment was fluidically isolated from all other compartments during the entire imaging experiment. The use of the VGSC blockers, TTX and lidocaine, confirmed the somal calcium influx relied upon action potential propagation from the periphery that was dependent upon sodium channels. Therefore, this *in vitro* preparation allowed for further pharmacological investigations of action potential propagation.

Much of the *in vitro* research into the expression of ion channels in DRG neurons has focused on the cell soma. Previous reports demonstrate that both TTX-s and TTX-r channels are expressed at the cell soma in a sufficient density to generate action potentials (Villière and McLachlan, 1996), however the expression of TTX-r subtypes in peripheral regions has been complicated by the use of different species, TTX concentrations, and the nerve region that has been investigated. For example, C-fibre compound action potential was unaffected by 100 µM TTX in an *ex vivo* preparation of the frog tibial nerve whilst Aβ- and Aδ-fibres were almost entirely blocked (Kobayashi et al., 1993). In a spinal cord and DRG *in vitro* slice preparation, 0.5 µM TTX failed to block the synaptic excitatory depolarisation of dorsal horn neurons induced by potassium stimulation of the sensory terminals (Jeftinija, 1994). Furthermore, in biopsied human sural nerves, 1-100 µM TTX addition to the bathing solution led to a complete abolition of conduction in Aβ and Aδ fibres, whereas approximately 50 % of the C-fibre action potential was resistant to TTX (Quasthoff et al., 1995). In apparent contradiction to these studies, *in vitro* experiments on a mouse peripheral nerve suggest that in all neurons, including those with a hump on the falling phase of the action potential (characteristic of C-fibre action potentials (Harper and Lawson, 1985)) impulse conduction is inhibited with 1 µM TTX application to the axon (Yoshida and Matsuda, 1979). Studies using the rat sciatic nerve have similarly shown that action potential propagation evoked by stimulation of the peripheral nerve was blocked by 0.3 or 1 µM TTX (Villière and McLachlan, 1996).

To investigate the effect that TTX has on action potential propagation in cultured DRG neurons, the 3 compartment chamber was used. Prior to these studies it has been difficult to assess the functional expression of VGSCs in peripheral regions of cultured DRG neurons. I have shown that in approximately 20 % of the total population, TTX-r channels are expressed at a sufficient density in the axon to allow action potential propagation to continue in the presence of 1 µM TTX . In regards to the current literature it is difficult to directly compare these findings as most other *in vitro* recordings were performed in dissected nerve preparations and not on cultured neurons. However, the presence of a population that continue to propagate in the presence of TTX, as measured in the compartmentalised chambers suggests that these neurons are actively expressing TTX-r VGSCs. Recordings from cultured DRG neurons derived from $Na_v1.8$ knockout mice show a reduced action potential peak amplitude, slowed rate of depolarisation and a failure to respond after repetitive stimulation (Renganathan et al., 2001). This therefore suggests that at least in acutely dissociated DRG somata the TTX-r, $Na_v1.8$ channel plays an important role in generating and maintaining action potential propagation in a subset of C-fibre DRG neurons. The expression of $Na_v1.8$ in the cell somata means that upon axonal regrowth, as is promoted in the microfluidic chambers, the channel is also likely to be expressed in the peripheral axon and terminals of these neurons. Using electron microscopy, Coggeshall and colleagues have demonstrated that $Na_v1.8$ is ordinarily expressed in the axon of both unmyelinated and myelinated neurons (Coggeshall et al., 2004). Other than $Na_v1.8$, $Na_v1.9$ is also TTX-r that is expressed in sensory neurons. The primary role of this VGSC is thought to be involved with modulating resting membrane potential (Herzog et al., 2001). Therefore it is

probable that the TTX-r current responsible for depolarising the cell somata is due to sodium conductance through $Na_v1.8$.

A consideration for these experiments is the influence of culture conditions that may affect the expression of proteins including sodium channels. Perhaps the main issue of the culture conditions is the addition of NGF to the culture medium. NGF is an established mediator of inflammatory pain (McMahon, 1996) and has been suggested to directly sensitise the peripheral terminals of nociceptive neurons and modify gene expression during inflammatory conditions (Woolf, 1996). The requirement of embryonic DRG neurons on NGF therefore may pose a problem, absence from the culture medium will result in the death of many neurons due to the embryonic dependence on neurotrophin signalling, whilst its presence may alter the phenotype of the neurons into a more sensitised state. However, a study by Bevan and Winter in 1995 investigated the effects of NGF on cultured DRG neurons. They demonstrated that the chemosensitivity of adult DRG neurons, in response to capsaicin, protons, GABA and ATP, was not increased by the addition of 200 ng/ml NGF (the same concentration that was used throughout this PhD project) (Bevan and Winter, 1995). Interestingly, transcriptome analysis of pure axonal mRNA from embryonic DRG axons did not contain any of the inflammatory genes that were contained in adult axons after both were cultured in NGF supplemented medium (Gumy et al., 2011). This suggests that *in vitro* embryonic cultures that have been in culture for 4 days, do not represent a model of inflammation and NGF does not upregulate the transcription of inflammatory-related genes.

The pharmacological properties of DRG neurons have been an important area of study for many decades. The nociceptive subpopulation have generally taken centre stage in this area of neuroscience research due to chronic pain becoming increasingly recognised as a disease accounting for substantial suffering and disability worldwide. Robust *in vitro* models of action potential propagation and peripheral transduction have been few and far between. Whilst *in vitro* culture of neurons cannot exactly replicate the neuron in its *in vivo* state, the combination of compartmentalised chambers and calcium imaging now allows for the functional characterisation of peripherally expressed ion channels.

Future perspectives

The reasonably quick preparation of these cultures can allow for a relatively high-throughput method of characterising novel compounds in an *in vitro* preparation. For example, this method can be used in addition to traditional somal recordings to study the inhibition of action potential propagation by novel compounds. Therefore, the next major step in this project would be to continue these investigations using novel compounds. The current major focus of analgesia research is focussed on the primary sensory neuron. This is primarily due to the characterisation of nociceptor specific transduction proteins including TRPV1, and the ATP receptor channel, P2X3. In addition, the characterisation of SCN9A mutations which result in both loss and gain of sensory

function, along with the cloning and characterisation of $Na_v1.7$, showing that it is an essential generator of action potentials in nociceptors, have helped to direct attention to the primary afferent neuron. The cell bodies of these neurons have long been used as a model of the peripheral terminals, however molecular and physiological observations made in the cell body may not necessarily relate to the often distantly located terminals. The combination of functional imaging and compartmentalised cultures as described in this thesis enables the accurate investigation of peripheral transduction and action potential propagation in an *in vitro* preparation. Importantly, this technique can be added to the diverse range of techniques neuroscientists have at their disposal to investigate sensory neurons. One technique alone cannot be used to answer all questions, however, in combination with others, functional evaluations of sensory neurons in microfluidic chambers can enable valuable translational research to take place.

An interesting continuation from the experiments described in chapter 3 would be to evaluate the contribution of TTX-s and TTX-r VGSC to the propagation of action potentials during a neuropathic pain state. TTX-r VGSC have been demonstrated to be especially important in the generation of neuropathic pain, selective knockdown of $Na_v1.8$ by antisense oligodeoxynucleotides reversed neuropathic pain induced by spinal nerve injury (Lai et al., 2002). Furthermore, spinal nerve injury resulted in the redistribution of $Na_v1.8$ to the axons of uninjured neurons which enabled a TTX-r current to propagate (Gold et al., 2003). The increase of $Na_v1.8$ expression and therefore TTX-r current has been shown to increase spontaneous activity in uninjured neurons contributing to the generation of neuropathic pain (Gold et al., 2003). This study provides an excellent example of the need to study the peripheral regions of sensory neurons as changes were predominantly observed in regions other than the soma. Therefore, the dissection and culture of DRG neurons from animals that have undergone surgery to induce neuropathic pain may enable an accurate method to functionally evaluate the redistribution of TTX-r channels to the axon. Currently, it is unknown whether the cell would remain in a neuropathic state once in culture, however, repeating the same experimental paradigm as in Figure 3.8.1, would enable the evaluation of TTX-r VGSC expression in the axon. A greater expression of TTX-r VGSCs in the axons of cultured neurons may relate to the neuropathic injury and therefore could greatly increase the potential of this system for research into neuropathic pain mechanisms.

Analysis of sensory neurons from rodent models of neuropathic pain would be an excellent method to characterise not only the axonal expression of VGSCs but also the changes in expression of peripheral transduction proteins. However, there is one issue that needs to be overcome before these experiments would be possible. The surgery would be performed on adult animals, therefore, adult neurons would need to be cultured in the microfluidic chambers. From personal observations, a considerably smaller percentage of adult DRG neurons project an axon through the microgroove array when cultured in the compartmentalised chambers. Adult cultures no longer rely on NGF for survival (Dodge et al., 2002), and also have transitioned through the neuronal 'pruning' period where

survival depends upon the growth of the axon reaching an area of target-derived neurotrophins (Lindsay, 1996). Therefore the use of an NGF chemoattraction protocol is not sufficient to encourage a high percentage of cells to project into the adjacent compartment which is likely to be due to the fact that TrkA expressing adult neurons are no longer dependent on NGF signalling for survival, and secondly, the proportion of TrkA expressing neurons in the adult is reduced compared to embryonic neurons. Despite this, adult DRG neurons still contain a very high regenerative capacity for axonal growth. Therefore refinement of the methods used to direct axonal growth is required so that adult cultures can be successfully used in compartmentalised chambers. One simple experiment would be to try a multiple neurotrophin approach, so that rather than selecting for a specific subpopulation, all populations are encouraged to grow through the microgrooves. However, as mentioned, adult DRG neurons no longer require neurotrophin signalling for survival, therefore the drive to reach an area of high neurotrophin concentration may not be sufficient for large growth through the microgroove array.

An alternative solution, which is highly compatible with microfluidic chambers is to co-culture DRG neurons with a second type of cell. A recent abstract presented at the Society for Neuroscience Meeting 2012 demonstrated that adult DRG neurons cultured in microfluidic chambers could be encouraged to grow neurites through the microgroove array by co-culturing epidermal keratinocytes in the adjacent compartment (Kumamoto et al., 2012) (Figure 7.3.1). In this protocol a manual neurotrophin gradient was not established, therefore the direction of axonal growth must be influenced by the release of factors from the epidermal keratinocytes (Figure 7.3.1).

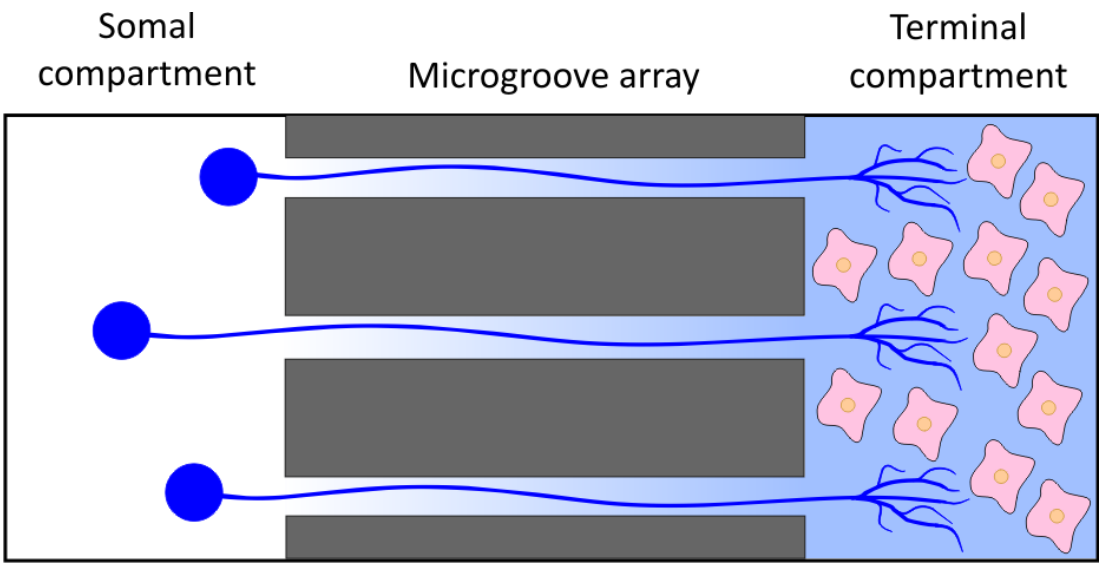

Figure 7.3.1
Schematic showing the co-culture of adult DRG neurons with keratinocytes. A manual neurotrophin gradient is not established in this protocol. Instead, the release of factors from the keratinocytes diffuses through the microgrooves and encourages the axonal growth in a uni-directional manner.

Personal communication with the abstract presenters suggested that using this co-culture method resulted in a highly successful growth of axons from adult neurons into the adjacent compartment. The fluidically isolating microgroove barrier also allows the use of different cell culture medium in the respective compartments to ensure optimal growth and survival of the different cell types (Figure 7.3.1). This may therefore provide a relatively easy mechanism to encourage adult DRG neurons to project through the microgroove array. A slight change in the design of the chamber mould may be required to reduce the length of the microgrooves. The 2 compartment chambers used throughout this thesis have 800 µm long microgrooves, reducing this length would most likely result in an increased number of projecting neurites. Kumamoto and colleagues used a design with 100 µm long microgrooves with apparent success.

Inflammatory conditions can also be created by adding inflammatory mediators to the culture medium. The addition of an 'inflammatory soup' including bradykinin, serotonin, prostaglandin E_2 and histamine can recapitulate the conditions during chronic inflammation *in vivo*. Furthermore, the fluidic isolation between compartments can enable the localised application of these mediators. Addition to the terminals can simulate peripheral inflammation, which for example is commonly associated with arthritis. Nociceptors are highly sensitised by inflammatory mediators (Huang et al., 2006), and when applied to the somata of cultured DRG neurons that had previously undergone chronic compression of the dorsal root ganglion (surgery performed *in vivo*), increased the discharge rate and reduced the number of silent neurons, compared to cultures derived from unoperated animals (Ma et al., 2006). Therefore, inflammatory mediators can clearly increase neuronal excitability which may lead to the development of hyperalgesia and allodynia. Application of an inflammatory soup to the terminals would enable thorough *in vitro* experimentation on the resulting processes that eventually can result in an upregulation/redistribution of $Na_v1.8$ in the axon.

In conclusion, the microfluidic chambers in combination with functional calcium imaging have great potential. With some slight modifications these techniques could be used to study both neuropathic and inflammatory conditions in a relatively simple *in vitro* preparation.

7.4. Proton sensitivity is differentially regulated between peripheral and somal regions in DRG neurons *in vitro*

Tissue acidosis is commonly associated with inflammation, ischemia and tissue damage, and is known to be a strong activator of nociceptive neurons (Reeh and Steen, 1996). The nerve endings of nociceptors are increasingly excited by falling pH in the skin, dura and visceral organs and psychophysical experiments have demonstrated a clear link between pain and proton concentration (Steen and Reeh, 1993). Previous investigations into proton sensitivity have found that in the skin-nerve preparation proton responses are largely restricted to capsaicin sensitive cells (Steen et al., 1992). Furthermore, analysis of DRG neurons from the TRPV1 knockout show that proton sensitivity is strongly reduced (Caterina et al., 2000; Davis et al., 2000). This was later confirmed by Leffler and

colleagues, who demonstrated that the disruption of the TRPV1 gene led to an almost complete elimination of proton responses in unmyelinated fibres with a proton stimulus of pH 5 (Leffler et al., 2006). These studies suggest that TRPV1 is a major transducer of acid stimuli.

The current findings detailed in chapter 4 however, suggest that ASICs play a greater role in proton transduction than these previous studies suggest. At pH 5.7, I have demonstrated that ASICs are responsible for acid transduction in approximately 80 % of neurons cultured in the microfluidic chambers. The difference between these findings and previous reports, may arise from variations in the neuronal region that has been tested. For example, in the rat, a high proportion of capsaicin sensitive cells have been shown to respond to acid stimuli when assessed at the cell soma (Leffler et al., 2006). However, I have demonstrated that the terminals and soma are significantly different in their respective sensitivity to protons. At pH 5.7, over 90 % of cells are excited by proton stimulation of the terminals, whereas in the same population of cells, less that 50 % respond to direct somal stimulation. The difference in capsaicin sensitivity is much less pronounced between these neuronal regions, therefore the proportion of proton sensitive cells that also display capsaicin sensitivity is likely to be much greater at the soma compared to the terminals. This may result in TRPV1 having a greater importance in proton detection at the soma compared with peripheral regions. The greater sensitivity of the terminals suggests that ASICs play a greater role in determining peripheral sensitivity compared with the soma *in vitro*.

Human psychophysical experiments involving the iontophoresis of acid has demonstrated that subcutaneous injection of amiloride significantly attenuated the pain induced by the iontophoresis of acid – suggesting that in this preparation which involves the stimulation of sensory terminals, ASICs are responsible for a substantial proportion of the pain (Jones et al., 2004). The human psychophysical data therefore coincides with the data gathered from stimulating the terminals in the microfluidic chambers, which suggest TRPV1 does not play an important role in acid detection. As discussed, the terminals still display robust sensitivity to capsaicin, so a lack of TRPV1 expression does not account for this reduced role. It seems likely that a preferential anterograde transport of ASICs out of the cell soma, establishes a greater sensitivity to acid stimuli in the peripheral terminals and that this relies predominantly on ASICs for transduction. It is particularly interesting that the psychophysical experiments in which the terminals are stimulated correspond closely with my data in which the terminals are also undergoing acid stimulation. Conversely, experimentation directly on the cell soma derived from animals which lack the capsaicin receptor suggest quite the opposite, that TRPV1 is the predominant transducer of acid in the cell body. This again illustrates the importance of differentiating between these neuronal regions, which the microfluidic chambers are highly adapted to do.

An important consideration for these experiments is the selection of the neuronal population that express TrkA and require NGF signalling for survival. In techniques such as the skin-

nerve preparation and human psychophysical experiments, all fibre types are present. Leffler and colleagues demonstrated that acid-evoked excitation of C-fibre cutaneous nociceptors *in situ* relied on TRPV1, whereas other mechanisms were responsible for excitation of the thin myelinated nociceptors. Furthermore, this study also reports that the transient ASIC-evoked currents were more prevalent in the IB4-negative, peptidergic neurons (Leffler et al., 2006) that has also been confirmed by other groups (Liu et al., 2004, Dirajlal et al., 2003). During embryogenesis, the peptidergic subpopulation continues to express TrkA and remain reliant on NGF signalling for survival (Crowley et al., 1994). The greater proportion of cells that rely on ASICs for proton transduction in the microfluidic chambers may be as a result of using NGF as a chemo-attractant, thereby positively selecting for the TrkA expressing neurons. Analysis of peptide expression from the cultured neurons when using only NGF as a chemo-attractant would provide more insight into the peptidergic identity of these cells, and may account for the greater reliance on ASICs for proton transduction.

In further support of the role for ASIC mediated proton transduction is the observation that acid stimuli induces very little tachyphylaxis when applied to the neuronal terminals. Protons are suggested to be unique amongst the algogenic substances in that they are able to excite nociceptors continuously without any obvious tachyphylaxis (Steen et al., 1992). Repeated activation of TRPV1 with capsaicin or protons typically leads to prominent desensitisation and tachyphylaxis. This process is induced by the rise in intracellular calcium levels that leads to TRPV1 dephosphorylation and the activation of calcineurin that interacts with TRPV1 (Numazaki et al., 2003, Rosenbaum et al., 2004). Consecutive proton stimulation rarely resulted in tachyphylaxis, therefore it seems likely that the transduction of protons is through ASICs that rapidly desensitise in response to proton stimulation but entirely recover during the 5 minute inter-stimulus wash-out period, so that they are able to respond to subsequent proton stimulation.

Future perspectives

These studies have confirmed ASICs play a major role in the transduction of proton stimuli in the peripheral terminals of cultured DRG neurons. Amiloride was used as a non-specific inhibitor of ASICs, investigations into the role of specific ASIC channels could be continued with the use of selective ASIC inhibitors. Venomous animals including spiders, scorpions and sea anemones contain a huge diversity of proteins that have been found to directly interact with many different classes of ion channels. These are commonly divided into toxins that produce inhibition by physically blocking the ion pore, and those that shift the voltage dependence of the channel to either a more negative or positive potential, therefore inhibiting or favouring channel opening, respectively.

APETx2 is a sea anemone toxin that is a selective inhibitor for homomeric ASIC3 and heteromeric channels containing ASIC3. This toxin reduces transient peak currents mediated by this channel (Diochot et al., 2004). On the other hand, a tarantula toxin – psalmotoxin 1 (PcTx1) has been isolated that selectively inhibits ASIC1a (Escoubas et al., 2003). The mechanism of inhibition of PcTx1

is by increasing the affinity of ASIC1a for H^+ which leads to chronic desensitisation at the resting pH of 7.4 (Chen et al., 2005). The use of toxins such as these would enable the exact contribution of each ASIC to be assessed in detail. When used in the microfluidic chambers, the fluidic isolation between compartments would enable further insight into the distribution of specific channels between neuronal regions. Inhibition may be more pronounced at the periphery due to the likely possibility that there is a greater dependence on ASICs for proton transduction.

A further continuation of this project would be to investigate the mechanism by which the terminals are significantly more sensitive to proton stimuli than the soma. I have hypothesised the differential regulation may be due to the preferential transport of ASICs out of the cell soma. Alternatively, local translation of the ASICs may also play a role in determining proton sensitivity. These mechanisms can be investigated using the microfluidic chambers. Firstly, blockade of axonal transport would quickly reveal if this mechanism was responsible for equipping the terminals with proton transducing proteins. Treatment of cultured mouse DRG neurons with the H_2O_2 donor – *tert*-butyl hydroperoxide (TBHP) inhibited anterograde and retrograde transport of organelles in a time and concentration dependent manner (Isonaka et al., 2011). Axonal transport was entirely inhibited with 10 µM TBHP in less than 1 hour, with higher concentrations of 100 µM and 1 mM producing a quicker inhibition but with associated organelle swelling. Actin filaments, neurofilaments and microtubules were unaffected even at the highest concentrations used (Isonaka et al., 2011). In order to investigate the role of axonal transport, cultures would first need to be established in the absence of any transport inhibitor. Axonal transport is critical during the regeneration of axons, therefore inhibition during early stages of the culture period would probably result in a major deficit of axonal growth through the microgroove array. A preliminary protocol would involve culturing the neurons for approximately 5-7 days *in vitro* in 3 compartment chambers, until a dense axonal network is established in the terminal compartment. TBHP could then be applied specifically to the middle axonal compartment which would negate any direct toxicity on the cell somata. The exact turnover rates of the membrane proteins would dictate how long the incubation period with TBHP would need to be. Therefore, after addition of TBHP proton sensitivity could be assessed at the peripheral terminals 24, 48, 72 and 96 hours later. This would enable a good indication into both the role of axonal transport and the membrane turnover rate of peripherally expressed proteins. I hypothesise that upon inhibition of axonal transport, the transportation of proton transducers would be inhibited, resulting in a subsequent downregulation of proton sensitivity in the peripheral terminals.

An alternative mechanism to investigate is the role of local translation. Cycloheximide is a commonly used inhibitor of eukaryotic translation (Schneider-Poetsch et al., 2010) that has been shown to completely inhibit the incorporation of labelled amino acids into proteins in the cell body of DRG cultures (Zheng et al., 2001). Therefore, the use of cycloheximide in peripheral compartments could give an important insight into the role of local translation in the peripheral

regions of cultured neurons. The study of axonal transport and local translation could also be extended to investigate other stimuli, such as TRP channel agonists, and even if VGSCs depend upon these mechanisms for the localisation to peripheral neuronal regions.

7.5. Expression of TRPV1 and the functional sensitivity to capsaicin in cultured DRG neurons

Expression of the capsaicin receptor is a classical marker of nociceptive neurons (Jancsó et al., 1967). Its expression has been extensively characterised throughout embryonic development and within neuronal subpopulations. These studies have demonstrated that in the mouse, functional TRPV1 expression is first observed at E12.5, this is followed by a rapid upregulation resulting in approximately 60 % of all DRG neurons displaying capsaicin sensitivity by E14.5 (Hjerling-Leffler et al., 2007). By adulthood approximately 30 - 40 % of all DRG neurons respond to capsaicin (Hjerling-Leffler et al., 2007) which are predominantly restricted to the peptidergic subpopulation (Cavanaugh et al., 2011). To investigate the expression of TRPV1 over time *in vitro*, embryonic cultures were prepared from mice and rats at ages after the onset of expression.

One of the most striking results in the experiments investigating TRPV1 expression was the profound downregulation of capsaicin sensitivity during the first 2-3 days *in vitro* in cultures prepared from younger embryos. This observation was found in both rat and mouse cultures, demonstrating the effect was not species specific. This suggests that other mammalian DRGs may also follow the same pattern of expression if cultured *in vitro*.

The downregulation of capsaicin sensitivity in earlier cultures suggests there may be a critical factor that is required for the maintenance of TRPV1 expression. This factor may not be expressed in earlier cultures, or may become downregulated once the neurons are in culture, coinciding with the loss of TRPV1 expression. A study by Michael and Priestley in 1999, demonstrated that after sciatic nerve axotomy, there was a concurrent reduction in TRPV1 mRNA in the ipsilateral L4 ganglion. *In situ* hybridisation performed on the L4 ganglia after sciatic nerve section revealed that the reduction in TRPV1 mRNA occurred between 4 – 7 days after axotomy and remained low even at 2 weeks after the lesion (Michael and Priestley, 1999). Cells positive for TRPV1 mRNA were detected in nearly 50 % of all cell bodies on the contralateral side, whereas this was reduced to 16 % on the ipsilateral side (Michael and Priestley, 1999). Additional phenotypic changes were also observed, including a reduction of CGRP, TrkA and IB4 immunofluorescence (Michael and Priestley, 1999). Spinal nerve section which axotomises all cells in the associated DRG resulted in a complete loss of TRPV1 mRNA in the L4 ganglion. The remaining TRPV1 expressing cells after sciatic nerve section are probably due to the partial lesion and therefore the sparing of some cells in the gangion. Section of the peripheral nerves obviously leads to profound changes in the phenotype of the axotomised cells. The changed availability of peripherally derived neurotrophins is likely to play an important role in the downregulation of TRPV1 and other associated changes in neuropeptide

and neurotrophin receptor expression. In support of this is the finding that adult DRGs cultured in the absence of NGF loose capsaicin sensitivity over time *in vitro* (Winter et al., 1988).

In terms of the downregulation of capsaicin sensitivity observed in the present investigations, these findings may be important. Crucially, during the dissection of the ganglia, the projecting axons are severed. Despite the abundant supplement of the medium with NGF, cultures prepared from earlier embryos loose capsaicin sensitivity during the first 1 – 3 days *in vitro*. In these earlier cultures, NGF/TrkA signalling is therefore unable to maintain capsaicin sensitivity. The current mechanism of how capsaicin sensitivity is downregulated is currently unknown. TRPV1 is regulated by several factors, and previous reports suggest that NGF induces an upregulation of TRPV1 expression which is dependent upon NGF signalling through TrkA (Buck and Winter, 1996). It therefore appears that in earlier cultures NGF is unable to activate mechanisms required to maintain TRPV1 expression. Experiments using cultured adult DRG neurons have investigated the role of mitogen activated protein (MAP) kinase signalling in mediating capsaicin sensitivity. Blockade of the NGF stimulated Shc-Ras-Raf-MAP kinase pathway using the Mitogen-activated protein kinase kinase (MEK) inhibitor - PB98059, resulted in a large downregulation of capsaicin sensitivity (Ganju et al., 1998). Therefore, the MEK inhibitor interferes with NGF induced upregulation of TRPV1, probably by inhibiting the transcription of TRPV1. Indeed, the downregulation of capsaicin sensitivity over several days *in vitro* (especially in E14.5 cultures) suggest that this may be due to a reduction of transcription rather than a prolonged desensitisation of the receptor, which presumably would happen over a much shorter time course. The time course of capsaicin sensitivity downregulation as detected in the microfluidic chambers is mirrored by the downregulation of capsaicin sensitivity in adult DRG neurons upon NGF removal (Winter et al., 1988). The downregulation of capsaicin sensitivity can be rescued by reapplying NGF to the culture medium, which upregulates capsaicin sensitivity over 4 – 6 days *in vitro* (Winter et al., 1988). The time course required to regain maximal capsaicin responses is similar to the duration in which it is lost in earlier microfluidic cultures, therefore both mechanisms may depend on synthesis, or loss of TRPV1 synthesis, respectively.

The small guanosine triphosphate (GTP)-ase, Ras plays an important role in intracellular pathways involved in neurotrophin-dependent survival and neuronal differentiation. Ras is a key component of the ERK/MAPK pathway and NGF induces the robust phosphorylation of ERK that then activates downstream cascades leading to gene transcription. Blockade of Ras has been shown to significantly reduce TRPV1 fluorescence in adult DRG neurons, whereas in the absence of both NGF and GDNF, activation of Ras induced TRPV1 expression in approximately 60 % of all cells (Bron et al., 2003). The authors suggest that a certain level of Ras activation is required to maintain the transcriptional machinery to synthesise TRPV1 (Bron et al., 2003). Upon overstimulation of Ras by increased NGF levels during inflammation may be involved in the overproduction of TRPV1 and other associated nociceptive molecules.

A separate mechanism suggested to regulate TRPV1 expression is that involving p38 MAPK. Activation of p38 has been demonstrated to be initiated by the retrograde transport of NGF from inflamed peripheral areas, which acts to increase translation and transport of TRPV1 to the peripheral terminals, which can then contribute towards the induction of inflammatory heat pain hypersensitivity (Ji et al., 2002). In this scenario the actual number of capsaicin receptors is upregulated rather than the sensitivity of the individual receptor. Interestingly, after activation of this pathway, the transport of TRPV1 occurs preferentially to the peripheral terminals. Only a very small increase was observed in the dorsal horn where the central terminals are located, suggesting that TRPV1 is specifically directed towards the periphery (Ji et al., 2002).

The many means by which the expression and sensitivity of TRPV1 is regulated make the exact mechanism of why the functional expression of TRPV1 is downregulated difficult to ascertain without further experiments. It may be possible that these pathways are affected by removing the neurons from their natural environment which subsequently influences the expression of TRPV1. For example, a downregulation of Ras activation may consequently result in a reduction of TRPV1 transcription, which potentially could lead to the loss of capsaicin sensitivity observed over several days in the E14.5 mouse cultures. Ultimately, this is the first description that TRPV1 expression during long term *in vitro* culture has a critical dependence on embryonic age and further experimentation may be able to provide important insight into the regulation of TRPV1 expression.

The blockade of action potential propagation by capsaicin has been previously examined in both *in vivo* (Petsche et al., 1983) and *in vitro* (Su et al., 1999) preparations. The indirect modulation of voltage gated sodium channels through TRPV1 activation, is likely to be the mechanism responsible for the conduction block detected in the microfluidic chambers (Liu et al., 2001; Onizuka et al., 2011). Furthermore, the finding that the TRPV1 expressing neurons can be excited by capsaicin application to the axon confirms previous investigations that TRPV1 is expressed at all points throughout the neuron, including the axon and terminals (Holzer, 1991). In conclusion, these results are in good agreement with findings from *in vivo* preparations and provide good proof of principle that the neurons under investigation in the compartmentalised culture chambers are similar to their *in vivo* counterparts.

7.6. Modality specificity in mouse and rat DRG neurons

Nociceptive sensory neurons are commonly divided into either a peptidergic population, or an IB4-binding population. These subpopulations target distinct zones in the dorsal horn, with the peptidergic terminating in lamina I and lamina II outer, and the non-peptidergic terminating in lamina II inner. There has been much investigation into whether these anatomical differences are paralleled by a similar division among somatosensory neurons to convey specific modalities. TRPV1 has commonly been used as a marker of nociceptive neurons (Jancsó et al., 1977), and its expression has been shown to become largely restricted to the peptidergic subpopulation in the mouse (Zwick

et al., 2002; Cavanaugh et al., 2011b). TRPV1 knockout does not result in a major deficit in thermal detection when tested behaviourally (Caterina et al., 2000; Davis et al., 2000), however ablation of the central terminals of TRPV1 expressing nociceptors results in a near complete loss of noxious heat sensitivity, with no deficit in noxious cold or mechanical detection (Cavanaugh et al., 2009). Recordings from the dorsal horn have shown that knockout of the TRPV1 gene, abolished heat-induced responses of wide dynamic range neurons in lamina V, but had no effect on heat responsiveness of lamina I neurons, suggesting the presence of an additional thermal detector (Eckert et al., 2006). Therefore, the restriction of the phenotype to only a deficit in noxious heat detection in mice with ablation of the central terminals, and the mild deficit observed in the TRPV1 knockout mouse, would argue that the TRPV1 expressing nociceptors are crucial for noxious thermal detection, which require both a TRPV1-dependent and TRPV1-independent mechanism for transduction. The restriction of this phenotype in the mouse suggests that the modality of noxious heat detection is restricted almost entriely to the TRPV1 expressing primary afferents.

The peripheral restriction of modalities is further supported by the finding that upon diphtheria toxin mediated ablation of the MrgprD positive neurons (all of which are non-peptidergic), a selective reduction of mechanical sensitivity is observed, with no change in noxious thermal detection (Cavanaugh et al., 2009). Collectively, these experiments suggest that in mouse primary afferent neurons, noxious heat detection relies upon TRPV1 expressing neurons (peptidergic) and noxious mechanical stimulation is detected by MrgprD expressing neurons (non-peptidergic). This finding has recently been validated by recording from lumbar dorsal horn neurons, which has shown that ablation of TRPV1 expressing neurons results in a loss of noxious heat responses in lamina I and V dorsal horn neurons. In contrast, diphtheria toxin mediated ablation of MrgprD expressing neurons resulted in a reduced number of WDR neurons excited by mechanical stimuli (Zhang et al., 2013).

The TRPA1 channel has been implicated in inflammatory nociception (Bautista et al., 2006), and has been shown to transduce both mechanical (Corey et al., 2004) and cold stimuli (Story et al., 2003). Using functional calcium imaging, the expression of TRPA1 has been shown to be largely restricted to the IB4-positive, nonpeptidergic subpopulation in both rat and mouse lumbar DRG cultures (Barabas et al., 2012). There is growing evidence suggesting that TRPA1 is integral in the initiation and maintenance of inflammatory mechanical hyperalgesia (Obata et al., 2005; Eid et al., 2008; da Costa et al., 2010), therefore the TRPA1 expressing, IB4-positive c-fibres may be crucial in conveying cutaneous mechanical pain in the mouse. The restriction of TRPA1 to the nonpeptidergic subpopulation, and the finding that TRPA1 may be important for the detection of mechanical stimuli, supports the hypothesis that the nonpeptidergic neurons in mice are vital for conveying noxious mechanical stimuli, again confirming the specificity of modality detection to neuronal subpopulations in this species.

With regard to rat DRG subpopulations, in contrast to the mouse, TRPV1 expression appears to be more evenly distributed among both peptidergic and nonpeptidergic subpopulations. Using colocalisation of immunoreactivity in the DRG, Tominaga and colleagues show that in the rat, whilst most (85 %) of the substance P-immunoreactive cells (peptidergic) costained for TRPV1, 60-80 % of the IB4-positive neurons (nonpeptidergic) were also positive for TRPV1 immunostaining (Tominaga et al., 1998). Similar patterns were observed in the superficial dorsal horn of the spinal cord, where widespread colocalisation of substance P and TRPV1 was observed in the lamina I and lamina II outer, corresponding to the termination zone of most peptidergic afferents, and colocalisation of dense TRPV1 immunoreactivity and IB4 in lamina II inner, where most nonpeptidergic afferent terminate (Tominaga et al., 1998). A more recent study has confirmed these observations, showing that in the rat L6 DRG, TRPV1 expression was almost equally divided between substance P and CGRP expressing peptidergic neurons, and IB4-positive nonpeptidergic neurons (Hwang et al., 2005).

With these TRPV1 expression patterns in mind, the findings in this thesis suggest that in the mouse, the peptidergic fibres can almost exclusively be blocked with the use of high concentration capsaicin (Figure 5.6), suggesting the neurons that continue to propagate through the capsaicin blockade may be comprised of nonpeptidergic population that do no express TRPV1. It is likely that if the same experiments were conducted in rat DRG cultures, propagation in TRPV1 expressing neurons would also be blocked by capsaicin, however, due to the more widespread expression of TRPV1 among peptidergic and nonpeptidergic c-fibres in the rat, the blockade would not be confined to the peptidergic population as it is likely to be in the mouse. In chapter 6, I detail the functional downregulation of TRPV1 in early embryonic cultures, this pattern was found in both rat and mouse preparations. Therefore, the mechanisms leading to the functional loss of capsaicin sensitivity in the mouse are likely to be restricted to the prospective peptidergic population, whereas in the rat, these mechanisms are likely to influence capsaicin sensitivity in both the peptidergic and nonpeptidergic populations.

Future perspectives

The downregulation of capsaicin sensitivity in cultures prepared prior to a critical developmental time point is an intriguing finding and further experiments are required to elucidate the mechanisms responsible. I have studied the effects of a range of neurotrophins on capsaicin sensitivity, and found that only retinoic acid was able to upregulate the functional expression of TRPV1 in cultured DRG neurons. Therefore the mechanism by which retinoic acid can induce upregulation of capsaicin sensitivity may be important in understanding why in earlier cultures it is downregulated.

Retinoids, are important factors for the survival of neurons, and it is suggested that the neurotrophin and retinoid pathways can interact. For example, in PC12 cells, a model of sympathetic neurons, one of the earliest genes upregulated by NGF is the orphan receptor – NGFI-B, that can

form a heterodimer with the Retinoid X receptors (RXRs) (Milbrandt, 1988). RXRs and associated orphan receptors can then mediate gene expression. Within DRG subpopulations there is a common and unique expression of retinoid receptors. All subpopulations express RXRα, RXRβ, RXRγ, and RARβ2, and it has been shown that retinoic acid mediated signalling through this latter receptor mediates neurite outgrowth in embryonic DRG neurons (Corcoran et al., 2000). However, the same study demonstrated that only NGF and NT3 dependent neurons extended neurites in response to retinoic acid and BDNF dependent neurons extended neurites regardless of the presence or absence of retinoic acid. The mechanisms by which retinoic acid upregulates capsaicin sensitivity is currently unclear, however the use of specific receptor agonists may be able to provide insight into the biological pathway responsible. For example, CD2019, is a specific RARβ2 agonist (Corcoran et al., 2000), therefore, any upregulation of capsaicin sensitivity induced by addition of this compound to the culture medium can be attributed to signalling through this receptor.

Retinoic acid clearly has an important role in the embryonic development of DRG neurons, predominantly by promoting the neurite growth, however a role in mediating the *in vivo* expression of TRPV1 has not been described. It therefore seems unlikely that a change in retinoic acid signalling is responsible for the downregulation of capsaicin sensitivity, despite the ability of this factor to rescue the TRPV1 phenotype in cultured neurons. To study the levels of TRPV1 protein, immunohistochemistry and western blots could be performed on cultured neurons prepared from various embryonic ages. Furthermore, *in situ* hybridisation and quantitative PCR could be used to assess the level of TRPV1 mRNA, which may provide insight into whether the transcription of the TRPV1 gene is reduced.

An interesting development to the capsaicin sensitivity studies would be to axotomise the axons that have grown through the microgroove array. Vacuum aspiration in the terminal compartment channel severs all axons at the point at which they emerge from the microgrooves. This enables the microfluidic chambers to be used as an *in vitro* model of axonal injury. Taylor and colleagues have performed these experiments using the same compartmentalised culture system, and demonstrated that there was a ~200 % increase in the induction of *c-fos* mRNA within 15 minutes when the soma was analysed by real-time PCR. This further increased to ~320 % within 2 hours after lesion (Taylor et al., 2005). Axotomy has been described to affect TRPV1 expression. In DRGs removed from human patients with a central axotomy, TRPV1 immunoreactive nerves significantly increased compared to controls (Facer et al., 2007). However, other studies have demonstrated that after sciatic nerve axotomy, TRPV1 mRNA in the L4 ganglion was reduced (Michael and Priestley, 1999) and TRPV1 expression was also decreased in the somata of neurons damaged by complete or partial nerve section (Hudson et al., 2001). Therefore, it would be interesting to section the axons of cultured DRG neurons, allow approximately 2 days for axonal regrowth, and then assess the functional expression of TRP channels at the sensory terminals. Furthermore, additional markers of injury could also be examined such as an upregulation of $Na_v1.3$,

neuropeptides and ATF3. Microfluidic chambers could therefore provide an *in vitro* platform to assess aspects of peripheral nerve injury. Factors that are involved in the regeneration of axons such as neurotrophins and retinoids could also be investigated in a relatively high-throughput *in vitro* method.

In regards to the capsaicin conduction block experiments, a continuation of the current experiment would be to investigate if the blockade could be reversed by washing out the high concentration capsaicin. This would enable investigations into whether the TRPV1 expressing cells could still propagate action potentials after the axons were exposed to a high concentration of capsaicin. An inability to propagate action potentials would suggest these cells have undergone excitotoxicity through a TRPV1-dependent mechanism that is observed in TRPV1 expressing HEK cells (Caterina et al., 1997). This mechanism would likely involve excessive ion influx including calcium and sodium, that induces cellular swelling (Bevan and Szolcsányi, 1990). As no histological changes such as swelling were observed in the cell somata or the axons, I would hypothesise that upon a prolonged wash out of capsaicin from the axonal compartment, most TRPV1 expressing cells would respond to a potassium stimulation of the terminals. Calcium influx is undoubtedly involved in the capsaicin induced conduction block of action potential propagation in cultured DRG neurons. To investigate if calcium is essential, or if the influx of other cations will also induce a conduction block, the middle axonal compartment could be bathed in calcium-free ECF, and the stock capsaicin diluted in the same ECF to make the 100 µM capsaicin solution. Therefore, at all times during the experiment, the middle axonal compartment would be free of calcium, test stimuli of potassium can then be applied to the terminals to determine if action potential propagation is inhibited when calcium is not present.

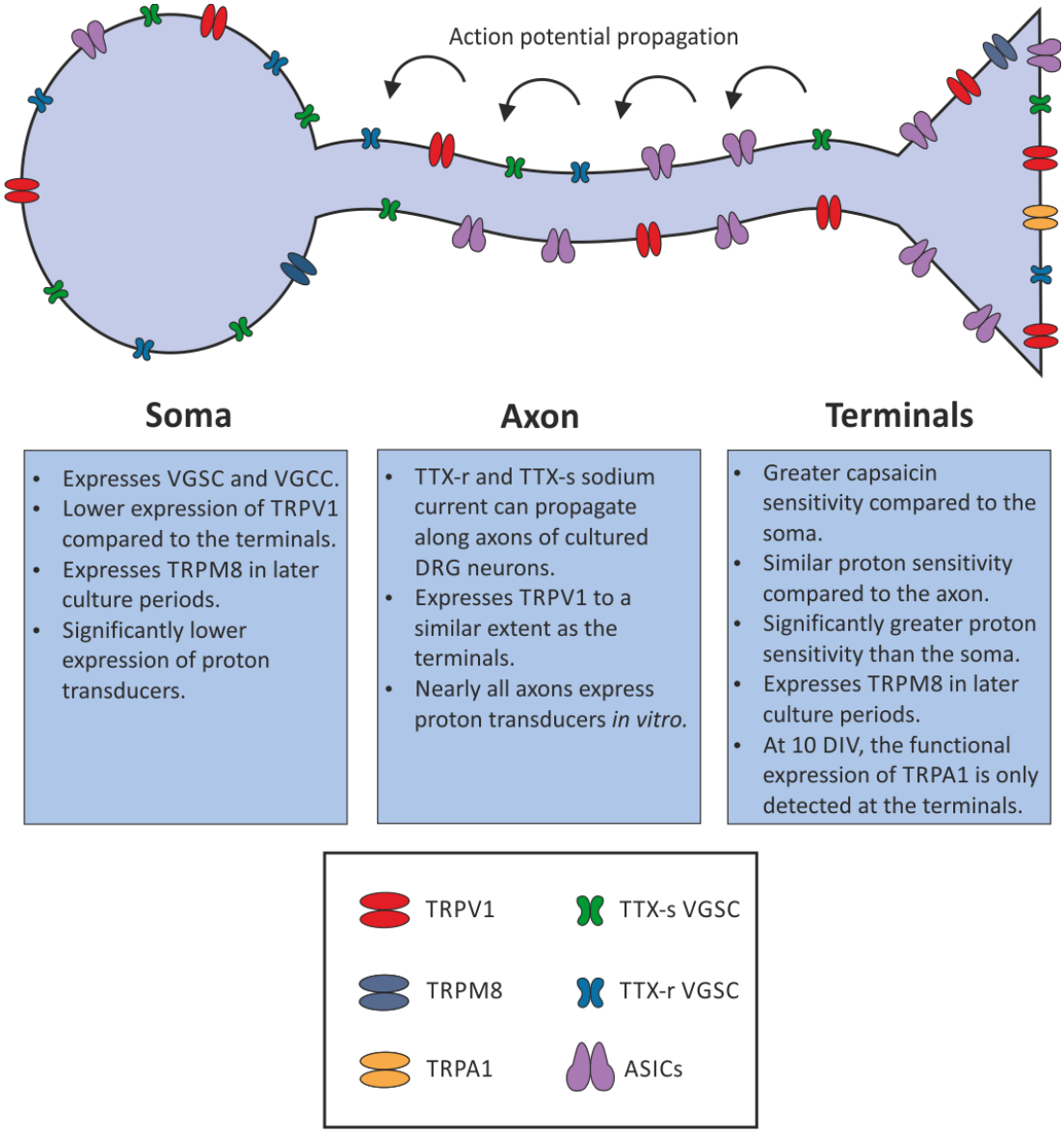

Figure 7.6.1
A summary of the functional expression of ion channels in cultured DRG neurons determined by functional calcium imaging of compartmentalised DRG cultures.

7.7. Final conclusions

The work in this thesis has described the novel combination of compartmentalised microfluidic chambers with functional calcium imaging. This has enabled the thorough investigation of sensory neurons in vitro, and allowed comprehensive comparisons of functional sensitivity between neuronal regions (Figure 7.6.1). The principal findings of this thesis include the initial confirmation that action potentials propagate from the terminals to the somata in cultured neurons. Pharmacological characterisations demonstrated that the majority of neurons cultured in the microfluidic chambers depend upon TTX-s VGSC, whilst a population of almost 20 % conduct a TTX-r sodium current (Figure 7.6.1). The EC50 of TTX was determined to be approximately 100 nM. Proton

sensitivity is differentially regulated in cultured DRG neurons, resulting in significantly greater proton sensitivity at the terminals and axons compared to the soma (Figure 7.6.1). The functional expression of TRPV1 also is greater at the terminals than the soma. Capsaicin robustly activates neurons when applied to the axon, which then causes a subsequent conduction block through a TRPV1 dependent mechanism. In both rat and mouse cultures, the expression of TRPV1 is highly influenced by the embryonic dissection age, with neurons unable to maintain capsaicin sensitivity if dissected prior to a critical developmental time point. Finally, the functional onset of TRPM8 expression is initiated in mouse cultures during the culture period, regardless of embryonic dissection age.

In summary, the microfluidic culture chambers provide an excellent *in vitro* platform in which to investigate specific regions of DRG neurons. The combination with functional imaging holds great potential to use these chambers in numerous biological applications, and make these a valuable tool for on-going neuroscience research. The findings discussed in this thesis illustrate that in cultured DRG neurons, the sensory terminals display considerably different properties to the cell soma, which emphasises the importance of studying these regions in isolation. Many questions still need to be answered regarding the mechanisms which govern the sensitivity differences, and continued use of the chambers may be able to unravel the biological processes responsible. Finally, these chambers enable the differentiation between neuronal regions which may be useful in modelling disease states *in vitro* and may provide important information into the regulation of protein expression in the periphery during normal and pathological states.

Bibliography

Adler CE, Fetter RD, Bargmann CI (2006) UNC-6/Netrin induces neuronal asymmetry and defines the site of axon formation. Nat Neurosci 9:511–518.

Adrian ED (1926) The impulses produced by sensory nerve endings: Part I. J Physiol 61:49–72.

Akopian AN, Sivilotti L, Wood JN (1996) A tetrodotoxin-resistant voltage-gated sodium channel expressed by sensory neurons. Nature 379:257–262.

Akopian AN, Souslova V, England S, Okuse K, Ogata N, Ure J, Smith A, Kerr BJ, McMahon SB, Boyce S, Hill R, Stanfa LC, Dickenson AH, Wood JN (1999) The tetrodotoxin-resistant sodium channel SNS has a specialized function in pain pathways. Nat Neurosci 2:541–548.

Alexander (2009) Acid-sensing (proton-gated) ion channels (ASICs). Br J Pharmacol 158:S124–S125.

Alving K, Sundström C, Matran R, Panula P, Hökfelt T, Lundberg JM (1991) Association between histamine-containing mast cells and sensory nerves in the skin and airways of control and capsaicin-treated pigs. Cell Tissue Res 264:529–538.

Arimura N, Kaibuchi K (2007) Neuronal polarity: from extracellular signals to intracellular mechanisms. Nat Rev Neurosci 8:194–205.

Armstrong CM (2006) Na channel inactivation from open and closed states. Proc Natl Acad Sci U S A 103:17991–17996.

Ascaño M, Richmond A, Borden P, Kuruvilla R (2009) Axonal targeting of Trk receptors via transcytosis regulates sensitivity to neurotrophin responses. J Neurosci 29:11674–11685.

Augustine GJ, Santamaria F, Tanaka K (2003) Local calcium signaling in neurons. Neuron 40:331–346.

Balmer JE, Blomhoff R (2002) Gene expression regulation by retinoic acid. J Lipid Res 43:1773–1808.

Bandell M, Patapoutian A (2009) Itching for insight. Cell 139:1224–1226.

Barabas ME, Kossyreva EA, Stucky CL (2012) TRPA1 is functionally expressed primarily by IB4-binding, non-peptidergic mouse and rat sensory neurons. Taylor B, ed. PLoS One 7:e47988.

Barde YA (1989) Trophic factors and neuronal survival. Neuron 2:1525–1534.

Barker PA, Shooter EM (1994) Disruption of NGF binding to the low affinity neurotrophin receptor p75LNTR reduces NGF binding to TrkA on PC12 cells. Neuron 13:203–215.

Barrett GL, Bartlett PF (1994) The p75 nerve growth factor receptor mediates survival or death depending on the stage of sensory neuron development. Proc Natl Acad Sci U S A 91:6501–6505.

Basbaum AI, Bautista DM, Scherrer G, Julius D (2009) Cellular and molecular mechanisms of pain. Cell 139:267–284.

Baumann TK, Burchiel KJ, Ingram SL, Martenson ME (1996) Responses of adult human dorsal root ganglion neurons in culture to capsaicin and low pH. Pain 65:31–38.

Baumann TK, Chaudhary P, Martenson ME (2004) Background potassium channel block and TRPV1 activation contribute to proton depolarization of sensory neurons from humans with neuropathic pain. Eur J Neurosci 19:1343–1351.

Bautista DM, Jordt S-E, Nikai T, Tsuruda PR, Read AJ, Poblete J, Yamoah EN, Basbaum AI, Julius D (2006) TRPA1 mediates the inflammatory actions of environmental irritants and proalgesic agents. Cell 124:1269–1282.

Beattie EC, Zhou J, Grimes ML, Bunnett NW, Howe CL, Mobley WC (1996) A signaling endosome hypothesis to explain NGF actions: potential implications for neurodegeneration. Cold Spring Harb Symp Quant Biol 61:389–406.

Benn SC, Costigan M, Tate S, Fitzgerald M, Woolf CJ (2001) Developmental expression of the TTX-resistant voltage-gated sodium channels Nav1.8 (SNS) and Nav1.9 (SNS2) in primary sensory neurons. J Neurosci 21:6077–6085.

Benson CJ, Xie J, Wemmie JA, Price MP, Henss JM, Welsh MJ, Snyder PM (2002) Heteromultimers of DEG/ENaC subunits form H+-gated channels in mouse sensory neurons. Proc Natl Acad Sci U S A 99:2338–2343.

Ben-Yakar A, Bourgeois F (2009) Ultrafast laser nanosurgery in microfluidics for genome-wide screenings. Curr Opin Biotechnol 20:100–105.

Bernardini N, Neuhuber W, Reeh PW, Sauer SK (2004) Morphological evidence for functional capsaicin receptor expression and calcitonin gene-related peptide exocytosis in isolated peripheral nerve axons of the mouse. Neuroscience 126:585–590.

Bessou P, Burgess PR, Perl ER, Taylor CB (1971) Dynamic properties of mechanoreceptors with unmyelinated (C) fibers. J Neurophysiol 34:116–131.

Bessou P, Perl ER (1969) Response of cutaneous sensory units with unmyelinated fibers to noxious stimuli. J Neurophysiol 32:1025–1043.

Bevan S, Szolcsányi J (1990) Sensory neuron-specific actions of capsaicin: mechanisms and applications. Trends Pharmacol Sci 11:331–333.

Bevan S, Winter J (1995) Nerve growth factor (NGF) differentially regulates the chemosensitivity of adult rat cultured sensory neurons. J Neurosci 15:4918–4926.

Bevan S, Yeats J (1991) Protons activate a cation conductance in a sub-population of rat dorsal root ganglion neurones. J Physiol 433:145–161.

Bezanilla F, Armstrong CM (1977) Inactivation of the sodium channel. I. Sodium current experiments. J Gen Physiol 70:549–566.

Black JA, Dib-Hajj S, McNabola K, Jeste S, Rizzo MA, Kocsis JD, Waxman SG (1996) Spinal sensory neurons express multiple sodium channel alpha-subunit mRNAs. Brain Res Mol Brain Res 43:117–131.

Black JA, Nikolajsen L, Kroner K, Jensen TS, Waxman SG (2008) Multiple sodium channel isoforms and mitogen-activated protein kinases are present in painful human neuromas. Ann Neurol 64:644–653.

Blair NT, Bean BP (2002) Roles of tetrodotoxin (TTX)-sensitive Na+ current, TTX-resistant Na+ current, and Ca2+ current in the action potentials of nociceptive sensory neurons. J Neurosci 22:10277–10290.

Brady ST, Lasek RJ, Allen RD (1982) Fast axonal transport in extruded axoplasm from squid giant axon. Science 218:1129–1131.

Bron R, Klesse LJ, Shah K, Parada LF, Winter J (2003) Activation of Ras is necessary and sufficient for upregulation of vanilloid receptor type 1 in sensory neurons by neurotrophic factors. Mol Cell Neurosci 22:118–132.

Brown AG, Iggo A (1967) A quantitative study of cutaneous receptors and afferent fibres in the cat and rabbit. J Physiol 193:707–733.

Buck H, Winter J (1996) K252a modulates the expression of nerve growth factor-dependent capsaicin sensitivity and substance P levels in cultured adult rat dorsal root ganglion neurones. J Neurochem 67:345–351.

Burgess PR, Perl ER (1967) Myelinated afferent fibres responding specifically to noxious stimulation of the skin. J Physiol 190:541–562.

Cabo R, Gálvez MA, San José I, Laurà R, López-Muñiz A, García-Suárez O, Cobo T, Insausti R, Vega JA (2012) Immunohistochemical localization of acid-sensing ion channel 2 (ASIC2) in cutaneous Meissner and Pacinian corpuscles of Macaca fascicularis. Neurosci Lett 516:197–201.

Cain DM, Khasabov SG, Simone DA (2001) Response properties of mechanoreceptors and nociceptors in mouse glabrous skin: an in vivo study. J Neurophysiol 85:1561–1574.

Caldwell JH, Schaller KL, Lasher RS, Peles E, Levinson SR (2000) Sodium channel Na(v)1.6 is localized at nodes of ranvier, dendrites, and synapses. Proc Natl Acad Sci U S A 97:5616–5620.

Campbell JN, Meyer RA (1983) Sensitization of unmyelinated nociceptive afferents in monkey varies with skin type. J Neurophysiol 49:98–110.

Campenot RB (1977) Local control of neurite development by nerve growth factor. Proc Natl Acad Sci U S A 74:4516–4519.

Caterina MJ, Julius D (2001) The vanilloid receptor: a molecular gateway to the pain pathway. Annu Rev Neurosci 24:487–517.

Caterina MJ, Leffler A, Malmberg AB, Martin WJ, Trafton J, Petersen-Zeitz KR, Koltzenburg M, Basbaum AI, Julius D (2000) Impaired nociception and pain sensation in mice lacking the capsaicin receptor. Science 288:306–313.

Caterina MJ, Rosen TA, Tominaga M, Brake AJ, Julius D (1999) A capsaicin-receptor homologue with a high threshold for noxious heat. Nature 398:436–441.

Caterina MJ, Schumacher MA, Tominaga M, Rosen TA, Levine JD, Julius D (1997) The capsaicin receptor: a heat-activated ion channel in the pain pathway. Nature 389:816–824.

Catterall WA (2012) Voltage-gated sodium channels at 60: structure, function and pathophysiology. J Physiol 590:2577–2589.

Catterall WA, Goldin AL, Waxman SG (2003) International Union of Pharmacology. XXXIX. Compendium of voltage-gated ion channels: sodium channels. Pharmacol Rev 55:575–578.

Catterall WA, Goldin AL, Waxman SG (2005) International Union of Pharmacology. XLVII. Nomenclature and structure-function relationships of voltage-gated sodium channels. Pharmacol Rev 57:397–409.

Cavanaugh DJ, Chesler AT, Bráz JM, Shah NM, Julius D, Basbaum AI (2011a) Restriction of transient receptor potential vanilloid-1 to the peptidergic subset of primary afferent neurons follows its developmental downregulation in nonpeptidergic neurons. J Neurosci 31:10119–10127.

Cavanaugh DJ, Chesler AT, Bráz JM, Shah NM, Julius D, Basbaum AI (2011b) Restriction of transient receptor potential vanilloid-1 to the peptidergic subset of primary afferent neurons follows its developmental downregulation in nonpeptidergic neurons. J Neurosci 31:10119–10127.

Cavanaugh DJ, Chesler AT, Jackson AC, Sigal YM, Yamanaka H, Grant R, O'Donnell D, Nicoll RA, Shah NM, Julius D, Basbaum AI (2011c) Trpv1 reporter mice reveal highly restricted brain distribution and functional expression in arteriolar smooth muscle cells. J Neurosci 31:5067–5077.

Cavanaugh DJ, Lee H, Lo L, Shields SD, Zylka MJ, Basbaum AI, Anderson DJ (2009) Distinct subsets of unmyelinated primary sensory fibers mediate behavioral responses to noxious thermal and mechanical stimuli. Proc Natl Acad Sci U S A 106:9075–9080.

Chao M V (2003) Neurotrophins and their receptors: a convergence point for many signalling pathways. Nat Rev Neurosci 4:299–309.

Chattopadhyay M, Mata M, Fink DJ (2008) Continuous delta-opioid receptor activation reduces neuronal voltage-gated sodium channel (NaV1.7) levels through activation of protein kinase C in painful diabetic neuropathy. J Neurosci 28:6652–6658.

Chen CC, England S, Akopian AN, Wood JN (1998) A sensory neuron-specific, proton-gated ion channel. Proc Natl Acad Sci U S A 95:10240–10245.

Chen C-C, Zimmer A, Sun W-H, Hall J, Brownstein MJ, Zimmer A (2002) A role for ASIC3 in the modulation of high-intensity pain stimuli. Proc Natl Acad Sci U S A 99:8992–8997.

Chen C-L, Broom DC, Liu Y, de Nooij JC, Li Z, Cen C, Samad OA, Jessell TM, Woolf CJ, Ma Q (2006) Runx1 determines nociceptive sensory neuron phenotype and is required for thermal and neuropathic pain. Neuron 49:365–377.

Chen X, Kalbacher H, Gründer S (2005) The tarantula toxin psalmotoxin 1 inhibits acid-sensing ion channel (ASIC) 1a by increasing its apparent H+ affinity. J Gen Physiol 126:71–79.

Chen Y-J, Huang C-W, Lin C-S, Chang W-H, Sun W-H (2009) Expression and function of proton-sensing G-protein-coupled receptors in inflammatory pain. Mol Pain 5:39.

Chuang HH, Prescott ED, Kong H, Shields S, Jordt SE, Basbaum AI, Chao M V, Julius D (2001) Bradykinin and nerve growth factor release the capsaicin receptor from PtdIns(4,5)P2-mediated inhibition. Nature 411:957–962.

Clapham DE (2003) TRP channels as cellular sensors. Nature 426:517–524.

Clapham DE, Julius D, Montell C, Schultz G (2005) International Union of Pharmacology. XLIX. Nomenclature and structure-function relationships of transient receptor potential channels. Pharmacol Rev 57:427–450.

Coggeshall RE, Tate S, Carlton SM (2004) Differential expression of tetrodotoxin-resistant sodium channels Nav1.8 and Nav1.9 in normal and inflamed rats. Neurosci Lett 355:45–48.

Corcoran J, Shroot B, Pizzey J, Maden M (2000) The role of retinoic acid receptors in neurite outgrowth from different populations of embryonic mouse dorsal root ganglia. J Cell Sci 113 (Pt 1:2567–2574.

Corey DP, García-Añoveros J, Holt JR, Kwan KY, Lin S-Y, Vollrath MA, Amalfitano A, Cheung EL-M, Derfler BH, Duggan A, Géléoc GSG, Gray PA, Hoffman MP, Rehm HL, Tamasauskas D, Zhang D-S (2004) TRPA1 is a candidate for the mechanosensitive transduction channel of vertebrate hair cells. Nature 432:723–730.

Coste B, Mathur J, Schmidt M, Earley TJ, Ranade S, Petrus MJ, Dubin AE, Patapoutian A (2010) Piezo1 and Piezo2 are essential components of distinct mechanically activated cation channels. Science 330:55–60.

Cox J, Reimann F, Nicholas A (2006) An SCN9A channelopathy causes congenital inability to experience pain. Nature 444:894–898.

Crabtree GR (2001) Calcium, calcineurin, and the control of transcription. J Biol Chem 276:2313–2316.

Crowley C, Spencer SD, Nishimura MC, Chen KS, Pitts-Meek S, Armanini MP, Ling LH, McMahon SB, Shelton DL, Levinson AD (1994) Mice lacking nerve growth factor display perinatal loss of sensory and sympathetic neurons yet develop basal forebrain cholinergic neurons. Cell 76:1001–1011.

Cui B, Wu C, Chen L, Ramirez A, Bearer EL, Li W-P, Mobley WC, Chu S (2007) One at a time, live tracking of NGF axonal transport using quantum dots. Proc Natl Acad Sci U S A 104:13666–13671.

Cummins TR, Aglieco F, Renganathan M, Herzog RI, Dib-Hajj SD, Waxman SG (2001) Nav1.3 sodium channels: rapid repriming and slow closed-state inactivation display quantitative differences after expression in a mammalian cell line and in spinal sensory neurons. J Neurosci 21:5952–5961.

Cummins TR, Dib-Hajj SD, Waxman SG (2004) Electrophysiological properties of mutant Nav1.7 sodium channels in a painful inherited neuropathy. J Neurosci 24:8232–8236.

Cummins TR, Sheets PL, Waxman SG (2007) The roles of sodium channels in nociception: Implications for mechanisms of pain. Pain 131:243–257.

Da Costa DSM, Meotti FC, Andrade EL, Leal PC, Motta EM, Calixto JB (2010) The involvement of the transient receptor potential A1 (TRPA1) in the maintenance of mechanical and cold hyperalgesia in persistent inflammation. Pain 148:431–437.

Dahlstrom AB (2010) Fast intra-axonal transport: Beginning, development and post-genome advances. Prog Neurobiol 90:119–145.

Davidson S, Giesler GJ (2010) The multiple pathways for itch and their interactions with pain. Trends Neurosci 33:550–558.

Davis JB, Gray J, Gunthorpe MJ, Hatcher JP, Davey PT, Overend P, Harries MH, Latcham J, Clapham C, Atkinson K, Hughes SA, Rance K, Grau E, Harper AJ, Pugh PL, Rogers DC, Bingham S, Randall A,

Sheardown SA (2000) Vanilloid receptor-1 is essential for inflammatory thermal hyperalgesia. Nature 405:183–187.

Delmas P, Hao J, Rodat-Despoix L (2011) Molecular mechanisms of mechanotransduction in mammalian sensory neurons. Nat Rev Neurosci 12:139–153.

Deval E, Noël J, Lay N, Alloui A, Diochot S, Friend V, Jodar M, Lazdunski M, Lingueglia E (2008) ASIC3, a sensor of acidic and primary inflammatory pain. Eur Mol Biol Organ J 27:3047–3055.

Deval E, Salinas M, Baron A, Lingueglia E, Lazdunski M (2004) ASIC2b-dependent regulation of ASIC3, an essential acid-sensing ion channel subunit in sensory neurons via the partner protein PICK-1. J Biol Chem 279:19531–19539.

Dib-Hajj SD, Cummins TR, Black JA, Waxman SG (2010) Sodium channels in normal and pathological pain. Annu Rev Neurosci 33:325–347.

Dib-Hajj SD, Estacion M, Jarecki BW, Tyrrell L, Fischer TZ, Lawden M, Cummins TR, Waxman SG (2008) Paroxysmal extreme pain disorder M1627K mutation in human Nav1.7 renders DRG neurons hyperexcitable. Mol Pain 4:37.

Dib-Hajj SD, Rush AM, Cummins TR, Hisama FM, Novella S, Tyrrell L, Marshall L, Waxman SG (2005) Gain-of-function mutation in Nav1.7 in familial erythromelalgia induces bursting of sensory neurons. Brain 128:1847–1854.

Dietrich PS, McGivern JG, Delgado SG, Koch BD, Eglen RM, Hunter JC, Sangameswaran L (1998) Functional analysis of a voltage-gated sodium channel and its splice variant from rat dorsal root ganglia. J Neurochem 70:2262–2272.

Dina OA, Green PG, Levine JD (2008) Role of interleukin-6 in chronic muscle hyperalgesic priming. Neuroscience 152:521–525.

Diochot S, Baron A, Rash LD, Deval E, Escoubas P, Scarzello S, Salinas M, Lazdunski M (2004) A new sea anemone peptide, APETx2, inhibits ASIC3, a major acid-sensitive channel in sensory neurons. EMBO J 23:1516–1525.

Dittert I, Benedikt J, Vyklický L, Zimmermann K, Reeh PW, Vlachová V (2006) Improved superfusion technique for rapid cooling or heating of cultured cells under patch-clamp conditions. J Neurosci Methods 151:178–185.

Dittrich PS, Manz A (2006) Lab-on-a-chip: microfluidics in drug discovery. Nat Rev Drug Discov 5:210–218.

Djouhri L, Fang X, Okuse K, Wood JN, Berry CM, Lawson SN (2003a) The TTX-resistant sodium channel Nav1.8 (SNS/PN3): expression and correlation with membrane properties in rat nociceptive primary afferent neurons. J Physiol 550:739–752.

Djouhri L, Newton R, Levinson SR, Berry CM, Carruthers B, Lawson SN (2003b) Sensory and electrophysiological properties of guinea-pig sensory neurones expressing Nav 1.7 (PN1) Na+ channel alpha subunit protein. J Physiol 546:565–576.

Docherty RJ, Robertson B, Bevan S (1991) Capsaicin causes prolonged inhibition of voltage-activated calcium currents in adult rat dorsal root ganglion neurons in culture. Neuroscience 40:513–521.

Docherty RJ, Yeats JC, Bevan S, Boddeke HWGM (1996) Inhibition of calcineurin inhibits the desensitization of capsaicin-evoked currents in cultured dorsal root ganglion neurones from adult rats. Pflügers Arch Eur J Physiol 431:828–837.

Dodge ME, Rahimtula M, Mearow KM (2002) Factors contributing to neurotrophin-independent survival of adult sensory neurons. Brain Res 953:144–156.

Dong X-W, Goregoaker S, Engler H, Zhou X, Mark L, Crona J, Terry R, Hunter J, Priestley T (2007) Small interfering RNA-mediated selective knockdown of Na(V)1.8 tetrodotoxin-resistant sodium channel reverses mechanical allodynia in neuropathic rats. Neuroscience 146:812–821.

Dotti C, Sullivan C, Banker G (1988) The establishment of polarity by hippocampal neurons in culture. J Neurosci 8:1454–1468.

Drew LJ, Rohrer DK, Price MP, Blaver KE, Cockayne DA, Cesare P, Wood JN (2004) Acid-sensing ion channels ASIC2 and ASIC3 do not contribute to mechanically activated currents in mammalian sensory neurones. J Physiol 556:691–710.

Duprat F, Lesage F, Fink M, Reyes R, Heurteaux C, Lazdunski M (1997) TASK, a human background K+ channel to sense external pH variations near physiological pH. EMBO J 16:5464–5471.

Eckert WA, Julius D, Basbaum AI (2006) Differential contribution of TRPV1 to thermal responses and tissue injury-induced sensitization of dorsal horn neurons in laminae I and V in the mouse. Pain 126:184–197.

Ehlers MD, Kaplan DR, Price DL, Koliatsos VE (1995) NGF-stimulated retrograde transport of trkA in the mammalian nervous system. J Cell Biol 130:149–156.

Eid SR, Crown ED, Moore EL, Liang HA, Choong K-C, Dima S, Henze DA, Kane SA, Urban MO (2008) HC-030031, a TRPA1 selective antagonist, attenuates inflammatory- and neuropathy-induced mechanical hypersensitivity. Mol Pain 4:48.

El Andaloussi-Lilja J, Lundqvist J, Forsby A (2009) TRPV1 expression and activity during retinoic acid-induced neuronal differentiation. Neurochem Int 55:768–774.

Elliott AM, Smith BH, Penny KI, Cairns Smith W, Alastair Chambers W (1999) The epidemiology of chronic pain in the community. Lancet 354:1248–1252.

England S, Bevan S, Docherty RJ (1996) PGE2 modulates the tetrodotoxin-resistant sodium current in neonatal rat dorsal root ganglion neurones via the cyclic AMP-protein kinase A cascade. J Physiol 495 (Pt 2:429–440.

Ernfors P (2001) Local and target-derived actions of neurotrophins during peripheral nervous system development. Cell Mol Life Sci 58:1036–1044.

Escoubas P, Bernard C, Lambeau G, Lazdunski M, Darbon H (2003) Recombinant production and solution structure of PcTx1, the specific peptide inhibitor of ASIC1a proton-gated cation channels. Protein Sci 12:1332–1343.

Eva R, Dassie E, Caswell PT, Dick G, ffrench-Constant C, Norman JC, Fawcett JW (2010) Rab11 and its effector Rab coupling protein contribute to the trafficking of beta 1 integrins during axon growth in adult dorsal root ganglion neurons and PC12 cells. J Neurosci 30:11654–11669.

Everill B, Cummins TR, Waxman SG, Kocsis JD (2001) Sodium currents of large (Abeta-type) adult cutaneous afferent dorsal root ganglion neurons display rapid recovery from inactivation before and after axotomy. Neuroscience 106:161–169.

Facer P, Casula MA, Smith GD, Benham CD, Chessell IP, Bountra C, Sinisi M, Birch R, Anand P (2007) Differential expression of the capsaicin receptor TRPV1 and related novel receptors TRPV3, TRPV4 and TRPM8 in normal human tissues and changes in traumatic and diabetic neuropathy. BMC Neurol 7:11.

Fang X, Djouhri L, Black JA, Dib-Hajj SD, Waxman SG, Lawson SN (2002) The presence and role of the tetrodotoxin-resistant sodium channel Na(v)1.9 (NaN) in nociceptive primary afferent neurons. J Neurosci 22:7425–7433.

Fitzgerald EM, Okuse K, Wood JN, Dolphin AC, Moss SJ (1999) cAMP-dependent phosphorylation of the tetrodotoxin-resistant voltage-dependent sodium channel SNS. J Physiol 516 (Pt 2:433–446.

Fitzgerald M (1987) Spontaneous and evoked activity of fetal primary afferents in vivo. Nature 326:603–605.

Frank E, Sanes JR (1991) Lineage of neurons and glia in chick dorsal root ganglia: analysis in vivo with a recombinant retrovirus. Development 111:895–908.

Gallo G, Lefcort FB, Letourneau PC (1997) The trkA Receptor Mediates Growth Cone Turning toward a Localized Source of Nerve Growth Factor. J Neurosci 17:5445–5454.

Ganju P, O'Bryan JP, Der C, Winter J, James IF (1998) Differential regulation of SHC proteins by nerve growth factor in sensory neurons and PC12 cells. Eur J Neurosci 10:1995–2008.

García-Añoveros J, Samad TA, Zuvela-Jelaska L, Woolf CJ, Corey DP (2001) Transport and localization of the DEG/ENaC ion channel BNaC1alpha to peripheral mechanosensory terminals of dorsal root ganglia neurons. J Neurosci 21:2678–2686.

Ginty DD, Segal RA (2002) Retrograde neurotrophin signaling: Trk-ing along the axon. Curr Opin Neurobiol 12:268–274.

Gissen AJ, Covino BG, Gregus J (1980) Differential sensitivities of mammalian nerve fibers to local anesthetic agents. Anesthesiology 53:467–474.

Godement P, Vanselow J, Thanos S, Bonhoeffer F (1987) A study in developing visual systems with a new method of staining neurones and their processes in fixed tissue. Development 101:697–713.

Gold MS, Levine JD, Correa AM (1998) Modulation of TTX-R INa by PKC and PKA and their role in PGE2-induced sensitization of rat sensory neurons in vitro. J Neurosci 18:10345–10355.

Gold MS, Weinreich D, Kim C-S, Wang R, Treanor J, Porreca F, Lai J (2003) Redistribution of NaV1.8 in Uninjured Axons Enables Neuropathic Pain. J Neurosci 23:158–166.

Golden JP, Hoshi M, Nassar MA, Enomoto H, Wood JN, Milbrandt J, Gereau RW, Johnson EM, Jain S (2010) RET signaling is required for survival and normal function of nonpeptidergic nociceptors. J Neurosci 30:3983–3994.

Goldstein LS, Yang Z (2000) Microtubule-based transport systems in neurons: the roles of kinesins and dyneins. Annu Rev Neurosci 23:39–71.

Goswami C, Schmidt H, Hucho F (2007) TRPV1 at nerve endings regulates growth cone morphology and movement through cytoskeleton reorganization. FEBS J 274:760–772.

Gu X, Olson EC, Spitzer NC (1994) Spontaneous neuronal calcium spikes and waves during early differentiation. J Neurosci 14:6325–6335.

Guler AD, Lee H, Iida T, Shimizu I, Tominaga M, Caterina M (2002) Heat-Evoked Activation of the Ion Channel, TRPV4. J Neurosci 22:6408–6414.

Gumy LF, Yeo GSH, Tung Y-CL, Zivraj KH, Willis D, Coppola G, Lam BYH, Twiss JL, Holt CE, Fawcett JW (2011) Transcriptome analysis of embryonic and adult sensory axons reveals changes in mRNA repertoire localization. RNA 17:85–98.

Harper AA, Lawson SN (1985) Conduction velocity is related to morphological cell type in rat dorsal root ganglion neurones. J Physiol 359:31–46.

Hayes AG, Hawcock AB, Hill RG (1984) The depolarising action of capsaicin on rat isolated sciatic nerve. Life Sci 35:1561–1568.

Hempstead BL (2002) The many faces of p75NTR. Curr Opin Neurobiol 12:260–267.

Hempstead BL, Martin-Zanca D, Kaplan DR, Parada LF, Chao M V (1991) High-affinity NGF binding requires coexpression of the trk proto-oncogene and the low-affinity NGF receptor. Nature 350:678–683.

Hensel H (1981) Thermoreception and temperature regulation. Monogr Physiol Soc 38:1–321.

HENSEL H, BOMAN KK (1960) Afferent impulses in cutaneous sensory nerves in human subjects. J Neurophysiol 23:564–578.

Herzog RI, Cummins TR, Ghassemi F, Dib-Hajj SD, Waxman SG (2003) Distinct repriming and closed-state inactivation kinetics of Nav1.6 and Nav1.7 sodium channels in mouse spinal sensory neurons. J Physiol 551:741–750.

Herzog RI, Cummins TR, Waxman SG (2001) Persistent TTX-resistant Na+ current affects resting potential and response to depolarization in simulated spinal sensory neurons. J Neurophysiol 86:1351–1364.

Hesselager M, Timmermann DB, Ahring PK (2004) pH Dependency and desensitization kinetics of heterologously expressed combinations of acid-sensing ion channel subunits. J Biol Chem 279:11006–11015.

Hille B (1975) The receptor for tetrodotoxin and saxitoxin. A structural hypothesis. Biophys J 15:615–619.

Hirokawa N (1982) Cross-linker system between neurofilaments, microtubules and membranous organelles in frog axons revealed by the quick-freeze, deep-etching method. J Cell Biol 94:129–142.

Hjerling-Leffler J, Alqatari M, Ernfors P, Koltzenburg M (2007) Emergence of functional sensory subtypes as defined by transient receptor potential channel expression. J Neurosci 27:2435–2443.

Hjerling-Leffler J, Marmigère F, Heglind M, Cederberg A, Koltzenburg M, Enerbäck S, Ernfors P (2005) The boundary cap: a source of neural crest stem cells that generate multiple sensory neuron subtypes. Development 132:2623–2632.

Holzer P (1991) Capsaicin: cellular targets, mechanisms of action, and selectivity for thin sensory neurons. Pharmacol Rev 43:143–201.

Huang C-W, Tzeng J-N, Chen Y-J, Tsai W-F, Chen C-C, Sun W-H (2007) Nociceptors of dorsal root ganglion express proton-sensing G-protein-coupled receptors. Mol Cell Neurosci 36:195–210.

Huang EJ, Wilkinson GA, Fariñas I, Backus C, Zang K, Wong SL, Reichardt LF (1999) Expression of Trk receptors in the developing mouse trigeminal ganglion: in vivo evidence for NT-3 activation of TrkA and TrkB in addition to TrkC. Development 126:2191–2203.

Huang J, Zhang X, McNaughton PA (2006) Inflammatory pain: the cellular basis of heat hyperalgesia. Curr Neuropharmacol 4:197–206.

Hudson LJ, Bevan S, Wotherspoon G, Gentry C, Fox A, Winter J (2001) VR1 protein expression increases in undamaged DRG neurons after partial nerve injury. Eur J Neurosci 13:2105–2114.

Hughes PA, Brierley SM, Young RL, Blackshaw LA (2007) Localization and comparative analysis of acid-sensing ion channel (ASIC1, 2, and 3) mRNA expression in mouse colonic sensory neurons within thoracolumbar dorsal root ganglia. J Comp Neurol 500:863–875.

Hwang SJ, Min Oh J, Valtschanoff JG (2005) Expression of the vanilloid receptor TRPV1 in rat dorsal root ganglion neurons supports different roles of the receptor in visceral and cutaneous afferents. Brain Res 1047:261–266.

Iggo A, Andres KH (1982) Morphology of cutaneous receptors. Annu Rev Neurosci 5:1–31.

Iggo A, Muir AR (1969) The structure and function of a slowly adapting touch corpuscle in hairy skin. J Physiol 200:763–796.

Ikoma A, Steinhoff M, Ständer S, Yosipovitch G, Schmelz M (2006) The neurobiology of itch. Nat Rev Neurosci 7:535–547.

Isonaka R, Hiruma H, Kawakami T (2011) Inhibition of axonal transport caused by tert-butyl hydroperoxide in cultured mouse dorsal root ganglion neurons. J Mol Neurosci 45:194–201.

Jackman A, Fitzgerald M (2000) Development of peripheral hindlimb and central spinal cord innervation by subpopulations of dorsal root ganglion cells in the embryonic rat. J Comp Neurol 418:281–298.

Jancsó G, Kiraly E, Jancsó-Gábor A (1977) Pharmacologically induced selective degeneration of chemosensitive primary sensory neurones. Nature 270:741–743.

Jancsó N, Jancsó-Gábor A, Szolcsányi J (1967) Direct evidence for neurogenic inflammation and its prevention by denervation and by pretreatment with capsaicin. Br J Pharmacol Chemother 31:138–151.

Jeffry JA, Yu S-Q, Sikand P, Parihar A, Evans MS, Premkumar LS (2009) Selective targeting of TRPV1 expressing sensory nerve terminals in the spinal cord for long lasting analgesia. Matsunami H, ed. PLoS One 4:e7021.

Jeftinija S (1994) The role of tetrodotoxin-resistant sodium channels of small primary afferent fibers. Brain Res 639:125–134.

Ji R-R, Samad TA, Jin S-X, Schmoll R, Woolf CJ (2002) p38 MAPK Activation by NGF in Primary Sensory Neurons after Inflammation Increases TRPV1 Levels and Maintains Heat Hyperalgesia. Neuron 36:57–68.

Jiménez-Díaz L, Géranton SM, Passmore GM, Leith JL, Fisher AS, Berliocchi L, Sivasubramaniam AK, Sheasby A, Lumb BM, Hunt SP (2008) Local translation in primary afferent fibers regulates nociception. PLoS One 3:e1961.

Johanek LM, Meyer RA, Friedman RM, Greenquist KW, Shim B, Borzan J, Hartke T, LaMotte RH, Ringkamp M (2008) A role for polymodal C-fiber afferents in nonhistaminergic itch. J Neurosci 28:7659–7669.

Jones NG, Slater R, Cadiou H, McNaughton P, McMahon SB (2004) Acid-induced pain and its modulation in humans. J Neurosci 24:10974–10979.

Jordt S-E, McKemy DD, Julius D (2003) Lessons from peppers and peppermint: the molecular logic of thermosensation. Curr Opin Neurobiol 13:487–492.

Kapp LD, Lorsch JR (2004) The molecular mechanics of eukaryotic translation. Annu Rev Biochem 73:657–704.

Karashima Y, Talavera K, Everaerts W, Janssens A, Kwan KY, Vennekens R, Nilius B, Voets T (2009) TRPA1 acts as a cold sensor in vitro and in vivo. Proc Natl Acad Sci U S A 106:1273–1278.

Kim Y, Bang H, Kim D (2000) TASK-3, a new member of the tandem pore K(+) channel family. J Biol Chem 275:9340–9347.

Kobayashi J, Ohta M, Terada Y (1993) C fiber generates a slow Na+ spike in the frog sciatic nerve. Neurosci Lett 162:93–96.

Kobayashi K, Fukuoka T, Obata K, Yamanaka H, Dai Y, Tokunaga A, Noguchi K (2005) Distinct expression of TRPM8, TRPA1, and TRPV1 mRNAs in rat primary afferent neurons with adelta/c-fibers and colocalization with trk receptors. J Comp Neurol 493:596–606.

Köbbert C, Apps R, Bechmann I, Lanciego JL, Mey J, Thanos S (2000) Current concepts in neuroanatomical tracing. Prog Neurobiol 62:327–351.

Koenig E, Martin R, Titmus M, Sotelo-Silveira JR (2000) Cryptic peripheral ribosomal domains distributed intermittently along mammalian myelinated axons. J Neurosci 20:8390–8400.

Koerber HR, Woodbury CJ (2002) Comprehensive phenotyping of sensory neurons using an ex vivo somatosensory system. Physiol Behav 77:589–594.

Koltzenburg M, Stucky CL, Lewin GR (1997) Receptive properties of mouse sensory neurons innervating hairy skin. J Neurophysiol 78:1841–1850.

Kramer I, Sigrist M, de Nooij JC, Taniuchi I, Jessell TM, Arber S (2006) A role for Runx transcription factor signaling in dorsal root ganglion sensory neuron diversification. Neuron 49:379–393.

Krishtal OA, Pidoplichko VI (1981) A receptor for protons in the membrane of sensory neurons may participate in nociception. Neuroscience 6:2599–2601.

Kuenzi FM, Dale N (1996) Effect of capsaicin and analogues on potassium and calcium currents and vanilloid receptors in Xenopus embryo spinal neurones. Br J Pharmacol 119:81–90.

Kumamoto J, Nakatani M, Tsutsumi M, Goto M, Denda S, Takei K, Denda M (2012) Coculture system of keratinocytes and dorsal-root-ganglion-derived cells for screening neurotrophic factors involved in guidance of neuronal axon growth. 2012 Neurosci Meet Plan Program 80.

Kuruvilla R, Zweifel LS, Glebova NO, Lonze BE, Valdez G, Ye H, Ginty DD (2004) A neurotrophin signaling cascade coordinates sympathetic neuron development through differential control of TrkA trafficking and retrograde signaling. Cell 118:243–255.

Kwan KY, Allchorne AJ, Vollrath MA, Christensen AP, Zhang D-S, Woolf CJ, Corey DP (2006) TRPA1 contributes to cold, mechanical, and chemical nociception but is not essential for hair-cell transduction. Neuron 50:277–289.

Lai J, Gold MS, Kim C-S, Bian D, Ossipov MH, Hunter JC, Porreca F (2002) Inhibition of neuropathic pain by decreased expression of the tetrodotoxin-resistant sodium channel, NaV1.8. Pain 95:143–152.

Lallemend F, Ernfors P (2012) Molecular interactions underlying the specification of sensory neurons. Trends Neurosci 35:373–381.

Lalli G, Schiavo G (2002) Analysis of retrograde transport in motor neurons reveals common endocytic carriers for tetanus toxin and neurotrophin receptor p75NTR. J Cell Biol 156:233–239.

Lapatsina L, Jira JA, Smith ESJ, Poole K, Kozlenkov A, Bilbao D, Lewin GR, Heppenstall PA (2012) Regulation of ASIC channels by a stomatin/STOML3 complex located in a mobile vesicle pool in sensory neurons. Open Biol 2:120096.

Latorre R, Vargas G, Orta G, Brauchi S (2007) TRP Ion Channel Function in Sensory Transduction and Cellular Signaling Cascades Chapter 21: Voltage and Temperature Gating of ThermoTRP Channels. CRC Press.

Lautermilch NJ, Spitzer NC (2000) Regulation of calcineurin by growth cone calcium waves controls neurite extension. J Neurosci 20:315–325.

Lawson SN, Perry MJ, Prabhakar E, McCarthy PW (1993) Primary sensory neurones: Neurofilament, neuropeptides and conduction velocity. Brain Res Bull 30:239–243.

Lechner SG, Frenzel H, Wang R, Lewin GR (2009) Developmental waves of mechanosensitivity acquisition in sensory neuron subtypes during embryonic development. EMBO J 28:1479–1491.

Lee KF, Davies AM, Jaenisch R (1994) p75-deficient embryonic dorsal root sensory and neonatal sympathetic neurons display a decreased sensitivity to NGF. Development 120:1027–1033.

Leem JW, Willis WD, Chung JM (1993) Cutaneous sensory receptors in the rat foot. J Neurophysiol 69:1684–1699.

Leffler A, Linte RM, Nau C, Reeh P, Babes A (2007) A high-threshold heat-activated channel in cultured rat dorsal root ganglion neurons resembles TRPV2 and is blocked by gadolinium. Eur J Neurosci 26:12–22.

Leffler A, Mönter B, Koltzenburg M (2006) The role of the capsaicin receptor TRPV1 and acid-sensing ion channels (ASICS) in proton sensitivity of subpopulations of primary nociceptive neurons in rats and mice. Neuroscience 139:699–709.

Lewin GR, Barde YA (1996) Physiology of the neurotrophins. Annu Rev Neurosci 19:289–317.

Lewin GR, Rueff A, Mendell LM (1994) Peripheral and Central Mechanisms of NGF-induced Hyperalgesia. Eur J Neurosci 6:1903–1912.

Lewin GR, Stucky CL (2000) Sensory neuron mechanotransduction: its regulation and underlying molecular mechanisms. In: Molecular basis of pain induction (Wood JN, ed), pp 129–149. New York.

Lewinter RD, Skinner K, Julius D, Basbaum AI (2004) Immunoreactive TRPV-2 (VRL-1), a capsaicin receptor homolog, in the spinal cord of the rat. J Comp Neurol 470:400–408.

Lindahl O (1961) Experimental skin pain induced by injection of water-soluble substances in humans. Acta Physiol Scand Suppl 179:1–89.

Lindsay RM (1996) Role of neurotrophins and trk receptors in the development and maintenance of sensory neurons: an overview. Philos Trans R Soc Lond B Biol Sci 351:365–373.

Lingueglia E, de Weille JR, Bassilana F, Heurteaux C, Sakai H, Waldmann R, Lazdunski M (1997) A modulatory subunit of acid sensing ion channels in brain and dorsal root ganglion cells. J Biol Chem 272:29778–29783.

Liu L, Oortgiesen M, Li L, Simon SA (2001) Capsaicin inhibits activation of voltage-gated sodium currents in capsaicin-sensitive trigeminal ganglion neurons. J Neurophysiol 85:745–758.

Liu Q, Tang Z, Surdenikova L, Kim S, Patel KN, Kim A, Ru F, Guan Y, Weng H-J, Geng Y, Undem BJ, Kollarik M, Chen Z-F, Anderson DJ, Dong X (2009) Sensory neuron-specific GPCR Mrgprs are itch receptors mediating chloroquine-induced pruritus. Cell 139:1353–1365.

LOEWENSTEIN WR, MENDELSON M (1965) COMPONENTS OF RECEPTOR ADAPTATION IN A PACINIAN CORPUSCLE. J Physiol 177:377–397.

Lonze BE, Riccio A, Cohen S, Ginty DD (2002) Apoptosis, axonal growth defects, and degeneration of peripheral neurons in mice lacking CREB. Neuron 34:371–385.

Lopes C, Liu Z, Xu Y, Ma Q (2012) Tlx3 and Runx1 act in combination to coordinate the development of a cohort of nociceptors, thermoceptors, and pruriceptors. J Neurosci 32:9706–9715.

Lorenzon P, Zacchetti D, Codazzi F, Fumagalli G, Meldolesi J, Grohovaz F (1995) Ca2+ waves in PC12 neurites: a bidirectional, receptor-oriented form of Ca2+ signaling. J Cell Biol 129:797–804.

Lukas J-R, Aigner M, Denk M, Heinzl H, Burian M, Mayr R (1998) Carbocyanine Postmortem Neuronal Tracing: Influence of Different Parameters on Tracing Distance and Combination with Immunocytochemistry. J Histochem Cytochem 46:901–910.

Luo W, Enomoto H, Rice FL, Milbrandt J, Ginty DD (2009) Molecular identification of rapidly adapting mechanoreceptors and their developmental dependence on ret signaling. Neuron 64:841–856.

Luo W, Wickramasinghe SR, Savitt JM, Griffin JW, Dawson TM, Ginty DD (2007) A hierarchical NGF signaling cascade controls Ret-dependent and Ret-independent events during development of nonpeptidergic DRG neurons. Neuron 54:739–754.

Ma C, Greenquist KW, Lamotte RH (2006) Inflammatory mediators enhance the excitability of chronically compressed dorsal root ganglion neurons. J Neurophysiol 95:2098–2107.

Maden M (2007) Retinoic acid in the development, regeneration and maintenance of the nervous system. Nat Rev Neurosci 8:755–765.

Mamet J, Baron A, Lazdunski M, Voilley N (2002) Proinflammatory mediators, stimulators of sensory neuron excitability via the expression of acid-sensing ion channels. J Neurosci 22:10662–10670.

Marmigère F, Ernfors P (2007) Specification and connectivity of neuronal subtypes in the sensory lineage. Nat Rev Neurosci 8:114–127.

Maro GS, Vermeren M, Voiculescu O, Melton L, Cohen J, Charnay P, Topilko P (2004) Neural crest boundary cap cells constitute a source of neuronal and glial cells of the PNS. Nat Neurosci 7:930–938.

McKemy DD, Neuhausser WM, Julius D (2002) Identification of a cold receptor reveals a general role for TRP channels in thermosensation. Nature 416:52–58.

McMahon SB (1996) NGF as a mediator of inflammatory pain. Philos Trans R Soc Lond B Biol Sci 351:431–440.

Melemedjian OK, Asiedu MN, Tillu D V, Peebles KA, Yan J, Ertz N, Dussor GO, Price TJ (2010) IL-6- and NGF-induced rapid control of protein synthesis and nociceptive plasticity via convergent signaling to the eIF4F complex. J Neurosci 30:15113–15123.

Menendez G (2010) Spatio-temporal control of neurotrophin trafficking and signalling in primary neurons cultured inside microfluidic chambers.

Meyer RA, Ringkamp M, Campbell JN, Raja SN (2006) Section 1: Neurobiology of Pain - Peripheral mechanisms of cutaneous pain. In: Textbook of Pain.

Michael GJ, Priestley J V. (1999) Differential Expression of the mRNA for the Vanilloid Receptor Subtype 1 in Cells of the Adult Rat Dorsal Root and Nodose Ganglia and Its Downregulation by Axotomy. J Neurosci 19:1844–1854.

Milbrandt J (1988) Nerve growth factor induces a gene homologous to the glucocorticoid receptor gene. Neuron 1:183–188.

Miller FD, Kaplan DR (2001) On Trk for Retrograde Signaling. Neuron 32:767–770.

Mishra SK, Tisel SM, Orestes P, Bhangoo SK, Hoon MA (2011) TRPV1-lineage neurons are required for thermal sensation. EMBO J 30:582–593.

Molliver DC, Snider WD (1997) Nerve growth factor receptor TrkA is down-regulated during postnatal development by a subset of dorsal root ganglion neurons. J Comp Neurol 381:428–438.

Molliver DC, Wright DE, Leitner ML, Parsadanian AS, Doster K, Wen D, Yan Q, Snider WD (1997) IB4-binding DRG neurons switch from NGF to GDNF dependence in early postnatal life. Neuron 19:849–861.

Nicholas RS, Winter J, Wren P, Bergmann R, Woolf CJ (1999) Peripheral inflammation increases the capsaicin sensitivity of dorsal root ganglion neurons in a nerve growth factor-dependent manner. Neuroscience 91:1425–1433.

Nordin M (1990) Low-threshold mechanoreceptive and nociceptive units with unmyelinated (C) fibres in the human supraorbital nerve. J Physiol 426:229–240.

Nykjaer A, Lee R, Teng KK, Jansen P, Madsen P, Nielsen MS, Jacobsen C, Kliemannel M, Schwarz E, Willnow TE, Hempstead BL, Petersen CM (2004) Sortilin is essential for proNGF-induced neuronal cell death. Nature 427:843–848.

Obara I, Géranton SM, Hunt SP (2012) Axonal protein synthesis: a potential target for pain relief? Curr Opin Pharmacol 12:42–48.

Obara I, Tochiki KK, Géranton SM, Carr FB, Lumb BM, Liu Q, Hunt SP (2011) Systemic inhibition of the mammalian target of rapamycin (mTOR) pathway reduces neuropathic pain in mice. Pain 152:2582–2595.

Obata K, Katsura H, Mizushima T, Yamanaka H, Kobayashi K, Dai Y, Fukuoka T, Tokunaga A, Tominaga M, Noguchi K (2005) TRPA1 induced in sensory neurons contributes to cold hyperalgesia after inflammation and nerve injury. J Clin Invest 115:2393–2401.

Ogata N, Tatebayashi H (1993) Kinetic analysis of two types of Na+ channels in rat dorsal root ganglia. J Physiol 466:9–37.

Olausson H, Lamarre Y, Backlund H, Morin C, Wallin BG, Starck G, Ekholm S, Strigo I, Worsley K, Vallbo AB, Bushnell MC (2002) Unmyelinated tactile afferents signal touch and project to insular cortex. Nat Neurosci 5:900–904.

Onizuka S, Yonaha T, Tamura R, Hosokawa N, Kawasaki Y, Kashiwada M, Shirasaka T, Tsuneyoshi I (2011) Capsaicin indirectly suppresses voltage-gated Na+ currents through TRPV1 in rat dorsal root ganglion neurons. Anesth Analg 112:703–709.

Pabbidi RM, Yu S-Q, Peng S, Khardori R, Pauza ME, Premkumar LS (2008) Influence of TRPV1 on diabetes-induced alterations in thermal pain sensitivity. Mol Pain 4:9.

Park JW, Vahidi B, Taylor AM, Rhee SW, Jeon NL (2006) Microfluidic culture platform for neuroscience research. Nat Protoc 1:2128–2136.

Park U, Vastani N, Guan Y, Raja SN, Koltzenburg M, Caterina MJ (2011) TRP vanilloid 2 knock-out mice are susceptible to perinatal lethality but display normal thermal and mechanical nociception. J Neurosci 31:11425–11436.

Paschal BM (1987) MAP 1C is a microtubule-activated ATPase which translocates microtubules in vitro and has dynein-like properties. J Cell Biol 105:1273–1282.

Patapoutian A, Peier AM, Story GM, Viswanath V (2003) ThermoTRP channels and beyond: mechanisms of temperature sensation. Nat Rev Neurosci 4:529–539.

Pazyra-Murphy MF, Segal RA (2008) Preparation and maintenance of dorsal root ganglia neurons in compartmented cultures. J Vis Exp.

Peier AM, Moqrich A, Hergarden AC, Reeve AJ, Andersson DA, Story GM, Earley TJ, Dragoni I, McIntyre P, Bevan S (2002a) A TRP Channel that Senses Cold Stimuli and Menthol. Cell 108:705–715.

Peier AM, Reeve AJ, Andersson DA, Moqrich A, Earley TJ, Hergarden AC, Story GM, Colley S, Hogenesch JB, McIntyre P, Bevan S, Patapoutian A (2002b) A heat-sensitive TRP channel expressed in keratinocytes. Science 296:2046–2049.

Peng YB, Ringkamp M, Meyer RA, Campbell JN (2003) Fatigue and paradoxical enhancement of heat response in C-fiber nociceptors from cross-modal excitation. J Neurosci 23:4766–4774.

Petsche U, Fleischer E, Lembeck F, Handwerker HO (1983) The effect of capsaicin application to a peripheral nerve on impulse conduction in functionally identified afferent nerve fibres. Brain Res 265:233–240.

Pezet S, McMahon SB (2006) Neurotrophins: mediators and modulators of pain. Annu Rev Neurosci 29:507–538.

Piñon LG, Minichiello L, Klein R, Davies AM (1996) Timing of neuronal death in trkA, trkB and trkC mutant embryos reveals developmental changes in sensory neuron dependence on Trk signalling. Development 122:3255–3261.

Pinto V, Derkach VA, Safronov B V (2008) Role of TTX-sensitive and TTX-resistant sodium channels in Adelta- and C-fiber conduction and synaptic transmission. J Neurophysiol 99:617–628.

Price DD, Hu JW, Dubner R, Gracely RH (1977) Peripheral suppression of first pain and central summation of second pain evoked by noxious heat pulses. Pain 3:57–68.

Price MP, Lewin GR, McIlwrath SL, Cheng C, Xie J, Heppenstall PA, Stucky CL, Mannsfeldt AG, Brennan TJ, Drummond HA, Qiao J, Benson CJ, Tarr DE, Hrstka RF, Yang B, Williamson RA, Welsh MJ (2000) The mammalian sodium channel BNC1 is required for normal touch sensation. Nature 407:1007–1011.

Price MP, McIlwrath SL, Xie J, Cheng C, Qiao J, Tarr DE, Sluka KA, Brennan TJ, Lewin GR, Welsh MJ (2001) The DRASIC cation channel contributes to the detection of cutaneous touch and acid stimuli in mice. Neuron 32:1071–1083.

Quasthoff S, Grosskreutz J, Schröder JM, Schneider U, Grafe P (1995) Calcium potentials and tetrodotoxin-resistant sodium potentials in unmyelinated C fibres of biopsied human sural nerve. Neuroscience 69:955–965.

Raper J, Mason C (2010) Cellular strategies of axonal pathfinding. Cold Spring Harb Perspect Biol 2:a001933.

Reeh PW (1986) Sensory receptors in mammalian skin in an in vitro preparation. Neurosci Lett 66:141–146.

Reeh PW, Steen KH (1996) Tissue acidosis in nociception and pain. Prog Brain Res 113:143–151.

Renganathan M, Cummins TR, Waxman SG (2001) Contribution of Na(v)1.8 sodium channels to action potential electrogenesis in DRG neurons. J Neurophysiol 86:629–640.

Renganathan M, Dib-Hajj S, Waxman S. (2002) Nav1.5 underlies the “third TTX-R sodium current” in rat small DRG neurons. Mol Brain Res 106:70–82.

Riccio A, Ahn S, Davenport CM, Blendy JA, Ginty DD (1999) Mediation by a CREB family transcription factor of NGF-dependent survival of sympathetic neurons. Science 286:2358–2361.

Rifkin JT, Todd VJ, Anderson LW, Lefcort F (2000) Dynamic expression of neurotrophin receptors during sensory neuron genesis and differentiation. Dev Biol 227:465–480.

Robertson D, Willard F, Vrana K (2001) Encyclopedia of Life Sciences: Phosphorimager. Chichester, UK: John Wiley & Sons, Ltd.

Rosenberg SS, Spitzer NC (2011) Calcium signaling in neuronal development. Cold Spring Harb Perspect Biol 3:a004259.

Ruit KG, Elliott JL, Osborne PA, Yan Q, Snider WD (1992) Selective dependence of mammalian dorsal root ganglion neurons on nerve growth factor during embryonic development. Neuron 8:573–587.

Rukwied R, Schley M, Forsch E, Obreja O, Dusch M, Schmelz M (2010) Nerve growth factor-evoked nociceptor sensitization in pig skin in vivo. J Neurosci Res 88:2066–2072.

Rush AM, Cummins TR, Waxman SG (2007) Multiple sodium channels and their roles in electrogenesis within dorsal root ganglion neurons. J Physiol 579:1–14.

Sangameswaran L, Fish LM, Koch BD, Rabert DK, Delgado SG, Ilnicka M, Jakeman LB, Novakovic S, Wong K, Sze P, Tzoumaka E, Stewart GR, Herman RC, Chan H, Eglen RM, Hunter JC (1997) A novel tetrodotoxin-sensitive, voltage-gated sodium channel expressed in rat and human dorsal root ganglia. J Biol Chem 272:14805–14809.

Sauer SK, Bove GM, Averbeck B, Reeh PW (1999) Rat peripheral nerve components release calcitonin gene-related peptide and prostaglandin E2 in response to noxious stimuli: evidence that nervi nervorum are nociceptors. Neuroscience 92:319–325.

Schmalhofer WA, Calhoun J, Burrows R, Bailey T, Kohler MG, Weinglass AB, Kaczorowski GJ, Garcia ML, Koltzenburg M, Priest BT (2008) ProTx-II, a selective inhibitor of NaV1.7 sodium channels, blocks action potential propagation in nociceptors. Mol Pharmacol 74:1476–1484.

Schmelz M, Schmidt R, Bickel A, Handwerker HO, Torebjörk HE (1997) Specific C-receptors for itch in human skin. J Neurosci 17:8003–8008.

Schmidt R, Schmelz M, Forster C, Ringkamp M, Torebjörk E, Handwerker H (1995) Novel classes of responsive and unresponsive C nociceptors in human skin. J Neurosci 15:333–341.

Schneider-Poetsch T, Ju J, Eyler DE, Dang Y, Bhat S, Merrick WC, Green R, Shen B, Liu JO (2010) Inhibition of eukaryotic translation elongation by cycloheximide and lactimidomycin. Nat Chem Biol 6:209–217.

Scholey JM, Heuser J, Yang JT, Goldstein LS (1989) Identification of globular mechanochemical heads of kinesin. Nature 338:355–357.

Scholz A, Kuboyama N, Hempelmann G, Vogel W (1998) Complex blockade of TTX-resistant Na+ currents by lidocaine and bupivacaine reduce firing frequency in DRG neurons. J Neurophysiol 79:1746–1754.

Serra J, Campero M, Ochoa J, Bostock H (1999) Activity-dependent slowing of conduction differentiates functional subtypes of C fibres innervating human skin. J Physiol 515 (Pt 3:799–811.

SHELLEY WB, ARTHUR RP (1955) Mucunain, the active pruritogenic proteinase of cowhage. Science 122:469–470.

Shu X-Q, Mendell LM (1999) Colloquium Paper: Neurotrophins and hyperalgesia. Proc Natl Acad Sci 96:7693–7696.

Slugg RM, Meyer RA, Campbell JN (2000) Response of cutaneous A- and C-fiber nociceptors in the monkey to controlled-force stimuli. J Neurophysiol 83:2179–2191.

Sluka KA, Price MP, Breese NM, Stucky CL, Wemmie JA, Welsh MJ (2003) Chronic hyperalgesia induced by repeated acid injections in muscle is abolished by the loss of ASIC3, but not ASIC1. Pain 106:229–239.

Smith ESJ, Omerbašić D, Lechner SG, Anirudhan G, Lapatsina L, Lewin GR (2011) The molecular basis of acid insensitivity in the African naked mole-rat. Science 334:1557–1560.

Smith GD, Gunthorpe MJ, Kelsell RE, Hayes PD, Reilly P, Facer P, Wright JE, Jerman JC, Walhin J-P, Ooi L, Egerton J, Charles KJ, Smart D, Randall AD, Anand P, Davis JB (2002) TRPV3 is a temperature-sensitive vanilloid receptor-like protein. Nature 418:186–190.

Snow PJ, Rose PK, Brown AG (1976) Tracing axons and axon collaterals of spinal neurons using intracellular injection of horseradish peroxidase. Science 191:312–313.

Staaf S, Franck MCM, Marmigère F, Mattsson JP, Ernfors P (2010) Dynamic expression of the TRPM subgroup of ion channels in developing mouse sensory neurons. Gene Expr Patterns 10:65–74.

Steen KH, Reeh PW (1993) Sustained graded pain and hyperalgesia from harmless experimental tissue acidosis in human skin. Neurosci Lett 154:113–116.

Steen KH, Reeh PW, Anton F, Handwerker HO (1992) Protons selectively induce lasting excitation and sensitization to mechanical stimulation of nociceptors in rat skin, in vitro. J Neurosci 12:86–95.

Steffens H, Hoheisel U, Eek B, Mense S (2001) Tetrodotoxin-resistant conductivity and spinal effects of cutaneous C-fibre afferents in the rat. Neurosci Res 39:413–419.

Stiess M, Bradke F (2011) Neuronal polarization: the cytoskeleton leads the way. Dev Neurobiol 71:430–444.

Story GM, Peier AM, Reeve AJ, Eid SR, Mosbacher J, Hricik TR, Earley TJ, Hergarden AC, Andersson DA, Hwang SW, McIntyre P, Jegla T, Bevan S, Patapoutian A (2003) ANKTM1, a TRP-like channel expressed in nociceptive neurons, is activated by cold temperatures. Cell 112:819–829.

Su X, Wachtel RE, Gebhart GF (1999) Capsaicin sensitivity and voltage-gated sodium currents in colon sensory neurons from rat dorsal root ganglia. Am J Physiol 277:G1180–8.

Sugiura Y, Lee CL, Perl ER (1986) Central projections of identified, unmyelinated (C) afferent fibers innervating mammalian skin. Science 234:358–361.

Sutherland SP, Benson CJ, Adelman JP, McCleskey EW (2001) Acid-sensing ion channel 3 matches the acid-gated current in cardiac ischemia-sensing neurons. Proc Natl Acad Sci U S A 98:711–716.

Szallasi A, Blumberg PM (1999) Vanilloid (Capsaicin) Receptors and Mechanisms. Pharmacol Rev 51:159–212.

Szallasi A, Nilsson S, Farkas-Szallasi T, Blumberg PM, Hökfelt T, Lundberg JM (1995) Vanilloid (capsaicin) receptors in the rat: distribution in the brain, regional differences in the spinal cord, axonal transport to the periphery, and depletion by systemic vanilloid treatment. Brain Res 703:175–183.

Takahashi J, Palmer TD, Gage FH (1999) Retinoic acid and neurotrophins collaborate to regulate neurogenesis in adult-derived neural stem cell cultures. J Neurobiol 38:65–81.

Talavera K, Nilius B, Voets T (2008) Neuronal TRP channels: thermometers, pathfinders and life-savers. Trends Neurosci 31:287–295.

Tanaka M, Cummins TR, Ishikawa K, Dib-Hajj SD, Black JA, Waxman SG (1998) SNS Na+ channel expression increases in dorsal root ganglion neurons in the carrageenan inflammatory pain model. Neuroreport 9:967–972.

Taylor AM, Blurton-Jones M, Rhee SW, Cribbs DH, Cotman CW, Jeon NL (2005) A microfluidic culture platform for CNS axonal injury, regeneration and transport. Nat Methods 2:599–605.

Taylor AM, Rhee SW, Tu CH, Cribbs DH, Cotman CW, Jeon NL (2003) Microfluidic Multicompartment Device for Neuroscience Research. Langmuir 19:1551–1556.

Tillman DB, Treede RD, Meyer RA, Campbell JN (1995) Response of C fibre nociceptors in the anaesthetized monkey to heat stimuli: estimates of receptor depth and threshold. J Physiol 485 (Pt 3:753–765.

Tohda C, Sasaki M, Konemura T, Sasamura T, Itoh M, Kuraishi Y (2001) Axonal transport of VR1 capsaicin receptor mRNA in primary afferents and its participation in inflammation-induced increase in capsaicin sensitivity. J Neurochem 76:1628–1635.

Tominaga M, Caterina MJ (2004) Thermosensation and pain. J Neurobiol 61:3–12.

Tominaga M, Caterina MJ, Malmberg AB, Rosen TA, Gilbert H, Skinner K, Raumann BE, Basbaum AI, Julius D (1998) The cloned capsaicin receptor integrates multiple pain-producing stimuli. Neuron 21:531–543.

Tong JX, Eichler ME, Rich KM (1996) Intracellular calcium levels influence apoptosis in mature sensory neurons after trophic factor deprivation. Exp Neurol 138:45–52.

Topilko P, Schneider-Maunoury S, Levi G, Baron-Van Evercooren A, Chennoufi AB, Seitanidou T, Babinet C, Charnay P (1994) Krox-20 controls myelination in the peripheral nervous system. Nature 371:796–799.

Treede RD, Meyer RA, Campbell JN (1998) Myelinated mechanically insensitive afferents from monkey hairy skin: heat-response properties. J Neurophysiol 80:1082–1093.

Treede RD, Meyer RA, Raja SN, Campbell JN (1995) Evidence for two different heat transduction mechanisms in nociceptive primary afferents innervating monkey skin. J Physiol 483 (Pt 3:747–758.

Ugawa S, Ueda T, Ishida Y, Nishigaki M, Shibata Y, Shimada S (2002) Amiloride-blockable acid-sensing ion channels are leading acid sensors expressed in human nociceptors. J Clin Invest 110:1185–1190.

Ugawa S, Ueda T, Yamamura H, Shimada S (2005) In situ hybridization evidence for the coexistence of ASIC and TRPV1 within rat single sensory neurons. Brain Res Mol Brain Res 136:125–133.

Usoskin D, Zilberter M, Linnarsson S, Hjerling-Leffler J, Uhlén P, Harkany T, Ernfors P (2010) En masse in vitro functional profiling of the axonal mechanosensitivity of sensory neurons. Proc Natl Acad Sci U S A 107:16336–16341.

Vallbo ÅB, Hagbarth K-E (1968) Activity from skin mechanoreceptors recorded percutaneously in awake human subjects. Exp Neurol 21:270–289.

Vassilev PM, Scheuer T, Catterall WA (1988) Identification of an intracellular peptide segment involved in sodium channel inactivation. Science 241:1658–1661.

Verdi JM, Birren SJ, Ibáñez CF, Persson H, Kaplan DR, Benedetti M, Chao M V, Anderson DJ (1994) p75LNGFR regulates Trk signal transduction and NGF-induced neuronal differentiation in MAH cells. Neuron 12:733–745.

Verma P, Chierzi S, Codd AM, Campbell DS, Meyer RL, Holt CE, Fawcett JW (2005) Axonal protein synthesis and degradation are necessary for efficient growth cone regeneration. J Neurosci 25:331–342.

Villière V, McLachlan EM (1996) Electrophysiological properties of neurons in intact rat dorsal root ganglia classified by conduction velocity and action potential duration. J Neurophysiol 76:1924–1941.

Vogt L, Giger RJ, Ziegler U, Kunz B, Buchstaller A, Hermens WTJMC, Kaplitt MG, Rosenfeld MR, Pfaff DW, Verhaagen J, Sonderegger P (1996) Continuous renewal of the axonal pathway sensor apparatus by insertion of new sensor molecules into the growth cone membrane. Curr Biol 6:1153–1158.

Voilley N, de Weille J, Mamet J, Lazdunski M (2001) Nonsteroid anti-inflammatory drugs inhibit both the activity and the inflammation-induced expression of acid-sensing ion channels in nociceptors. J Neurosci 21:8026–8033.

Von Holst A, Rodriguez-Tébar A, Michaille JJ, Dhouailly D, Bäckström A, Ebendal T, Rohrer H (1995) Retinoic acid-mediated increase in TrkA expression is sufficient to elicit NGF-dependent survival of sympathetic neurons. Mol Cell Neurosci 6:185–198.

Von Schack D, Casademunt E, Schweigreiter R, Meyer M, Bibel M, Dechant G (2001) Complete ablation of the neurotrophin receptor p75NTR causes defects both in the nervous and the vascular system. Nat Neurosci 4:977–978.

Vriens J, Owsianik G, Hofmann T, Philipp SE, Stab J, Chen X, Benoit M, Xue F, Janssens A, Kerselaers S, Oberwinkler J, Vennekens R, Gudermann T, Nilius B, Voets T (2011) TRPM3 is a nociceptor channel involved in the detection of noxious heat. Neuron 70:482–494.

Waldmann R (1997) Molecular Cloning of a Non-inactivating Proton-gated Na+ Channel Specific for Sensory Neurons. J Biol Chem 272:20975–20978.

Waldmann R, Champigny G, Bassilana F, Heurteaux C, Lazdunski M (1997) A proton-gated cation channel involved in acid-sensing. Nature 386:173–177.

Watanabe S, Hong M, Lasser-Ross N, Ross WN (2006) Modulation of calcium wave propagation in the dendrites and to the soma of rat hippocampal pyramidal neurons. J Physiol 575:455–468.

Watson FL, Heerssen HM, Moheban DB, Lin MZ, Sauvageot CM, Bhattacharyya A, Pomeroy SL, Segal RA (1999) Rapid nuclear responses to target-derived neurotrophins require retrograde transport of ligand-receptor complex. J Neurosci 19:7889–7900.

Waxman SG, Kocsis JD, Black JA (1994) Type III sodium channel mRNA is expressed in embryonic but not adult spinal sensory neurons, and is reexpressed following axotomy. J Neurophysiol 72:466–470.

Wetzel C, Hu J, Riethmacher D, Benckendorff A, Harder L, Eilers A, Moshourab R, Kozlenkov A, Labuz D, Caspani O, Erdmann B, Machelska H, Heppenstall PA, Lewin GR (2007) A stomatin-domain protein essential for touch sensation in the mouse. Nature 445:206–209.

White FA, Silos-Santiago I, Molliver DC, Nishimura M, Phillips H, Barbacid M, Snider WD (1996) Synchronous onset of NGF and TrkA survival dependence in developing dorsal root ganglia. J Neurosci 16:4662–4672.

William A. Catterall, Edward Perez-Reyes, Terrance P. Snutch JS (2009) Voltage-gated calcium channels | INTRODUCTION. IUPHAR database Available at: http://www.iuphar-db.org/DATABASE/FamilyIntroductionForward?familyId=80.

Winter J, Bevan S, Campbell EA (1995) Capsaicin and pain mechanisms. Br J Anaesth 75:157–168.

Winter J, Forbes CA, Sternberg J, Lindsay RM (1988) Nerve growth factor (NGF) regulates adult rat cultured dorsal root ganglion neuron responses to the excitotoxin capsaicin. Neuron 1:973–981.

Woodbury CJ, Zwick M, Wang S, Lawson JJ, Caterina MJ, Koltzenburg M, Albers KM, Koerber HR, Davis BM (2004) Nociceptors lacking TRPV1 and TRPV2 have normal heat responses. J Neurosci 24:6410–6415.

Woolf CJ (1996) Phenotypic modification of primary sensory neurons: the role of nerve growth factor in the production of persistent pain. Philos Trans R Soc Lond B Biol Sci 351:441–448.

Yang Y, Wang Y, Li S, Xu Z, Li H, Ma L, Fan J, Bu D, Liu B, Fan Z, Wu G, Jin J, Ding B, Zhu X, Shen Y (2004a) Mutations in SCN9A, encoding a sodium channel alpha subunit, in patients with primary erythermalgia. J Med Genet 41:171–174.

Yang Y, Wang Y, Li S, Xu Z, Li H, Ma L, Fan J, Bu D, Liu B, Fan Z, Wu G, Jin J, Ding B, Zhu X, Shen Y (2004b) Mutations in SCN9A, encoding a sodium channel alpha subunit, in patients with primary erythermalgia. J Med Genet 41:171–174.

Yeomans DC, Levinson SR, Peters MC, Koszowski AG, Tzabazis AZ, Gilly WF, Wilson SP (2005) Decrease in inflammatory hyperalgesia by herpes vector-mediated knockdown of Nav1.7 sodium channels in primary afferents. Hum Gene Ther 16:271–277.

Yoshida S, Matsuda Y (1979) Studies on sensory neurons of the mouse with intracellular-recording and horseradish peroxidase-injection techniques. J Neurophysiol 42:1134–1145.

Yuen EC, Howe CL, Li Y, Holtzman DM, Mobley WC (n.d.) Nerve growth factor and the neurotrophic factor hypothesis. Brain Dev 18:362–368.

Zeng D, Kyle JW, Martin RL, Ambler KS, Hanck DA (1996) Cardiac sodium channels expressed in a peripheral neurotumor-derived cell line, RT4-B8. Am J Physiol 270:C1522–31.

Zhang J, Cavanaugh DJ, Nemenov MI, Basbaum AI (2013) The modality-specific contribution of peptidergic and non-peptidergic nociceptors is manifest at the level of dorsal horn nociresponsive neurons. J Physiol 591:1097–1110.

Zhang X, Huang J, McNaughton PA (2005) NGF rapidly increases membrane expression of TRPV1 heat-gated ion channels. EMBO J 24:4211–4223.

Zheng J-Q, Kelly TK, Chang B, Ryazantsev S, Rajasekaran AK, Martin KC, Twiss JL (2001) A Functional Role for Intra-Axonal Protein Synthesis during Axonal Regeneration from Adult Sensory Neurons. J Neurosci 21:9291–9303.

Zhuang Z-Y, Xu H, Clapham DE, Ji R-R (2004) Phosphatidylinositol 3-kinase activates ERK in primary sensory neurons and mediates inflammatory heat hyperalgesia through TRPV1 sensitization. J Neurosci 24:8300–8309.

Zimmermann K, Hein A, Hager U, Kaczmarek JS, Turnquist BP, Clapham DE, Reeh PW (2009) Phenotyping sensory nerve endings in vitro in the mouse. Nat Protoc 4:174–196.

Zimmermann K, Leffler A, Babes A, Cendan CM, Carr RW, Kobayashi J, Nau C, Wood JN, Reeh PW (2007) Sensory neuron sodium channel Nav1.8 is essential for pain at low temperatures. Nature 447:855–858.

Zolessi FR, Poggi L, Wilkinson CJ, Chien C-B, Harris WA (2006) Polarization and orientation of retinal ganglion cells in vivo. Neural Dev 1:2.

Zwick M, Davis BM, Woodbury CJ, Burkett JN, Koerber HR, Simpson JF, Albers KM (2002) Glial cell line-derived neurotrophic factor is a survival factor for isolectin B4-positive, but not vanilloid receptor 1-positive, neurons in the mouse. J Neurosci 22:4057–4065.